

**Influence of Microbial
Community on Nitrogen
Loss through
Denitrification in
Agriculture**

Claire Elizabeth Moulton-Brown

PhD

University of York

Biology

September 2022

Abstract

Global food demand is expected to rise by up to 62% by 2050, with an increasing population and finite land available for food production. Denitrification causes loss of fixed nitrogen from soil systems, thereby reducing crop productivity. Current nitrogen cycling models cannot fully explain the variation in nitrogen use efficiency at the field scale; this variation is thought to be associated with microbial community dynamics. The dynamics of denitrification and denitrifying communities are affected by the physicochemical properties of the soil, and therefore the land management practices which alter them. In this thesis, we look at the effects of land management history and innate environmental variation using a long-term factorial field trial, a working commercial farm, and laboratory-based experiments. By studying the denitrifier community composition, abundance and diversity in the context of environmental data, we were able to address the question of how specific land management practices and innate spatiotemporal variation affects the distribution of denitrifiers within arable soils.

It was found that bacterial and denitrifier communities are largely unaffected by land management history, and cluster predominantly along environmental gradients. Additionally, there was a high degree of spatiotemporal variation in soil denitrifying communities, with implications for future sampling strategies as well as computer modelling. Finally, it was established that isolation of bacteria from the environment is a viable method for culturing non-model organisms that can be characterized and used to inform nitrogen-cycling models. In this combination of well-established agricultural field trial and working commercial farm, the major identifiable determinant of bacterial community dissimilarity was a blend of physicochemical factors. The importance of selection on bacterial communities, relative to ecological drift, may have consequences for attempts to understand and model nutrient availabilities in arable farming systems, and improve agricultural productivity to feed the growing global population.

Table of Contents

Abstract	2
Table of Contents.....	3
Table of Figures.....	8
Table of Tables	14
Acknowledgements.....	16
Author's Declaration.....	17
Chapter 1: General Introduction.....	19
1.1. Population growth and food security.....	19
1.2. The microbial nitrogen cycle.....	21
1.2.1. Nitrogen fixation	23
1.2.2. Nitrate assimilation	23
1.2.3. ANAMMOX	24
1.2.4. Nitrification.....	24
1.2.5. DNRA	25
1.2.6. Denitrification	25
1.3. Rational for studying denitrifying communities.....	31
1.4. Measuring denitrification.....	33
1.4.1. Acetylene inhibition.....	33
1.4.2. ¹⁵ N tracers	35
1.4.3. Direct N ₂ quantification.....	35
1.4.4. Mass balance approaches.....	35
1.4.5. Molecular methods	36

1.4.6.	Direct measurement of denitrification intermediates.....	41
1.5.	Soil bacterial biodiversity	41
1.5.1.	Soil heterogeneity.....	42
1.5.2.	Microbial biodiversity	42
1.5.3.	Biogeography and community assembly.....	42
1.5.4.	Land management interventions.....	43
1.5.5.	Predicting function from genes	45
1.5.6.	Cultivating denitrifiers	45
1.6.	Thesis aims and objectives.....	46
1.6.1.	Chapter 2 aims:.....	47
1.6.2.	Chapter 3 aims:.....	48
1.6.3.	Chapter 4 aims:.....	48
Chapter 2: Long-term fertilization and tillage regimes have limited effects on structuring bacterial and denitrifier communities in a block designed long-term field trial		
		49
2.1.	Introduction.....	49
2.1.1.	Experimental aims	52
2.2.	Methods	52
2.2.1.	Nafferton long-term field experiment and sampling.....	52
2.2.2.	Quantification of 16S rRNA using spike-in <i>T. thermophilus</i>	55
2.2.3.	DNA extraction and amplicon sequencing	56
2.2.4.	Determination of soil properties.....	58
2.2.5.	Statistical and diversity analysis.....	59
2.2.6.	Accession numbers	59
2.3.	Results	60

2.3.1.	Soil physicochemical properties.....	60
2.3.2.	The effect of tillage and fertilizer on bacterial taxa and abundance	61
2.3.3.	The effect of tillage and fertilizer on bacterial 16S rRNA and denitrification gene alpha diversity	64
2.3.4.	The effect of tillage, fertilizer and sample location on bacterial community composition	66
2.3.5.	Spatial and environmental effects on bacterial community composition.....	67
2.4.	Discussion	70
2.4.1.	Conclusions.....	72
Chapter 3: Spatiotemporal distribution of bacteria and denitrification genes in a commercially farmed arable field and their association with yield variability		74
3.1.	Introduction.....	74
3.1.1.	Spatial effects.....	74
3.1.2.	Denitrification as a marker of functional diversity.....	76
3.1.3.	Experimental objectives	76
3.2.	Methods	77
3.2.1.	Harold Smiths field experiment and sampling.....	77
3.2.2.	Development of a spike-in quantification system for amplicon sequences...	81
3.2.3.	DNA extraction and amplicon sequencing	83
3.2.4.	qPCR of 16S and denitrification genes	85
3.2.5.	Determination of soil physicochemical properties	89
3.2.6.	Statistical and diversity analysis.....	89
3.3.	Results	91
3.3.1.	Physicochemical field properties.....	91

3.3.2.	Bacterial and denitrification gene abundance	93
3.3.3.	Verification of spike-in DNA for calculating absolute gene abundance.....	95
3.3.4.	Taxonomic spatiotemporal distribution.....	97
3.3.5.	Alpha diversity	101
3.3.6.	Community beta diversity.....	104
3.3.7.	Spatial and environmental links to community composition.....	107
3.4.	Discussion	110
3.4.1.	Spatial patterns of microbial distribution	110
3.4.2.	Temporal stability of microbial populations.....	112
3.4.3.	Associations between denitrifier population and low yield.....	113
3.4.4.	Utilization of synthetic spike-in standards for gene quantification	114
Chapter 4: Isolation and characterisation of potential denitrifying bacteria.....		116
4.1.	Introduction.....	116
4.1.1.	Experimental aims	117
4.2.	Methods	119
4.2.1.	Microbial isolation field site and experimental overview	119
4.2.2.	Isolation devices	120
4.2.3.	Culturing microbial isolates.....	121
4.2.4.	High-throughput nitrate and nitrite reduction assays	122
4.2.5.	16S rRNA sequencing of all isolates	124
4.2.6.	Selection of isolates for further study	125
4.2.7.	Quantifying utilised substrate	125
4.2.8.	Nitrate loss rate experiments in pure culture	126
4.2.9.	Whole genome sequencing of selected isolates.....	130

4.3.	Results	131
4.3.1.	Isolation of culturable soil bacteria.....	131
4.3.2.	Diversity captured through isolation.....	131
4.3.3.	High-throughput screening for nitrate & nitrite reduction.....	134
4.3.4.	Selection of isolates for further study	134
4.3.5.	Nitrate reduction profile in selected isolates.....	135
4.3.6.	Comparative genomic analysis of nitrogen cycling gene profiles.....	142
4.4.	Discussion	145
4.4.1.	Tackling the great plate count anomaly.....	145
4.4.2.	Characterisation of cultured environmental microbes	147
4.4.3.	Nitrate reduction in the absence of denitrification.....	148
	Chapter 5: General Discussion	151
	Appendix 1: Published Manuscript: Environmental Microbiology (2022) 24(1), 298–308 doi:10.1111/1462-2920.15873	158
	Appendix 2:Electrical conductivity and yield maps of Harold Smiths field	170
	Appendix 3:Arduino code used to transfer data from nitric oxide and oxygen sensors	177
	References.....	179

Table of Figures

Figure 1 World population in billions from 1950 to 2050. Observed population from 1950-2022, and projected population from 2022 onwards. High, medium and low fertility variants for modelling population are given in white, pale blue and medium blue respectively. Data from United Nations, Department of Economic and Social Affairs, Population Division (2022) (United Nations, 2022b).	19
Figure 2 Microbial pathways in the nitrogen cycle. Background colours indicate processes occurring under oxic (blue) or anoxic conditions (brown). The compounds are positioned according to the oxidation state of N. Solid coloured lines show microbial pathways, and the genes encoding the respective enzymes that catalyse each step. Dotted lines indicate the contributing pathways to atmospheric loading of gaseous nitrogen compounds. Enzyme codes are as follows: amo, ammonia monooxygenase; hao, hydroxylamine oxidoreductase; hdh (also known as hzo), hydrazine dehydrogenase; hzs, hydrazine synthase, nar/nap, cytoplasmic and periplasmic dissimilatory nitrate reductases, respectively; nas, assimilatory nitrate reductase; nif, nitrogenase; nas/nirB, assimilatory nitrite reductase; nirS/nirK, cytochrome-cd1 and copper-based dissimilatory nitrite reductases, respectively; nor, nitric oxide reductases; nosZ, nitrous oxide reductase; nrf, formate-dependent dissimilatory nitrite reductase; nxr, nitrite oxidoreductase. Figure reproduced from Hallin et al. 2018 (Hallin et al., 2018).....	22
Figure 3 Location of Nafferton Factorial Systems Comparison study showing (A) position in the UK, (B) satellite view of the field site and (C) ordnance survey map of the field site with 10m spaced contour lines indicating elevation above sea level.	53
Figure 4 Schematic of Nafferton Factorial Systems Comparison (NFSC) East Hemmel Experiment 3 Plots indicating plots used in this study. MT = minimum tillage, CT = conventional tillage, OF = organic fertilizer and MF = mineral fertilizer. Each individual plot measured 6 x 24m (4 blocks of 32 plots are separated from other blocks by 7m).	54
Figure 5 Relative (A) and absolute (B) abundance of bacterial phyla in soils treated with different combinations of tillage and fertilizer. ‘Others’ refers to all phyla with an abundance	

of less than 1% across samples. Labels indicate field plot. MT and CT denote minimum and conventional tillage respectively. OF and SF denote organic and synthetic fertilizer respectively. 62

Figure 6 Boxplots of alpha diversity measures of each sample treatment. (A) Observed amplicon sequence variants by sample treatment. (B) Shannon diversity index. (C) Pielou’s evenness index. Conventional tillage is shown in black, with minimum tillage shown in white. OF and SF denote organic and synthetic fertilizer respectively. 64

Figure 7 Non-metric multidimensional scaling (NMDS) of gene amplicon Bray-Curtis dissimilarity from NFSC soils. (A) Whole bacterial community 16S rRNA. (B) nirK amplicon variants. (C) nirS amplicon variants. (D) nosZ amplicon variants. Samples are indicated with points, conventional tillage (CT) plots are shown in white, with minimum tillage (MT) in black; organic fertilizer (OF) is denoted by circles, synthetic fertilizer (SF) treatments are shown by triangles. Points are grouped by polygons indicating block position of sample in the field study, from block 1 shown in white to block 4 shown with the dark grey. Labels indicate environmental variables which significantly explain sample Bray Curtis beta diversity. 66

Figure 8 Distance-decay relationship between geographic distance between samples and Bray-Curtis dissimilarity index for 16S rRNA (A), nirK (B), nirS (C) and nosZ (D) genes. 69

Figure 9 Location of Harold Smiths field site showing (A) position in the UK, (B) satellite view of the field site and (C) ordnance survey map of the field site with 5m spaced contour lines in orange indicating elevation above sea level, (D) 2018 spring bean yield – low yield samples with 1.43 t ha⁻¹ are in pale green and high yield sites with 2.75 t ha⁻¹ are in medium blue, (E) shallow electrical conductivity scan – low conductivity samples were 16.8 mS m⁻¹ are coloured orange and high conductivity samples with 27.1 mS m⁻¹ are coloured turquoise . See Appendix 2: for high resolution maps. Image credits: (A,B) Google maps, 2022; (C) Ordnance survey, 2022; (D,E) Precision Decisions. 77

Figure 10 Schematic showing sampling locations within Harold Smiths field and sampling strategies. (A) Stratified sampling of four 40 m² zones with distinct properties: low yield and low conductivity (pink), low yield and high conductivity (green), high yield and low conductivity (blue) and high yield and high conductivity (purple). Within each zone, there are

four 2 m² blocks, which were distributed to give a wide spread of distances between blocks. Within the sixteen blocks, there are three randomly located sampling sites. (B) Schematic of spatial investigation sampling, with 48 spatially explicit sampling sites (black dots) sampled in 2018. (C) Schematic of temporal investigation sampling, with four pooled sampled (from twelve 10 cm deep cores) taken each year over three years. 78

Figure 11 Overview of production of synthetic spike-in DNA standards for spike-AMP quantification of amplicon abundance during sequencing..... 81

Figure 12 C_q values obtained during qPCR inhibition test on qPCR Plate 1 (A) and Plate 2 (B). The red line indicates median C_q value obtained from the no-template control (NTC) for each plate. All samples contained equal amounts of pUC18 template DNA..... 93

Figure 13 qPCR derived gene copy numbers per g soil. Bars indicate mean of three replicates with standard error shown. Colours indicate field zone of soil sample: pink = low yield, low conductivity, green = low yield, high conductivity; blue = high yield low conductivity and purple = high yield, high conductivity. 94

Figure 14 qPCR and spike-in DNA derived gene abundance comparison. (A) *T. thermophilus* spike-in derived 16S rRNA copy numbers, (B) synthetic 16S spike-in derived 16S copy number, (C) synthetic nirK spike-in derived nirK copy number and (D) synthetic nirS spike-in derived nirS copy number..... 96

Figure 15 Relative (A) and absolute abundance (B) of phyla in Harold Smiths 2018 soils. ‘Others’ refers to all phyla with an abundance of less than 1% across samples. 97

Figure 16 Changes to relative (A) and absolute (B) phyla abundances in Harold Smiths soils from 2018 – 2020. ‘Others’ refers to all phyla with an abundance of less than 1% across samples. 99

Figure 17 Monthly rainfall at Linton on Ouse weather station from 2016 – 2020. Red line indicates the fifteen-year average monthly rainfall. Vertical dashed lines indicate sampling date. Rainfall data obtained from the MET Office (Met Office, 2019)..... 100

Figure 18 Alpha diversity for 2018 soil samples for 16S rRNA, nirK and nirS. (A) shows species richness through observed ASVs, (B) indicates Shannon Index of diversity and (C) shows Pielou’s evenness index. Bars represent mean of twelve samples, with error bars

showing one standard error. Colours indicate field zone of soil sample: pink = low yield, low conductivity; green = low yield, high conductivity; blue = high yield low conductivity and purple = high yield, high conductivity. Note variable y axis scale. 101

Figure 19 Alpha diversity from 2018 – 2020 soil samples. (A) species richness through observed ASVs, (B) Shannon Index of diversity and (C) Pielou’s evenness index. Colours indicate field zone of soil sample: pink = low yield, low conductivity; green = low yield, high conductivity; blue = high yield low conductivity and purple = high yield, high conductivity. Colour intensity shows year: palest = 2018, medium = 2019, darkest = 2020. Note variable y axis scale. 103

Figure 20 Non-metric multidimensional scaling (NMDS) of 2018 soil gene amplicon Bray-Curtis dissimilarity (top) and Weighted UniFrac distance (bottom). (A) 16S rRNA gene, (B) nirK nitrite reductase gene, (c) nirS nitrite reductase gene. Colours indicate field zone of soil sample: pink = low yield, low conductivity; green = low yield, high conductivity; blue = high yield low conductivity and purple = high yield, high conductivity. Labels indicate environmental variables which significantly explain beta diversity. 104

Figure 21 Non-metric multidimensional scaling (NMDS) of 2018 – 2020 soils showing Bray-Curtis dissimilarity (top) and Weighted UniFrac distance (bottom) for (A) 16S, (B) nirK, (C) nirS, and (D) nosZ(I). Colours indicate year of sampling: red = 2018, green = 2019 and blue = 2020. Shapes indicate site of soil sample: circle = low yield low conductivity, triangle = low yield high conductivity, square = high yield low conductivity and plus = high yield high conductivity. 106

Figure 22 Association between spatial distance and community dissimilarity in Harold Smiths 2018 soils. Euclidean distance versus Bray-Curtis dissimilarity (top) and Weighted UniFrac distance (bottom) for (A) 16S, (B) nirK, (C) nirS genes. Statistics show mantel test r statistic and p value for each association. Stars indicate p value size with *** indicating $p < 0.001$. 108

Figure 23 Variation partitioning of Weighted UniFrac distances in 2018-20 samples. 109

Figure 24 Schematic overview of the experiments in Chapter 4, from culturing soil microbes from isolation devices, to characterising potential nitrogen cycling capabilities. 119

Figure 25 Isolation device & components. (A) From left to right: intact isolation device, front panel, central panel with 396 1 ul pores, back panel. Once assembled, membranes (not shown) are attached to either side of the central panel and the isolation device is held together by screws and bolts (left). (B) Technical drawing of the isolation chip device this device was based on. Figure reproduced from (Berdy et al., 2017)..... 120

Figure 26 Schematic diagram representing the high-throughput nitrate and nitrite reduction assays. (A) Griess reaction principle. Under acidic conditions, nitrite reacts with sulphanilamide to produce a diazonium ion, which is then coupled to NED to produce a chromophoric azo product, which strongly absorbs at 540 nm. (B) nitrate reduction assay to determine whether isolated microbes can reduce nitrate to nitrite, reduce nitrate beyond nitrite or cannot reduce nitrate. (C) nitrite reduction assay to determine if isolated microbes can reduce nitrite. Figure part (A) reproduced from Giustarini et al. (Giustarini et al., 2008). . 123

Figure 26 Nitrate loss in pure culture experimental setup. (A) Structure of the ISO-NOP nitric oxide probe. (B) Components of the dissolved oxygen (Clark) electrode. (C) Photograph of experimental setup including nitric oxide probe, Clark electrode, Arduino interface and isolated nitric oxide meter. Panels A and B adapted from WPI-Europe & Rank Brothers respectively 126

Figure 27 Arduino Due circuit to transfer data from the oxygen and nitric oxide detectors. (A) Photograph depicting breadboard mounted circuit connected to Arduino Due microcontroller board. (B) Schematic view of the circuits..... 129

Figure 28 Phylogenetic tree of 16S rRNA for all bacteria isolated and cultured from Harold Smiths soils. Coloured tip points indicate isolate genus. Starred isolates indicate those selected for further study. Coloured bars around the outside indicate screening assay results for aerobic and anaerobic nitrate and nitrite reduction..... 132

Figure 29 Species accumulation curve for Harold Smiths soil samples. Inset panel is zoomed in on 0 - 205 samples to represent the equivalent of the 205 cultured isolates. 133

Figure 30 Rank abundance curve of 16S rRNA amplicon sequence variants from Harold Smiths field 2018-2020. Arrows indicate abundance of twelve isolates chosen for further study. Arrow colour indicates isolate genus. 134

Figure 31 Percent of 500 μ M nitrate or nitrite used after four hours under anoxic or oxic conditions with a starting cell density of 5×10^6 cells. Bars show mean of three replicates with error bars representing standard error. 136

Figure 32 Nitrate loss in pure culture in 5 ml TSB supplemented with 500 μ M potassium nitrate. Nitric oxide and oxygen measurements were taken continuously, with nitrate and nitrite measurements taken every 15 minutes as indicated by the points on the graph. Bacterial isolates are shown in facet name. The nitrate (black), nitrite (grey) and oxygen (light grey) scale is shown on the left axis, with nitric oxide (dark grey) on the right-hand axis. 138

Figure 33 Rate of oxygen use in relation to dissolved oxygen concentration in Clark electrode experiments. Each panel shows a bacterial isolate. Black points show experimental data from the Clark electrode, with red line showing a Michaelis–Menten model fitted to the data. V_{max} (μ M s^{-1}) and K_M (μ M) values derived from the Michaelis-Menten model are shown in the bottom right of each panel. 139

Figure 34 Rate of nitrate loss over time in Clark electrode experiments. Each panel shows a bacterial isolate. Black points show experimental data from the Clark electrode, 140

Figure 35 Rate of nitrite production and loss over time. Positive rate values indicate nitrite production with negative values showing rate of nitrite loss. 141

Figure 36 Outputs from agent-based denitrification model after (A) 1, (B) 50, (C) 100 and (D) 150 generations of bacterial growth. Nitrate concentration is elevated on the right-hand side of the landscape and oxygen is elevated at the top of the landscape. Red dots indicate oxygen metabolism, green shows nitrate usage and blue shows nitrite usage. In this model, oxygen respiration has a value of 8 points, nitrate respiration has a value of 5 points. Movement rate is set to 0.5 and costs 1 point and there are no maintenance costs in this scenario. 156

Table of Tables

Table 1 Genes for the denitrification process and their functions. Updated from Zumft (Zumft, 1997)	27
Table 2 Primers pairs with the highest coverage for amplification of genes in the bacterial denitrification pathway.....	39
Table 3 Vellend's four processes for community assembly, reproduced from Nemergut et al. (Vellend, 2010; Nemergut et al., 2013).....	43
Table 4 Primers and PCR conditions used to amplify 16S rRNA, nirK, nirS and nosZ gene amplicons.....	57
Table 5 Summary of a 16-year cropping systems management experiment at Nafferton Factorial Systems Comparison study (A) and soil physicochemical properties (B). All values are interaction means of four replicates with standard errors given in brackets. ¹ MT = minimum tillage, CT = conventional tillage, OF = organic fertilizer & SF = synthetic fertilizer.	60
Table 6 Crops and treatments applied to Harold Smiths field during the 2018-2020 growing seasons.....	80
Table 7 Primers used to produce synthetic spike-in DNA standards for gene copy number quantification using pUC18 plasmid as template DNA.	82
Table 8 Primers and thermal profiles of PCR reactions for amplicon sequencing.....	84
Table 9 Primers used for the construction of qPCR-standards	87
Table 10 Quantitative PCR primers, reaction mixtures and thermal profiles for the different target genes	88
Table 11 Summary of sampling location details within Harold Smiths Field (A) and soil physicochemical soil properties (B). All values are interaction means of three replicates with standard errors given in brackets. ¹ LY = low yield, HY = high yield, LC = low conductivity & HC = high conductivity.	91

Table 12 Nitrate and nitrite reduction profiles of selected bacterial isolates under oxic and anoxic conditions in three experiments: high-throughput screening, substrate utilisation and Clark electrode . + indicates loss of nitrate or nitrite. + O ₂ indicates oxic conditions and - O ₂ indicates anoxic.	137
Table 13 Nitrogen cycling gene profiles of selected bacterial isolates based on whole genome sequencing. Annotations were made using Prokka.....	144

Acknowledgements

The work detailed in this thesis was undertaken as part of an NPIF DTP project funded by the BBSRC in partnership with Precision Decisions Ltd. and was carried out at the University of York.

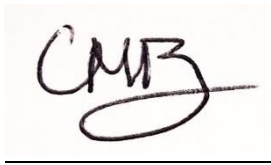
I am grateful to Professor James Moir, who guided me and supported me throughout this PhD. Special thanks to Professor Thorunn Helgason who helped me every time I needed advice. I am also very grateful to Professor Calvin Dytham for his supervision and support during the project. Thank you to my TAP panel, Dr Sylvia Toet and Dr Kelly Redeker, for their helpful and knowledgeable suggestions.

Thank you to my lab mates in L1 and J1, especially Hannah, Victor, Ed, Elena, Pan and Amy who always made time for coffee breaks.

Finally, I would like to thank my family and friends for their support and patience throughout my studies, particularly John, Mum, Dad, and Willow.

Author's Declaration

I declare that the work presented in this thesis is my own original work, unless explicitly stated otherwise. This work has not previously been presented for an award at this, or any other, University. All sources are acknowledged as references. My PhD has benefited from the contribution of others for the setup of long-term field experiments, sample collection and technical support, who are acknowledged below.



Claire Elizabeth Moulton-Brown

September 2022

Chapter 2: Experimental plots in Nafferton Factorial Systems Comparison (NFSC) study were designed and implemented by members of the University of Newcastle in 2001. Soil sampling was carried out by Tianer Feng, Shreiya Shivagni Kumar and Luxi Xu under the supervision of Dr Julia Cooper. The hypothesis generated and experiment conducted using this system was my own. All molecular work, data analysis and writing of the chapter was carried out independently.

A modified version of **Chapter 2** has been published as a peer-reviewed journal paper:

Claire E. Moulton-Brown, Tianer Feng, Shreiya Shivagni Kumar, Luxi Xu, Calvin Dytham, Thorunn Helgason, Julia M. Cooper, James W. B. Moir. Long-term fertilization and tillage regimes have limited effects on structuring bacterial and denitrifier communities in a sandy loam UK soil. *Environmental Microbiology* (2022) 24(1), 298–30. doi: 10.1111/1462-2920.15873 The

published version of the manuscript has been included as Appendix 1 (Moulton-Brown *et al.*, 2022).

The ion-chromatography work presented in **Chapter 3** to measure nitrate, nitrite and phosphate concentrations within the soil was performed under the guidance of Dr Matt Pickering for the 2018 samples and performed by Dr Pickering for the 2019-2020 soils due to Covid-19 access restrictions.

The denitrification model discussed in the **General Discussion** was produced in collaboration with Professor Calvin Dytham who wrote the code.

Chapter 1: General Introduction

1.1. Population growth and food security

The challenge of ending world hunger, a UN sustainable development goal (United Nations, 2022a), is becoming increasingly difficult with global food demand expected to increase by 30-62% from 2010 to 2050 (van Dijk *et al.*, 2021). This increase is largely driven by population increases, as the global population is predicted to reach over 9 billion by 2050 (United Nations, 2022b) and may reach up to 10.5 billion if high fertility rates occur (Figure 1). To compound this issue, global land area characterised as agricultural land has been decreasing from its peak in 2001 (FAO, 2022). With increased food demand coupled with conflict, climate change and growing competition for land, it is imperative that agricultural productivity increases to avoid food insecurity.

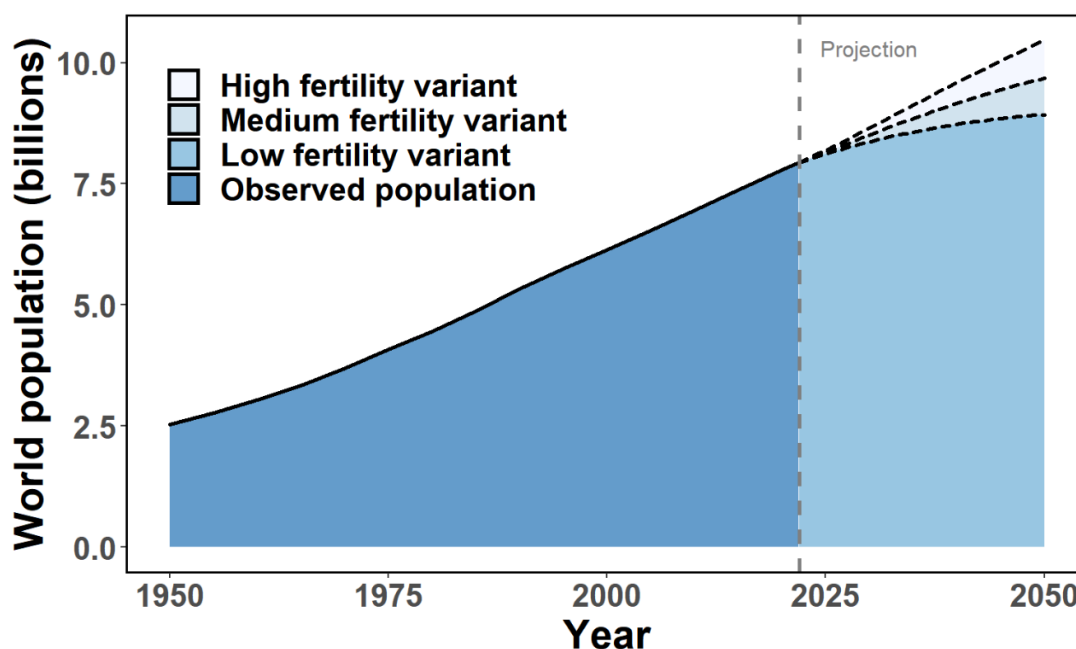


Figure 1 World population in billions from 1950 to 2050. Observed population from 1950-2022, and projected population from 2022 onwards. High, medium and low fertility variants for modelling population are given in white, pale blue and medium blue respectively. Data from United Nations, Department of Economic and Social Affairs, Population Division (2022) (United Nations, 2022b).

The intensification of food production through conventional agricultural practices, such as deep inversion tillage, high mineral fertilizer, herbicide and pesticide inputs during the ‘Green Revolution’, have seen historical rapid gains in crop yield (Tilman *et al.*, 2002). However, the gains achieved through agricultural intensification have been stagnating (Ray *et al.*, 2012, 2013) and even declining in certain cases such as that of cereal production within the UK (FAO, 2022). Further to this, world cereal production is predicted to decline by 1.3% from 2.81 billion tonnes in 2021/22 to 2.77 billion tonnes in 2022/23 (FAO, 2023).

The intensification of agriculture has created a number of problems relating to sustainability. Intensive agricultural practices reduce soil quality through the loss of earthworm numbers, soil organic matter (SOM), fertility and water holding capacity (Bai *et al.*, 2018; Muhammed *et al.*, 2018). These properties mean that the soil is more vulnerable to erosion and compaction, (Foucher *et al.*, 2014; Kopittke *et al.*, 2019) so more susceptible to crop failures, particularly as a result of extreme weather events such as flooding and drought, which are increasingly likely due to climate change (IPCC, 2022).

One option for improving crop productivity whilst reducing some of the harms associated with intensive agriculture is through precision agriculture. Precision agriculture is a farming management practice with the goal of optimising returns on inputs while preserving resources. It is based on principles of measuring and responding to intra- and inter-field variation in crop production (McBratney *et al.*, 2005). This site-specific crop management concept aims to reduce the variability in agricultural production in an economic and environmentally efficient manner. By targeting agricultural interventions to where they are most needed, crop yield can potentially be increased whilst nutrient and other crop inputs are reduced. In practice, precision agriculture has been found to improve yield stability as well as resilience to climate change (Yost *et al.*, 2017). Precision agriculture has the secondary benefit of reducing chemical losses into the environment, such as through leaching, which are more likely to occur when agrochemicals are added in excess (Wick *et al.*, 2012; Gao *et al.*, 2016). This improves overall ecosystem functioning.

1.2. The microbial nitrogen cycle

Nitrogen use efficiency is the focus of this thesis because nitrogen is the major limiting nutrient for agroecosystem productivity (Rütting *et al.*, 2018) and therefore a key factor in meeting the sustainable development goal of zero hunger (United Nations, 2022a). Current agronomic models are unable to explain the variation in efficiency with which nitrogen is assimilated into plants, based on soil physicochemical and environmental properties alone. It is thought that the inclusion of information on microbial nitrogen cycling potential will enable better modelling of nitrogen use efficiency and ultimately lead to more sustainable use of nitrogenous fertilizer. At present, nitrogen-rich fertilizer is typically added to soils uniformly to reduce this nutrient limitation, but this is costly and increases environmental problems including the leaching of nitrate into watercourses and the release of the ozone depleting greenhouse gas nitrous oxide by altering the dynamics of the nitrogen cycle. The nitrogen cycle is a complex biogeochemical cycle where nitrogen is physically or biologically transformed into different chemical forms as it circulates in atmospheric, terrestrial and marine ecosystems.

The microbial pathways within the nitrogen cycle can be split into six distinct processes (Figure 2). These include: (1) nitrogen fixation, (2) nitrate assimilation, (3) anaerobic ammonium oxidation (ANAMMOX), (4) nitrification, (5) dissimilatory nitrate reduction to ammonia (DNRA), and (6) denitrification. Additionally, there are abiotic processes which convert one form of nitrogen into another (Doane, 2017) and contribute to altered nitrogen reservoir sizes as well as atmospheric loading.

Nitrogen fixation **ANAMMOX** **DNRA**
Nitrate assimilation **Nitrification** **Denitrification**

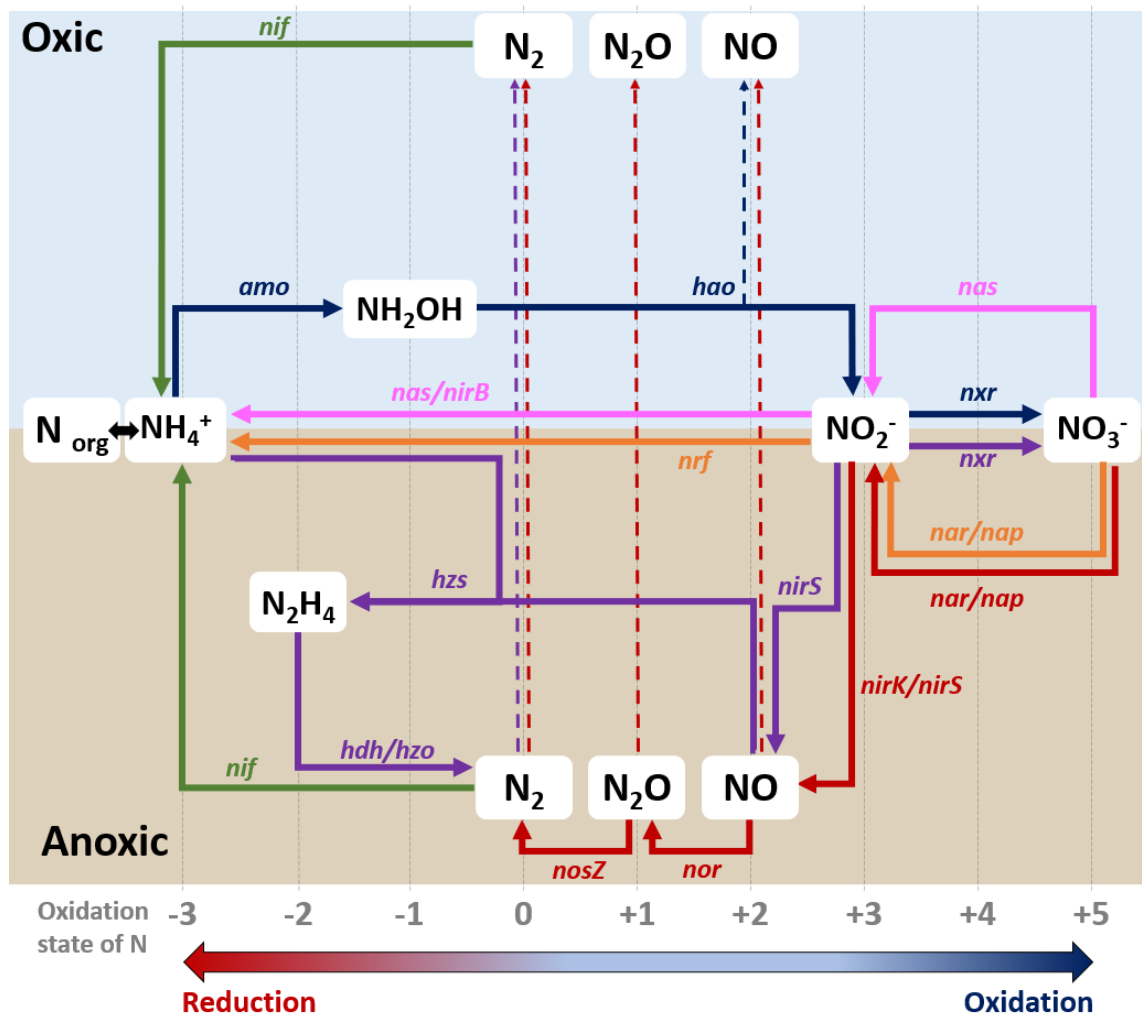


Figure 2 Microbial pathways in the nitrogen cycle. Background colours indicate processes occurring under oxic (blue) or anoxic conditions (brown). The compounds are positioned according to the oxidation state of N. Solid coloured lines show microbial pathways, and the genes encoding the respective enzymes that catalyse each step. Dotted lines indicate the contributing pathways to atmospheric loading of gaseous nitrogen compounds. Enzyme codes are as follows: amo, ammonia monooxygenase; hao, hydroxylamine oxidoreductase; hdh (also known as hzo), hydrazine dehydrogenase; hzs, hydrazine synthase, nar/nap, cytoplasmic and periplasmic dissimilatory nitrate reductases, respectively; nas, assimilatory nitrate reductase; nif, nitrogenase; nas/nirB, assimilatory nitrite reductase; nirS/nirK, cytochrome-cdI and copper-based dissimilatory nitrite reductases, respectively; nor, nitric oxide reductases; nosZ, nitrous oxide reductase; nrf, formate-dependent dissimilatory nitrite reductase; nrx, nitrite oxidoreductase. Figure reproduced from Hallin et al. 2018 (Hallin et al., 2018).

1.2.1. *Nitrogen fixation*

Nitrogen fixation is the biological process where diazotroph prokaryotes reduce dinitrogen gas to ammonia (green reactions, Figure 2). The majority of fixed nitrogen derives from biological nitrogen fixation; this dominates the input of the nitrogen budget (Zhang *et al.*, 2020). Because the triple bond of dinitrogen is very stable, diazotrophs exclusively use a large, structurally complex, iron-rich nitrogenase, with significant amounts of ATP and reductant to achieve the difficult conversion under ambient conditions (Young, 1992). The *nif* genes encode the nitrogenase complex used for nitrogen fixation. The structural subunit of dinitrogenase reductase and the two subunits of dinitrogenase are encoded by the *nifH*, *nifD*, and *nifK* genes, respectively (Hoffman *et al.*, 2014). Nitrogen fixation increases the amount of reactive nitrogen in the terrestrial ecosystem, so contributes positively to nitrogen use efficiency in agriculture.

1.2.2. *Nitrate assimilation*

Nitrate assimilation refers to the utilisation of nitrate as a nitrogen source to synthesise organic nitrogen (pink reactions, Figure 2). The bacterial assimilation of dissolved inorganic nitrogen as nitrate is common, but metabolically costly. The nitrate must first be reduced to nitrite and then ammonium with *nas* - the assimilatory nitrate reductase, and *nas/nirB* - assimilatory nitrite reductases - before the nitrogen can be assimilated into biomolecules (Luque-Almagro *et al.*, 2011). This reaction typically occurs under oxic conditions, with nitrate and nitrite reduction highly coupled such that nitrite does not accumulate during assimilation (Gates *et al.*, 2011).

During prokaryotic nitrate assimilation, microbes directly compete with plants for available nitrate, reducing the concentration of plant-available nitrogen. However, plants can also use ammonium as a nitrogen source. Ammonium is more energetically efficient in terms of assimilation compared with nitrate because ammonium can be directly incorporated into glutamate via an ammonium assimilation pathway (Krapp, 2015), whereas nitrate must first be reduced. However, nitrate is usually more available for uptake in many ecosystems, owing to its higher mobility. Nitrate can be incorporated into organic compounds in both root and leaf tissues whereas ammonium is only synthesized into amino acids in the root tissues near the site of uptake

to avoid toxic accumulation. In well aerated agricultural soils, nitrate is the principal inorganic nitrogen source (Hachiya and Sakakibara, 2016). Studies suggest that provision of both nitrate and ammonium stimulates plant growth beyond that observed with either nitrogen source alone (Miller and Cramer, 2005). Therefore, microbial nitrate assimilation may increase nitrogen use efficiency in agriculture under a specific set of conditions.

1.2.3. **ANAMMOX**

Anaerobic ammonium oxidation (ANAMMOX) is a route for loss of fixed nitrogen from the terrestrial ecosystem. ANAMMOX bacteria, all of which belong to the phylum Planctomycetes (Oshiki *et al.*, 2016), oxidise ammonium to dinitrogen gas using nitrite as the electron acceptor under anoxic conditions (purple reactions, Figure 2). ANAMMOX uses a combination of *nxr*, nitrite oxidoreductase, *nirS*, cytochrome-cd1 nitrite reductase, *hzs*, hydrazine synthase, and *hdh* (also known as *hzo*), hydrazine dehydrogenase. The hydrazine synthase and hydrazine dehydrogenase enzymes are thought to be unique to ANAMMOX, so the genes which encode them can be a useful signature for diagnosis and quantification (Oshiki *et al.*, 2016). Loss of fixed nitrogen through ANAMMOX is thought to account for 29% of global dinitrogen gas emissions (Zhang *et al.*, 2020), and therefore decreases nitrogen use efficiency in agriculture by removing sources of fixed nitrogen. ANAMMOX is connected to the loss of fixed nitrogen from marine ecosystems in particular.

1.2.4. **Nitrification**

Nitrification is the sequential oxidation of ammonium to nitrite and nitrate (blue reactions, Figure 2). Nitrification involves *amo*, ammonia monooxygenase; *hao*, hydroxylamine oxidoreductase and *nxr*, nitrite oxidoreductase. Interestingly, the nitrite oxidoreductase used in nitrification is homologous to the enzyme used in ANAMMOX. Like nitrate assimilation, nitrification results in the internal cycling of nitrogen between different fixed forms but does not directly affect integrated nitrogen reservoir sizes. Nitrification is generally carried out by chemoautotrophic nitrifying microbes that use ammonia or nitrite as a source of energy and as sources of biomass (Kuypers *et al.*, 2018). Nitrification generally occurs in two stages by separate bacteria: the

ammonia oxidising bacteria oxidise ammonia to nitrite with oxygen, then the nitrite oxidizing bacteria oxidise nitrite aerobically to nitrate (Vlaeminck *et al.*, 2011). More recently, bacteria have been found which catalyse both steps in the reaction, known as complete ammonia oxidation (comammox) (Van Kessel *et al.*, 2015). Although nitrification contributes to gain of plant-available nitrate in the soil it also leads to nitrate leaching and gaseous nitrous oxide production with up to 50% loss of nitrogen availability for the plant (Beeckman *et al.*, 2018) and therefore has a net loss in nitrogen use efficiency in agriculture.

1.2.5. **DNRA**

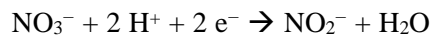
In dissimilatory nitrate reduction to ammonium (DNRA) nitrate is used as an electron acceptor for anaerobic respiration of organic matter by chemoheterotrophs. Nitrate is first reduced to nitrite and then to ammonium (orange reactions, Figure 2). DNRA uses *nar/nap*, cytoplasmic or periplasmic dissimilatory nitrate reductases respectively and *nrf*, formate-dependent dissimilatory nitrite reductase (Kraft *et al.*, 2011). Like many processes described above, DNRA recycles fixed N within an ecosystem, so should have limited impact on ecosystem productivity. Bacteria performing DNRA and those performing denitrification are in competition for nitrate; DNRA is favoured at higher organic carbon/nitrate ratios, while lower ratios favour denitrification (King and Nedwell, 1985). DNRA is also reported to be less sensitive to oxygen than denitrification (Yang *et al.*, 2015). By altering soil management practices to increase soil organic carbon or increase soil oxygenation, it may be possible to alter the amount of nitrogen cycled in the terrestrial ecosystem by DNRA compared to that lost through denitrification. This means that more nitrogen would be available for crops, when appropriately transformed.

1.2.6. **Denitrification**

Denitrification is the stepwise reduction of nitrate to nitrite, nitric oxide, nitrous oxide and dinitrogen gas (red reactions, Figure 2). Most denitrifying organisms are facultatively aerobic, heterotrophic bacteria that use nitrate as a terminal electron acceptor for respiration when oxygen concentration is low (Zumft, 1997). Aerobic denitrification, which follows the same pathway, has also been observed in a small number of bacteria. It is thought to be the result of differential

regulation of aerobic and anaerobic pathways, under oscillating oxygen conditions (Zumft, 1997; Ji *et al.*, 2015).

Denitrification starts with one of the nitrate reductases: *nap* or *nar* catalysing the reduction of nitrate to nitrite (Table 1; Equation 1) *nap* encodes the periplasmic dissimilatory enzyme in prokaryotes, with *nar* encoding the membrane-bound, cytoplasm-facing enzyme (González *et al.*, 2006). *Nar* is the enzyme typically associated with denitrification, and its cytoplasmic orientation is consistent with generation of proton motive force, allowing ATP synthesis during denitrification (Moreno-Vivián *et al.*, 1999). The mechanism for energy generation is less clear in *Nap*, with the proton motive force reportedly insufficient to synthesise ATP (Moreno-Vivián *et al.*, 1999). *Nap* is the version of the enzyme found in microbes capable of aerobic denitrification.



Equation 1

Table 1 Genes for the denitrification process and their functions. Updated from Zumft (Zumft, 1997)

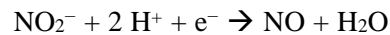
Category	Gene ^a	Molecular mass of product (kDa) ^b	Encoded gene product, function, or observation	Reference(s)
Regulation	<i>anr</i>	27.1	<i>P. aeruginosa</i> FNR-like global redox regulator for expression of denitrification genes	(Galimand <i>et al.</i> , 1991; Sawers, 1991)
	<i>dnr, fnrD</i>	24.5–26.2	<i>Pseudomonas</i> FNR-like regulators; affect the expression of <i>nirS</i> and <i>norCB</i>	(Arai <i>et al.</i> , 1995a)
	<i>fixK₂</i>		<i>B. japonicum</i> FNR-like regulator; affects anaerobic growth on nitrate	(Fischer, 1994)
	<i>fnrP</i>	28	<i>Paracoccus</i> FNR-like regulator; affects the expression of <i>narGH</i>	(Van Spanning <i>et al.</i> , 1997)
	<i>narL</i>	24.4	Activates the expression of the nitrate reductase <i>narGHJI</i> in two component system with <i>narX</i>	(Nohno <i>et al.</i> , 1989)
	<i>nirI</i>	73.1	Transcriptional activator of <i>NosZ</i> , <i>homologue of NosR</i>	(Saunders <i>et al.</i> , 1999)
	<i>nirR</i>	25.6	Global transcription regulator for anaerobic respiration	(Neubauer <i>et al.</i> , 1999)
	<i>nirY</i>	32.7	LysR-like regulator	(Glockner and Zumft, 1996)
	<i>nnr, nnrR, nnrS</i>	26	<i>Paracoccus</i> and <i>Rhodobacter</i> FNR-like regulators; affect <i>nirS</i> and <i>norCB</i> expression. Activates transcription of <i>nirK</i> and <i>nor</i> genes in <i>R. sphaeroides</i>	(Van Spanning <i>et al.</i> , 1995; Tosques <i>et al.</i> , 1996; Kwiatkowski <i>et al.</i> , 1997)
	<i>nosR</i>	81.9	Membrane-bound regulator required for transcription of <i>nosZ</i>	(Viebrock and Zumft, 1988)
Nitrate respiration	<i>narK</i>	46.1	Nitrate/nitrite transporter	(Noji <i>et al.</i> , 1989)
	<i>narG</i>	139	Large or a subunit of nitrate reductase; binds MGD	(Philippot <i>et al.</i> , 1997)
	<i>narH</i>	57.3	<i>b</i> subunit of respiratory nitrate reductase; binds Fe-S clusters	(Berks, Page, <i>et al.</i> , 1995)
	<i>narI</i>	26.1	Cytochrome <i>b</i> subunit of respiratory nitrate reductase	(Berks, Page, <i>et al.</i> , 1995)
	<i>narJ</i>	25	Nitrate reductase molybdenum cofactor assembly chaperone	(Berks, Page, <i>et al.</i> , 1995; Liu and DeMoss, 1997)
Periplasmic nitrate reduction	<i>napA</i>	92.6–93.3	Large subunit of periplasmic nitrate reductase; binds MGD and Fe-S cluster	(Siddiqui <i>et al.</i> , 1993; Berks, Richardson, <i>et al.</i> , 1995)
	<i>napB</i>	17.8–18.9	Small subunit of periplasmic nitrate reductase; a diheme cytochrome <i>c</i>	(Siddiqui <i>et al.</i> , 1993; Berks, Richardson, <i>et al.</i> , 1995)
	<i>napC</i>	27.2	Mediates electron flow from quinones to the NapAB complex	(Berks, Richardson, <i>et al.</i> , 1995)
	<i>napD</i>	12.1	Catalytic subunit of the periplasmic nitrate reductase complex NapAB. Receives electrons from NapB and catalyses the reduction of nitrate to nitrite	(Siddiqui <i>et al.</i> , 1993; Berks, Richardson, <i>et al.</i> , 1995; Grove <i>et al.</i> , 1996; Thomas <i>et al.</i> , 1999)
	<i>napE</i>	6.6	May be involved in mediating interactions between NapC and a quinol oxidase	(Berks, Richardson, <i>et al.</i> , 1995)
Nitrite respiration	<i>nirB</i>	30.4	Nitrite reductase (NADH) large subunit	(Peakman <i>et al.</i> , 1990)
	<i>nirC</i>	11.9	Catalyses nitrite uptake and nitrite export across the cytoplasmic membrane	(Klünemann <i>et al.</i> , 2020)
	<i>nirK, nirU</i>	36.9–41	Copper-containing nitrite reductase	(Glockner <i>et al.</i> , 1993; Nishiyama <i>et al.</i> , 1993; Chen <i>et al.</i> , 1996)
	<i>nirN</i>	55.5	Affects anaerobic growth and in vivo nitrite reduction; similarity to NirS. Involved in heme d1 biosynthesis	(Glockner and Zumft, 1996; Kawasaki <i>et al.</i> , 1997)
	<i>nirQ</i>	29.2	Gene product affects catalytic function of NirS and NorCB. Activator of nitrite and nitric oxide reductases.	(Jüngst and Zumft, 1992; Arai <i>et al.</i> , 1994)
	<i>nirS</i>	62	Cytochrome <i>cd₁</i> nitrite reductase	(de Boer <i>et al.</i> , 1994; Klünemann <i>et al.</i> , 2020)

Heme D ₁ biosynthesis	<i>nirD</i>	16.9	Gene product affects heme D ₁ biosynthesis or processing. Nitrite reductase (NADH) small subunit	(de Boer <i>et al.</i> , 1994; Palmedo <i>et al.</i> , 1995; Kawasaki <i>et al.</i> , 1997)
	<i>nirE</i>	29.6	Inactivation of uroporphyrinogen-III methyltransferase results in the loss of nitrite and nitric oxide reductase activities. Involved in heme D ₁ biosynthesis	(de Boer <i>et al.</i> , 1994)
	<i>nirF</i>	43.1	Required for the biosynthesis of heme d1 of nitrite reductase NirS	(Palmedo <i>et al.</i> , 1995)
	<i>nirG</i>	16.6	Siroheme decarboxylase. Involved in heme D ₁ biosynthesis	(Palmedo <i>et al.</i> , 1995)
	<i>nirH</i>	18.8	Siroheme decarboxylase subunit. Involved in heme D ₁ biosynthesis	(Bali <i>et al.</i> , 2011)
	<i>nirJ</i>	44.4	Pre-heme D ₁ synthase, yielding the heme D ₁ precursor dihydro-heme D ₁	(Brindley <i>et al.</i> , 2010)
	<i>nirL</i>	19.6	Siroheme decarboxylase subunit. Catalyses the decarboxylation of siroheme into didecarboxysiroheme	(Palmedo <i>et al.</i> , 1995; Kawasaki <i>et al.</i> , 1997)
	<i>nirM</i>	10.8	Cytochrome <i>c</i> ₅₅₁	(Jüngst <i>et al.</i> , 1991)
	<i>nirT</i>	22.8	Putative membrane-anchored tetraheme <i>c</i> -type cytochrome	(Jüngst <i>et al.</i> , 1991)
NO respiration	<i>norB</i>	52–53.1	Cytochrome <i>b</i> subunit of NO reductase. Catalytic subunit of the enzyme complex.	(Arai <i>et al.</i> , 1995b; De Boer <i>et al.</i> , 1996; Bartnikas <i>et al.</i> , 1997)
	<i>norC</i>	16–17	Cytochrome <i>c</i> subunit of NO reductase	(Arai <i>et al.</i> , 1995b; De Boer <i>et al.</i> , 1996; Bartnikas <i>et al.</i> , 1997)
	<i>norD</i>	69.7	Part of the operon <i>norEFCBQD</i> encoding nitric oxide reductase	(Arai <i>et al.</i> , 1995b; De Boer <i>et al.</i> , 1996; Bartnikas <i>et al.</i> , 1997)
	<i>norE</i>	17.7–19.5	Membrane protein; homologous with COX III	(Arai <i>et al.</i> , 1994; De Boer <i>et al.</i> , 1996; Glockner and Zumft, 1996)
	<i>norF</i>	8.2	Nitric oxide reductase activation protein	(De Boer <i>et al.</i> , 1996)
	<i>norQ</i>	30.5	Affects NirS and NorCB function; homolog of NirQ	(De Boer <i>et al.</i> , 1996; Bartnikas <i>et al.</i> , 1997)
N ₂ O respiration	<i>norZ</i>	84.5	Chromosomally encoded <i>R. eutropha</i> NO reductase	(Cramm <i>et al.</i> , 1997)
	<i>fhp</i>	44.8	Flavohemoprotein: nitric oxide dioxygenase (NOD)	(Cramm <i>et al.</i> , 1994)
	<i>nosA, oprC</i>	74.9–79.2	Channel-forming outer membrane protein; affects Cu-processing for NosZ	(Lee <i>et al.</i> , 1991)
	<i>nosD</i>	48.2	ABC transporter binding protein (NosDFY). Required for the assembly of the copper chromophores of N ₂ O reductase	(Zumft <i>et al.</i> , 1990; Hoeren <i>et al.</i> , 1993; Holloway <i>et al.</i> , 1996)
	<i>nosF</i>	33.8	ATP/GTP-binding protein involved in Cu insertion into NosZ	(Zumft <i>et al.</i> , 1990; Holloway <i>et al.</i> , 1996)
	<i>nosL</i>	20.4	Part of <i>nos</i> gene cluster; putative outer membrane lipoprotein	(Chan <i>et al.</i> , 1997)
	<i>nosX</i>	34.1	Affects nitrous oxide reduction in <i>S. meliloti</i>	(Chan <i>et al.</i> , 1997)
	<i>nosY</i>	29.4	Inner membrane protein involved in Cu processing for NosZ	(Zumft <i>et al.</i> , 1990; Holloway <i>et al.</i> , 1996)
	<i>nosZ</i>	70.8	Nitrous oxide reductase	(Viebrock and Zumft, 1988; Hoeren <i>et al.</i> , 1993; Holloway <i>et al.</i> , 1996)

^a Mnemonics for gene designations: *anr*, arginine nitrate regulation; *cyc*, cytochrome *c*; *dnr*, dissimilatory nitrate respiration regulator; *fhp*, flavohemeprotein; *fix*, nitrogen fixation; *fnr*, fumarate and nitrate respiration; *nap*, nitrate reductase, periplasmic; *nar*, nitrate respiration; *nir*, nitrite respiration; *nnr*, nitrite and nitric oxide reductase regulator; *nor*, nitric oxide respiration; *nos*, nitrous oxide respiration.

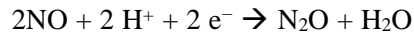
^b Molecular masses of unprocessed gene products without cofactors.

Following nitrate reduction to nitrite, the nitrite is reduced to nitric oxide (Equation 2) by one of two structurally unrelated enzymes. *nirS* encodes cytochrome-cd1 nitrite reductase whilst *nirK* encodes copper-based dissimilatory nitrite reductase containing both type-I and type-II copper sites (Table 1). These genes were thought to be mutually exclusive and functionally redundant, however a few organisms have been reported to possess both genes (Sánchez and Minamisawa, 2018). *nirS* is found to be more strongly associated with complete denitrifiers than *nirK*, as it more frequently co-occurs with *nosZ* nitrous oxide reductase (Graf *et al.*, 2014). *nirS*, along with *cNOR* and *nosZ*, have been reported to be associated with areas of higher soil moisture, nitrate and annual denitrification rates (Nadeau *et al.*, 2019). Nitrite reduction is often considered to be the commitment step of denitrification because the following step of nitric oxide reduction is so strongly coupled with it to avoid accumulation of nitric oxide which can be toxic to the cell.



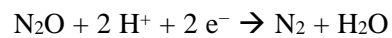
Equation 2

NOR, an iron-containing, membrane-integrated enzyme (Shiro, 2012), then reduces the nitric oxide to nitrous oxide (Equation 3; Table 1). This gene is very common due to the toxicity of nitric oxide as well as its ubiquitous nature as a signalling molecule. Nitric oxide reductases (NORs) occur in two main types: *qNOR*, which obtains its electrons from membrane-bound quinones (quinone-oxidizing), and *cNOR*, which gets its electrons from soluble electron carriers, mostly cytochromes (cytochrome-oxidizing) (Hendriks *et al.*, 2000). *cNOR* tends to co-occur with *nar*, which fits with *nar*, *nirS* and *cNOR* being more strongly associated with higher denitrification rate (Nadeau *et al.*, 2019). *qNOR* is more likely to cooccur with *nap*.



Equation 3

The nitrous oxide is then converted to dinitrogen (Equation 4). The nitrous oxide reductase encoded by *nosZ* is a complex Cu enzyme (Table 1). Although there is only one nitrous oxide reductase, it has two distinct clades which mainly differ in their signal peptides (Jones *et al.*, 2013), indicating differences in the translocation pathway of the nitrous oxide reductase across the membrane. *NosZI* is predominantly found in Proteobacteria, whereas *nosZII* is found in a broader range of organisms (Jones *et al.*, 2014). Bacteria with *nosZII* often do not contain complete denitrification pathways, with 51% of the organisms with clade II *nosZ* appearing to be nondenitrifying N₂O reducers (Graf *et al.*, 2014). And, with greater abundance of *nosZII* than *nosZI* (Jones *et al.*, 2013), this may lead to a nitrous oxide sink. Further study is needed to develop predictive models of nitrous oxide fluxes using this information to generate improved land management strategies.



Equation 4

Notably, denitrification is a modular process, with not all denitrifiers possessing the full suite of genes for the enzymes needed for complete denitrification (Graf *et al.*, 2014). Meta-transcriptomic data also demonstrates evidence of modular denitrification (Masuda *et al.*, 2019). Under standard conditions, the final transition from nitrous oxide to dinitrogen is the most favourable, followed by nitric oxide reduction, nitrate reduction and finally nitrite reduction (Milazzo *et al.*, 1978). However, the nitrate to nitrite transition is thought to be the most widespread amongst bacteria. It is unclear why this is. The likelihood is that complete denitrification is performed by a diverse

group of microorganisms, with each one carrying out one to two steps of the pathway (Roco *et al.*, 2017). The modularity of the pathway in natural environments implies that microbial community structure is important in determining the fate of fixed N in terrestrial soils.

1.3. Rational for studying denitrifying communities

The complexity of microbial pathways in the nitrogen cycle, which have multiple regulatory pathways and accessory genes (Table 1), makes understanding the influence of the microbial community on the nitrogen cycle a challenging prospect. This thesis focuses on the process of denitrification for two key reasons: environmental concerns from gases released during incomplete denitrification, and concerns relating to agricultural productivity linked to loss of fixed N from the terrestrial ecosystems.

Denitrification is primarily studied through an environmental lens as it accounts for 60% of global nitrous oxide emissions (Kroeze *et al.*, 1999), with 60-80% of the anthropogenic flux originating directly from agriculture (Coskun *et al.*, 2017). Nitrous oxide, which is produced through incomplete denitrification and nitrification (Figure 2), is a long-lived greenhouse gas that has a global warming potential 273 times greater than a molar equivalent of carbon dioxide over a 100-year period (IPCC, 2021). Nitrous oxide remains in the atmosphere for an estimated average of 116 ± 9 years (Prather *et al.*, 2015). It is currently the third most important long-lived greenhouse gas contributor to global warming, accounting for approximately 10% of global radiative forcing (IPCC, 2022).

In addition to global warming potential, nitrous oxide is the most important stratospheric ozone-depleting substance emitted in the 21st century (Ravishankara *et al.*, 2009; IPCC, 2021). Nitrous oxide emissions have steadily been rising, with a 33% increase since 1990 (IPCC, 2022).

Conversely, denitrification should also be considered in terms of reducing nitrous oxide emissions. The final stage of converting nitrous oxide to dinitrogen is the only biological sink for nitrous oxide (Seitzinger *et al.*, 2006; Conthe *et al.*, 2019). Research is now considering the role of non-denitrifying nitrous oxide-reducing bacteria as a sink for nitrous oxide in soil (Domeignoz-

Horta *et al.*, 2016; Hallin *et al.*, 2018). As the main sources of anthropogenic nitrous oxide emissions are agriculture, industry and biomass burning (Mosier, 1998; Galloway *et al.*, 2004; Reay *et al.*, 2012) and with a growing population with greater food and manufacturing demands (Figure 1), it is increasingly important to understand the drivers of denitrification in the agricultural setting.

For these reasons, denitrification is primarily studied from an environmental perspective, whereas this thesis focuses on the role of denitrification in agricultural productivity. Nitrogen is the main limiting factor for productivity in agroecosystems (Rütting *et al.*, 2018). Denitrification contributes to the loss of plant-available nitrogen from the terrestrial ecosystem through loss of gaseous products, unlike other nitrate reducing processes such as DNRA, which retain nitrogen in the terrestrial biosphere (Figure 2).

It is difficult to quantify the effects of denitrification on the UK nitrogen budget. The Lord *et al.* study of the nitrogen balance in UK agricultural land, argued that estimates of denitrification were too uncertain to include in their analysis (Lord *et al.*, 2002). This may be due to the heterogeneous nature of terrestrial ecosystems (Zhang *et al.*, 2020). Other studies consider only fluxes of reactive nitrogen as opposed to total nitrogen flux (Galloway *et al.*, 2004; Parfitt *et al.*, 2008; Sutton, 2011; Ti *et al.*, 2012), and therefore do not include denitrification or industrial emissions of dinitrogen.

Where estimates of terrestrial denitrification losses have been published, all have reported an increase from preindustrial to contemporary estimates. Global preindustrial denitrification losses are reported to range from approximately 27×10^9 kg N yr⁻¹ (Houlton and Bai, 2009; Schlesinger and Bernhardt, 2013) to approximately 100×10^9 kg N yr⁻¹ (Galloway *et al.*, 2004; Gruber and Galloway, 2008), whereas modern soils are thought to lose between 44×10^9 to 160×10^9 kg N yr⁻¹ (Galloway *et al.*, 2004; Gruber and Galloway, 2008; Fowler *et al.*, 2013, 2015; Schlesinger and Bernhardt, 2013; Scheer *et al.*, 2020). Minimising these losses from agroecosystems could play an important role in increasing nitrogen use efficiency and reaching the sustainable development goal of zero hunger.

1.4. Measuring denitrification

Denitrification is difficult to measure. Available methods are problematic for a number of reasons including the alteration of substrate concentrations, physical disturbance of the process, lack of sensitivity, or are prohibitively costly in time and expenditure. Fundamentally, it is difficult to quantify the dinitrogen produced as the end-product of denitrification, due to the high background concentration in the atmosphere. Quantification of denitrification is also hindered by high spatial and temporal variation; particularly in terrestrial environments, where denitrification occurs at ecosystem, landscape, regional, and global scales and no single method is capable of capturing the full picture (Groffman *et al.*, 2006). Some of the methodological approaches for quantifying denitrification in terrestrial systems include: (1) acetylene inhibition, (2) ¹⁵N tracers, (3) direct N₂ quantification, (4) mass balance approaches, (5) molecular approaches and (6) direct measurement of denitrification intermediates.

1.4.1. Acetylene inhibition

The most common method used to estimate denitrification rate in terrestrial systems is through acetylene inhibition (Yoshinari and Knowles, 1976; Tiedje *et al.*, 1989; Groffman *et al.*, 2006). This sensitive method involves injecting acetylene (C₂H₂) to inhibit the final step of denitrification: N₂O reduction to N₂ by nitrous oxide reductase. This causes the accumulation of nitrous oxide, which reflects the denitrification rate and can be quantified using gas chromatography. The nitrous oxide is relatively easy to measure due to low atmospheric concentrations as well as the availability of sensitive detectors such as the electron capture detector (ECD) used for gas chromatography. Acetylene inhibition is sometimes used with static core methods, where acetylene is injected or added to the headspace of a sealed soil core and nitrous oxide accumulation is measured over incubation times ranging from 1 - 24 hours (Groffman *et al.*, 2006). This method is time and cost effective and allows for large numbers of samples to be tested at the same time.

On the other hand, the acetylene inhibition technique is limited by its propensity to underestimate denitrification rates in low nitrate environments. This is because acetylene also inhibits nitrate

production via nitrification (specifically ammonia oxygen encoded by *amo*, Figure 2), which is closely coupled to denitrification (Arth *et al.*, 1998). Additionally, nitrogen fixation is inhibited by acetylene, as the nitrogenase responsible for nitrogen fixation also reduces acetylene (C₂H₂) to ethylene (C₂H₄) (Hardy *et al.*, 1968), creating a confounding factor. Other problems that occur when using acetylene inhibition are that the presence of sulphide can remove the inhibition (Sørensen, 1978), that microbes have been reported to degrade acetylene (Brzezińska *et al.*, 2011), and contamination of acetylene with other gases that can affect denitrification (Gross and Bremner, 1992). More recently, it has been found that denitrification-related parameters are also linked to the underestimation of denitrification rate using the acetylene inhibition method with increases in soil nitrate and water content linked to the increased underestimation of denitrification (Yuan *et al.*, 2019). Acetylene-catalysed nitric oxide oxidation was found to account for most of this bias, with incomplete acetylene inhibition of nitrous oxide reductase accounting for the rest. From a natural ecosystem perspective, the biggest drawback of this technique is the reliance on disturbed samples i.e. extracted cores rather than *in-situ* methods. Loss of environmental cues that regulate denitrification poses the risk of measuring artificially-induced denitrification rates that do not reflect what would occur in the field (Groffman *et al.*, 2006).

Despite these challenges, there have been developments in the acetylene inhibition technique. Amendments of nitrate and carbon as well as protein synthesis inhibitors, to prevent further enzyme synthesis and ensure the measured rates reflect activity due to pre-existing enzymes only, have been added to improve quantification of potential denitrification rate (Joye and Paerl, 1994). Additionally, whilst the acetylene inhibition method is typically used on fresh soil, research has been ongoing to enable denitrification rate measurements of air dried soils after rewetting (Kaden *et al.*, 2020). These developments have led to the acetylene inhibition technique becoming widely adopted.

1.4.2. *¹⁵N tracers*

In this method ¹⁵N labelled nitrate is added directly to soil and the ¹⁵N labelled dinitrogen produced is measured to quantify denitrification (Hauck and Melsted, 1956). Although this method is considered highly accurate, its adoption has been limited by the laborious procedures and expensive instrumentation required. Two other drawbacks associated with this method are the need to know the ratio of ¹⁵N to ¹⁴N, something that has been quickly resolved (Hauck *et al.*, 1958), and that the ¹⁵N enrichment itself can increase denitrification rate by providing more available nitrogen, which is rarely an issue in well-fertilized agricultural soils but becomes problematic in nitrate limited areas. Additionally, previous iterations of this method could only measure the labelled nitrogen that was transformed through denitrification, however novel methods can distinguish between denitrification, ANAMMOX and DNRA using different isotopes (Sheng *et al.*, 2021). Whilst ¹⁵N tracer methods are thought to be accurate and provide estimates that integrate well over larger spatial scales (Bai *et al.*, 2012), the heterogeneity of the soil and its microbial communities over field scales means that this method would be difficult to implement to understand the effects of soil microbial communities on denitrification.

1.4.3. *Direct N₂ quantification*

Directly quantifying dinitrogen emissions from soil is highly problematic due to the high background atmospheric concentration (79%). Soils (either mixed or intact cores) therefore need to be incubated with reduced atmospheric dinitrogen. N₂ stored in pores or aggregates must be removed and the entire system must remain gas-tight and built from materials that do not release N₂ (Butterbach-Bahl *et al.*, 2002). Direct N₂ quantification of denitrification has advantages of being non-destructive, label free, inhibition free and sensitive (a detection limit of <1 kg N₂-N·ha⁻¹·yr⁻¹ (Groffman *et al.*, 2006)). However, the design, construction and operation of these gas flow incubation systems can be complex, expensive and difficult.

1.4.4. *Mass balance approaches*

Mass balance approaches apply the concept of mass conservation to the analysis of a physical system. To study denitrification with a mass balance approach all nitrogen fluxes and changes in

nitrogen storage must be measured or estimated. Assumptions are often made that the system is in a steady state with only inputs and outputs quantified (Groffman *et al.*, 2006). Inputs include biological nitrogen fixation, atmospheric deposition and fertilizer application, and outputs include biomass harvest, general exports and runoff. The difference between inputs and outputs is attributed to denitrification. One of the main limitations of mass balance approaches are the assumptions used. Many mass balance based denitrification studies ignore changes in nitrogen storage because they are assumed to be very small, whereas the storage pool size can be extremely large, and so can have a big impact on mass balance calculations (David *et al.*, 2001). Mass balance can provide some insight into the potential importance of denitrification but is mainly useful for constraining estimates of other methods used because it relies so heavily on the ability to quantify all nitrogen fluxes accurately, and to accurately determine changes in nitrogen storage pools.

1.4.5. *Molecular methods*

Denitrification rates are affected by complex interactions of physical, chemical and hydrological environmental factors, but abiotic factors alone cannot reliably be used to predict denitrification rates in terrestrial ecosystems. In fact, the response of denitrifying organisms to these factors is highly dependent on characteristics of the microbial community. Therefore, the overall goal of this thesis is to understand how the composition and physiology of the denitrifying microbial community affects and is affected by nitrogen transformations in the environment and how this links to increasing nitrogen use efficiency in agriculture.

Molecular methods are proving increasingly popular to study denitrification. These include, DNA probes (Kloos *et al.*, 1998; Hou *et al.*, 2018), terminally labelled restriction-length fragment polymorphism (T-RFLP) (Cui *et al.*, 2016), denaturing gradient gel electrophoresis (DGGE) (Throbäck *et al.*, 2004), PCR (Ma *et al.*, 2019), quantitative PCR (qPCR) (Henry *et al.*, 2004, 2006) and an increasing use of multi-omics technologies (Frostegård *et al.*, 2022). PCR and qPCR are widely used in the experiments described in this thesis to better understand the diversity, distribution and abundance of the soil microbial community. PCR-based techniques are often used

because of their speed and accuracy in amplifying a specific segment of DNA. This can be used for detection, sequenced to understand the diversity or amplified using known standards for quantification of gene numbers.

To understand which organisms (including denitrifiers) are present in the soil, the 16S ribosomal RNA (rRNA) gene is often used for phylogenetic identification (Weisburg *et al.*, 1991). This gene is widely used in environmental microbiology because it has highly conserved regions between bacteria and archaea (Coenye and Vandamme, 2003), which facilitates the design of universal PCR primers which bind to the conserved regions and amplify the hypervariable regions for sequencing that can provide species-specific signature sequences useful for identification. Curated databases such as Ribosomal Database Project (Cole *et al.*, 2014), SILVA (McLaren and Callahan, 2021) and GreenGenes (DeSantis *et al.*, 2006; McDonald *et al.*, 2012) that include 16S rRNA sequences are often used for taxonomic identification. Notably, these databases can yield different results (Balvočiūtė and Huson, 2017), so care should be taken during the planning process to select the most appropriate database.

As denitrification is catalysed by an extremely diverse group of organisms (Zumft, 1997), most research focusses on the functional genes within the pathway (Figure 2, 1.2.6.), not just the organisms themselves. PCR primers have been developed for the denitrification genes (Table 2) and have been used to study the distribution, abundance and diversity of denitrifying bacteria in many studies. Some studies focus on the nitrate reductases *napA* and *narG* (Flanagan *et al.*, 1999; Gregory *et al.*, 2000; Mergel *et al.*, 2001; Philippot *et al.*, 2002; Delorme *et al.*, 2003; López-Gutiérrez *et al.*, 2004; Bru *et al.*, 2007; Chen *et al.*, 2012). Others focus on nitric oxide reductases *qNOR* and *cNOR* (Braker and Tiedje, 2003; Casciotti and Ward, 2005; Dandie *et al.*, 2007; Verbaendert *et al.*, 2014) or nitrous oxide reductase *nosZ* (Chèneby *et al.*, 1998; Scala and Kerkhof, 1998b; Delorme *et al.*, 2003; Throbäck *et al.*, 2004; Sanford *et al.*, 2012; Jones *et al.*, 2014).

The majority of molecular-based studies of denitrification in natural environments focus on the nitrite reductases *nirK* and *nirS* (Braker *et al.*, 1998; Michotey *et al.*, 2000; Casciotti and Ward, 2001; Henry *et al.*, 2004; Chen *et al.*, 2010), because they represent the first committed step that leads to a gaseous intermediate. Like these studies, much of this thesis will focus on bacterial nitrite reductase genes to study the distribution, abundance, diversity of denitrifiers, with additional insight provided through the study of the nitrous oxide reductase gene which determines much of the environmental impact of denitrification in terms of nitrous oxide emissions. Targeting these genes provides a profile of the denitrification gene population that reflects the diversity and abundance of each of the target sequences and can be used to detect changes in community dynamics related to environmental properties.

Denitrification gene primers are based on conserved regions within the genes and may only have limited population coverage (Table 2). Additionally, different sequencing technologies lend themselves to different sized amplicons. Therefore, selecting primer pairs can become a compromise between maximum coverage of the broadest range of organisms and achieving the amplicon size that will result in the highest quality sequencing. For example, the Illumina MiSeq platform can sequence reads of up to 300bp, which would give a theoretical maximum amplicon length of 600bp. In reality, the maximum amplicon length is shorter than this due to length of adapters, spacers, barcodes and significant quality loss after approximately 200bp. It is also important to achieve significant overlap in order merge paired-end reads, so amplicon sizes must be below 500bp. On the other hand, optimal qPCR efficiency requires amplicon sizes of under 200bp (Van Holm *et al.*, 2021).

Table 2 Primers pairs with the highest coverage for amplification of genes in the bacterial denitrification pathway

Target gene	Primer	Sequence	Amplicon size (bp)	^a % Coverage	Reference
narG	narG1960f	TAYGTSGGSCARGAR AA	650	99.6	(Philippot <i>et al.</i> , 2002)
	narG2650r	TTYTCRTACCABGTB GC			
napA clade I-III	V16F	GCNCCNTGYMGNTTY TGYGG	1002	95.8	(Flanagan <i>et al.</i> , 1999)
	V17R	RTGYTGRTTRAANCC CATNGTCCA			
nirK clade I	nirKC1F	ATGGCGCCATCATGG TNYTNCC	487	89.3	(Wei <i>et al.</i> , 2015)
	nirKC1R	TCGAAGGCCTCGATN ARRTTRTG			
nirK clade II	nirKC2F	TGCACATCGCCAACG GNATGTWYGG	458	76.7	(Wei <i>et al.</i> , 2015)
	nirKC2R	GGCGCGGAAGATGSH RTGRTCNAAC			
nirS clade I	cd8F	GGNTAYGCNGTNCAY AT	369	91.5	(Michotey <i>et al.</i> , 2000)
	cd2R	CCNGTYTCYTTNACR TTNAC			
nirS clade II	nirSC2F	TGGAGAACGCCGGNC ARGTNTGG	386	25	(Wei <i>et al.</i> , 2015)
	nirSC2R	GATGATGTCCACGGC NACRTANGG			
nirS clade III	nirSC3F	TTCGCCCTGAARGAY GGNGG	374	50	(Wei <i>et al.</i> , 2015)
	nirSC3R	AGGTGCCACGAANA RNCCNCC			
qnorB	qnorB2F	GGNCAYCARGGNTAY GA	262	45.8	(Braker and Tiedje, 2003)
	qnorB5R	ACCCANAGRTGNACN ACCCACCA			
cnorB	cnorB2F	GACAAGNNNTACTGG TGGT	454	81.9	(Braker and Tiedje, 2003)
	cnorB7R	TGNCCRTGNGCNGCN GT			
nosZ clade I	nosZf	AACGACAAGDYCAA	1433	93.6	(Delorme <i>et al.</i> , 2003)
	nosZr	AKSGCRTGGCAGAA			
nosZ clade II	nosz-II-F	CTIGGICCIYTKCAYAC	698	86.1	(Jones <i>et al.</i> , 2013)
	nosZ-II-R	GCIGARCARAAITCBG TRC			

^a Percentage coverage of de-duplicated isolate genomes from Functional gene Repository (Fish *et al.*, 2013) or National Center for Biotechnology Information (NCBI) allowing a maximum of two base pair mismatches as reported by Ma *et al.* (Ma *et al.*, 2019)

There are a number of limitations when using molecular methods to study denitrifying bacteria. When using DNA, not all of it will represent viable soil organisms (Blagodatskaya and Kuzyakov, 2013) and it is unclear what the impact of this is in terms of assessing community function. This addition of dead/dormant microbial biomass may explain why molecular studies have revealed a much higher diversity of denitrification genes in the environment than expected which are often divergent from the genes of cultured denitrifiers (Scala and Kerkhof, 1998b; Flanagan *et al.*, 1999; Braker *et al.*, 2000; Gregory *et al.*, 2000).

Additionally, DNA-based denitrification studies show only genetic potential for denitrification, rather than denitrification itself. However, if RNA is used instead to demonstrate which genes are actively being transcribed it is strongly affected by environmental conditions and can be quickly degraded (Blazewicz *et al.*, 2013), making results much harder to replicate. This thesis focuses on DNA rather than RNA, as it shows a more stable pool of potentially active microbes and has been reported to better reflect the soil enzyme activity than RNA-based methods (Zhu *et al.*, 2020).

Another notable limitation of PCR based methods is the large potential for bias. Primer sequences have limited coverage (Table 2), and not all sequences will be equally amplified due to small mismatches with primers. Additional errors will occur because of the polymerase used, with lower fidelity enzymes such as Taq having an error rate of approximately 1.8×10^{-4} errors/base/doubling (Potapov and Ong, 2017). High fidelity polymerases have approximately 10-fold lower error rates (McInerney *et al.*, 2014), but this is still significant. Additionally errors during PCR are difficult to quantify as an incorrectly amplified sequence may still be sequenced with complete accuracy and have an associated high quality score (Schirmer *et al.*, 2015). Molecular methods such as metagenomics can overcome some of this bias and are becoming 'best-practice' for microbiome analysis (Knight *et al.*, 2018), despite their prohibitive cost. Full integration of metagenomics, metatranscriptomics, proteomics and metabolomics, combined with dynamic culture dependent methods may be seen as aspirational for analysing complex microbial communities, but may soon

become the gold standard (Knight *et al.*, 2018). What remains clear, is the need for robust experimental design and reproducible research.

1.4.6. *Direct measurement of denitrification intermediates*

One final method to measure denitrification is through measurement of denitrification intermediates. Nitrate and nitrite concentrations can be measured using a spectrophotometric methods (Miranda *et al.*, 2001; García-Robledo *et al.*, 2014). Electrochemical nitric oxide sensors can be used to determine nitric oxide concentrations (Privett *et al.*, 2010; Brown and Schoenfisch, 2019). And nitrous oxide can be measured using gas chromatography coupled to an electron capture detector (Rapson and Dacres, 2014). As discussed previously, the final product of denitrification, dinitrogen, proves extremely difficult to measure, with relatively small fluctuations against a high atmospheric background. This can be overcome using a low N₂ atmosphere setup as described in section 1.4.3. Measuring denitrification intermediates faces a number of limitations such as the need to use destructive sampling for the spectrophotometric components, and the absence of *in situ* measurements. However, the ability to track production and utilization of denitrification intermediates in a cost-effective manner is highly useful for providing a clear picture of nitrogen cycling dynamics during denitrification and is utilised in this thesis.

1.5. **Soil bacterial biodiversity**

Much of the nitrogen cycle is microbially mediated (Figure 2), but despite this, little is currently known about how microbial community structure affects denitrification rate. Assessing the abundance, diversity and function of the soil microbial community presents a significant technical challenge. The soil microbiome is extremely diverse and may include up to one quarter of the diversity found on earth (Wagg *et al.*, 2019), with thousands of different taxa in a single gram of soil (Fierer, 2017).

1.5.1. Soil heterogeneity

Assessing this diversity is further complicated by the heterogeneous structure of soil. With limited pore connectivity, soil maintains high microbial biodiversity by creating spatially distinct environments with differing abiotic characteristics (Carson *et al.*, 2010). Soils are highly variable in terms of pH, organic carbon concentration, salinity, texture, oxygen concentration and available nitrogen concentration (Fierer, 2017). Even in a single soil profile, there is considerable variation; linked to the rhizosphere, preferential water flow paths (such as cracks in the soil), animal burrows, intra-aggregate and inter-aggregate environments (Sexstone *et al.*, 1985). These factors affect the variables listed above and subsequently the microbial community and its functioning.

1.5.2. Microbial biodiversity

Most studies quantify and compare microbial biodiversity using alpha diversity – the diversity within an environment (Shannon, 1948; Pielou, 1966; Thukral, 2017) – or beta diversity – the turnover in diversity between environments (Roger, Bray and Curtis, 1957; Chang *et al.*, 2011; Mori *et al.*, 2018). In other words, a community with high alpha diversity has high biodiversity within a habitat at a defined spatial scale, while two distinct communities with high beta diversity have few species in common. Importantly, to understand microbial biodiversity, particular thought should be given to biogeography and the distribution of microorganisms across space and time.

1.5.3. Biogeography and community assembly

Two of the fundamental biogeographic patterns that we would expect to see in the soil microbiome are the positive power law between species richness and area, known as taxa-area relationships (F. W. Preston, 1980; Lawton, 1999; Horner-Devine *et al.*, 2004) and the distance-decay relationship (Nekola and White, 1999), the decay of community similarity with geographic distance. Microbial biogeography has predominantly been studied through a taxonomic lens. However, functional properties of microbial communities, such as denitrification potential, are often decoupled from their taxonomic compositions, emphasising the need to study the biogeography of microbial functional genes directly.

To further comprehend the structure of soil denitrifying bacterial communities, it is important to understand the relative importance of the processes of community assembly. Vellend's four processes of community assembly (Table 3) operate in combination, with two processes that act to bring new organisms into communities (diversification/ speciation and dispersal) and two processes that affect changes in the relative abundance of organisms over time (drift and selection) (Vellend, 2010; Nemergut *et al.*, 2013). The interactions and relative input of these factors will have large impacts on community assembly.

Table 3 Vellend's four processes for community assembly, reproduced from Nemergut et al. (Vellend, 2010; Nemergut et al., 2013).

Process	Description
Diversification	Generation of new genetic variation
Dispersal	Movement of organisms through space
Selection	Changes in community structure caused by deterministic fitness differences between taxa
Drift	Stochastic changes in the relative abundances of taxa

Our current understanding of how assembly processes might ultimately influence ecosystem function remains limited. Similarly to the overall bacterial community, functional guilds such as denitrifiers form communities using the same processes, with stochastic 'drift' processes reportedly dominating denitrifying community structure (Li *et al.*, 2022). Alternatively, other studies report selection as the primary driver of denitrifier community assembly (Kou *et al.*, 2021; Liu and Sheng, 2021), although some note community assembly differences in different environments (Jones and Hallin, 2010).

1.5.4. Land management interventions

One of the biggest questions in microbial ecology from an agricultural perspective is 'what will the impact be of land management decisions?' It is important to understand the role of physical and chemical interventions in shaping the microbial community and their functioning. As

previously discussed, nitrogen deficiency is the major nutrient limitation for agricultural productivity, this results in widespread addition of nitrogen rich fertilizers. This is costly, both financially and environmentally (Good and Beatty, 2011). The effects of nitrogen fertilizer on denitrification within agricultural soils has been extensively studied. A significant increase in denitrification has been linked to the application of synthetic nitrogen fertilizers (Ryden, 1983; Kim *et al.*, 2013; Gerber *et al.*, 2016; Krauss, Krause, *et al.*, 2017; Liu *et al.*, 2017). On average, this increase was found to be 174% (Wang *et al.*, 2017). Other studies have found that nitrogen input can only be used as a reliable predictor for denitrification, but only with the addition of soil water content measurements (Tenuta and Beauchamp, 2003). Additionally, nitrogen deposition can cause soil acidification and associated major losses in biodiversity once nitrogen inputs exceed a critical load (Galloway *et al.*, 2003; Tian and Niu, 2015). This shows that the effects of chemical treatments may interact with soil physicochemical properties, and understanding these interactive effects are important for the development of accurate predictive denitrification models.

Another commonly used land management technique for agricultural soil is tillage – the mechanical agitation of soil. Reduced tillage treatments are often considered to be more sustainable than conventional tillage because of links to reduced soil erosion, improved water conservation and decreased nitrous oxide emissions when applied long term (Six *et al.*, 2004; Rochette, 2008; Derpsch *et al.*, 2010; van Kessel *et al.*, 2013; Powlson *et al.*, 2014). Alternatively, other studies have found that reduced tillage is actually associated with increased nitrous oxide and carbon dioxide emissions (Krauss, Ruser, *et al.*, 2017). Reduced tillage is known to be associated with stratification of soil organic matter (Luo *et al.*, 2010), which alters aeration and organic carbon availability, affecting microbial community structure and function (Wallenstein *et al.*, 2006; Baudoin *et al.*, 2009; Melero *et al.*, 2011; Kuntz *et al.*, 2013; Tellez-Rio *et al.*, 2014).

Few studies have investigated the combined effect of fertilizer and tillage on nitrous oxide emissions, yet Krauss *et al.* (2017) found that the highest N₂O emissions were found in the soil treated with inorganic fertilizer (calcium ammonium nitrate) and minimum tillage treatment.

More studies are now needed to confirm interactions between land-management techniques and the effects on denitrifying communities and individuals.

1.5.5. *Predicting function from genes*

To understand denitrification in the context of the soil microbial community, many studies utilise RNA and DNA based methods (section 1.4.5.). However, it remains important to link genotype and phenotype, given that it remains unclear whether genomic measures of functionality in soil are useful predictors of ecosystem process rates and stability (Eisenhauer *et al.*, 2017).

Some studies have found clear links between genomic potential and denitrification rate. Several studies report that *nosZ* abundance is significantly correlated to potential denitrification rate (PDR) (Hallin *et al.*, 2009; Philippot *et al.*, 2009; Petersen *et al.*, 2012). Other studies have linked *nirK/S* abundances to potential denitrification rate (PDR) (Chroňáková *et al.*, 2009; Dong *et al.*, 2009; Čuhel *et al.*, 2010). Alternatively, other studies report that abundances of denitrification genes are not correlated to PDR (Dandie *et al.*, 2008; Miller *et al.*, 2008; Baudoin *et al.*, 2009; Djigal *et al.*, 2010; Song *et al.*, 2010; Attard *et al.*, 2011). This lack of consensus suggests that further integration of molecular methods and physiological measurements may be needed to better understand the link between genomic potential and denitrification rate.

1.5.6. *Cultivating denitrifiers*

To understand the contribution of individual taxa to denitrification rate, soil microbes must be cultured in the lab. However, there are considerable challenges when culturing diverse soil microbes under lab conditions (Staley and Konopka, 1985; Amann *et al.*, 1995; Torsvik and Øvreås, 2002). As a result, many groups of denitrifying bacteria currently have no cultivable representatives available in biobanks (Zumft, 1997; Lycus *et al.*, 2017), with studies revealing much higher diversity of denitrification genes in the environment than expected based on the genes of cultured denitrifiers (Scala and Kerkhof, 1998a; Flanagan *et al.*, 1999; Braker *et al.*, 2000; Gregory *et al.*, 2000). This suggests that most organisms in the environment are not similar to the organisms used in laboratory experiments designed to test our ideas of how denitrifying

communities respond to environmental factors. It is likely that some of the most abundant and/or significant denitrification guilds have not yet been extensively studied.

Several techniques have been developed to increase the cultivability of wider range of soil microbes, to solve the ‘great plate count anomaly’, a phrase coined by Staley and Konopka (1985), to describe the gap between what is in the soil (as measured by culture-independent measures such as 16S rRNA sequencing) and what can be cultured in the lab using traditional microbiology methods. These methods include *in situ* cultivation (Nichols *et al.*, 2010; Alessi *et al.*, 2018), targeted phenotypic culturing (Browne *et al.*, 2016), diffusion chambers and bioreactors (Kaeberlein *et al.*, 2002; Chaudhary *et al.*, 2019), encapsulation (Zengler *et al.*, 2002) high dilution (Rappé *et al.*, 2002) and microfluidics (Alekklett *et al.*, 2018) approaches. By developing these techniques that enable the cultivable soil community to better reflect the total soil community, a greater understanding of the links between microbial community and denitrification dynamics can be established.

1.6. Thesis aims and objectives

The central question presented in this thesis is ‘How does the microbial community influence nitrogen loss through denitrification in agriculture?’. This was approached through the lens of the microbial community dynamics involved in denitrification in arable soils. Particular attention was paid to the effects of long-term land management techniques (tillage and fertilizer type), spatiotemporal variation and the isolation and cultivation of denitrifiers that are not considered model organisms.

Denitrifier diversity and community composition are important for their potential to improve nitrogen availability for crops whilst reducing greenhouse gas emissions. It is estimated that global food demand is expected to increase by 35% to 56% between 2010 and 2050 (van Dijk *et al.*, 2021). By making changes to reduce excess denitrification and divert nitrogen into crops or other microbial processes which retain the nitrogen in the terrestrial ecosystem (Figure 2), there is potential to improve crop yield through improving nitrogen use efficiency and bridge the gap

between the food we produce now and the food we need for the growing global population. It is important that we look beyond the presence of denitrifiers within agricultural systems to the individual species and communities that assemble in response to different land management strategies, as the modular nature of denitrification means that some bacteria will be sources of nitrogen molecules, with others as potential sinks.

Achieving a better understanding of the denitrification capabilities of soil microbial functional guilds under various management practices including minimum tillage and organic fertilizer will allow us to make informed agricultural decisions to maximise the benefits of agroecosystems in a less polluting way. Agroecosystems can be shifted to deliver maximum yields while minimising their environmental impact and ensuring the resilience of yields to future challenges.

The specific objectives of this thesis are listed below according to the chapter they are addressed in.

1.6.1. Chapter 2 aims:

- Understand the impact of long-term fertilizer regime (synthetic versus organic) and tillage (minimum versus conventional) on denitrifying functional guilds in arable soils.
- Investigate the importance of inherent environmental variation including rainfall, temperature, water filled pore space, soil moisture, soil organic carbon, total nitrogen, ground topography, pH and soil texture on bacteria and denitrification gene abundance and diversity within the field site.
- Explore the importance of intrinsic neutral processes on microbial and denitrifier community composition, with potentially overlapping niches predicating that all species are identical in their demographic rates (birth, death, dispersal and speciation) and exclusion processes are completely random.

1.6.2. **Chapter 3 aims:**

- Determine whether spatial distance drives diversity patterns in denitrifying bacterial communities.
- Elucidate whether the variation in bacterial community diversity maps onto the scales currently used in precision farming.
- Establish how stable soil bacterial and denitrifier communities are over time.
- Investigate if bacterial or denitrifier community composition or abundance is associated with low yield areas of the field with otherwise favourable soils.
- Test whether spike-in DNA can be used to obtain absolute quantitation of microbiota and denitrification gene abundance .

1.6.3. **Chapter 4 aims:**

- Isolate and culture bacteria that are not denitrification model organisms from arable soil using a custom-made isolation device.
- Determine whether isolated bacteria are representative of the soil bacterial community by comparing cultured bacteria to genomic 16S rRNA amplicon sequence variants.
- Establish what proportion of the cultivable bacteria are able to reduce nitrate or nitrite using an optimised high-throughput screening assay.
- Assess whether a greater proportion of denitrifiers are cultivable from low yield or high conductivity soils than their counterparts.
- Track the individual denitrification reaction dynamics in a representative sample of bacterial isolates.
- Investigate the denitrification genomic potential in a representative sample of bacterial isolates to understand the link between phenotype and genotype.

Chapter 2: Long-term fertilization and tillage regimes have limited effects on structuring bacterial and denitrifier communities in a block designed long-term field trial¹

2.1. Introduction

Below-ground biodiversity plays a major role in the functioning of soil ecosystems and is considered a key measure of soil health and essential for the supply of ecosystem goods and services (Bardgett and van der Putten, 2014; Bender *et al.*, 2016; Delgado-Baquerizo *et al.*, 2016). Whilst farming practices are changing and efforts are being made to become more sustainable, in terms of meeting current food requirements whilst having minimal negative environmental effects (Rockström *et al.*, 2017), it is important to consider what effects agricultural management practice will have on microbial communities and what the consequences of this will be for crop productivity and biogeochemical cycles.

The effect of soil microbial biodiversity on the nitrogen cycle is critical, as nitrogen is the primary limiting factor for productivity in agroecosystems (Rütting *et al.*, 2018). To keep up with global crop demands, 110 Mt nitrogen fertilizer was applied in 2016 (FAO, 2018). Nitrogen fertilizer

¹ A modified version of Chapter 2 has been published as a peer-reviewed journal paper: Claire E. Moulton-Brown, Tianer Feng, Shreiya Shivagni Kumar, Luxi Xu, Calvin Dytham, Thorunn Helgason, Julia M. Cooper, James W. B. Moir. Long-term fertilization and tillage regimes have limited effects on structuring bacterial and denitrifier communities in a sandy loam UK soil. *Environmental Microbiology* (2022) 24(1), 298–30. doi: 10.1111/1462-2920.15873 The published version of the manuscript has been included as Appendix 1. (Moulton-Brown *et al.*, 2022)

use remains a controversial issue, because of the need to balance high crop yield with the expense of fertilizers and the environmental impact associated with overuse, including eutrophication of waters, global warming and stratospheric ozone depletion (Ravishankara *et al.*, 2009; IPCC, 2019; Stevens, 2019).

One option for balancing yield and environmental impact is through the use of organic fertilizers which do not require fossil fuels for manufacture. Long-term organic fertilizer (OF) amendments have been shown to increase microbial species richness relative to synthetic fertilizers (SF) (Hartmann *et al.*, 2015; Francioli *et al.*, 2016), which benefits ecosystem functioning. Additionally, farmers may seek to adopt different tillage practices to reduce their environmental impact. Reduced tillage, including no tillage (NT) and minimum tillage (MT), is thought to increase microbial diversity relative to conventional tillage (CT) by increasing soil organic carbon stocks (Cooper *et al.*, 2016; Sun *et al.*, 2016; Wang *et al.*, 2016; Chen *et al.*, 2020), with the added benefits of reduced soil erosion and improved water conservation (Derpsch *et al.*, 2010). It should be noted, however, that there is often little consensus on the effects of tillage, with recent studies finding that reduced tillage does not increase soil carbon (Keel *et al.*, 2019; Camarotto *et al.*, 2020) or prokaryotic biodiversity (Degruene *et al.*, 2016; Piazza *et al.*, 2019). There is also little consensus on whether reduced tillage increases or decreases nitrogen losses through N₂O emissions (Six *et al.*, 2004; Rochette, 2008; Krauss, Krause, *et al.*, 2017; Krauss, Ruser, *et al.*, 2017).

Denitrification, the microbially-mediated dissimilatory reduction of nitrate to nitrogen gases, accounts for 60% of global N₂O emissions (Kroeze *et al.*, 1999) and contributes to decreased crop productivity through loss of available nitrogen from terrestrial ecosystems (Syakila and Kroeze, 2011). Although denitrification is considered beneficial for wastewater treatment and aquatic ecosystems, in terms of removing fixed nitrogen from the ecosystem and preventing undesirable consequences such as algal bloom (Lu *et al.*, 2014), in agriculture the loss of nitrates from fertilizers is detrimental and costly. Understanding the impact of land management practices in structuring the denitrification community may enable the mitigation of these nitrogen losses

Whilst the effects of tillage and fertilization regimes have received considerable attention, the potential impact on denitrifying bacteria remains relatively unclear. Previous studies have looked at the effect of no tillage (NT) compared to conventional tillage, with results suggesting that NT leads to an increase in denitrifier abundance and activity (Wang and Zou, 2020). This effect was shown to be fertilizer dependent (with increased denitrification with mineral N fertilizer and minimum tillage) (Krauss, Krause, *et al.*, 2017; Wang and Zou, 2020). Less is known about the effects of type of nitrogen fertilizer used, or the combined effects of fertilizer type and minimum tillage on total soil and denitrifier community structure.

The highly heterogenous soil matrix contains many microscale soil habitats which affect microbial activity, diversity and abundance. Whilst many studies demonstrate the impact of long-term land management on microbial and denitrifier diversity, there is a conspicuous knowledge gap in how this is linked to neutral processes in shaping the denitrifying community. Despite relatively weaker biogeographic patterns being observed in microbial taxa than in plants and animals (Meyer *et al.*, 2018), it remains clear that microbial and denitrifier community assembly is driven by local environmental conditions, dispersal limitations and selection (Dumbrell *et al.*, 2010; Vos *et al.*, 2013; Domeignoz-Horta *et al.*, 2018; Jiang *et al.*, 2020). However, little is known about how long-term agricultural practices affect these drivers.

The initial aim of this study was therefore to gain understanding about the impact of fertilizer regime (synthetic versus organic) and tillage (minimum versus conventional) on denitrifying functional guilds in arable soils in a long-term field trial. We hypothesized that (1) minimum tillage would be associated with increased denitrifier diversity due to reduced physical disturbance, reduced aeration and increased soil organic carbon which provides optimum conditions for full and partial denitrification; and (2) synthetic fertilizer would be associated with increased microbial abundance and denitrification gene diversity due to increased initial nitrate concentration relative to composted dairy manure. An additional objective of the study was to investigate the importance of inherent environmental variation within the field site, and intrinsic

neutral processes, on microbial community composition. This study uses bacterial and select denitrifier gene diversity to address these specific objectives.

2.1.1. Experimental aims

The specific objectives of this chapter were to:

- Understand the impact of long-term fertilizer regime (synthetic versus organic) and tillage (minimum versus conventional) on denitrifying functional guilds in arable soils.
- Investigate the importance of inherent environmental variation on bacteria and denitrification gene abundance and diversity within the field site.
- Explore the importance of intrinsic neutral processes on microbial and denitrifier community composition.

2.2. Methods

2.2.1. Nafferton long-term field experiment and sampling

Experiment 3 of the Nafferton Factorial Systems Comparison (NFSC) study, is a long-term field experiment established in 2001 in the Tyne Valley, UK (54:59:27 N; 1:53:54 W, Figure 3) to compare the effects of tillage and fertilizer regimes on crops in an eight-year crop rotation (Orr *et al.*, 2011).

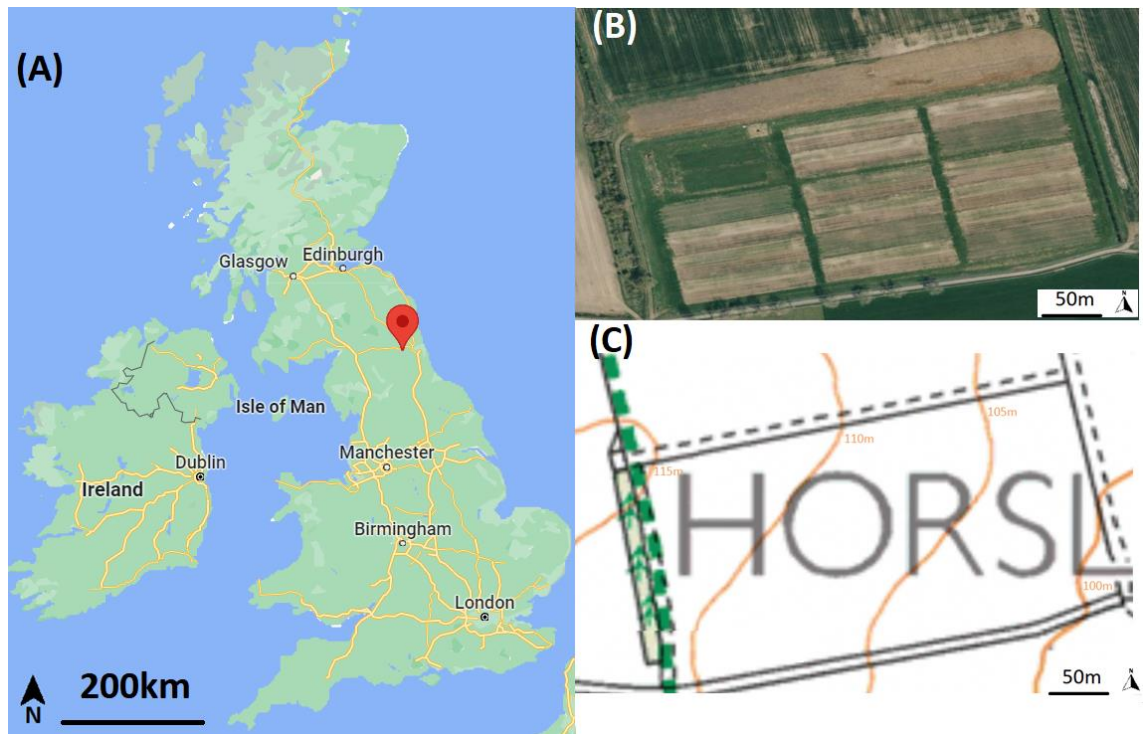


Figure 3 Location of Nafferton Factorial Systems Comparison study showing (A) position in the UK, (B) satellite view of the field site and (C) ordnance survey map of the field site with 10m spaced contour lines indicating elevation above sea level.

The soils were sampled from the site in April 2017 when all plots were planted with spelt and rye and were at the same stage in the crop rotation. The 24m x 6m plots were treated with synthetic (SF) or organic (OF) fertilizer (100 kg total N ha⁻¹ year⁻¹ ammonium nitrate fertilizer or composted dairy manure respectively) and deep inversion conventional tillage (CT) or shallow inversion minimum tillage (MT), with each treatment replicated four times in blocks distributed across the field site (Figure 4). The topsoil of the 4ha trial site is a uniform sandy loam formed in slowly permeable glacial till deposits: Dystric Stagnosol (Soil Survey Staff, 2014).

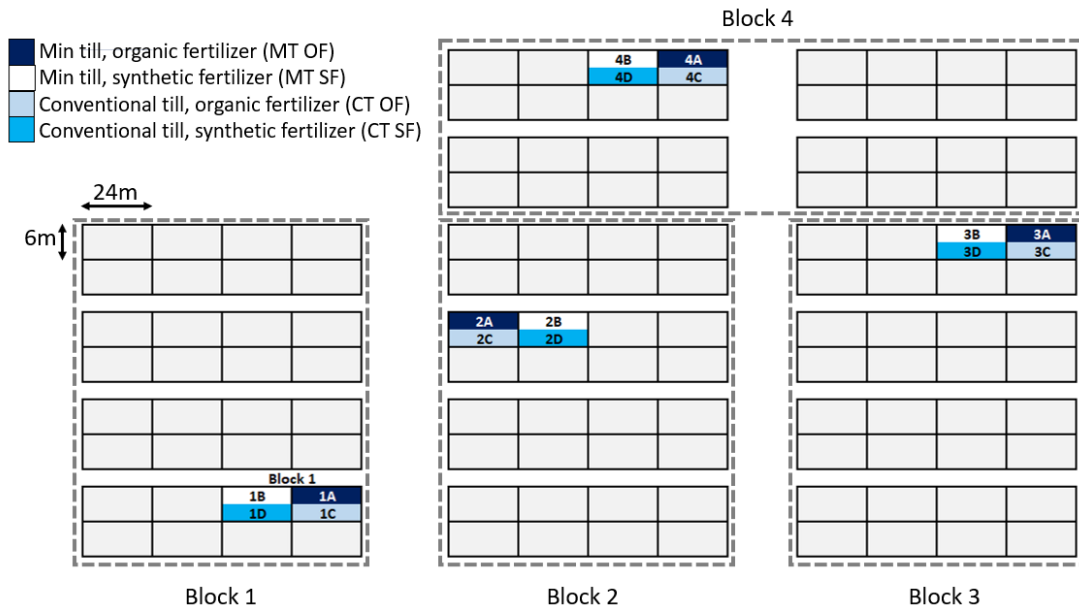


Figure 4 Schematic of Nafferton Factorial Systems Comparison (NFSC) East Hemmel Experiment 3 Plots indicating plots used in this study. MT = minimum tillage, CT = conventional tillage, OF = organic fertilizer and MF = mineral fertilizer. Each individual plot measured 6 x 24m (4 blocks of 32 plots are separated from other blocks by 7m).

The synthetic fertilizer was applied in mid-April 2016, with P and K in the mineral fertilizer plots only added at maintenance levels based on soil analysis. Compost was added in October 2016 for the 2016/17 season, at the same total N-input level as the mineral fertilizer. The compost was produced on site at Nafferton Farm from cow manure and straw and applied prior to sowing. The two tillage levels were also applied prior to sowing. Minimum tillage was shallow (< 20 cm depth) non-inversion tillage using a Dyna-Drive cultivator (Bomford Turner Ltd.) while conventional tillage treatments were mouldboard ploughed to a depth of 25 - 30 cm. All plots were sown with a 1.5 m wide Sow-Lite seed drill (Jordan Engineering Ltd.). Plots were not sprayed with pesticides to remove possible impacts on microbial and denitrifier populations. To allow for within-plot variability, ten cores of soil (0 -10 cm depth) were randomly sampled within each plot and immediately mixed to form one composite sample per plot. Soils were sieved through a 4 mm sieve then stored at -20°C prior to DNA extraction.

2.2.2. *Quantification of 16S rRNA using spike-in T. thermophilus*

A 16S rRNA gene copy number quantification technique (Smets *et al.*, 2016) was carried out for soils by spiking them with an internal DNA standard (*Thermus thermophilus* DSM 46338) prior to DNA extraction. The *Thermus thermophilus* DSM 46338 strain was selected as it is unlikely to be found in UK soils as it grows optimally at 72°C.

T. thermophilus was grown in liquid culture at 72°C for 72 hours without shaking in tryptic soy broth (Fluka Analytical) supplemented with yeast extract (4 g L⁻¹) and NaCl (3 g L⁻¹) at pH 7.5 (Wilquet *et al.*, 2004). DNA was extracted from *T. thermophilus* using the DNeasy PowerSoil DNA isolation kit (Qiagen). Twenty-five ml of culture was centrifuged at 2000 rpm for 10 minutes. The pellet was washed with 5 ml of sterile saline (0.85% NaCl Fisher Scientific) and re-centrifuged. Pellets were resuspended with lysis buffer and DNA was extracted following the manufacturer's protocol. DNA concentration was quantified using NanoDrop (Thermo Fisher Scientific). *T. thermophilus* DNA totalling 0.1% of the expected DNA extracted from the soil, based on a pilot DNA extraction of four of the soils (14.1 ng), was added to each soil sample before DNA extraction.

To determine the number of 16S rRNA genes found in each sample, the equation given below was used (Equation 5; Smets *et al.*, 2016).

$$\frac{R_i}{R_s} = \frac{\omega_i * c_i}{X} \Rightarrow X = \frac{R_s * \left(\frac{\omega_i * c_i}{g_i} \right)}{R_i}$$

Equation 5

In this equation, X represents the number of 16S rRNA genes found in each extracted soil sample. Here R_i is the number of reads assigned to the bacterial taxon used as the internal standard (*T. thermophilus*), R_s is the number of reads assigned to other taxa found in the soil, ω_i is the

weight of internal standard genomic DNA added to the samples, g_i is the weight of the genome of the internal standard and c_i is the 16S copy number of the internal standard.

Briefly, the number of reads assigned to each taxon is multiplied by a constant, made by multiplying the 16S copy number of the internal standard by the weight of DNA added to the sample, divided by the genome weight of the internal standard. This value is then divided by the number of reads assigned to the internal standard. A gene copy number of two and a weight of 2.16×10^{-15} g per *T. thermophilus* genome were assumed (Hallin and Ussery, 2004).

2.2.3. *DNA extraction and amplicon sequencing*

Genomic DNA was extracted from all sixteen soil samples for community 16S rRNA gene and denitrification gene amplicon sequence analysis. The denitrification genes used were nitrite reductases *nirK* and *nirS*, and nitrous oxide reductase *nosZ* (clade I).

DNA was extracted from 0.25 g soil using the DNeasy PowerSoil DNA isolation kit (Qiagen), used according to the manufacturer's protocol. The quality of nucleic acid extractions was verified in SybrSafe-stained (Thermo Fisher Scientific) 1.0% agarose gels. DNA concentration and purity were quantified using a NanoDrop spectrophotometer (Thermo Fisher Scientific).

To amplify genes involved in specific processes in the N cycle, we conducted PCR using primers for the nitrite reductase genes *nirK* (Braker et al., 1998) and *nirS* (Throbäck et al., 2004) and the N₂O reductase gene *nosZ(I)* (Henry et al., 2006) using the published reaction conditions (Table 4). In addition, the V4-V5 region of the 16S rRNA gene was amplified (Walters et al., 2016) for study of the total bacterial community diversity.

For 16S rRNA and *nirK* amplification, PCR was performed in a total volume of 50 µl containing 10 µl 5X GoTaq colourless PCR buffer (7.5 mM MgCl₂) (Promega), 200 µM of each deoxynucleotide triphosphate, 1.25 U of GoTaq polymerase (Promega), 200 mM of each primer and 37.5 ng DNA. In accordance with Braker et al. (Braker et al., 2000), an additional 1.0 mM MgCl₂ and 15 µg BSA were also added. Primer sequences and reaction conditions are shown in Table 4.

For *nirS* and *nosZ* PCR amplification, reactions were performed in a total volume of 25 μ l containing 5 μ l 5X GoTaq colourless PCR buffer (7.5 mM MgCl₂) (Promega), 200 μ M of each deoxynucleotide triphosphate, 1.25 U of GoTaq polymerase (Promega), 400 mM of each primer and 50 ng DNA. Fifteen micrograms BSA was also added. Primer sequences and reaction conditions are shown in Table 4.

Table 4 Primers and PCR conditions used to amplify 16S rRNA, *nirK*, *nirS* and *nosZ* gene amplicons

Gene	Primers	Primer sequence (5'-3')	PCR conditions	Reference
16S rRNA	515F / 806R	GTGYCAGCMGCCGCGGTAA / GGACTACNVGGGTWTCTAAT	Initial denaturation at 95 °C for 2 min, followed by 35 cycles of 30 s at 95 °C, 45 s at 53 °C and 1 min at 72 °C. The reaction was completed after 10 min at 72 °C.	(Walters <i>et al.</i> , 2016)
<i>nirK</i>	nirK1F / nirK3R	GGMATGGTKCCSTGGCA / GAACTTGCCGGTVGYCCAGAC	Initial denaturation at 95 °C for 2 min, followed by 35 cycles of 30 s at 95 °C, 45 s at 53 °C and 1 min at 72 °C. The reaction was completed after 10 min at 72 °C.	(Braker <i>et al.</i> , 1998)
<i>nirS</i>	nirS_cd3aF / nirS_R3cd	G TSAACG TSAAGGARACSGG / GASTTCGGRTGSGTCTTGA	Initial denaturation at 94 °C for 2 min, followed by 35 cycles of 30 s at 94 °C, 1 min at 57 °C and 1 min at 72 °C. The reaction was completed after 10 min at 72 °C.	(Throback <i>et al.</i> , 2004)
<i>nosZ</i>	nosZ2F / nosZ2R	CGCRACGGCAASAAGGTSMSSTG / TCAKRTGCAKSGCRTGGCAGAA	Initial denaturation at 95 °C for 90 s, followed by 35 cycles of 24 s at 95 °C, 24 s at 56 °C and 24 s at 58 °C. The reaction was completed after 10 min at 72 °C.	(Henry <i>et al.</i> , 2006)

PCR products were purified using QIAquick PCR Purification Kit (Qiagen) and quantified using NanoDrop (Thermo Fisher Scientific). PCR products were sequenced using the Illumina MiSeq platform with 2 x 300bp reads by the Bioscience Technology Facility, University of York.

Raw fastq files were demultiplexed, then trimmed to 100,000 reads per sample and quality-filtered using QIIME2 version 2018.2 (Bolyen *et al.*, 2018) to a quality score above 25. Sequences were denoised, dereplicated and chimeras removed using the dada2 denoise-paired function in the dada2 R package (Callahan *et al.*, 2016). Feature IDs were summarized before taxonomy was assigned using the Greengenes 16S rRNA database (DeSantis *et al.*, 2006). For denitrification genes, amplicon sequence variants (ASVs) were used, with reads manually verified using the FunGene database (Fish *et al.*, 2013).

2.2.4. *Determination of soil properties*

Soil was chemically analysed for carbon and nitrogen content using the Vario MACRO Cube CN Elemental Analyser (Elementar). Extractable phosphorus was determined using the Olsen P test (Olsen *et al.*, 1954) and extractable potassium was determined following extraction with 1M ammonium nitrate using a flame photometer. pH was measured in H₂O in 1:2.5 w/v suspensions using a pH probe.

Gravimetric water content was calculated by dividing the mass of water lost when soil was dried at 105°C for 24 hours by the mass of the dry soil. Particle size distribution (PSD) was determined by a Low Angle Laser Light Scattering technique using a Malvern Mastersizer 2000 optical bench with recirculating wet cell enhancement and a Hydro 2000MU sample introduction unit. Organic matter content was determined using the Loss on Ignition method (Ball, 1964). Active soil bacterial carbon biomass was determined by substrate induced respiration (Beare *et al.*, 1990) through addition of glucose to the MicroResp™ system. CO₂ respiration rates were converted to mL CO₂ 100 g⁻¹ of dry soil weight h⁻¹ using the ideal gas law equation. Microbial carbon biomass was calculated using the formula described by Anderson and Domsch (Anderson and Domsch, 1978).

2.2.5. *Statistical and diversity analysis*

Statistical and diversity analyses were performed using R version 3.5.1 (R Core Team, 2022) implemented in RStudio version 1.2.1335 (RStudio Team, 2018). Physicochemical soil data was analysed using two-way analysis of variance (ANOVA) following normality and homoscedasticity testing with the ‘shapiro_test’ and ‘levene_test’ functions respectively. ANOVA was carried out using the lmer function from the lmerTest package (Kuznetsova *et al.*, 2017), with tillage method and fertilizer type as factors and block as a random factor. Percentage data was arcsine-square root transformed prior to analysis.

The ‘multipatt’ function from the indicpecies package (De Cáceres and Legendre, 2009) was used to perform Dufrene-Legendre indicator species analysis to identify bacteria that were specifically associated with different treatments. Alpha diversity was compared across samples using species richness (observed OTUs/ASVs), the Shannon index and Pielou’s evenness index (Shannon, 1948; Pielou, 1966). Differences in alpha diversity were tested using two-way ANOVA as described above. Beta-diversity was represented by Bray-Curtis distance matrices generated from the OTU/ASV table (Roger, Bray and Curtis, 1957). Function ‘adonis2’ in the R package vegan (Oksanen *et al.*, 2013) was used to quantify the possible effects of tillage, fertilizer and field-trial block on beta-diversity, using the Bray-Curtis distance matrix and non-metric multidimensional scaling plots (NMDS) were used to visually represent community dissimilarities between samples based on the Bray-Curtis index using the metaMDS function in vegan. Distance matrices were composed using the vegdist function in vegan before Mantel tests were conducted to measure the correlation between spatial distance and Bray-Curtis dissimilarity and also between environmental data and Bray-Curtis dissimilarity using the mantel function in vegan.

2.2.6. *Accession numbers*

Raw reads for 16S rRNA, *nirK*, *nirS* and *nosZ(I)* amplicons and sample metadata were deposited in the European Nucleotide Archive under study accession number PRJEB49432.

2.3. Results

2.3.1. Soil physicochemical properties

Table 5 Summary of a 16-year cropping systems management experiment at Nafferton Factorial Systems Comparison study (A) and soil physicochemical properties (B). All values are interaction means of four replicates with standard errors given in brackets.¹ MT = minimum tillage, CT = conventional tillage, OF = organic fertilizer & SF = synthetic fertilizer.

A. Cropping system	MT OF	MT SF	CT OF	CT SF
Tillage	Shallow non-inversion	Shallow non-inversion	Deep inversion	Deep inversion
Fertility	Composted dairy manure	Ammonium nitrate	Composted dairy manure	Ammonium nitrate
Pest Control	None	None	None	None
Weed Control	None	None	None	None
B. Soil chemical, physical and biological properties				
C (%)	2.24 (±0.09)	2.16 (±0.04)	2.21 (±0.05)	2.06 (±0.05)
N (%)	0.22 (±0.009)	0.21 (±0.003)	0.21 (±0.009)	0.21 (±0.005)
C:N	10.21 (±0.11)	10.35 (±0.08)	10.41 (±0.25)	10.08 (±0.21)
Extractable P (mg kg ⁻¹)	22.19 (±2.91)	17.14 (±3.24)	18.42 (±4.14)	18.42 (±3.92)
Extractable K (mg kg ⁻¹)	109.3 (±10.1) ^a	82.6 (±7.3) ^b	107.7 (±12.5) ^a	68.2 (±2.2) ^b
Moisture content (%)	23.0 (±0.92)	22.6 (±0.64)	22.4 (±1.26)	22.4 (±0.82)
pH	6.74 (±0.10)	6.51 (±0.13)	6.66 (±0.08)	6.69 (±0.16)
Clay (%)	16.50 (±0.65)	16.50 (±0.87)	16.50 (±0.29)	17.25 (±0.85)
Sand (%)	64.75 (±0.63)	64.25 (±1.80)	63.50 (±1.19)	62.50 (±1.55)
Silt (%)	18.75 (±0.25)	19.25 (±1.03)	20.00 (±1.00)	20.25 (±0.75)
Microbial biomass (µg C g ⁻¹ soil)	209.6 (±25.9) ^a	203.1 (±33.8) ^a	143.9 (±23.7) ^b	144.2 (±25.7) ^b
Organic matter (%)	6.19 (±0.19)	6.11 (±0.10)	5.99 (±0.13)	5.80 (±0.16)

¹ Means followed by the same letter in the same row are not significantly different. All soil properties measured were compared using Linear Mixed Effects model ($p < 0.05$).

Soil physicochemical properties were measured to ascertain whether land management treatments affected soil properties, which could influence bacterial community composition. There was little chemical difference in the soil between treatments apart from extractable potassium content, which was significantly higher in soils treated with organic fertilizer compared to synthetic mineral fertilizer (Table 5; Fertilizer: $F_{1,13} = 23.07$; $p = 0.0009$). This is because animal manure contains significant potassium levels (Qian *et al.*, 2011). All potassium concentrations had a K Index of 1, indicating a potential risk of potassium deficiency, whereas all soils were within range of P Index 2, the target index for arable crops (Alexander *et al.*, 2008). Soil carbon was also slightly elevated in soils treated with organic fertilizer, although this was not statistically significant ($p = 0.055$).

Treatment did not affect soil texture or pH. However, active microbial carbon biomass, measured through bacterial respiration, was greater in plots with minimum tillage compared to conventional tillage (Tillage: $F_{1,13} = 17.72$; $p = 0.002$). And, although not significant at the $p < 0.05$ level ($p = 0.054$), organic matter was also increased in sites which used minimum tillage.

These results suggest that reducing soil disturbance through the adoption of minimum tillage strategies can have a positive impact on below-ground biomass, regardless of fertility management strategy. The results also show that use of organic fertilizer (manure) has a positive impact on extractable potassium and may also increase available carbon in the soil.

2.3.2. *The effect of tillage and fertilizer on bacterial taxa and abundance*

The 16S ribosomal RNA gene sequence was used to investigate bacterial abundance and diversity. By adding a known quantity of foreign DNA, it was possible to simultaneously evaluate the absolute 16S rRNA gene abundance per gram of soil and the bacterial diversity, rather than using only relative abundance.

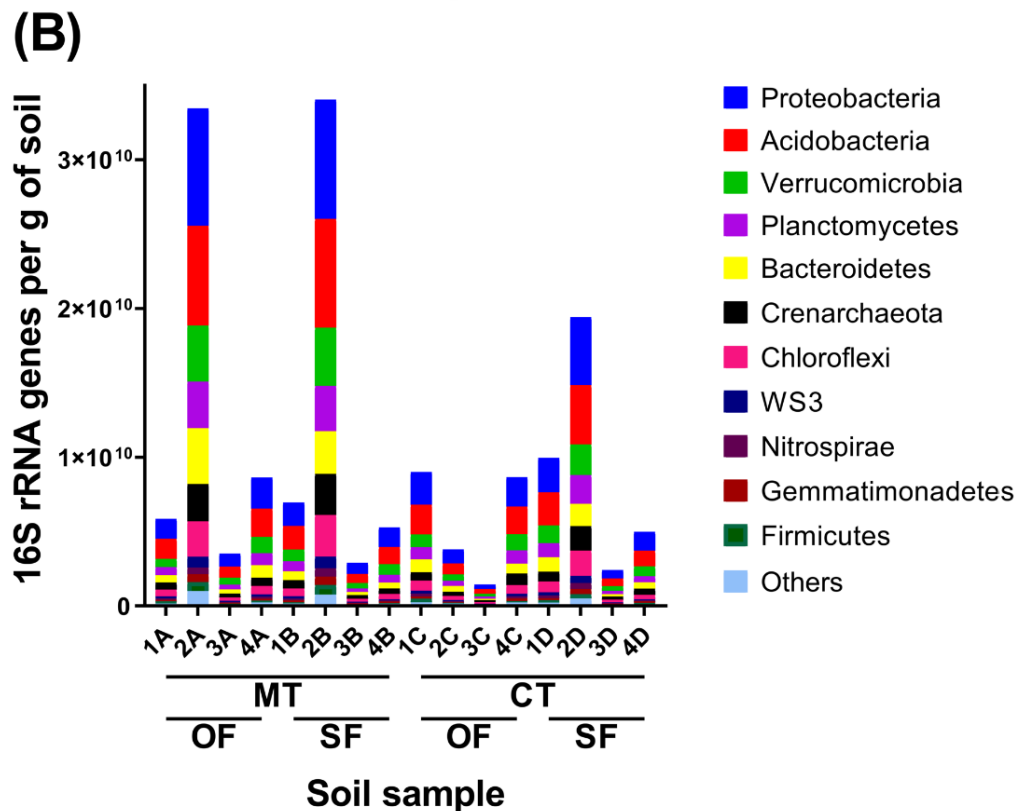
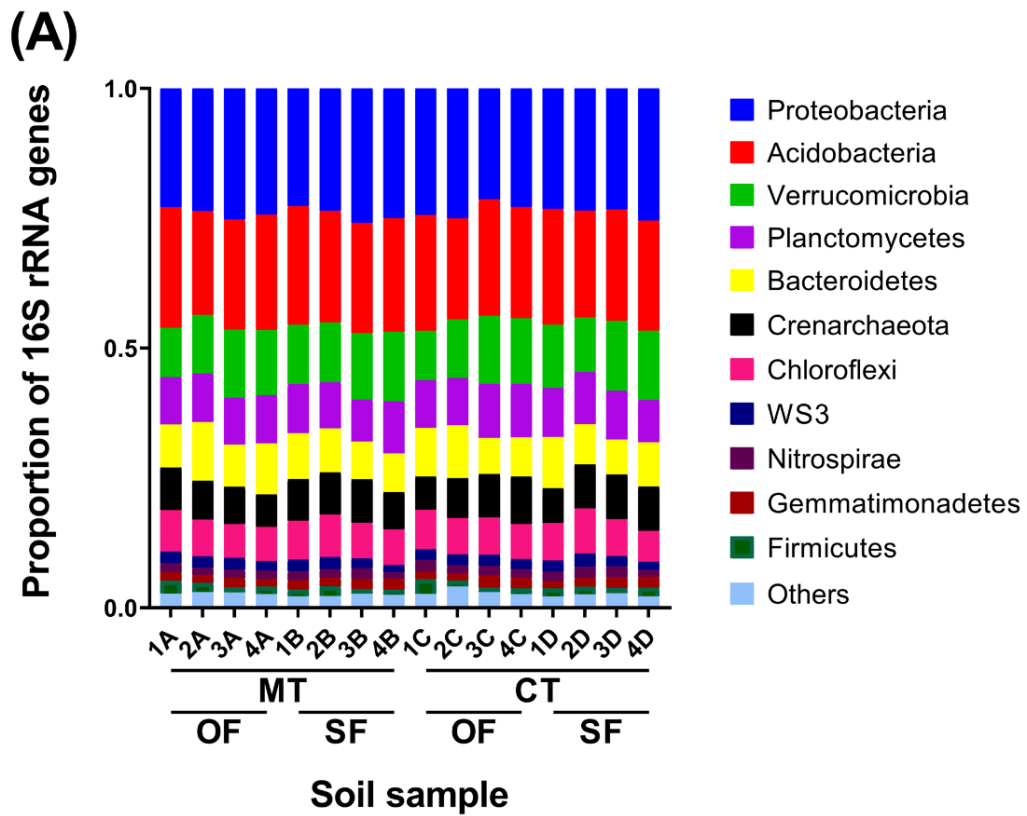


Figure 5 Relative (A) and absolute (B) abundance of bacterial phyla in soils treated with different combinations of tillage and fertilizer. 'Others' refers to all phyla with an abundance of less than 1% across samples. Labels indicate field plot. MT and CT denote minimum and conventional tillage respectively. OF and SF denote organic and synthetic fertilizer respectively.

The relative abundance of each phylum remained relatively constant across plots (Figure 5A), but clear differences can be observed in the total abundance, with plots having between 1.45×10^9 and 3.41×10^{10} 16S rRNA genes per gram of soil (Figure 5B). Although no significant difference was found between treatments due to high variance, minimum tillage appears to be associated with greater bacterial abundance. This is in accordance with the bacterial biomass result discussed above. When investigating the high sample variance further, it was clear that field-block had a significant effect on the 16S rRNA abundance in each soil sample (Block: $F_{3, 12} = 5.77$; $p = 0.0111$), with Block 2 soils having significantly more 16S copies per gram of soil than any other block.

The dominant phylum across all plots was found to be proteobacteria, with mainly Alphaproteobacteria, Betaproteobacteria and Gammaproteobacteria dominating all samples. Acidobacteria, in particular actinobacteria, was the next most abundant phylum across all samples (Figure 5). Indicator species analysis identified OTUs that were specifically associated with land management history. Although 3,716 OTUs were detected in total, only 32 were associated with specific treatments, indicating that land management treatment did not affect the majority of taxa within the soil.

Five indicator species were specifically associated with plots treated with synthetic fertilizer. These were the ammonia oxidising *Nitrosospora multiformis*, a Chloroflexi in the Kouleothrixaceae family, a *Spartobacterium* thought to be an obligate symbiont of plant pathogenic nematodes of the *Xiphinema americanum* group (Vandekerckhove *et al.*, 2000), and two Phycisphaerae (a bacterial class of mainly unknown ecophysiologicals often found in ANAMMOX communities (Costa *et al.*, 2014)). Two OTUs were specifically associated with minimum tillage treatments. One is a member of the DA101 genus of the Chthoniobacteraceae family that is known to be common in grassland soils (Felske and Akkermans, 1998), the other is a Gammaproteobacteria of the Sinobacteraceae family.

*The effect of tillage and fertilizer on bacterial 16S rRNA and
denitrification gene alpha diversity*

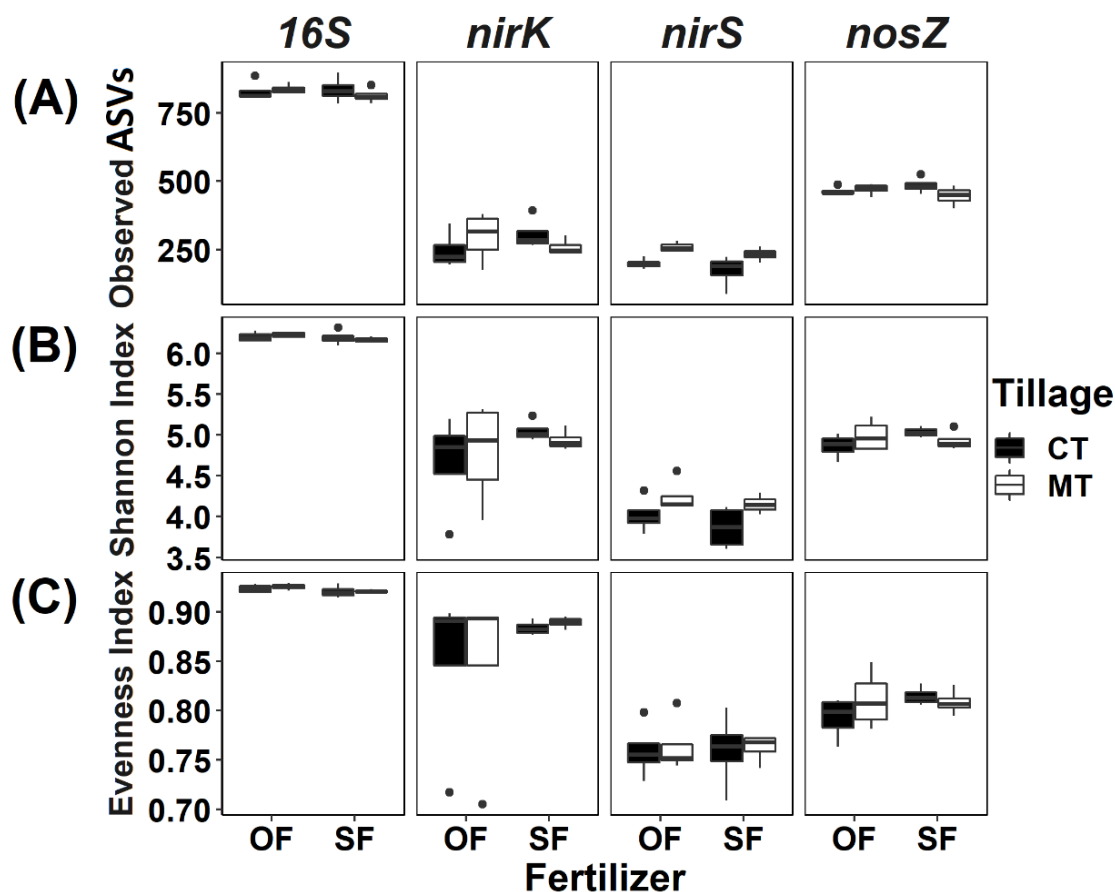


Figure 6 Boxplots of alpha diversity measures of each sample treatment. (A) Observed amplicon sequence variants by sample treatment. (B) Shannon diversity index. (C) Pielou's evenness index. Conventional tillage is shown in black, with minimum tillage shown in white. OF and SF denote organic and synthetic fertilizer respectively.

To compare the effects of land management on within-plot biodiversity, three measures of alpha diversity were used. The number of observed variants did not differ significantly in the 16S rRNA, *nirK* or *nosZ* amplicons, but there were approximately 32% more observed *nirS* variants in the minimum tillage treated plots than the conventional tillage (Figure 6A; Tillage: $F_{1,9} = 13.7$; $p = 0.0048$). Likewise, *nirS* had significantly greater Shannon diversity when treated with minimum tillage compared to conventional tillage (Figure 6B; Tillage: $F_{1,9} = 12.08$; $p = 0.0069$). Notably, land management treatment was not associated with any differences in variant evenness for any

of the amplicons (Figure 6C). Overall, this suggests that minimum tillage is associated with slightly increased below-ground biodiversity, but fertilizer has little effect.

All genes had significantly different levels of evenness, with 16S rRNA variants being more evenly distributed within plots compared to the other genes which had more dominant variants, particularly *nirS* (Figure 6C; Evenness by gene: $F_{3, 60} = 106.4$; $p = 2e^{-16}$). *NirS* genes are less diverse than *nirK* and *nosZ* genes, which could indicate a higher level of conservation within the cytochrome *cd₁* variant of the nitrite reductase compared to the copper-containing enzyme of the same function, consistent with the greater conservation of *nirS* reported previously (Braker *et al.*, 2000).

2.3.4. *The effect of tillage, fertilizer and sample location on bacterial community composition*

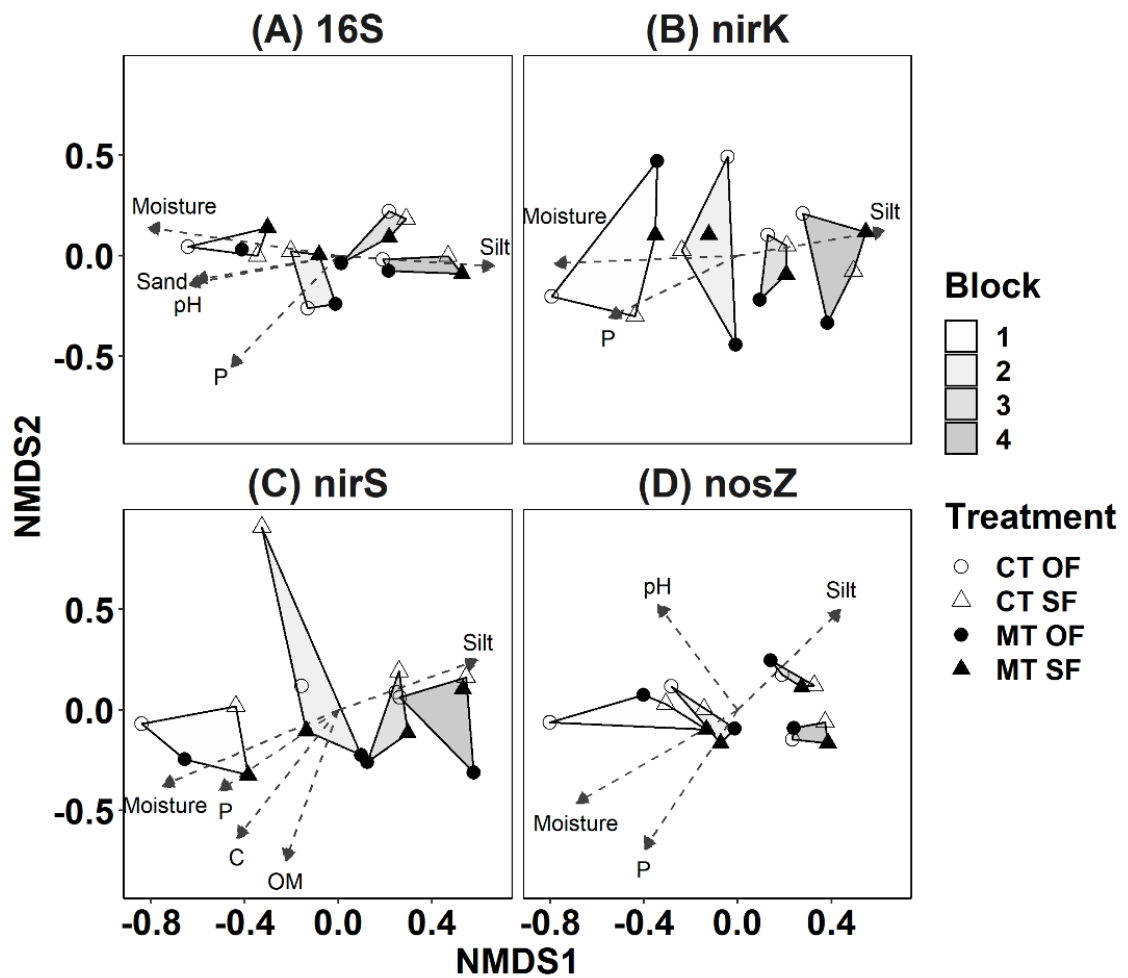


Figure 7 Non-metric multidimensional scaling (NMDS) of gene amplicon Bray-Curtis dissimilarity from NFSC soils. (A) Whole bacterial community 16S rRNA. (B) nirK amplicon variants. (C) nirS amplicon variants. (D) nosZ amplicon variants. Samples are indicated with points, conventional tillage (CT) plots are shown in white, with minimum tillage (MT) in black; organic fertilizer (OF) is denoted by circles, synthetic fertilizer (SF) treatments are shown by triangles. Points are grouped by polygons indicating block position of sample in the field study, from block 1 shown in white to block 4 shown with the dark grey. Labels indicate environmental variables which significantly explain sample Bray Curtis beta diversity.

To explore the differences in the composition of bacterial communities between land management treatments, a non-metric multidimensional scaling (NMDS) ordination of whole bacterial

community 16S rRNA gene amplicons was constructed (Figure 7A). To confirm if the differences between community compositions can be explained by land-management factors, a PERMANOVA test was used. Neither tillage method nor fertility treatment were found to have significant effects on community composition (Tillage: $F_{1, 15} = 0.73$; $p = 0.81$; Fertilizer: $F_{1, 15} = 1.2$; $p = 0.18$; Tillage x Fertilizer: $F_{1, 15} = 0.59$; $p = 0.98$), despite block effects being accounted for as a random factor. The variable accounting for most differentiation among samples was block, i.e. the location of the plots (Fig. 4; Block: $F_{3, 15} = 5.7$; $p = 0.001$), suggesting that field location had a greater effect on soil bacterial community than either tillage or fertilizer treatments.

Amplicon analyses for the denitrification genes *nirK*, *nirS* and *nosZ* (clade I) were then used to ascertain whether functional diversity followed the same patterns as taxonomic diversity in the treated soils. Similarly to bacterial taxa, the variants of the nitrite reductase gene *nirK* were not significantly associated with tillage or fertilizer treatment (Tillage: $F_{1, 15} = 0.92$; $p = 0.53$; Fertilizer: $F_{1, 15} = 1.02$; $p = 0.35$; Tillage x Fertilizer: $F_{1, 15} = 0.70$; $p = 0.96$), but were strongly associated with field block (Figure 7B; Block: $F_{3, 12} = 2.41$; $p = 0.001$). This was also true for *nirS*, which was not significantly affected by land management (Tillage: $F_{1, 15} = 1.0$; $p = 0.37$; Fertilizer: $F_{1, 15} = 0.65$; $p = 0.6$; Tillage x Fertilizer: $F_{1, 15} = 0.29$; $p = 0.99$), but was significantly affected by block (Figure 7C; Block: $F_{3, 12} = 6.18$; $p = 0.001$). The same pattern was evident in nitrous oxide reductase *nosZ* (Figure 7D; Tillage: $F_{1, 15} = 0.73$; $p = 0.67$; Fertilizer: $F_{1, 15} = 1.0$; $p = 0.32$; Tillage x Fertilizer: $F_{1, 15} = 0.56$; $p = 0.92$; Block: $F_{3, 12} = 3.58$; $p = 0.001$), suggesting that field-block location is the major determinant of bacterial community and denitrification functional gene composition.

2.3.5. *Spatial and environmental effects on bacterial community composition*

Once it had become apparent that bacterial communities and denitrification genes appear largely unaffected by land management history, and cluster predominantly by field block, we began investigating the role of environmental factors and spatial location in bacterial community composition. Environmental vector fitting revealed that five soil variables: soil moisture, phosphorous, pH, silt, and sand content were significantly related to total bacterial community

composition (Figure 7A; Envfit: Moisture $r^2=0.68$, $p=0.001$; Phosphorus $r^2=0.52$, $p=0.009$; pH $r^2=0.43$, $p=0.021$; Silt $r^2=0.44$, $p=0.025$; Sand $r^2=0.38$, $p=0.04$). Since none of these factors were affected by land management treatment (Table 5), this suggests that innate environmental differences have more effect on bacterial community composition than long-term tillage or fertilizer treatments.

Additionally, the distribution of each of the denitrification genes was significantly associated with moisture (Envfit moisture: *nirK* $r^2=0.61$, $p=0.002$; *nirS* $r^2=0.70$, $p=0.001$; *nosZ* $r^2=0.69$; $p=0.001$). Phosphorus and silt content were also significantly correlated with denitrification gene distribution (Figure 7B:D). *NirS* variation was significantly associated with carbon content and organic matter (Envfit *nirS*: carbon $r^2=0.59$, $p=0.005$; organic matter $r^2=0.61$; $p=0.005$), suggesting that *nirS* organisms may be more sensitive to carbon than their *nirK* counterparts.

To further investigate variation in community composition, a spatial analysis was completed. A Euclidean distance matrix (with the distances between the centre of each plot) was compared against the Bray-Curtis dissimilarity matrix using a Mantel test. The test indicated that there was significant positive correlation between the physical distance between plots and their community dissimilarity for all of the amplicons tested (Figure 8; 16S rRNA: $R^2 = 0.590$, $p = 0.001$; *nirK*: $R^2 = 0.429$, $p = 0.001$; *nirS*: $R^2 = 0.559$, $p = 0.002$; *nosZ*: $R^2 = 0.589$, $p = 0.001$). This result indicates a clear distance decay effect, with increased physical distance being associated by increased dissimilarity between bacterial communities and denitrification gene distributions. Here, spatial distance is found to account for approximately 55% variation in bacterial communities and denitrification genes.

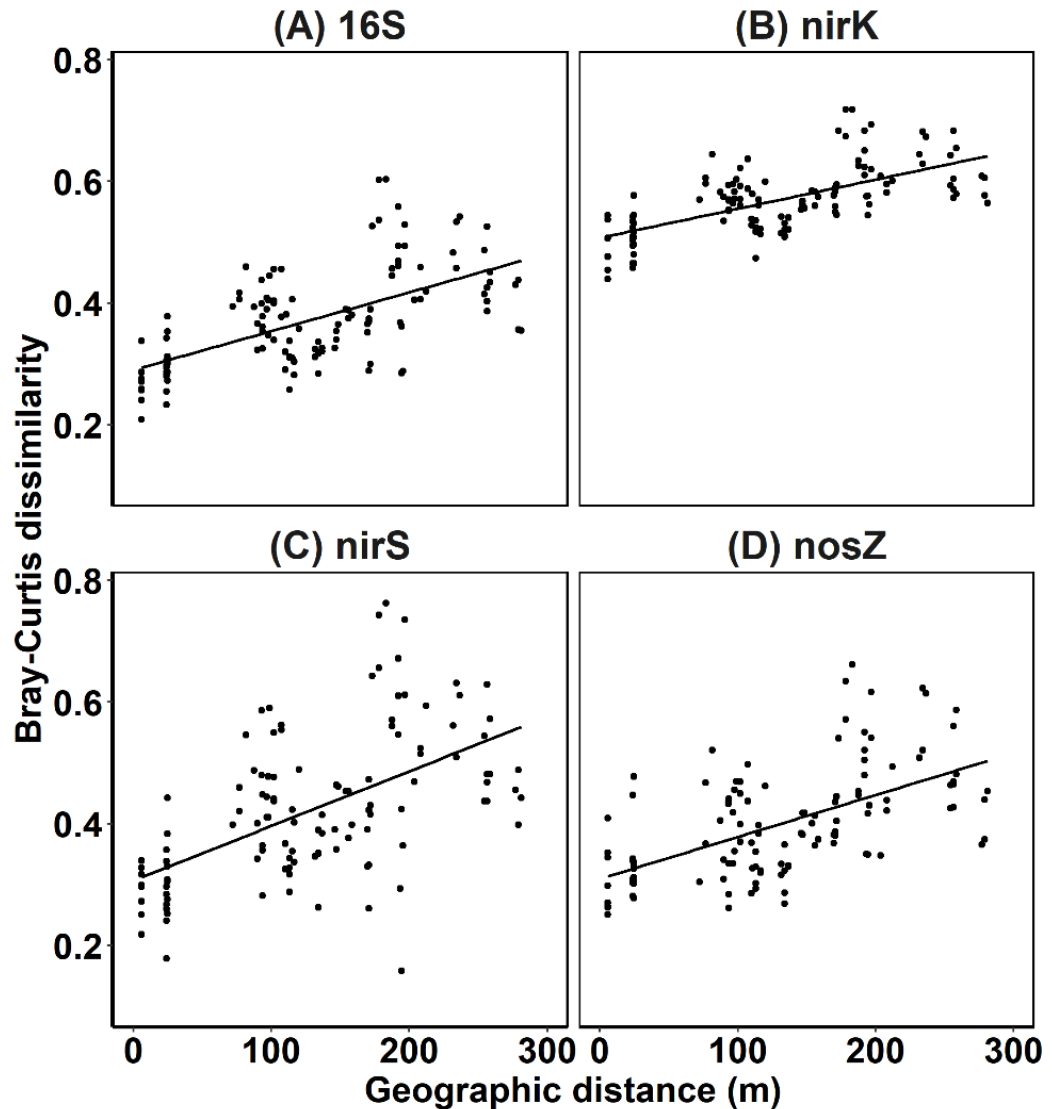


Figure 8 Distance-decay relationship between geographic distance between samples and Bray-Curtis dissimilarity index for 16S rRNA (A), *nirK* (B), *nirS* (C) and *nosZ* (D) genes.

To separate the effects of space alone from environmental gradients on community composition, the `calc.relimp` function in R was used. This indicated that environmental and spatial variation together accounted for 63.6% variation in 16S rRNA diversity, with 18.9% of this attributable to space alone and 44.7% attributable to environmental variables. Spatial and environmental gradients together accounted for 28.5%, 63.0% and 50.8% of community variation in *nirK*, *nirS* and *nosZ* respectively. Spatial distance had a relatively stronger effect on the denitrification genes

than on the overall microbial population, with space alone attributable to 13.1%, 21.1% and 22.6% of variation respectively. Together these analyses indicate that spatial distance is a major determinant of bacterial community similarity and has a much stronger effect than long-term tillage or fertilizer regimes.

2.4. Discussion

This study demonstrates the surprisingly limited effect of long-term tillage and fertilizer regimes on soil microbial community and denitrification gene diversity, with clear field-scale patterns across distance and environmental gradients.

Minimum tillage was associated with an increase in microbial biomass, which is in accordance with several studies which demonstrate that conservation tillage systems, including no tillage and minimum tillage, have increased microbial biomass (Mathew *et al.*, 2012; Zhang *et al.*, 2012; Murugan *et al.*, 2014). The increase is thought to be due to increased levels of microbially available, labile soil carbon and nitrogen in surface soils under conservation tillage (Chen *et al.*, 2009). While labile C may represent a relatively small proportion of total soil organic C (Li *et al.*, 2018), it plays a key role in driving soil microbial activity. We did not directly measure labile C in this study, but values for soil basal respiration were significantly higher in the minimum tillage treatment compared to conventional tillage, suggesting a higher proportion of labile C in the minimum tillage soils, which were not observed in this long-term field trial.

Similarly, the increased number of *nirS* variants in the minimum tillage plots suggests that minimum tillage has similar effects to no-tillage, in increasing denitrifier diversity (Wang and Zou, 2020). This effect is thought to be primarily due to increased bulk density in conservation-tilled soils, resulting in reduced aeration, which is favourable for denitrifiers as anoxic conditions are most suitable for denitrification (Doran, 1980).

Nitrogen deficiency is the major nutrient limitation for agricultural productivity, and results in widespread addition of environmentally and financially costly nitrogen rich fertilizers (e.g. Good and Beatty, 2011; Rütting et al., 2018). Furthermore, a significant increase in denitrification and denitrifier diversity has been linked to the application of synthetic nitrogen fertilizers (Gerber *et al.*, 2016; Krauss, Ruser, *et al.*, 2017). Practices which improve efficiency of fertilizer N use and reduce reliance on synthetic inputs can reduce these impacts. While substitution of organic N sources has been proposed as a strategy to reduce losses of mineral N, in this study we found no discernible difference in denitrifier populations due to N source. This may have been due to the application of equivalent levels of total N for each treatment, suggesting that the total nitrogen supplied rather than the nitrogen source that has the primary effect on denitrifier community diversity.

Environmental variation through oxygen and nitrate content; organic matter quantity, quality, and availability; redox potential; temperature; pH; and soil type are all known to affect microbial communities and denitrification (Drenovsky *et al.*, 2004; Wallenstein *et al.*, 2006; Enwall *et al.*, 2010; Nadeau *et al.*, 2019). Here, we show significant effects of moisture, potassium, pH and soil textural class on all of the denitrification gene diversities. Cytochrome *cd₁* type nitrite reductase *nirS* is further associated with increased soil carbon and soil organic matter, which may be due to the relatively greater energy demands needed for enzyme assembly for *nirS* type denitrifiers, which requires at least ten genes for assembly of the mature nitrite reductase enzyme, compared to *nirK* type denitrifiers, which requires only a single gene (Rinaldo *et al.*, 2016). Additionally, a combination of other physical factors, including those not measured in this experiment such as oxygen concentration, may also be important drivers of soil microbial community structure. Whilst environmental gradients can be attributed to approximately 32.6% variation across all of the genes studied, it remains clear that geographical distance is also a driver of microbial and denitrifier gene community diversity.

Distance-decay and other spatial effects are well-known ecological phenomena (e.g. Green et al., 2004; Martiny et al., 2011; O'Brien et al., 2016; Zhou et al., 2008) that appear to be driving

bacterial and denitrifier gene diversity in this study. Here, community similarity decays as a function of distance, which suggests that dispersal ability is a significant force behind the bacterial diversity observed in this study (Martiny *et al.*, 2011). The denitrification genes in this analysis appear to show greater dispersal limitation than the background bacterial population. This may indicate that the genetic backgrounds in which these genes occur have either restricted niches or lower motility – both of which are consistent with the anoxia required for denitrification. The combination of spatial effects and environmental gradients observed here suggests that a combination of niche and neutral processes drives observed community structure, and that the balance of the processes may further be related to function.

The United Nations promote the use of reduced tillage for improved and sustained crop production (FAO, 2015) and the use of organic fertilizers to maintain and enhance soil productivity. This experiment demonstrates that long-term reduced tillage and organic fertilizer regimes have no significant negative effects on soil physico-chemical properties. Indeed, organic fertilizer use led to an increase in soil potassium which may improve crop yield (Pettigrew, 2008) and minimum tillage led to increased active microbial carbon biomass, which can improve crop yield through increased nutrient cycling, suppression of soil-borne pathogenic microorganisms, and the decomposition of organic matter, which is closely associated with the aboveground performance of crops (Marschner, 2007; Berg and Smalla, 2009).

This study evaluated the role of agricultural management practices on microbial and denitrification gene diversity through the use of a long-term randomised complete block fully factorial field trial. Whilst land-management had a limited effect on microbial community abundance, distance and physico-chemical properties were the main drivers of total bacterial and denitrification gene diversity.

2.4.1. Conclusions

This chapter highlights that whilst the microbial community can be “diagnosed”, it is unlikely that long-term land management strategies will significantly alter the community to improve

nitrogen use efficiency. This result goes some way to explaining the frequent inconsistencies in field studies and demonstrates unequivocally that field studies of microbiomes cannot rely on standard replicated designs to reveal the effect of land management scale interventions, even when applied long term. Furthermore, this may lead to a model for agricultural intervention that is led by soil microbial community information rather than purely physicochemical data to allow a more holistic view of factors affecting crop production.

Chapter 3: Spatiotemporal distribution of bacteria and denitrification genes in a commercially farmed arable field and their association with yield variability

3.1. Introduction

Following an investigation into the effects of tillage and fertilizer regimes in a long-term field trial (Chapter 2), it was found that microbial communities and denitrification genes were largely unaffected by long-term land management history, and cluster predominantly by spatial location within the field. This is a trend that cannot be fully explained by measurable environmental variation. This led us to devise an experiment to explicitly test the role of spatial location in driving diversity patterns in both bacteria and denitrification genes.

3.1.1. Spatial effects

Although much is known about the biogeographic patterns of macroorganisms, there is often little in the way of consensus on the spatial patterns of microorganisms (Constancias *et al.*, 2015; Ramirez *et al.*, 2018). Since microorganisms and macroorganisms often form associations, it would seem logical that the spatial distribution of microorganisms mirrors that of macroorganisms. Although some studies have found that microbes do exhibit the same biogeographic patterns as macroorganisms (Hillebrand *et al.*, 2001; Horner-Devine *et al.*, 2004; Zhou *et al.*, 2008), they are generally found to be much weaker than associations that are found in plants and animals (Meyer *et al.*, 2018). Two of the fundamental biogeographic

patterns that we would expect to see are the positive power law between species richness and area, known as taxa-area relationships (F. W. Preston, 1980; Lawton, 1999; Horner-Devine *et al.*, 2004), and the distance-decay relationship (Nekola and White, 1999): the decay of community similarity with geographic distance.

As well as these two theories, there is also a third: “Everything is everywhere” (Beijerinck, 1913) was coined to suggest that microbial taxa are found ubiquitously. The phrase was later amended to: “Everything is everywhere, but, the environment selects” (Baas-Becking, 1934), to note that microbial taxa are found anywhere on earth that there is suitable habitat for them. Over time this theory has evolved into the niche versus neutral theory whereby it is debated whether habitat features alone can explain the presence of a given taxa (Fenchel and Finlay, 2004) or whether biodiversity arises at random (McGill, 2003). The neutral theory will help form our null hypothesis: there will be no significant association between physical distance (Euclidean distance) and phylogenetic distance between bacterial and denitrifier communities (Weighted UniFrac distance).

Since the emergence of high-throughput, culture-independent measures of assessing microbial communities, such as 16S rRNA sequencing, studies can measure biogeographic patterns of microbes at scales which can capture more microbial diversity than would ever have been possible using microbiological culture-based methods. Understanding biogeographic patterns in microorganisms is fundamental because microorganisms are the most abundant and diverse living entities on Earth, and they have important roles in biogeochemical cycling of materials that are vital for ecosystem functioning (Griffiths *et al.*, 2011). With this in mind, it is important to consider microbial communities both in terms of their taxonomy, but also in terms of their functionality, for example, whether gene-area relationships are quantitatively similar to taxa-area relationships.

3.1.2. *Denitrification as a marker of functional diversity*

The functional process in this study is denitrification, a community process within the nitrogen cycle, that catalyses the stepwise reduction of nitrate to dinitrogen. This hugely important process accounts for 60% of global nitrous oxide emissions (Kroeze *et al.*, 1999) and is also the only biological sink for nitrous oxide, which is a potent greenhouse gas (Seitzinger *et al.*, 2006). Notably, denitrification is a modular process, with not all denitrifiers possessing the full suite of genes for the enzymes needed for complete denitrification (Graf *et al.*, 2014). This adds a level of complexity as to which organisms execute which denitrification step within the microbial community to achieve complete denitrification and which genes are the best predictors of denitrification rate. Several studies have linked copper-containing nitrite reductase (*nirK*), cytochrome cd1 nitrite reductase (*nirS*) or nitrous oxide reductase gene *nosZ(I)* abundances to potential denitrification rate (Chroňáková *et al.*, 2009; Dong *et al.*, 2009; Čuhel *et al.*, 2010; Petersen *et al.*, 2012). Abundance and diversity of these genes will therefore be a focus of this study to investigate spatial scaling of functional gene diversity across bacterial taxa.

3.1.3. *Experimental objectives*

The specific aims of this chapter were to:

- Determine whether spatial distance drives diversity patterns in denitrifying bacterial communities.
- Elucidate whether the variation in bacterial community diversity maps onto the scales currently used in precision farming.
- Establish how stable soil bacterial and denitrifier communities are over time.
- Investigate if bacterial or denitrifier community composition or abundance is associated with low yield areas of the field with otherwise favourable soils.

- Test whether spike-in DNA can be used to obtain absolute quantitation of microbiota and denitrification gene abundance.

3.2. Methods

3.2.1. Harold Smiths field experiment and sampling

Soil sampling took place at Harold Smiths field (54:00:37.0 N; 1:08:40.4 W, Figure 9), a 6 ha arable field located in North Yorkshire, UK. The field is part of a working commercial farm, Church Farm, owned by PD N Blacker & Son. The topsoil is predominantly clay loam, with small areas of silty clay loam and sandy silt loam. The field is largely flat, with two patches that are slightly elevated at the north and centre of the field (Figure 9C), with a drainage ditch running around the north and eastern field perimeters.

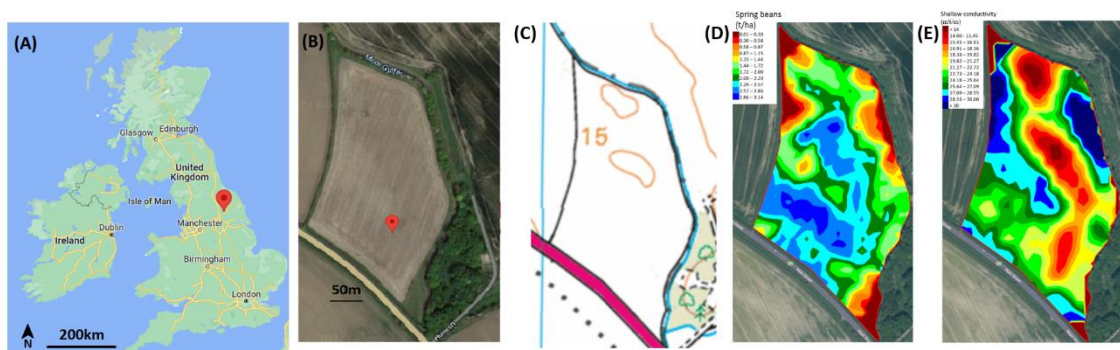


Figure 9 Location of Harold Smiths field site showing (A) position in the UK, (B) satellite view of the field site and (C) ordnance survey map of the field site with 5m spaced contour lines in orange indicating elevation above sea level, (D) 2018 spring bean yield – low yield samples with 1.43 t ha^{-1} are in pale green and high yield sites with 2.75 t ha^{-1} are in medium blue, (E) shallow electrical conductivity scan – low conductivity samples were 16.8 mS m^{-1} are coloured orange and high conductivity samples with 27.1 mS m^{-1} are coloured turquoise. See Appendix 2: for high resolution maps. Image credits: (A,B) Google maps, 2022; (C) Ordnance survey, 2022; (D,E) Precision Decisions.

A sampling strategy was devised to investigate both spatial and temporal microbial and denitrifier variation within the field. To investigate spatial variation, soils were collected from 48 locations within the field (**Error! Reference source not found.**), which were grouped into four zones with similar properties (combinations of low and high yield and low and high conductivity as described below). Additionally, to investigate temporal community variation,

samples were collected each year over three years (2018 - 2020). In the temporal samples, twelve cores of soil (0 - 20 cm depth) were randomly sampled within each zone and immediately mixed to form one composite sample per zone per year to allow for within-zone variability.

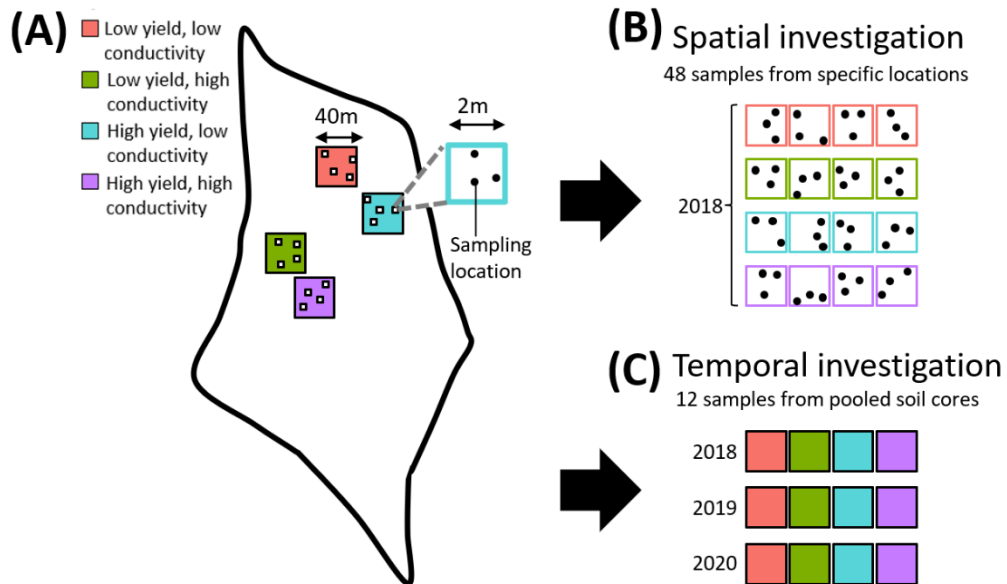


Figure 10 Schematic showing sampling locations within Harold Smiths field and sampling strategies. (A) Stratified sampling of four 40 m² zones with distinct properties: low yield and low conductivity (pink), low yield and high conductivity (green), high yield and low conductivity (blue) and high yield and high conductivity (purple). Within each zone, there are four 2 m² blocks, which were distributed to give a wide spread of distances between blocks. Within the sixteen blocks, there are three randomly located sampling sites. (B) Schematic of spatial investigation sampling, with 48 spatially explicit sampling sites (black dots) sampled in 2018. (C) Schematic of temporal investigation sampling, with four pooled sampled (from twelve 10 cm deep cores) taken each year over three years.

To assess whether microbial community may be associated with poor crop yield, when other factors are favourable, a stratified sampling method was used. This method targeted field regions with high and low yield which had favourable levels of acidity and soil textural indices. Overall, most of the yield variation within the field in 2018 can be explained by shallow electrical conductivity (Figure 9D-E). Soil electrical conductivity (EC) is a measurement that correlates with soil properties that affect crop productivity, including soil

texture, cation exchange capacity, drainage conditions, organic matter, salinity, and subsoil characteristics. Where the electrical conductivity in the soil was high, the yield tended to be poorest. This is likely because high EC is a good indicator of high clay content and high water-holding capacity, which can set hard during high temperatures, preventing roots from getting adequate water and soil nutrients. Whilst the correlation between high electrical conductivity and low yield site was expected ($R^2 = -0.52$, $p = 2.2e^{-16}$), this study also includes high EC high yield sites and low EC low yield sites to understand how the microbial communities differ.

Sampling site locations were selected using a stratified sampling strategy with four zones of interest in Harold Smiths field, combinations of low yield, LY, (less than 1.43 t ha^{-1} Spring Beans in 2018); high yield, HY, (over 2.75 t ha^{-1}); low conductivity, LC, (shallow conductivity below 16.91 mS m^{-1}); and high conductivity, HC, (above 27.09 mS m^{-1}). Yield and shallow electrical conductivity maps are shown in Appendix 2.

All zones had a pH range of 6.1-6.5 and a soil texture index of 6-8, indicating clay loam soils and silt clay loam soils respectively. By ensuring these variables were as similar as possible, clearer inferences could be made regarding associations with microbial community composition. Within each zone, four 2 m^2 blocks were located to maximize the spread of distances between all 16 blocks (**Error! Reference source not found.**). Within each block, three sampling locations were randomly located using a random number generator to generate coordinates. Soil cores of 10 cm depth were taken at each site, soils were sieved through a 2 mm sieve then stored at -20°C prior to DNA extraction.

In the months prior to sampling, the field was treated with herbicides, fungicides, insecticides and lime (Table 6), with additional adjuvants for spraying (not listed). Sampling was completed post-harvest each year to account for microbial variation due to cropping practices and to ensure weather conditions were similar at the time of sampling. Sampling took place on 12/09/18, 31/07/19 and 17/08/20 for the 2018-2020 growing seasons. Spring beans were grown in 2018, winter wheat was grown in 2019 and the field was fallow in 2020.

Table 6 Crops and treatments applied to Harold Smiths field during the 2018-2020 growing seasons.

Growing season	Treatment type	Date applied	Treatment details
2018	Crop	23/04/18	250 kg ha ⁻¹ Vertigo spring beans
	Fungicide	22/06/18	40 g ha ⁻¹ cyproconazole and 375 g ha ⁻¹ chlorothalonil
		17/07/18	40 g ha ⁻¹ cyproconazole and 375 g ha ⁻¹ chlorothalonil
		28/06/18	100 g ha ⁻¹ azoxystrobin and 500 g ha ⁻¹ chlorothalonil
		25/04/18	36 g ha ⁻¹ clomazone
	Herbicide	25/04/18	2.4 kg ha ⁻¹ prosulfocarb
		05/06/18	81.8 g ha ⁻¹ propaquizafop
		25/04/18	1.1 kg ha ⁻¹ pendimethalin
		24/03/18	1.44 kg ha ⁻¹ glyphosate
		25/04/18	360 g ha ⁻¹ glyphosate
		20/08/18	1.44 kg ha ⁻¹ glyphosate
		Insecticide	04/07/18
	17/07/18		7.5 g ha ⁻¹ lambda-cyhalothrin
	Lime	28/06/18	2 t ha ⁻¹ calcium lime
2019	Crop	14/09/18	165.5 kg ha ⁻¹ Dunston C2 winter wheat
	Herbicide	15/09/18	2.4 kg ha ⁻¹ prosulfocarb
		26/10/18	50 g ha ⁻¹ diflufenican
		26/10/18	2.5 g ha ⁻¹ florasulam
		15/09/18	60 g ha ⁻¹ diflufenican and 240 g ha ⁻¹ flufenacet
		26/10/18	32 g ha ⁻¹ picolinafen and 640 g ha ⁻¹ pendimethalin
	Insecticide	08/10/18	15 g ha ⁻¹ zetacypermethrin
		26/10/18	5 g ha ⁻¹ lambda-cyhalothrin
	Lime	09/04/19	2 t ha ⁻¹ calcium lime
	Molluscicide	14/09/18	90 g ha ⁻¹ ferric phosphate
	Trace Elements	08/10/18	300 g ha ⁻¹ manganese
08/10/18		640 g ha ⁻¹ manganese	
2020	Herbicides	30/10/19	2.5 g ha ⁻¹ arylex and 12 g ha ⁻¹ picloram
		10/10/19	100 g ha ⁻¹ propaquizafop
		16/06/20	1.08 kg ha ⁻¹ glyphosate
		27/03/20	1.08 kg ha ⁻¹ glyphosate
	Insecticides	14/09/19	72 g ha ⁻¹ thiacloprid
		14/09/19	7.5 g ha ⁻¹ lambda-cyhalothrin
		30/10/19	7.5 g ha ⁻¹ lambda-cyhalothrin
	Lime	20/04/20	200 kg ha ⁻¹ calcifert
		19/05/20	200 kg ha ⁻¹ calcifert
	Molluscicides	25/08/19	167.8 g ha ⁻¹ ferric phosphate

3.2.2. *Development of a spike-in quantification system for amplicon sequences*

Following the use of a spike-in 16S rRNA gene copy number quantification technique (2.2.2) using *Thermus thermophilus* DNA, a technique was developed to quantify the functional denitrification genes during amplicon sequencing.

As it was not possible to find a bacterium possessing the denitrification genes of interest that would reliably not be found in UK soils, synthetic spike-in DNA standards were designed instead. Primers were designed that would amplify regions of the pUC18 *E. coli* plasmid that were the same length as the gene amplicons (16S rRNA, *nirK*, *nirS* and *nosZ(I)*), with 5' overhangs on the primers that were complementary to the amplicon primers for sequencing using the process shown in Figure 11.

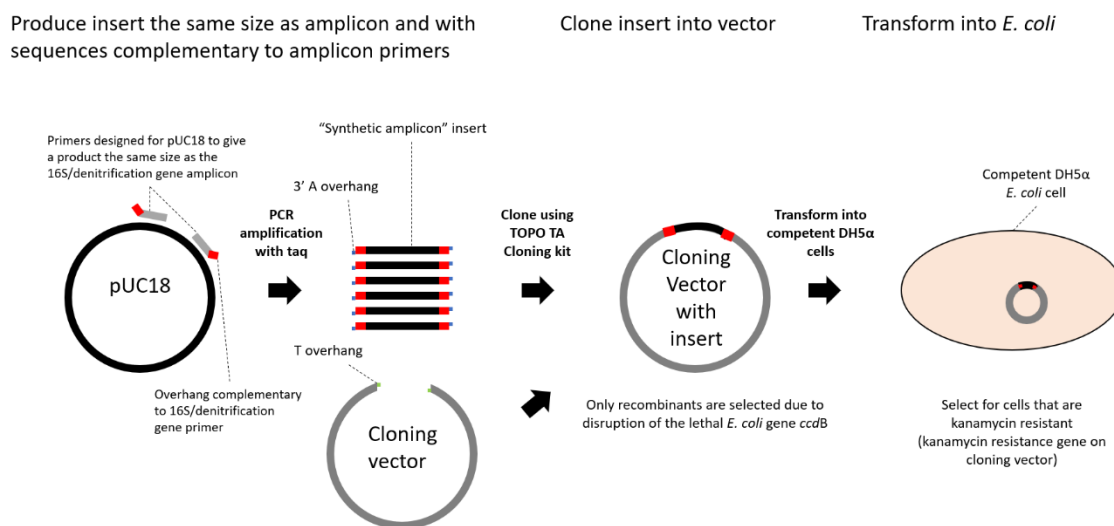


Figure 11 Overview of production of synthetic spike-in DNA standards for spike-AMP quantification of amplicon abundance during sequencing.

pUC18 plasmid was isolated from DH5α cells using a Plasmid Miniprep kit (Qiagen). Synthetic internal standard amplicons were produced by PCR amplification with the primers shown in Table 7 using pUC18 plasmid as template DNA. (PCR conditions: 2 min at 95°C;

25 cycles of 30s at 95°C, 45s at 55°C, 1 min at 72°C; and a final extension of 10 min at 72°C). PCR was performed in a total volume of 50µl containing 10µl 5X GoTaq colourless PCR buffer (7.5mM MgCl₂) (Promega), 200µM of each deoxynucleotide triphosphate, 1.25U of GoTaq polymerase (Promega), 200mM of each primer and 37.5ng template DNA. The PCR products were purified using QIAquick PCR Purification Kit (Qiagen) and then cloned into pCRII-TOPO Vector using TOPO TA cloning (Thermo Fisher Scientific) and transformed into chemically competent DH5α cells to increase DNA stability, following the manufacturer's protocol (Figure 11).

Plasmids containing the spike-in DNA standard were then isolated using QIAprep Spin Miniprep Kit (Qiagen) and quantified using Qubit fluorometric quantitation (Thermo Fisher Science). 1% of the expected DNA extracted from the soil (19.47 ng), based on triplicate DNA extraction from Harold Smiths soils, was added to each soil sample prior to DNA extraction. Gene copy number was then calculated based on the number of reads containing the spike-in DNA sequences obtained during sequencing as described in section 2.2.2.

Table 7 Primers used to produce synthetic spike-in DNA standards for gene copy number quantification using pUC18 plasmid as template DNA.

Gene for standard	Overhang (5'-3') for PCR with soil DNA	pUC18 primer (5'-3')	Product size (bp)	Anneal temp. (°C)
16S rRNA	GTGYCAGCMGCCGCGGTAA	TTGGTAGCTCTTGATCCGGC	372	55
	GGACTACNVGGGTWTCTAAT	AGCCCTCCCGTATCGTAGTT		
<i>nirK</i>	GGMATGGTKCCSTGGCA	ACTACGATACGGGAGGGCTT	392	55
	GAACTTGCCGGTVGYCCAGAC	AGTGATAAACTGCGGCCAA		
<i>nirS</i>	G TSAACG TSAAGGARACSGG	CCTGGGGTGCCTAATGAGTG	413	55
	GASTTCGGRTGSGTCTTGA	TTCGCCACCTCTGACTTGAG		
<i>nosZ(I)</i>	CGYTGTTTCMTCGACAGCCAG	TGTAGGCGGTGCTACAGAGTTC	415	58

3.2.3. *DNA extraction and amplicon sequencing*

Genomic DNA was extracted from all 48 spatial study samples and 12 temporal study samples for community 16S rRNA gene and denitrification gene amplicon sequence analysis and quantification. DNA was extracted from 0.25 g soil using the DNeasy PowerSoil DNA isolation kit (Qiagen), used according to the manufacturer's protocol. The quality of nucleic acid extractions was verified in SybrSafe-stained (Thermo Fisher Scientific) 1.0% agarose gels. DNA concentration and purity were quantified using a NanoDrop spectrophotometer (Thermo Fisher Scientific).

For total bacterial community analyses, the V4-V5 region of the 16S rRNA gene was amplified for each soil using 515F/806R primers (Walters *et al.*, 2016). To assess nitrogen cycling gene abundance and diversity, primers for the nitrite reductases *nirK* (Braker *et al.*, 1998) and *nirS* (Throbäck *et al.*, 2004) were used as well as nitrous oxide reductase *nosZ* clade (I) (Kloos *et al.*, 2001; Throbäck *et al.*, 2004) using the primers and thermal profiles listed in Table 8. All primers included overhang adapters (forward:TCGTCGGCAGCGTCAGATGTGTATAAAGAGACAG, adapter:GTCTCGTGGGCTCGGAGATGTGTATAAAGAGACAG) to allow the subsequent addition of multiplexing index-sequences. Additionally, a 13-base random sequence was added between the adapter and locus-specific sequence of the forward primer to prevent false clustering during sequencing.

For 16S rRNA and *nirK* amplification, PCR was performed in a total volume of 50µl containing 10µl 5X GoTaq colourless PCR buffer (7.5mM MgCl₂) (Promega), 200µM of each deoxynucleotide triphosphate, 1.25U of GoTaq polymerase (Promega), 200mM of each primer and 37.5ng template DNA. In accordance with Braker *et al.* (Braker *et al.*, 2000), an additional 1.0mM MgCl₂ and 15µg BSA were also added. For *nirS* and *nosZ(I)* PCR

amplification, reactions were performed in a total volume of 25µl containing 5µl 5X GoTaq colourless PCR buffer (7.5mM MgCl₂) (Promega), 200µM of each deoxynucleotide triphosphate, 1.25U of GoTaq polymerase (Promega), 400mM of each primer and 50ng DNA. 15µg BSA was also added.

Table 8 Primers and thermal profiles of PCR reactions for amplicon sequencing

Target gene	Primer	Sequence	Thermal profile	Amplicon size (bp)	Reference
16S rRNA	515F	GTGYCAGCMGC CGCGGTAA	2 min at 95°C followed by 35 cycles of 30s at 95°C, 45s at 53°C and 60s at 72°C with an additional 10 min extension at 72°C	372	(Walters <i>et al.</i> , 2016)
	806R	GGACTIONVGGG TWTCTAAT			
<i>nirK</i>	<i>nirK1F</i>	GGMATGGTKCCS TGGCA	2 min at 95°C followed by 35 cycles of 30s at 95°C, 45s at 53°C and 60s at 72°C with an additional 10 min extension at 72°C	392	(Braker <i>et al.</i> , 1998)
	<i>nirK3R</i>	GAACTTGCCGGT VGYCCAGAC			
<i>nirS</i>	cd3aF	G TSAACG TSAAG GARACSGG	2 min at 95°C followed by 35 cycles of 30s at 95°C, 60s at 57°C and 60s at 72°C with an additional 10 min extension at 72°C	413	(Throbäck <i>et al.</i> , 2004)
	R3cd	GASTTCGGRTGS GTCTTGA			
<i>nosZ</i> (I) ^a	nosZ-F	CGYTGTTCMTCG ACAGCCAG	2 min at 95°C followed by 35 cycles of 30s at 95°C, 60s at 53°C and 60s at 72°C with an additional 10 min extension at 72°C	415	(Kloos <i>et al.</i> , 2001)
	nosZ1622R	CGCRASGGCAAS AAGGTSCG			
<i>nosZ</i> (I) ^b	nosZ2F	CGCRACGGCAAS AAGGTSMSSGT	2 min at 95°C followed by 35 cycles of 30s at 95°C, 30s at 56°C and 30s at 72°C with an additional 10 min extension at 72°C	267	(Henry <i>et al.</i> , 2006)
	nosZ2R	TCAKRTGCAKSG CRTGGCAGAA			

^a primers *nosZ-F/nosZ1622R* were used for the 2018 spatial samples but found to amplify non-specific targets, so were not included in the analysis. ^b primers *nosZ2F/nosZ2R* were used to amplify *nosZ* for all temporal samples (2018-2020).

PCR products were purified using QIAquick PCR Purification Kit (Qiagen) and quantified using NanoDrop spectrophotometer (Thermo Fisher Scientific) and Qubit Fluorometer

(Thermo Fisher Scientific). Amplicons libraries were prepared for sequencing using Nextera XT DNA Library Preparation Kit (Illumina) by the Bioscience Technology Facility at the University of York and sequenced using the Illumina MiSeq platform with 300bp paired-end sequencing.

Sequences were analysed using the dada2 pipeline in the dada2 R package (Callahan *et al.*, 2016). Sequences were filtered and trimmed to a quality score above 25. Error rates were calculated from the first 100 million bases using the LearnErrors function from dada2. Sequences were dereplicated and dada2 high resolution sample inference was used to resolve exact amplicon sequence variants (ASVs). Paired reads were merged, chimeras removed, and a sequence table was assembled. Taxonomy was assigned to the 16S rRNA using the SILVA reference database version 138.1 (McLaren and Callahan, 2021). For denitrification genes, ASVs were used, with reads manually verified using the FunGene database (Fish *et al.*, 2013). All reads relating to eukaryotic, mitochondrial and chloroplast DNA was removed from the 16S ASV table prior to community analysis, along with all spike-in DNA reads following gene copy number quantification. The *nosZ(I)* primers in the spatial experiment (*nosZ-F/nosZ1622R*) were found to have amplified many non-specific targets at this stage, so the analysis was discontinued for *nosZ* amplicons. Alternative primers (*nosZ2F/nosZ2R*) were used for the temporal analysis.

3.2.4. *qPCR of 16S and denitrification genes*

To assess the effects of variability in gene copy number and evaluate the accuracy of the spike-in DNA quantification system, real-time qPCR was used. Absolute quantification of target genes 16S rRNA and denitrification genes (*nirK* and *nirS*) was carried out in triplicate on a QuantStudio 3 Real-Time PCR System (Thermo Fisher Scientific).

Prior to quantification of specific genes, a qPCR inhibition assay was carried out to assess the levels of PCR inhibition caused by co-extracted inhibitors in the samples. This was done by adding a known amount of pUC18 plasmid (purified from *Escherichia coli* DH5 α using

QIAprep Spin Miniprep Kit (Qiagen) according to the manufacturer's protocol) to 10 ng of template DNA or nuclease-free water, followed by real-time quantitative PCR (qPCR) with plasmid-specific primers for each sample. The primers were designed using Benchling and produced a 124 bp amplicon, (pUC18F_qPCR: ATCCGGCAAACAAACCACCGCT and pUC18R_qPCR: CCACTGAGCGTCAGACCCCGTA). The PCR was performed in a total volume of 20 μ l containing 10 μ l Fast SYBR Green Master Mix (Thermo), 250 mM of each primer, 10 ng soil extracted DNA and 0.152ng pUC18 plasmid or nuclease-free water for the no-template controls. PCR included an initial denaturation step of 20 s at 95°C followed by forty cycles of 1 s at 95°C with 30 s at 60°C and a melt curve analysis was used to check target specificity. Inhibition was tested by comparing quantification cycle (Cq) values between reactions with soil DNA template and non-template controls using "pairwise.wilcox.test" using the FDR method of p adjustment for multiple comparisons.

To generate quantification standards for qPCR, longer regions of the gene of interest were amplified from bacterial isolates for 16S rRNA and *nirK* using the primers and strains shown in Table 9. (PCR conditions: 2 min at 95°C; 25 cycles of 30 s at 95°C, 45 s at 55°C, 1 min at 72°C; and a final extension of 10 min at 72°C.) PCR was performed in a total volume of 50 μ l containing 10 μ l 5X GoTaq colourless PCR buffer (7.5 mM MgCl₂) (Promega), 200 μ M of each deoxynucleotide triphosphate, 1.25 U of GoTaq polymerase (Promega), 200 mM of each primer and 37.5 ng template DNA. The PCR products were purified using QIAquick PCR purification kit (Qiagen) and subsequently cloned into pCRII-TOPO Vector using TOPO TA cloning (Thermo Fisher Scientific) with chemically competent DH5 α cells. Plasmids were isolated using QIAprep spin miniprep kit (Qiagen), quantified using Qubit fluorometric quantitation (Thermo Fisher Science) and standard curves ranging from 10³ to 10⁹ gene copies μ l⁻¹ were generated. Plasmids generated in section 3.2.2. were used as qPCR standards for *nirS*, as they contained primer sites complementary to the qPCR primers.

Table 9 Primers used for the construction of qPCR-standards

Gene	Strain/template DNA	Primer	Sequence	Amplicon size (bp)
16S rRNA	<i>Acinetobacter guillouiae</i>	27F	AGAGTTTGATCMTGGCTCAG	1465
		1492R	GGWTACCTTGTTACGACTT	
<i>nirK</i>	<i>Achromobacter xylosoxidans</i>	A.xyl <i>nir</i> KF	GACAAGCTGCCCCATACCAA	972
		A.xyl <i>nir</i> KR	CTGCTTCATCAGGTCGTCGT	
<i>nirS</i>	pUC18 isolated from <i>Escherichia coli</i> DH5 α	pUC18 <i>nir</i> SF	G TSAACG TSAAGGARACSGGCCTGGG GTGCCTAATGAGTG	413
		pUC18 <i>nir</i> SR	GASTTCGGRTGSGTCTTGATTCGCCA CCTCTGACTTGAG	

Absolute quantification of all investigated target genes was carried out in 20 μ l samples with the primers, reagents and thermal profiles given in Table 10. The specificity of the amplification products was confirmed by melt-curve analysis. No template controls gave a null or negligible values. Standard curves with efficiencies ranging from 88 to 99% were obtained for DNA quantification standards.

Table 10 Quantitative PCR primers, reaction mixtures and thermal profiles for the different target genes

Target gene	Primer	Sequence	Amplicon size (bp)	Reaction mixture	Volume (µl)	Thermal profile	Reference
16S rRNA	341f	CCTACGGGAGGCAGCAG	194	Fast SYBR® Green Master Mix	10	95 °C 20 s	(Watanabe <i>et al.</i> , 2001)
	534r	ATTACCGCGGCTGCTGGCA		341f (5 µM)	1	40 cycles	
				534r (5 µM)	1	95 °C 1 s	
				BSA (20% w/v)	0.5	60 °C 30 s	
				Nuclease free water	5.5		
			Template (5-50 ng µl ⁻¹)	2			
<i>nirK</i>	<i>nirK876C</i>	ATYGGCGGVCA YGGCGA	164	Fast SYBR® Green Master Mix	10	95 °C – 20 s	(Henry <i>et al.</i> , 2004)
	<i>nirK1040</i>	GCCTCGATCAGRTRTGG		<i>nirK876C</i> (5 µM)	1	40 cycles	
				<i>nirK1040</i> (5 µM)	1	95 °C – 1 s	
				Nuclease free water	6	59 °C – 30 s	
				Template (5-50 ng µl ⁻¹)	2		
<i>nirS</i>	cd3af	GTNAA YGTNAARGARACNGG	413	Fast SYBR® Green Master Mix	10	95 °C – 20 s	(Michotey <i>et al.</i> , 2000)
	R3cd	GASTTCGGRTGSGTCTTGA		cd3af (5 µM)	2	40 cycles	
				R3cd (5 µM)	2	95 °C – 1 s	
				Nuclease free water	4	57 °C – 40 s	
				Template (5-50 ng µl ⁻¹)	2	72 °C – 40 s	

3.2.5. *Determination of soil physicochemical properties*

Soil physicochemical analyses were carried out in triplicate to determine soil properties. pH was measured in H₂O in 1:2.5 w/v suspensions using a pH probe (Fisherbrand accumet AB315, FisherSci) (Avery and Bascomb, 1974). Soil organic matter (SOM) content was determined using the Loss on Ignition method, with 0.1 g soil heated at 550 °C overnight (Ball, 1964). Gravimetric water content was calculated by dividing the mass of water lost when soil was dried at 105 °C for 24 hours by the mass of the dry soil (Avery and Bascomb, 1974). Bulk density was calculated by heating 5 cm³ soil at 105 °C for 24 hours and dividing the dried soil weight by the wet soil volume (Avery and Bascomb, 1974). Water filled pore space (WFPS) was derived from gravimetric water content and bulk density using a particle density of 2.65 g cm⁻³ (Franzluebbers, 1999).

Ion-exchange chromatography was used to measure the concentration of nitrate, nitrite and phosphate in the soils using a Dionex ICS-2000 (Thermo Scientific). Chromatography samples were prepared by suspending soil in water 10% (w/v) with vigorous shaking, before centrifugation for 5 minutes at 1,800 x g at room temperature. Supernatant was filtered (0.22 μm) and loaded onto the Dionex ICS-2000 using the AS40 autosampler (Dionex) with a 25 μl loop. Area under the chemical trace peak (μS*min) was calculated using Chromeleon Chromatography Data System software (Thermo Fisher Scientific). Nitrate and phosphate standards from 0.5 – 30 μg/ml and nitrite standards from 0.05 – 2 μg/ml were used to formulate a standard curve to calculate the concentrations of the target molecules. Derived C:N ratios were calculated by dividing soil organic matter by available N (defined as total nitrate and nitrite percentage per g soil (w/w)).

3.2.6. *Statistical and diversity analysis*

Statistical and diversity analyses were performed using R version 4.2.0 (R Core Team, 2022) implemented in RStudio version 2022.02.3.492 (RStudio Team, 2022). Physicochemical soil data was analysed using two-way analysis of variance (ANOVA) using the lmer function from the lmerTest package (Kuznetsova *et al.*, 2017), with yield category and shallow conductivity

category as factors with year as a random factor. Percentage data was arcsine-square root transformed prior to analysis.

For sequence analysis, the `multipatt` function from the `indicspecies` package (De Cáceres and Legendre, 2009) was used to perform Dufrene-Legendre indicator species analysis to identify bacteria that were specifically associated with different environments. Alpha diversity was compared across samples using species richness (observed ASVs), the Shannon index and Pielou's evenness index (Shannon, 1948; Pielou, 1966). Differences in alpha diversity were tested using two-way ANOVA as described above. Beta-diversity was represented by Bray-Curtis distance (Roger, Bray and Curtis, 1957) and weighted UniFrac distance (Lozupone and Knight, 2005). Bray-Curtis was calculated from the ASV table using the `vegdist` function from `vegan` (Oksanen *et al.*, 2022). Weighted UniFrac was calculated using the `UniFrac` function from the `phyloseq` package (McMurdie and Holmes, 2013). Weighted UniFrac distance was generated from the normalised ASV table and phylogenetic tree produced through amplicon sequence alignment, neighbour joining of distance matrix and rooting using the longest branch.

Pearson product-moment correlation was used to test for correlation between gene copy number as calculated using spike-in standards during sequencing to gene copy number calculated using qPCR with the `cor.test` function. Function `adonis2` in the R package `vegan` (Oksanen *et al.*, 2013) was used to quantify the possible associations between yield or conductivity and beta-diversity. Non-metric multidimensional scaling plots (NMDS) were used to visually represent community dissimilarities between samples based on the Bray-Curtis or Weighted UniFrac index using the `isoMDS` function in `MASS`. Euclidean distance matrices were composed using the `vegdist` function in `vegan` before Mantel tests were conducted to measure the correlation between spatial distance and beta diversity and between environmental data and beta diversity.

3.3. Results

3.3.1. Physicochemical field properties

Table 11 Summary of sampling location details within Harold Smiths Field (A) and soil physicochemical soil properties (B). All values are interaction means of three replicates with standard errors given in brackets. ¹ LY = low yield, HY = high yield, LC = low conductivity & HC = high conductivity.

A. Sampling location details												
Year	2018				2019				2020			
Crop	Spring beans				Winter wheat				Fallow			
Site designation	LYLC	LYHC	HYLC	HYHC	LYLC	LYHC	HYLC	HYHC	LYLC	LYHC	HYLC	HYHC
2018 Yield (t ha ⁻¹)	1.43	1.43	2.75	2.75	1.43	1.43	2.75	2.75	1.43	1.43	2.75	2.75
Conductivity (mS m ⁻¹)	< 16.9	> 27.1	< 16.9	> 27.1	< 16.9	> 27.1	< 16.9	> 27.1	< 16.9	> 27.1	< 16.9	> 27.1
Soil type	Clay loam	Clay loam	Clay loam	Clay loam	Clay loam	Clay loam	Clay loam	Clay loam	Clay loam	Clay loam	Clay loam	Clay loam
B. Soil physicochemical properties												
Bulk density (g cm ⁻³)	1.22 (±0.01)	1.05 (±0.01)	1.12 (±0.01)	1.15 (±0.02)	0.74 (±0.01)	0.99 (±0.02)	0.97 (±0.02)	1.02 (±0.01)	1.16 (±0.01)	1.04 (±0.01)	1.06 (±0.01)	1.00 (±0.01)
Derived C:N ***	5.81 (±0.66)	9.70 (±0.79)	8.41 (±0.92)	6.16 (±0.32)	5.06 (±0.69)	8.62 (±0.48)	3.13 (±0.07)	3.25 (±0.08)	12.9 (±1.18)	23.8 (±1.85)	7.53 (±0.38)	11.1 (±1.48)
Gravimetric water content (%)	3.80 (±0.02)	9.16 (±0.18)	5.63 (±0.04)	6.71 (±0.07)	34.5 (±0.28)	22.4 (±0.07)	28.1 (±0.33)	24.5 (±0.07)	19.9 (±0.02)	24.3 (±0.14)	21.9 (±0.01)	23.5 (±0.12)
Nitrate (mg kg ⁻¹) ***	17.0 (±1.40)	10.4 (±0.35)	10.3 (±1.07)	12.7 (±1.00)	28.5 (±0.06)	12.2 (±0.01)	32.6 (±0.04)	23.9 (±0.06)	7.51 (±0.01)	4.47 (±0.01)	8.99 (±0.01)	6.79 (±0.01)
Nitrite (mg kg ⁻¹)	7.70 x 10 ⁻³ (±1 x 10 ⁻³)	4.43 x 10 ⁻³ (±1 x 10 ⁻³)	6.38 x 10 ⁻³ (±2 x 10 ⁻³)	8.53 x 10 ⁻³ (±3 x 10 ⁻³)	2.03 x 10 ⁻³ (±3 x 10 ⁻⁵)	1.23 x 10 ⁻³ (±3 x 10 ⁻⁵)	9.70 x 10 ⁻⁴ (±3 x 10 ⁻⁵)	6.70 x 10 ⁻⁴ (±3 x 10 ⁻⁵)	6.30 x 10 ⁻³ (±3 x 10 ⁻⁵)	6.30 x 10 ⁻⁴ (±1 x 10 ⁻⁴)	2.13 x 10 ⁻³ (±2 x 10 ⁻⁴)	3.47 x 10 ⁻³ (±3 x 10 ⁻⁵)
Organic matter (%) ***	9.72 (±0.37)	10.1 (±0.46)	8.50 (±0.22)	7.74 (±0.22)	14.4 (±2.00)	10.5 (±0.59)	10.2 (±0.25)	7.77 (±0.19)	9.69 (±0.89)	10.7 (±0.83)	6.78 (±0.34)	7.52 (±1.01)
Phosphate (mg kg ⁻¹) *	0.36 (±0.02)	0.30 (±0.03)	0.44 (±0.01)	0.25 (±0.01)	0.38 (±0.01)	0.33 (±0.01)	0.46 (±0.01)	0.49 (±0.01)	0.09 (±0.01)	0.19 (±0.01)	0.09 (±0.01)	0.24 (±0.01)
pH *	6.28 (±0.11)	6.51 (±0.02)	6.25 (±0.07)	6.26 (±0.07)	5.61 (±0.01)	5.51 (±0.03)	5.45 (±0.02)	5.75 (±0.02)	6.82 (±0.01)	6.42 (±0.02)	6.56 (±0.03)	7.01 (±0.01)

¹ Stars indicate p values of Linear Mixed Effects model with year as a random factor (* indicates p < 0.05, ** p < 0.01, *** p < 0.001).

Harold Smiths field soil properties were assessed to determine how much variation occurred spatially within the field and how stable these within-field trends were over time. Bulk density

was not found to differ significantly across the field. And, although bulk density was considerably lower in 2019, particularly for the LYLC soil, this may be attributed to factors such as rainfall. 2019 had much higher annual rainfall than the other years, with the effect being seen through increased gravimetric water content in 2019 soils (Table 11). Interestingly however, there were no significant trends in gravimetric water content across the four sites, despite the expectation that shallow soil electrical conductivity results would provide a good proxy for soil moisture content. The temporal instability of gravimetric water content, bulk density and derived water filled pore space within these four sampling locations suggests that soil water retention may be more variable than previously anticipated.

Available nitrate was higher in low conductivity sites relative to the high conductivity sites (Table 11; Conductivity: $F_{1,30} = 21.47$; $p = 6.54e-05$). Available nitrite was relatively higher for low conductivity sites in areas of high yield, but higher for high conductivity sites in areas of low yield (Conductivity * Yield: $F_{1,30} = 10.16$; $p = 0.0033$). Available phosphate was higher in high yield sites (Yield: $F_{1,30} = 5.77$; $p = 0.23$). However, none of the trends for available molecules were fully consistent over the three-year period.

pH also differed over time, but in general, the high conductivity sites had an increased pH in the high yield areas and a decreased pH in the low yield sites (Conductivity * Yield: $F_{1,30} = 10.26$; $p = 0.0032$). One of the strongest and most consistent associations was increased soil organic matter within the low yield sites (Yield: $F_{1,30} = 29.5$; $p = 6.86e-06$). The derived C:N, based on soil organic matter and total available nitrate and nitrite, was highest in the 2020 soils, when the field had been fallowed for one year. As with SOM, C:N was significantly increased in low yield sites (Yield: $F_{1,30} = 20.81$; $p = 7.99e-05$), additionally, high conductivity sites had increased C:N (Conductivity: $F_{1,30} = 11.72$; $p = 0.0018$), with a significant interaction present between the two variables (Conductivity * Yield: $F_{1,30} = 8.66$; $p = 0.006$). These results indicate that there was substantial environmental variation across the field, beyond the factors accounted for in the sampling strategy.

3.3.2. *Bacterial and denitrification gene abundance*

The qPCR inhibition test described in 3.2.4. showed that no significant inhibition was detected for the amount of template DNA used in the reactions based on comparing quantification cycle (C_q) values between reactions with soil DNA template and non-template controls, with none of the FDR adjusted p values of the multiple Kruskal-Wallis pairwise comparisons below 0.05. Interestingly many of the soil DNA samples reduced C_q, rather than increasing it as would be expected by inhibition (Figure 12). However, since none of these values differed significantly from the no-template control, it was assumed that there was no significant effect of soil extracted DNA on qPCR efficiency.

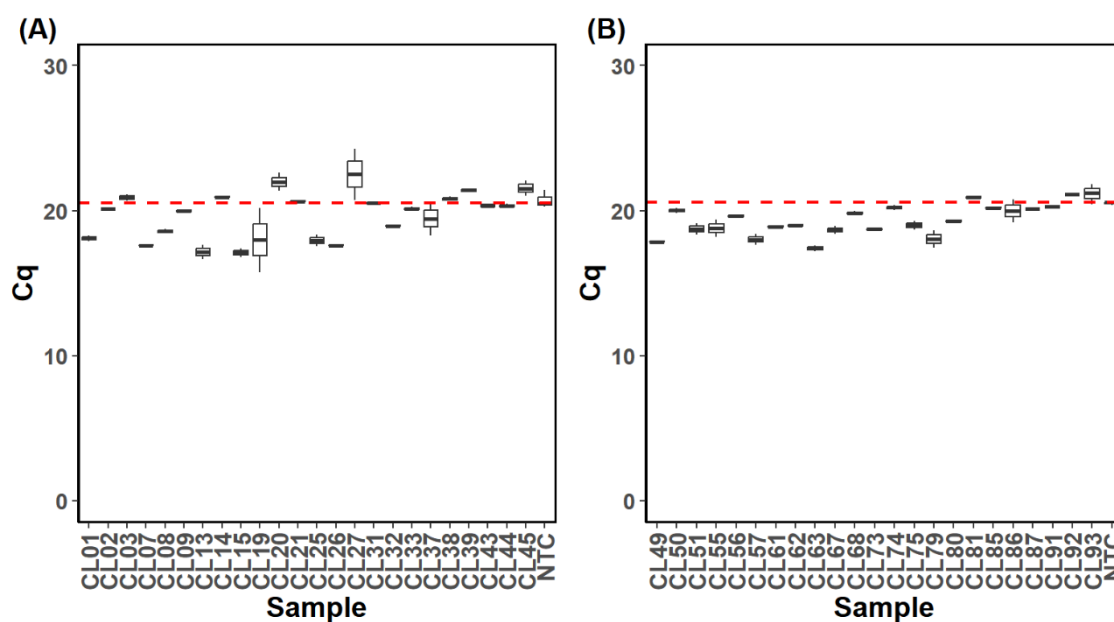


Figure 12 C_q values obtained during qPCR inhibition test on qPCR Plate 1 (A) and Plate 2 (B). The red line indicates median C_q value obtained from the no-template control (NTC) for each plate. All samples contained equal amounts of pUC18 template DNA.

Following this inhibition assay, qPCR was completed on soil samples using the conditions stated in Table 10 to determine the copy number of 16S rRNA and denitrification genes (*nirK*, *nirS* and *nosZ(I)*) to assess gene abundance and also to validate the spike-in synthetic DNA quantification method proposed in 3.2.2.

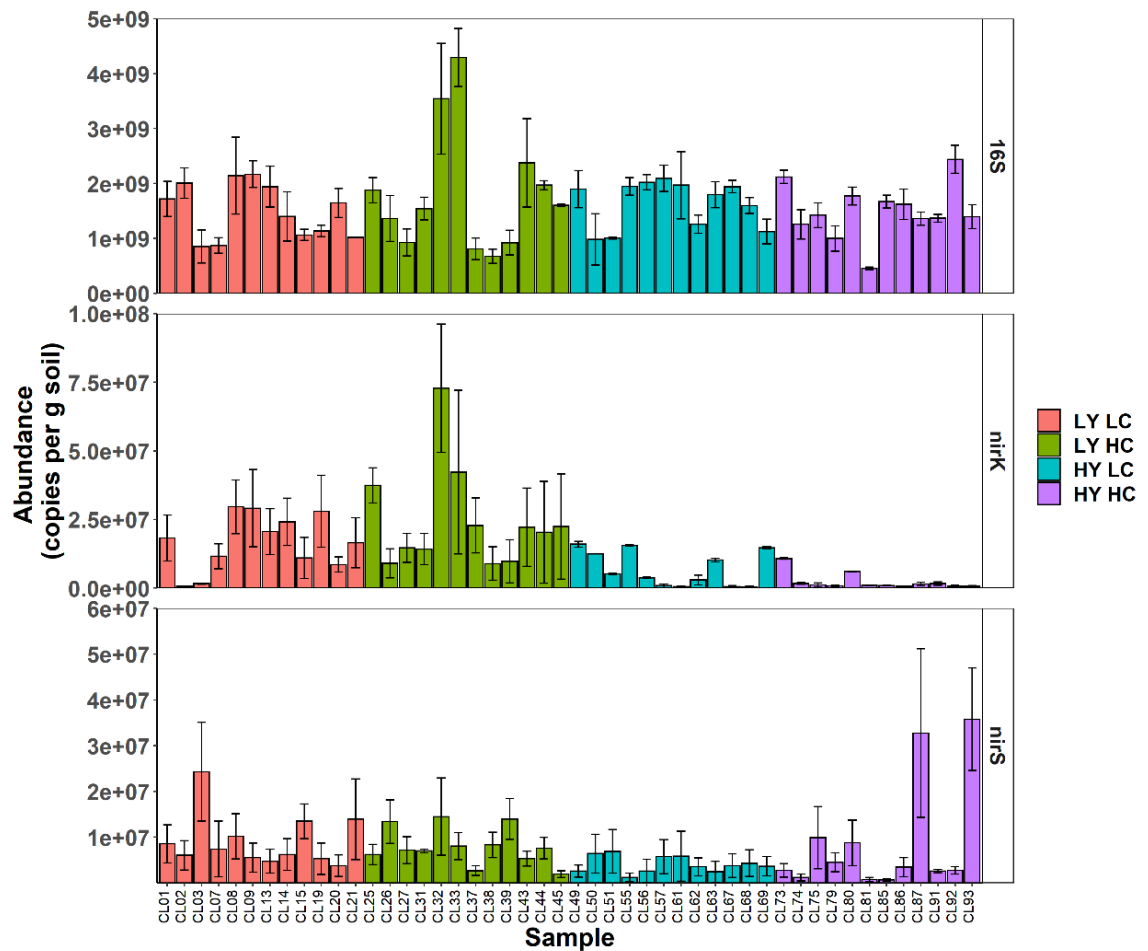


Figure 13 qPCR derived gene copy numbers per g soil. Bars indicate mean of three replicates with standard error shown. Colours indicate field zone of soil sample: pink = low yield, low conductivity, green = low yield, high conductivity; blue = high yield low conductivity and purple = high yield, high conductivity.

The average number of 16S rRNA genes per g soil was 1.61×10^9 ($\pm 9.92 \times 10^7$ standard error) and this did not differ significantly between sample areas (Conductivity: $F_{1,138} = 0.21$; $p = 0.64$; Yield: $F_{1,138} = 0.16$; $p = 0.68$; Conductivity * Yield: $F_{1,138} = 2.31$; $p = 0.13$). However, it was notable that samples CL32 and CL33 from the low yield high conductivity soil had more than double the mean copies of 16S (Figure 13).

NirK copies were found to be significantly higher in low yield soils (2.07×10^7 *nirK* per g soil $\pm 2.18 \times 10^6$) compared to high yield soils (8.44×10^5 *nirK* per g soil $\pm 8.78 \times 10^4$); (Yield: F = 58.1338, Df = 1, 134, p = 4.024e-12). Yield was also significantly associated with *nirS* copies with low yield soils having a mean of 8.56×10^6 *nirS* per g soil ($\pm 7.13 \times 10^5$) compared to high yield soils which only had 6.44×10^6 *nirS* per g soil ($\pm 1.28 \times 10^6$); (Yield: F = 4.2200, Df = 1, 136, p = 0.04187). The association between field area and *nirS* is relatively weaker than that of *nirK* due to high *nirS* abundances in two high yield, high conductivity samples (CL87 and CL93, Figure 13).

These results indicate that 16S abundance was much higher than *nirK* or *nirS* in these samples, with a ratio of 1:147 *nirK* genes compared to 16S, and 1:215 *nirS* genes compared to 16S. Our results also indicate that low yield areas of the field have comparable overall bacterial abundance to high yield areas, but relatively more nitrite reductase genes (for both *nirK* and *nirS*). This may be a key result for precision farming companies to make decisions surrounding fertilizer applications, but further study is needed to confirm this result.

3.3.3. *Verification of spike-in DNA for calculating absolute gene abundance*

These qPCR results were also used to verify the use of spike-in DNA to calculate gene abundance during amplicon sequencing (3.2.2.). Having previously used spike-in *Thermus thermophilus* DNA to quantify 16S rRNA abundance during amplicon sequencing (2.3.2.), a synthetic gene spike in method was developed to quantify the abundance of denitrification genes. Here, *T. thermophilus* derived 16S abundance was found to be strongly correlated to qPCR derived 16S rRNA abundance ($R^2 = 0.797$, p = 1.17×10^{-11} ; Figure 14A), despite different primers being used for qPCR and amplicon sequencing.

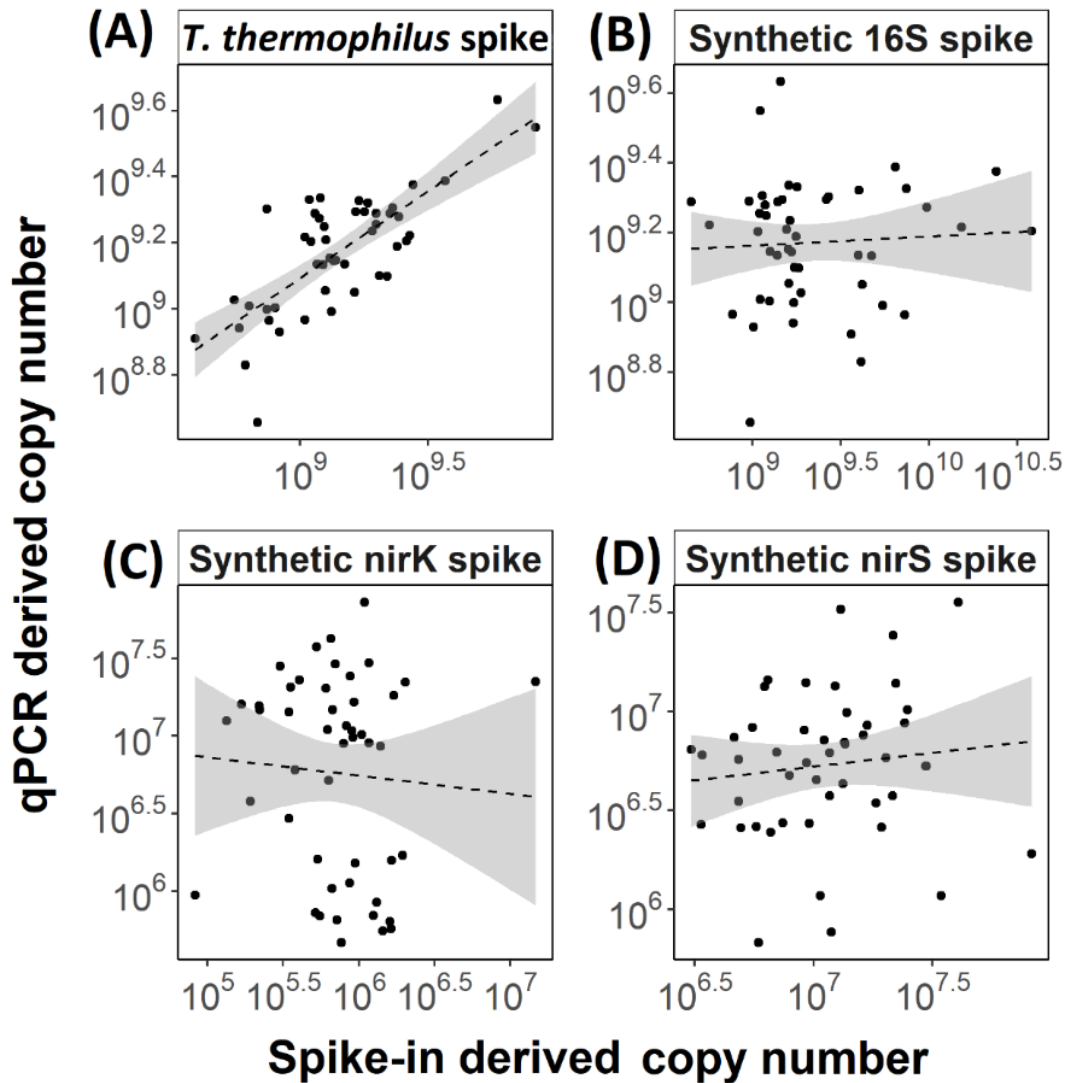


Figure 14 qPCR and spike-in DNA derived gene abundance comparison. (A) *T. thermophilus* spike-in derived 16S rRNA copy numbers, (B) synthetic 16S spike-in derived 16S copy number, (C) synthetic *nirK* spike-in derived *nirK* copy number and (D) synthetic *nirS* spike-in derived *nirS* copy number.

Disappointingly, there were no significant correlations between the synthetic DNA spike-in derived abundances and qPCR copy numbers for any of the genes tested (16S rRNA, *nirK* and *nirS*; Figure 14B:D). The synthetic spike was more likely to overestimate 16S and *nirS* copies, but underestimate *nirK*. Together, these results indicate that spike-in DNA for gene abundance quantification may be a reliable option using spike in DNA from organisms that won't be found in that environment but cannot reliably be determined using DNA constructs. Therefore, further

analysis will focus on the *T. thermophilus* derived 16S abundance and relative abundance of denitrification genes will be used.

3.3.4. Taxonomic spatiotemporal distribution

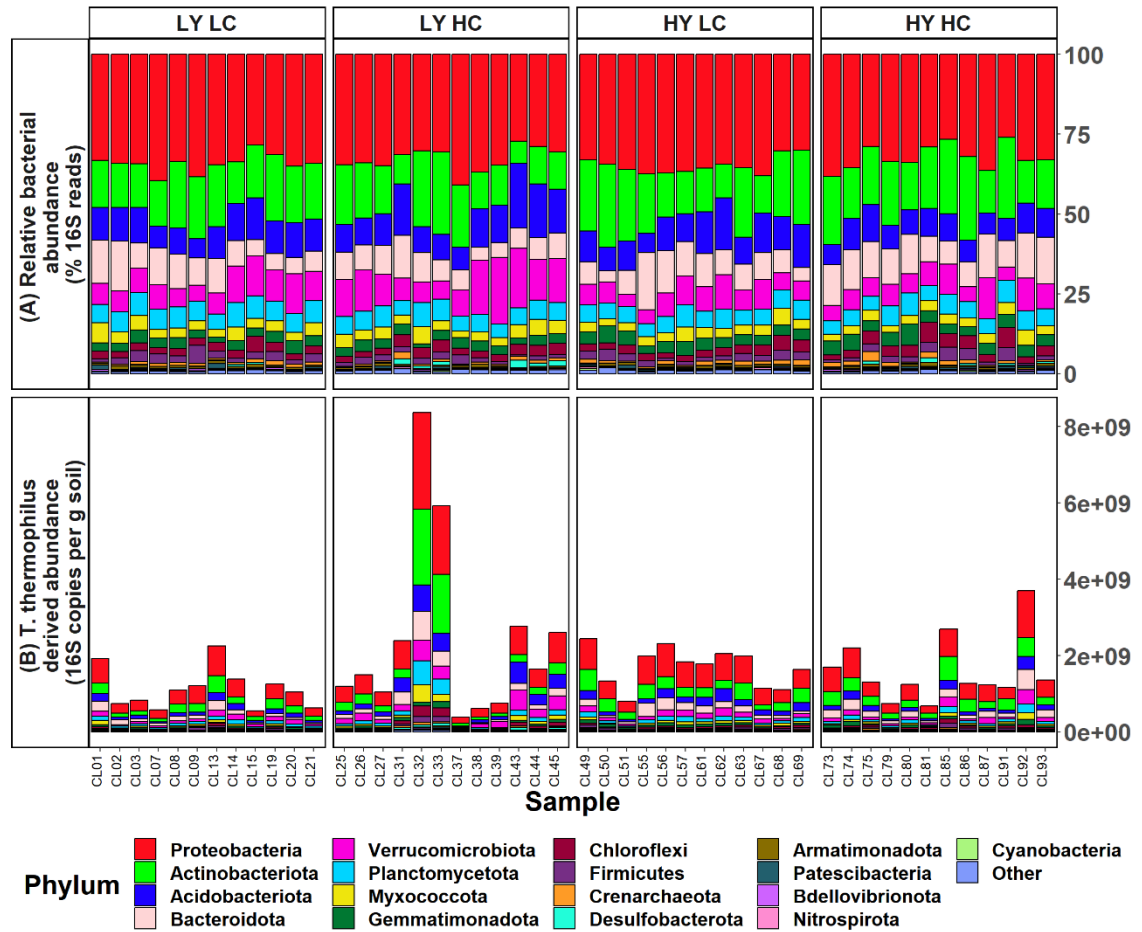


Figure 15 Relative (A) and absolute abundance (B) of phyla in Harold Smiths 2018 soils. 'Others' refers to all phyla with an abundance of less than 1% across samples.

In the 2018 soils microbial community was relatively evenly distributed over the four field zones (Figure 15A). Proteobacteria accounted for an average of 33.5% total reads, Actinobacteria 17.3%, with Acidobacteria and Bacteroidota (previously named Bacteroidetes) accounting for an average of 10% of total reads each. As observed previously, using absolute abundance in addition to relative abundance of 16S rRNA copies enables more in-depth community comparisons (Figure

15B). For example, where total number of 16S reads are reduced (CL07, CL38, CL39), there appears to be an increased proportion of Proteobacteria in the community. Low yield high conductivity samples (CL25 – CL45) had the most 16S copies with an average of 2.43×10^9 ($\pm 6.90 \times 10^8$); with low yield low conductivity samples (CL01 – CL21) having the fewest (1.12×10^9 16S per g soil $\pm 1.53 \times 10^8$). This is in accordance with the results obtained through qPCR. The low yield high conductivity samples showed the most variance, with samples CL32 and CL33 once again having more than double the average 16S abundance per gram of soil, and CL37-39 having the lowest copy numbers.

4,412 16S rRNA amplicon sequences variants (ASVs) were detected overall in the 2018 soils, with 462 ASVs associated with a given field zone or condition. Far more ASVs were associated with conductivity than yield with 207 ASVs compared to 53.

2018 low yield sites were specifically associated with 22 ASVs. These included four Planctomycetota and Verrucomicrobiota, three Actinobacteriota, Bacteroidota and Proteobacteria, two Acidobacteriota and one of Crenarchaeota, Chloroflexi and Firmicutes respectively. ASVs for *Nitrososphaera* and a *Solirubrobacter* were most strongly associated with the low yield sites ($p = 0.001$). The *Nitrososphaera* has close 16S sequence identity to *Nitrososphaera viennensis*, an ammonia oxidizing archaeon (Tourna *et al.*, 2011). The *Solirubrobacter* is likely to be a gram-positive aerobic endophyte (Wei *et al.*, 2014). High yield was associated with 31 ASVs. High yield sites were most strongly associated with two *Gemmatimonas*, a Roseiflexaceae, a *Desulfobulbus* and a *Nocardioides* ($p = 0.001$).

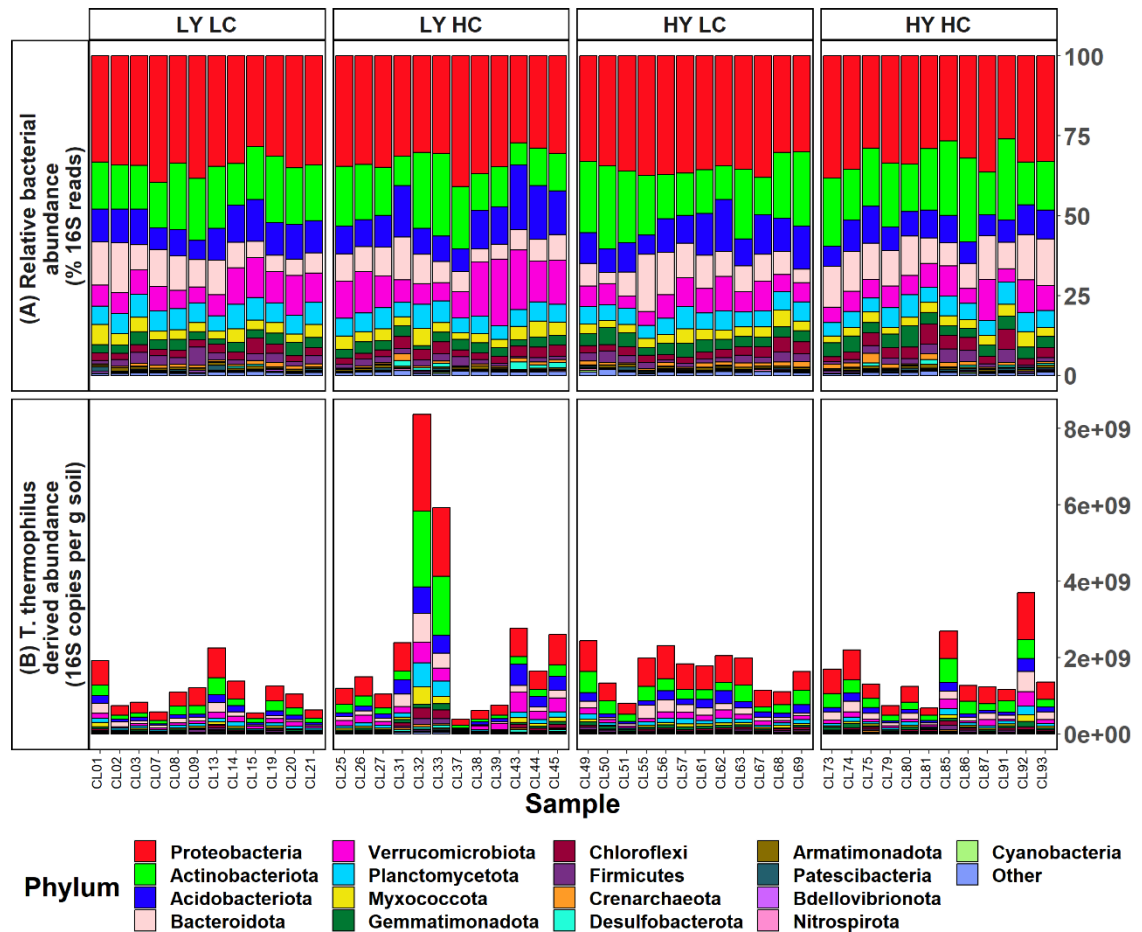


Figure 16 Changes to relative (A) and absolute (B) phyla abundances in Harold Smiths soils from 2018 – 2020. 'Others' refers to all phyla with an abundance of less than 1% across samples.

When studying temporal variation in soils, bacterial copy number was highly variable over the three years (Figure 16B; Year: $F = 4.00$, $Df = 1$, 168 , $p = 0.047$). 2019 soils generally had much lower abundance of 16S, with the exception of site HYLC which had a large increase in 16S during 2019. It is thought that these temporal changes may be associated with environmental differences, with 2019 having much higher monthly precipitation than the ten-year average (Figure 17), compared to 2018 and 2020, which had lower rainfall. This increased rainfall in 2019 has had a particularly strong effect in reducing bacterial numbers in the high conductivity sites, which are known to become more waterlogged. What remains unclear is why the HY LC site experienced such an increase in 16S abundance under these conditions.

LY LC soils generally had the lowest bacterial abundance, and low yield soils had significantly fewer 16S copies than high yield sites (Figure 16; Yield: $F = 10.66$, $Df = 1$, $1.67e+23$, $p = 0.001$). High yield sites may be associated with healthier soil, with more available carbon and nitrogen, which is favourable for most soil microbes.

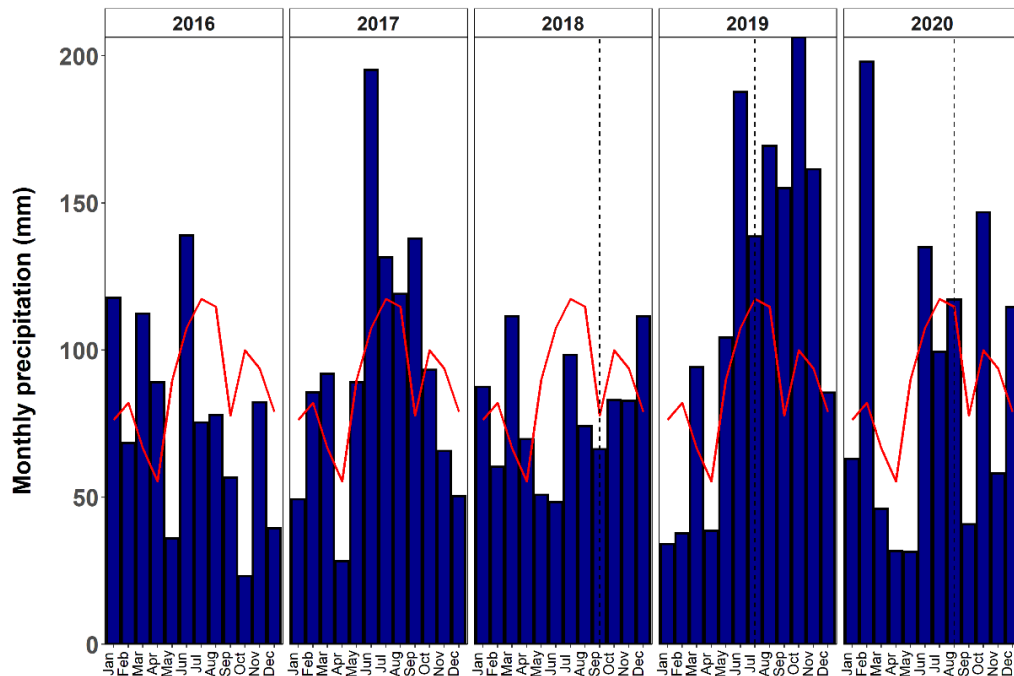


Figure 17 Monthly rainfall at Linton on Ouse weather station from 2016 – 2020. Red line indicates the fifteen-year average monthly rainfall. Vertical dashed lines indicate sampling date. Rainfall data obtained from the MET Office (Met Office, 2019).

In terms of indicator species over the three-year sampling period, out of 7,166 ASVs, only 37 were significantly associated with a specific field site or characteristic (yield or conductivity). One ASV was associated with high yield sites: *Paraccoccus korensis*. This Gram-negative and short rod- to coccus-shaped bacterium was found not to be capable of denitrification, in contrast to its three nearest phylogenetic neighbours (La *et al.*, 2005). No ASVs were specifically associated with low yield sites over the three-year period.

In contrast to yield, 18 ASVs were associated with conductivity (four for high conductivity and fourteen for low conductivity). A *Nocardioides* species, *Chthoniobacter*, *Ferruginibacter* and

Geobacter were associated with high conductivity. This is unsurprising for the strictly anaerobic *Nocardioides* and *Geobacter* due to the reduced oxygen concentration in high conductivity soils, but more surprising for the free living aerobic chemoheterotroph *Chthoniobacter*. It is thought that *Chthoniobacter* is likely involved in the breakdown of organic carbon in the soil as it is found associated with plant biomass, but incapable of growth on amino/organic acids apart from pyruvate (Kant *et al.*, 2011).

The two ASVs most associated with low conductivity soils ($p < 0.01$) were an uncultured Sphingobacteriales found in wastewater treatment plants (Begmatov *et al.*, 2022) and a Holophagae subgroup 7 isolate with little characterisation. Additionally, there were four Planctomycetota, two Acidobacteriota, Verrucomicrobiota and one Bacteroidota, Gemmatimonadota, Myxococcota and Gammaproteobacteria that were significantly associated with the low yield sites.

3.3.5. Alpha diversity

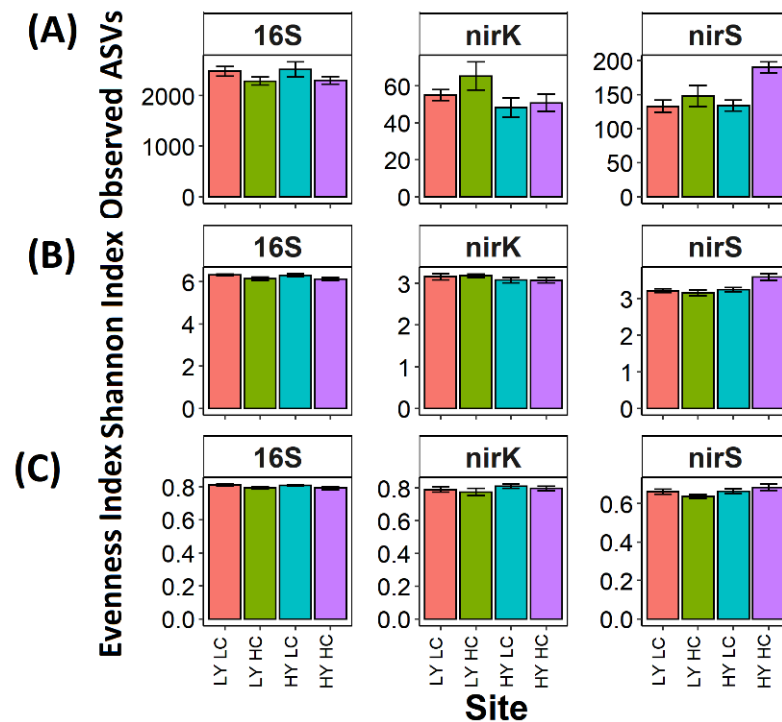


Figure 18 Alpha diversity for 2018 soil samples for 16S rRNA, *nirK* and *nirS*. (A) shows species richness through observed ASVs, (B) indicates Shannon Index of diversity and (C) shows Pielou's evenness index. Bars represent mean of twelve samples, with error bars showing one standard error. Colours indicate field zone of soil sample: pink = low

yield, low conductivity; green = low yield, high conductivity; blue = high yield low conductivity and purple = high yield, high conductivity. Note variable y axis scale.

Having predicted that high yield sites would have increased available carbon and nitrogen relative to low yield sites (although actually finding increased biomass in low yield sites Table 11), it was predicted that alpha diversity would be greater in high yield sites. This was the case for *nirS* species richness (defined as observed ASVs) in the 2018 soils, with significantly more variants in high yield samples compared to low (Figure 18A, Yield: $F = 4.56$, $Df = 1,43$, $p = 0.038$), but not for 16S rRNA or *nirK* genes. Additionally, there were significantly more *nirS* ASVs in the high conductivity samples than the low conductivity samples that are drier (Figure 18A, Conductivity: $F = 10.8$, $Df = 1,43$, $p = 0.002$). This result is similar to that in section 2.3.3., where only the *nirS* species richness was significantly different under different conditions. There were no significant interactions between the effects of yield and conductivity for any of the genes investigated.

For the Shannon index of diversity, which accounts for both species richness and evenness, 16S populations were more diverse in low conductivity soils which may be drier (Figure 18B, Conductivity: $F = 7.11$, $Df = 1,44$, $p = 0.011$), this result was driven by a greater evenness index in the low conductivity 16S samples (Figure 18C). As with the species richness measure of diversity, *nirS* was significantly more diverse in high yield low conductivity soils (Figure 18B, Yield: $F = 9.85$, $Df = 1,43$, $p = 0.003$), however conductivity was not significantly associated with the Shannon metric. In terms of evenness for the gene diversity within the 2018 soils, *nirS* was considerably less even than 16S or *nirK* (Figure 18C), despite having more variants than *nirK*. Evenness did not vary significantly across the sites for *nirK* or *nirS*.

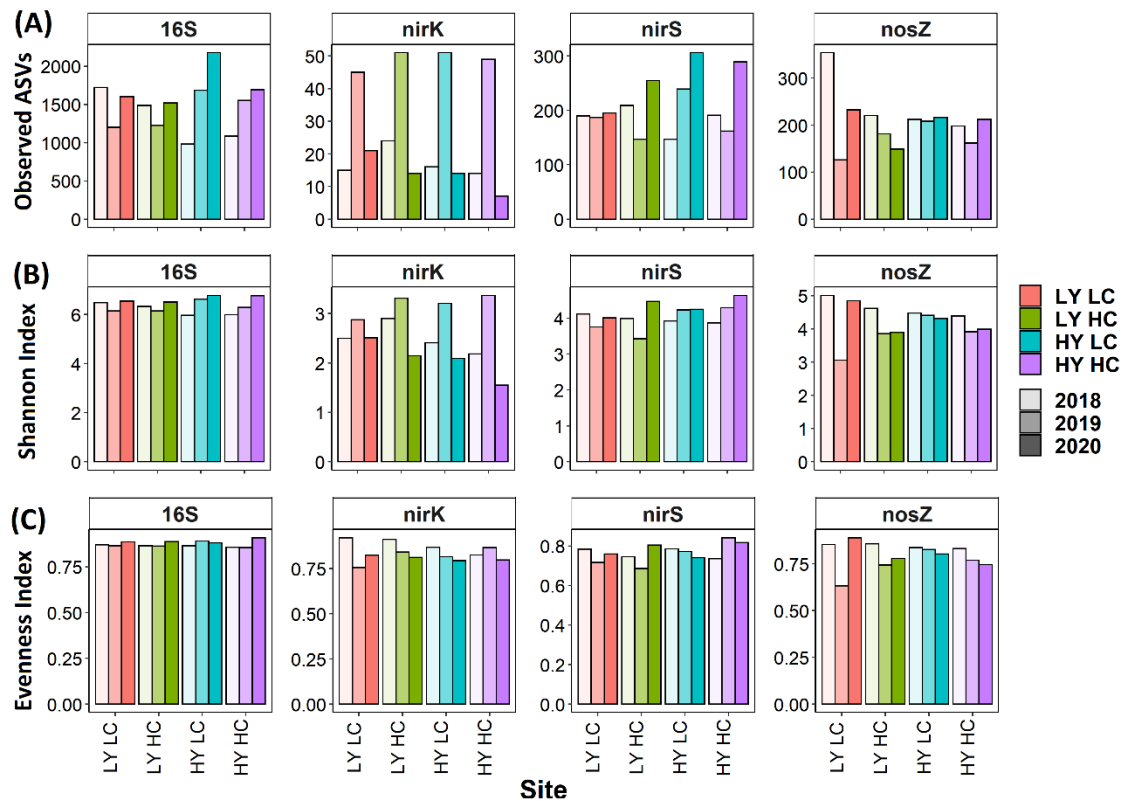


Figure 19 Alpha diversity from 2018 – 2020 soil samples. (A) species richness through observed ASVs, (B) Shannon Index of diversity and (C) Pielou's evenness index. Colours indicate field zone of soil sample: pink = low yield, low conductivity; green = low yield, high conductivity; blue = high yield low conductivity and purple = high yield, high conductivity. Colour intensity shows year: palest = 2018, medium = 2019, darkest = 2020. Note variable y axis scale.

For 2018-2020 soil samples, there were many changes in observed ASVs over time (Figure 19A). For 16S, the low yield sites saw a drop in richness in 2019 followed by recovery in 2020. In contrast, the low yield soils saw a steady increase in 16S ASVs from 2018-2020. The *nirK* gene had the biggest change over time with observed ASVs more than doubling from a mean of 17.25 (± 2.3) in 2018 to 49 (± 1.4) in 2019, and then a large drop to 14 (± 2.9) in 2020. *NosZ(I)* observed ASVs remained the most constant over the three-year period. Evenness index and the derived Shannon index remained fairly constant over this period, regardless of changes in ASV numbers (Figure 19).

Together, these results suggest that species and gene richness change significantly over time as microbial community dynamics alter. This can likely be attributed to a combination of biotic and

abiotic environmental factors. *NirK* and *nirS* ASV richness seems more susceptible to change in relation to environmental factors than *nosZ(I)*. Additionally, 16S species richness changes considerably over time but its consistently high evenness index indicates that loss of ASVs is not associated with increased species dominance as may be expected from adaptation.

3.3.6. Community beta diversity

To visualise the differences in the composition of bacterial communities between field zones in 2018, a non-metric multidimensional scaling (NMDS) ordination of whole bacterial community 16S rRNA gene and denitrification gene amplicons was constructed (Figure 20). With both Bray Curtis dissimilarity and Weighted UniFrac distance used, it was possible to compare compositional dissimilarity with phylogenetic diversity.

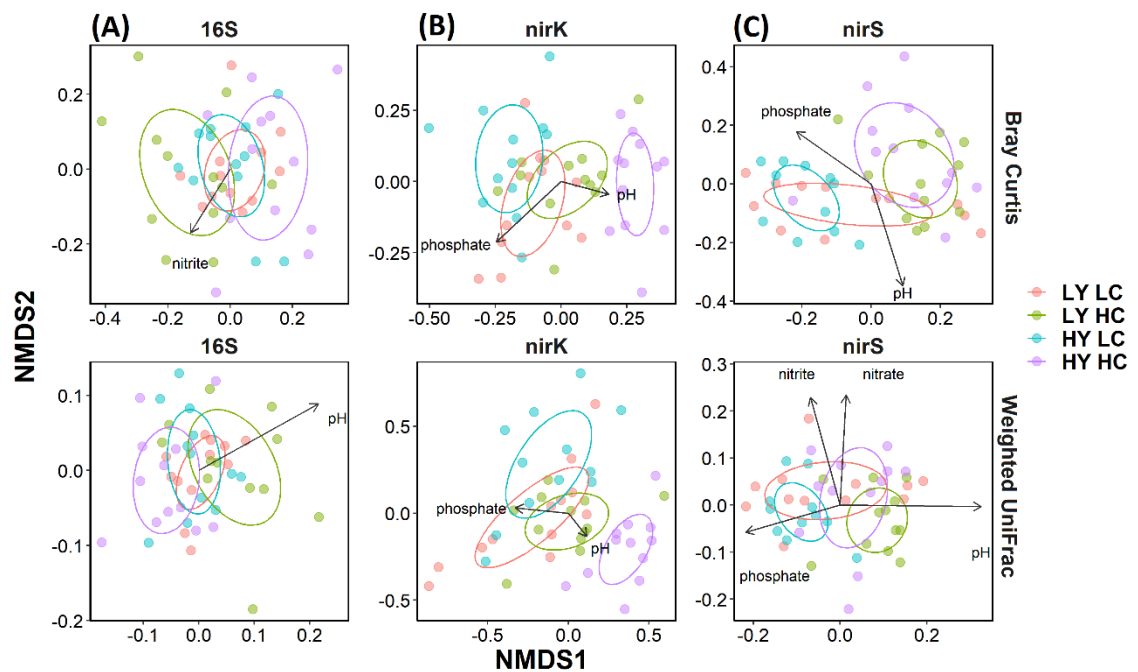


Figure 20 Non-metric multidimensional scaling (NMDS) of 2018 soil gene amplicon Bray-Curtis dissimilarity (top) and Weighted UniFrac distance (bottom). (A) 16S rRNA gene, (B) *nirK* nitrite reductase gene, (c) *nirS* nitrite reductase gene. Colours indicate field zone of soil sample: pink = low yield, low conductivity; green = low yield, high conductivity; blue = high yield low conductivity and purple = high yield, high conductivity. Labels indicate environmental variables which significantly explain beta diversity.

To confirm if the differences between community compositions can be explained by field site properties, a PERMANOVA test was used. Both yield and conductivity had a significant effect on the community composition of 16S when using the Bray Curtis dissimilarity matrix (Figure 20A; Bray Curtis 16S - Yield: $F_{1,44} = 3.44$; $p = 0.001$; Conductivity: $F_{1,44} = 3.62$; $p = 0.001$; Yield x Conductivity: $F_{1,44} = 2.68$; $p = 0.003$). When comparing the Weighted UniFrac distance between communities, yield had a relatively stronger effect compared to conductivity, but both remained significant factors (Figure 20A; Weighted UniFrac 16S - Yield: $F_{1,44} = 3.53$; $p = 0.001$; Conductivity: $F_{1,44} = 2.17$; $p = 0.024$; Yield x Conductivity: $F_{1,44} = 2.77$; $p = 0.007$). This suggests that the total bacterial population was distributed according to which field position it was sampled from, and that yield had a stronger association with bacterial selection than conductivity in these samples.

Amplicon analyses for the nitrite reductase genes *nirK* and *nirS* were then used to ascertain whether functional diversity followed the same patterns as taxonomic diversity in the 2018 soils. Similar to 16S distribution, *nirK* was significantly associated with both yield and conductivity factors (Figure 20B; Bray Curtis NirK - Yield: $F_{1,44} = 3.05$; $p = 0.003$; Conductivity: $F_{1,44} = 8.47$; $p = 0.001$; Yield x Conductivity: $F_{1,44} = 3.22$; $p = 0.001$), with conductivity having a stronger influence. This was almost identical for the Bray Curtis and Weighted UniFrac distance (Figure 20B; Weighted UniFrac NirK - Yield: $F_{1,44} = 3.74$; $p = 0.001$; Conductivity: $F_{1,44} = 8.14$; $p = 0.001$; Yield x Conductivity: $F_{1,44} = 3.30$; $p = 0.007$). Like *nirK*, *nirS* distribution was significantly associated with both factors but had a stronger association with conductivity (Figure 20C; Bray Curtis NirS - Yield: $F_{1,43} = 4.40$; $p = 0.002$; Conductivity: $F_{1,43} = 10.2$; $p = 0.001$; Yield x Conductivity: $F_{1,43} = 2.70$; $p = 0.023$). This result was mirrored in the phylogenetic diversity (Figure 20C; Weighted UniFrac NirS - Yield: $F_{1,43} = 2.94$; $p = 0.018$; Conductivity: $F_{1,43} = 8.82$; $p = 0.001$; Yield x Conductivity: $F_{1,43} = 2.78$; $p = 0.027$). These results suggest that the denitrification genes in this study are more strongly associated with conductivity trends than the total bacterial population, indicating a selective pressure.

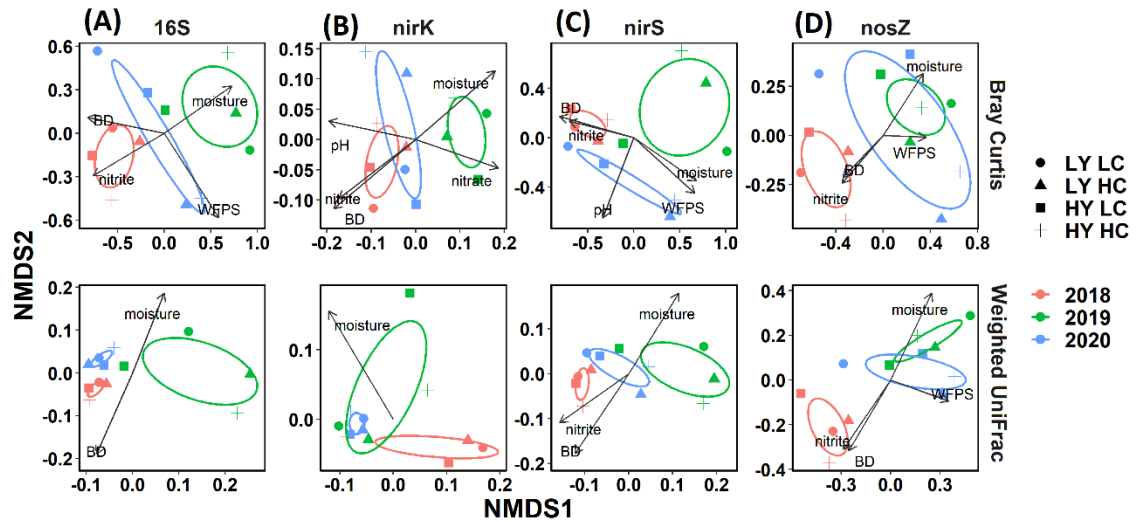


Figure 21 Non-metric multidimensional scaling (NMDS) of 2018 – 2020 soils showing Bray-Curtis dissimilarity (top) and Weighted UniFrac distance (bottom) for (A) 16S, (B) *nirK*, (C) *nirS*, and (D) *nosZ(I)*. Colours indicate year of sampling: red = 2018, green = 2019 and blue = 2020. Shapes indicate site of soil sample: circle = low yield low conductivity, triangle = low yield high conductivity, square = high yield low conductivity and plus = high yield high conductivity.

Although there were clear effects of yield and conductivity in the 2018 samples, these were much less apparent in the 2018-2020 samples, where clustering was significantly associated with year of sampling (Figure 21). Interestingly, when year was used to constrain permutations, 16S diversity was affected by conductivity (Figure 21A; Bray Curtis 16S - Conductivity: $F_{1,8} = 1.19$; $p = 0.023$) with the same effect shown using Weighted UniFrac (Weighted UniFrac 16S - Conductivity: $F_{1,8} = 1.01$; $p = 0.014$).

In terms of the functional genes of interest (*nirK*, *nirS* and *nosZ(I)*), the only significant effect apart from year of sampling was that of conductivity on *nirS* Weighted UniFrac distance (Figure 21C, Weighted UniFrac *nirS* - Conductivity: $F_{1,8} = 1.23$; $p = 0.028$), shown by circle and square symbols diverging from pluses and triangles on the NMDS2 axis. Interestingly, conductivity was also trending towards significance for *nirK* and *nosZ(I)*, and stronger effects may have been visible with greater replication. Once again, these results indicate that conductivity is a strong

driver for bacterial and denitrifier community assembly, but also demonstrates the high microbial turnover present in these sites over time.

3.3.7. *Spatial and environmental links to community composition*

To explore the drivers of community composition in more detail and to determine whether spatial distance drives diversity patterns in denitrifying bacterial communities, environmental and spatial analysis was undertaken. Environmental vector fitting revealed that four soil variables: water filled pore space (WFPS), bulk density (BD), nitrite and soil moisture content were significantly related to total bacterial community composition (Figure 21A; Envfit: WFPS $r^2=0.68$, $p=0.005$; BD $r^2=0.68$, $p=0.004$; nitrite $r^2=0.67$, $p=0.012$ and soil moisture content $r^2=0.63$, $p=0.011$). Since none of these factors were significantly different across sampling sites but did change considerably over time (Table 11), this suggests that bacterial community composition is largely driven by environmental factors.

Similarly, the distribution of each of the denitrification genes was significantly associated with moisture (Figure 21B-D; Envfit moisture: *nirK* $r^2=0.62$, $p=0.018$; *nirS* $r^2=0.72$, $p=0.006$; *nosZ* $r^2=0.86$; $p=0.001$). In terms of phylogenetic diversity, *nirS* and *nosZ* were also significantly affected by nitrite concentration (*nirS* $r^2=0.58$, $p=0.031$; *nosZ* $r^2=0.71$; $p=0.004$), bulk density (*nirS* $r^2=0.75$, $p=0.002$; *nosZ* $r^2=0.66$; $p=0.005$) and WFPS for *nosZ* (*nosZ* $r^2=0.53$; $p=0.027$). Comparing phylogenetic diversity using Weighted UniFrac distance rather than compositional dissimilarity yielded fewer significant environmental associations (Figure 21). However, these environmental associations are more likely to be drivers of adaptation, as Weighted UniFrac distance accounts for relatedness between the ASVs. Together these results suggest that moisture and available nitrite are strongly associated with distribution of denitrification genes.

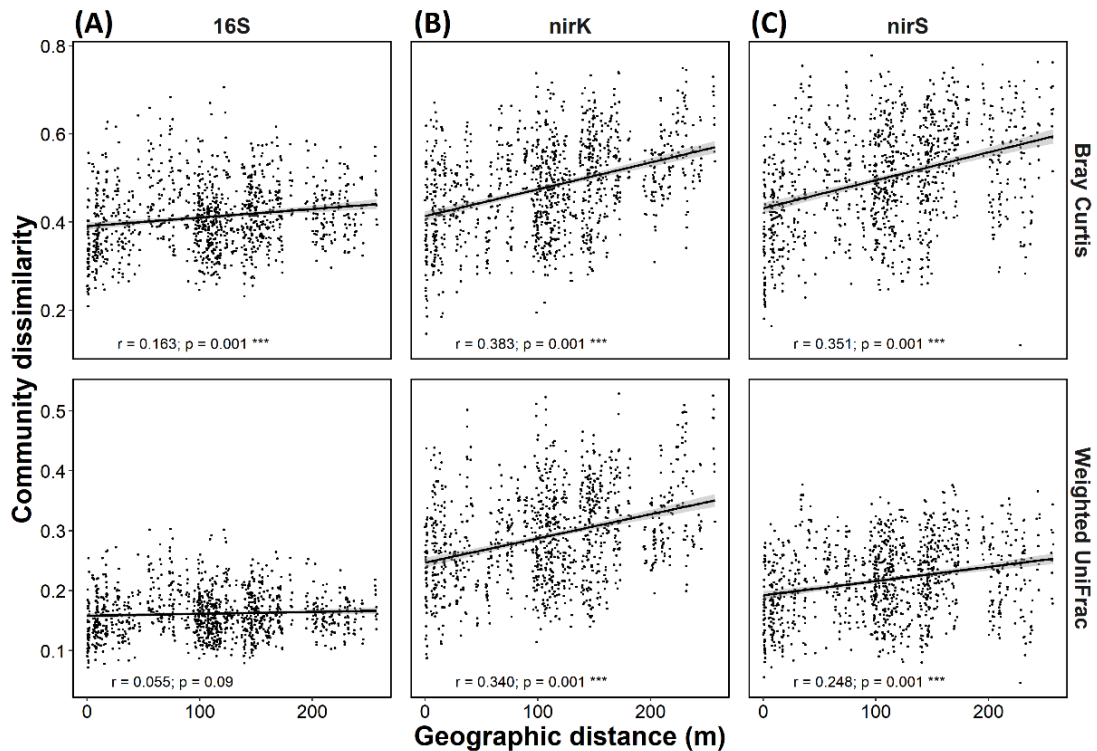


Figure 22 Association between spatial distance and community dissimilarity in Harold Smiths 2018 soils. Euclidean distance versus Bray-Curtis dissimilarity (top) and Weighted UniFrac distance (bottom) for (A) 16S, (B) *nirK*, (C) *nirS* genes. Statistics show mantel test r statistic and p value for each association. Stars indicate p value size with *** indicating $p < 0.001$.

To further investigate variation in community composition, a spatial analysis was completed. A Euclidean distance matrix was compared against the Bray-Curtis dissimilarity matrix or Weighted UniFrac distance matrix using a Mantel test. This test indicated a weak positive correlation for 16S, and a slightly stronger correlation for nitrite reductase genes *nirK* and *nirS* using Bray Curtis (Figure 22; 16S rRNA: $R^2 = 0.163$, $p = 0.001$; *nirK*: $R^2 = 0.383$, $p = 0.001$; *nirS*: $R^2 = 0.351$, $p = 0.001$). When comparing phylogenetic distance to spatial distance, there was no significant correlation for 16S, but the weak positive association for *nirK* and *nirS* remained (*nirK*: $R^2 = 0.340$, $p = 0.001$; *nirS*: $R^2 = 0.248$, $p = 0.001$). All of these values are considerably below those observed in the previous chapter (2.3.5.). The flatter gradient of Harold Smiths field compared to NFSC at Nafferton Farm may explain why a weaker distance-decay effect was observed here.

Although spatial distance was still found to drive diversity in denitrifying bacterial communities, spatial distance could not account for much of the variation between samples.

To detangle the effects of space from environmental variation on community composition, the `calc.relimp` function in R was used. In the 2018 samples only a small proportion of the phylogenetic diversity was explained by spatial and environmental factors with an average of 10% explained. 16S rRNA variation was least well explained, with only 1.2%. 0.33% 16S variation was attributed to spatial distance and the rest attributable to measured environmental variables (3.3.1. Table 11). By contrast, far more *nirK* and *nirS* phylogenetic diversity was explained overall (22.5 and 6.42% respectively), with a greater proportion explained by spatial distance (9.61 and 5.82% respectively; Figure 22B-C). The remainder of measurable phylogenetic variation was explained by environmental variables, predominantly by pH differences between sites.

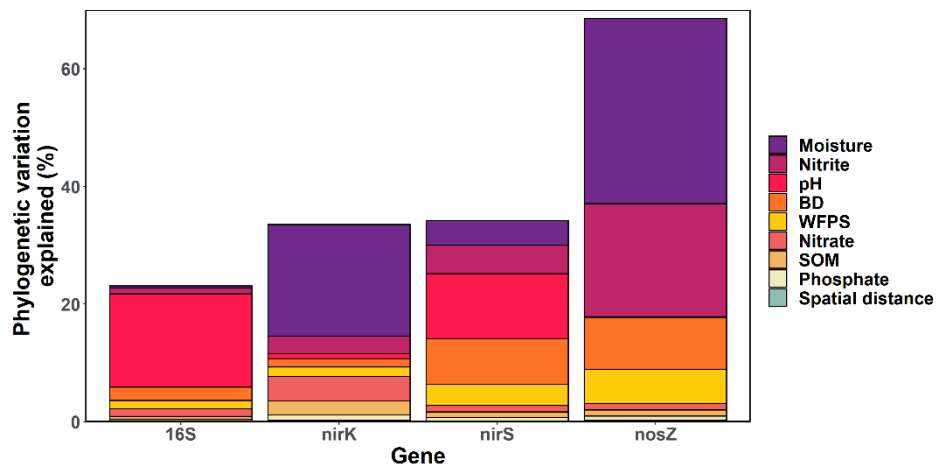


Figure 23 Variation partitioning of Weighted UniFrac distances in 2018-20 samples.

In the 2018-2020 samples a much greater proportion of phylogenetic diversity was accounted for, with an average of 39.8% variation explained (Figure 23). For 16S rRNA environmental and spatial variation together accounted for 23.1% variation of the Weighted UniFrac distance, with 0.10% attributable to space and 23% attributable to measured environmental variables. In particular, pH accounted 15.9% of 16S phylogenetic variation. A larger proportion of

denitrification gene phylogenetic diversity was attributable to measured variables (Figure 23), with moisture being the key driver for *nirK* and *nosZ(I)* and pH for *nirS*. Spatial variation played a much smaller role in differentiating between these annual samples, due to repeated sampling at the same sites and high variation between sampling dates (Figure 21).

In all of the Harold Smiths field samples less of the community diversity can be attributed to spatial and measured environmental samples than in the Nafferton Farm NFSC study (2.3.5.). This may be because of the nature of the long-term field trial at Nafferton and may reflect the stochastic properties that affect a commercial farm compared to a more standardized field trial.

3.4. Discussion

3.4.1. Spatial patterns of microbial distribution

Since the earliest days of soil microbial ecology, it has been fundamental to map the diversity and functionality of microbial communities to the factors that drive them. Since microbial processes such as denitrification can vary significantly over field scale (Philippot *et al.*, 2009), it is important to understand the spatial distribution of the microbial guilds which mediate this process. Using a spatially-structured, stratified sampling regime we used amplicon sequencing and novel methods of abundance measurement of 16S rRNA and nitrite reductase genes *nirK* and *nirS* to investigate how denitrifying communities vary between soils with similar physicochemical properties. Having found strong evidence for distance decay effects at Nafferton Farm where samples were pooled by experimental treatment block, (Moulton-Brown *et al.*, 2022), we predicted that taking samples with high spatial resolution would enable us to test the strength of distance-decay relationship of microbial distribution over scales ranging from 6.7 cm to 257 m.

The results of our study of samples obtained by systematic sampling of four zones within an agricultural field indicates that weaker patterns of distance-decay are present for Harold Smiths field soils compared to Nafferton farm (2.3.5.), with only denitrification functional genes following this pattern and not 16S rRNA (Figure 8). Electrical conductivity has been found to drive soil microbial community composition in other studies (Van Horn *et al.*, 2013; Kim *et al.*,

2016), with the likelihood that electrical conductivity is a proxy for a water content gradient that is the true driver of diversity. The slope of Nafferton site relative to that of Harold Smiths field may therefore explain why a weaker distance decay pattern is observed here. Although space alone had little effect on the microbial community, pH was found to have a strong effect bacterial phylogenetic diversity, a phenomena that has been widely documented for both the total bacterial community and also denitrifying microbial communities (Fierer and Jackson, 2006; Hallin *et al.*, 2009; Bru *et al.*, 2011; Shi *et al.*, 2018).

Interestingly the functional gene-distance relationships did not behave in the same way as the taxa-distance relationship represented by 16S rRNA. In fact, the nitrite reductases *nirK* and *nirS* phylogenetic diversities both showed significant spatial patterning in terms of distance decay relationships. This is in accordance with other studies (Schulz *et al.*, 2017), but with comparable patterns between *nirK* and *nirS* unlike the niche partitioning between the nitrite reductases as observed in other studies (Philippot *et al.*, 2009; Enwall *et al.*, 2010).

The relatively stronger distance decay relationship in the denitrification genes compared to the 16S rRNA gene suggests that denitrifiers incur greater habitat selection than the total microbial population. Our findings revealed that deterministic processes are more important for denitrification community assembly, with stochastic processes being relatively more important in shaping the total bacterial community. With high diversity between samples, even at the centimetre scale, precision farming would currently struggle to reach the required resolution for most agricultural interventions. The highest resolution mapping currently offered from drones measured at 10s of cm per pixel (Späti *et al.*, 2021). Additionally, these images require digital processing, auxiliary data and variable rate technologies for the practical application of precision agriculture (Dong *et al.*, 2019), so may be unsuitable for the widescale use in medium or small-scale farming systems.

3.4.2. *Temporal stability of microbial populations*

Our results show that microbial and denitrifier community composition can change considerably in relation to environmental variation over time and that more highly resolved temporal sampling is crucial for observing this variation (Emilia Hannula *et al.*, 2019). Although our temporal resolution was low, with annual sampling over three years immediately following crop harvest, these snapshots provided a clear image of the factors affecting community composition.

Compared to other community types, soil communities are thought to be fairly stable (Shade *et al.*, 2013), with the suggestion that the high proportion of dormant soil organisms that would mask changes in microbial community (Locey *et al.*, 2020) or that the high spatial heterogeneity of soils may conceal local changes in microbial communities due to high variability across sites close by to one another. In fact, our study showed high microbial and denitrifier turnover at the annual scale, with large changes in both the composition and abundance of these communities. This is similar to temporal changes in nitrogen cycling gene copy number observed by Behnke *et al.* (Behnke *et al.*, 2022), although their samples were taken monthly over a single growing season rather than focusing on annual variation.

Although the majority of annual variation in microbial and denitrifying communities in our study was attributed to specific environmental properties, it is notable that agricultural management is likely to have also contributed directly and indirectly to the temporal changes in the soil microbial communities (Babin *et al.*, 2019). The different levels of nitrogen input would likely have altered the composition and diversity of the bacterial community (Liu *et al.*, 2020), but it is difficult to decouple short and long-term effects of N input from environmental factors such as precipitation. This work highlights the complex and temporal effect agricultural management has on key microbial functions related to denitrification as well as one of the limitations for incorporation of microbial work into precision agriculture.

3.4.3. *Associations between denitrifier population and low yield*

Despite nitrogen being the most limiting nutrient in agroecosystem productivity (Rütting *et al.*, 2018), little is known about the effects of denitrifying microbial community structure on crop yield. Process-based biogeochemical models offer a simulation of crop yields and greenhouse gas emissions caused by denitrification with input regarding land management interventions. One of the most commonly used biogeochemical models is the DeNitrification DeComposition (DNDC) model (Changsheng Li *et al.*, 1992), which has been widely adopted to predict greenhouse gas emissions and recently updated to simulate crop yield (Musafiri *et al.*, 2021). However, at present the model cannot be updated with data regarding the soil microbial community and instead uses broader scale inputs such as land management treatments and climate data. In future iterations of the model, finer scale information regarding soil and denitrifier community structure may allow for within-field estimates of crop yield and greenhouse gas emissions with

In this study for example, copy numbers of both *nirK* and *nirS* were significantly higher in low yield soils compared to high yield. This information could potentially be used to diagnose the soil, potentially utilizing Loop-Mediated Isothermal Amplification (LAMP) technology for in-field diagnosis, to influence applications of nitrogen fertilizer. Several studies have also linked *nirK/S* abundances to potential denitrification rate (Chroňáková *et al.*, 2009; Dong *et al.*, 2009; Čuhel *et al.*, 2010), which may explain some of the drop in yield in these areas. However, the association between denitrification gene copy numbers and potential denitrification rate has not been observed universally.

In terms of community composition, the 2018 soils had significantly altered phylogenetic diversity between low and high yield sites for 16S, *nirK* and *nirS* genes, as well as 53 indicator ASVs, indicating that a form of microbial fingerprinting may be a useful contribution for the DNDC model. However, it should be noted that no significant associations were found between yield and community profile in the longitudinal study apart from one indicator species related to *Paraccoccus koreensis*, which was associated with high yield sites. It is thought that the high heterogeneity of the soil microbiome may have masked associations between yield and bacterial

community profile, however, and that increased sampling effort may have clarified potential associations. Since microbial abundances and community structures are associated with crop yield (Wang *et al.*, 2022), it seems useful to incorporate this information predictive biogeochemical models.

3.4.4. *Utilization of synthetic spike-in standards for gene quantification*

Relative microbiome profiling has limited capacity to detect changes in microbial community profile relating to abundance. As such high-throughput sequencing is increasingly being combined with absolute microbiome profiling to gain a more comprehensive understanding of microbiome dynamics (Smets *et al.*, 2016; Vandeputte *et al.*, 2017; Tkacz *et al.*, 2018). In this study we compared two spike-in amplification methods (spike-AMP) to quantitative PCR combined with sequencing data (qPCR-AMP), the current preferred method in soil microbiome quantitative research (Zhang *et al.*, 2022).

We found that spike-AMP using *T. thermophilus*, with a known amount of DNA single-spike added to environmental samples prior to total DNA extraction, provided a reliable method of quantifying 16S rRNA copy number when added at low concentrations as used in the literature (Smets *et al.*, 2016). This method provided valuable quantitative insight, with minimal labour intensity.

Similar methods of using synthetic DNA spikes have been published to assess the abundance of taxonomy-associated genes (Tkacz *et al.*, 2018), although as of yet, this hasn't been attempted with functional genes. To understand the community dynamics of the denitrifying community, we therefore proposed using synthetic spikes of nitrite reductase genes *nirK* and *nirS* alongside a synthetic 16S rRNA. Unfortunately, this method did not correlate with the qPCR generated copy number for any of the genes tested and could not reliably be used to infer copy numbers. This may be for a number of reasons, including the use of primers with greater affinity to the spike-DNA compared to the native microbial DNA due to the degenerate nature of denitrification primers. Additionally, the selection of a suitable spike concentration is challenging because low

levels of spikes can easily be retained in environmental samples (Tkacz *et al.*, 2018). And, since large variations in microbial population abundance have been reported, the optimal spike level for different samples may be variable. This difficulty may be overcome by using a spike with gradient concentrations (Tkacz *et al.*, 2018; Guo *et al.*, 2020) or a known spike mixture (Tourlousse *et al.*, 2017; Jiang *et al.*, 2019).

Overall, there is certainly value in measuring the absolute abundance of each organism or sequence variant when comparing microbial diversity across samples because effects caused by overall abundance may be missed when purely assessing relative abundance (Vandeputte *et al.*, 2017). In the absence of a gold-standard quantitative method for microbiome profiling, spike-AMP remains a feasible method with low labour intensity which produces reliable results where optimal spike level and primer efficiency for the spike DNA is predetermined.

Altogether, these results lay the foundations for a better understanding of the role of soil microbial communities on agricultural productivity and how it may ultimately be targeted by farming practices to meet the growing global food demand.

Chapter 4: Isolation and characterisation of potential denitrifying bacteria

4.1. Introduction

Existing knowledge surrounding the process of denitrification is predominantly based on select model organisms. However, many groups of denitrifying bacteria currently have no cultivable representatives available in biobanks (Zumft, 1997; Janssen *et al.*, 2002; Lycus *et al.*, 2017). Denitrification is widely spread among taxonomically diverse groups of bacteria and more fundamental understanding is needed from a wider range of organisms to fully understand the regulatory biology of denitrification and subsequent gas fluxes and nutrient implications. Since many soil-dwelling microorganisms are not easily cultivable in the laboratory using traditional microbiological methods (Staley and Konopka, 1985; Amann *et al.*, 1995; Torsvik and Øvreås, 2002), it is likely that some of the most abundant and/or significant denitrification guilds have not yet been extensively studied.

Previous studies which attempted to isolate denitrifying bacteria used fully anoxic conditions (Chèneby *et al.*, 2000; Heylen *et al.*, 2006; Hashimoto *et al.*, 2009). However, some denitrifying bacteria would have been unable to grow under these conditions because a gradual change to anoxia is needed to initiate enzyme production, as otherwise they may enter anoxia without energy to produce the enzymes needed for denitrification and energy production (Hassan *et al.*, 2014). This limits the isolates to the ones that can manage such abrupt shifts. Additionally, this approach may overlook aerobic denitrifiers which often perform nitrification and denitrification simultaneously (Robertson and Kuenen, 1990).

In this study, we use an *in-situ* cultivation approach to isolate and culture a broad taxonomic range of soil bacteria, which are then screened for denitrification activity using a high-throughput assay.

Isolation devices, such as the isolation chip (iChip) proposed by Nichols et al. (Nichols *et al.*, 2010), enable microbial isolation through the dilution of soil microbes. Environmental material such as soil is diluted to an average of one cell per diffusion chamber, with membranes to prevent contamination but allow nutrient exchange, to result in mono-specific culture. This technology improves microbial cultivability through *in-situ* incubation in soil with naturally present growth factors and nutrients. Isolation devices have been shown to facilitate the growth of a greater diversity and different species profile from the complex soil microorganism community than traditional plating techniques (Alessi *et al.*, 2018). Therefore, it is predicted that a broader range of denitrifying bacteria will be isolated through use of isolation devices than has been achieved in previous studies.

Since our current knowledge of denitrification is predominantly based on model organisms, the primary aim of this experiment is to isolate and culture a representative range of environmental denitrifiers. We extracted bacteria from three soils from an agricultural field which had varying levels of moisture and crop yield. We hypothesised that in the high moisture areas, there would be a greater number of denitrifiers due to reduced oxygen in the soil and therefore increased denitrification, and we hypothesized that there would be an increased number of denitrifiers in the low yield areas of the field, as increased denitrification could account for some of the yield loss due to nitrogen limitation. We also expected that detailed phenotypic analyses of nitrate and nitrite reduction would reveal a variety of phenotypes, not always reflecting the genomic potential of the organisms. Further, with comprehensive genotyping and high-throughput phenotyping methods, we hoped to find evidence of differing denitrification gene clusters among isolates that provides insight into key regulatory mechanisms involved in denitrification.

4.1.1. Experimental aims

The specific objectives of this chapter were to:

- Isolate and culture bacteria that are not model organisms from soil using a custom-made isolation device.

- Determine whether isolated bacteria are representative of the soil bacterial community.
- Establish how many of the isolated bacteria are able to reduce nitrate or nitrite using an optimised high-throughput screening assay.
- Assess whether a greater proportion of denitrifiers are cultivable from low yield or high conductivity soils than their counterparts.
- Track the denitrification reaction dynamics in a representative sample of bacterial isolates.
- Investigate the denitrification genomic potential in a representative sample of bacterial isolates to understand the link between phenotype and genotype.

4.2. Methods

4.2.1. Microbial isolation field site and experimental overview

Soil sampling and isolation device incubation took place at Harold Smiths field (54:00:37.0 N; 1:08:40.4 W), with the site described in Chapter 3. Four isolation devices were placed around the field in the centre of the zones set out in 3.2.1., which correspond to combinations of low and high yield based on the 2018 spring bean harvest ($< 1.43 \text{ t ha}^{-1}$ or $> 2.75 \text{ t ha}^{-1}$) and low and high shallow soil electrical conductivity ($< 16.9 \text{ mS m}^{-1}$ or $> 27.1 \text{ mS m}^{-1}$). Soils were sampled at a depth of 10cm on 31/07/19 when the field was planted with winter wheat.

An overview of the experiments in Chapter 4 are shown in Figure 24. The experiment began by using isolation devices to culture difficult-to-culture microbial isolates and plating them onto non-selective media. This was followed by characterisation of all 205 viable isolates developing high-throughput aerobic and anaerobic nitrate and nitrite utilisation assays and also by Sanger sequencing the 16S rRNA gene. From this, twelve isolates were selected for further study using the criteria given in 4.3.4. and further characterised with substrate utilisation assays, nitrate loss rate experiments in pure culture and whole genome sequencing.

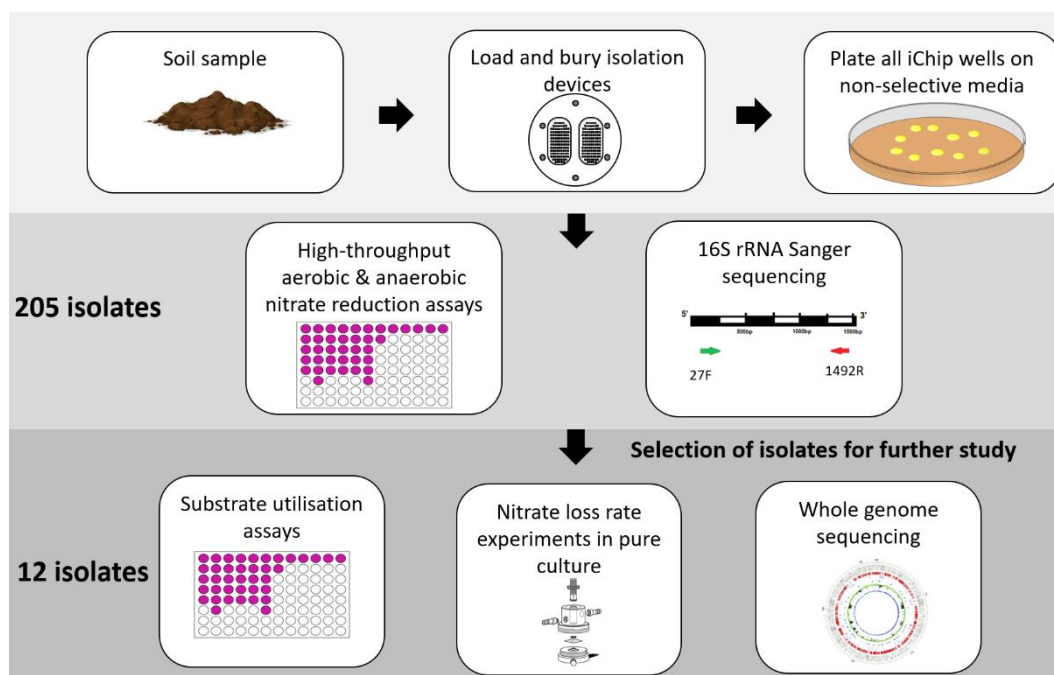


Figure 24 Schematic overview of the experiments in Chapter 4, from culturing soil microbes from isolation devices, to characterising potential nitrogen cycling capabilities.

4.2.2. Isolation devices

Isolation devices were used to separate individual microbes from the soil and increase the diversity of microbial cultivation through *in-situ* incubation. Isolation devices consist of 384 miniature (1 μ l) diffusion chambers that allow the growth of individual microbial species with access to metabolites from their natural environment. Devices were custom made in the Biology Mechanical Workshop, University of York, based on the Nichols *et al.* specifications (Nichols *et al.*, 2010), with altered design (Figure 25) to fit the Whatman Nuclepore Track-Etched, polycarbonate 0.05 μ m pore size 47 mm diameter membrane (VWR).

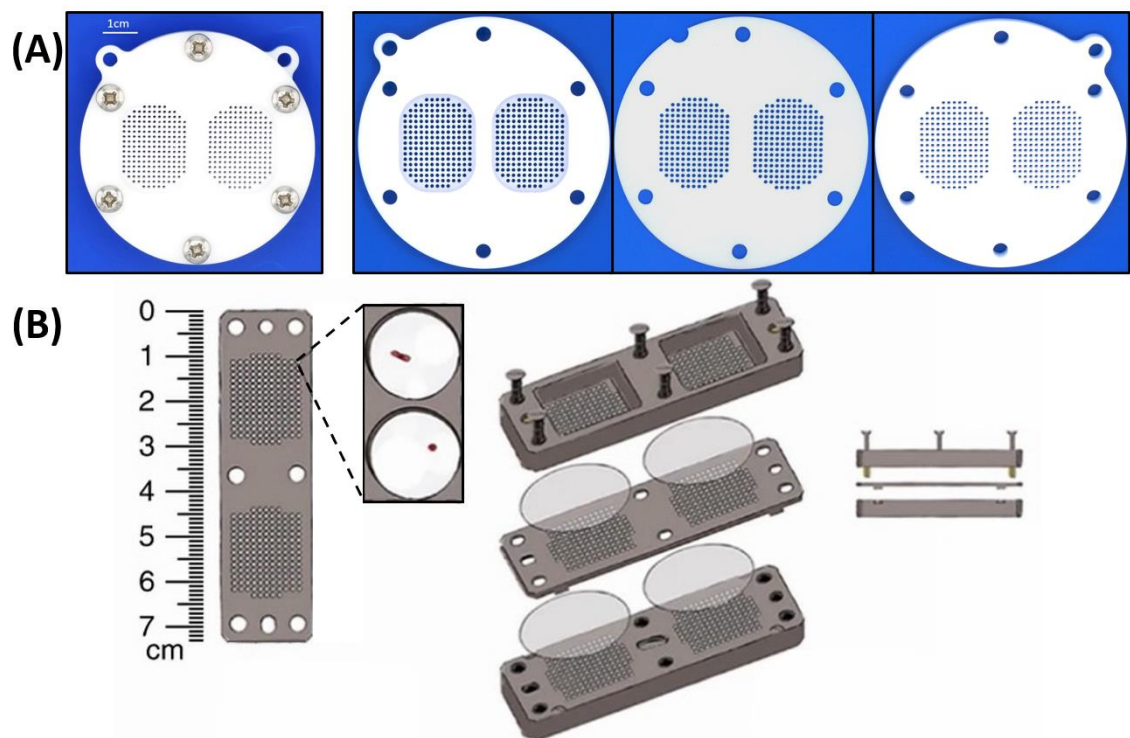


Figure 25 Isolation device & components. (A) From left to right: intact isolation device, front panel, central panel with 384 1 μ l pores, back panel. Once assembled, membranes (not shown) are attached to either side of the central panel and the isolation device is held together by screws and bolts (left). (B) Technical drawing of the isolation chip device this device was based on. Figure reproduced from (Berdy *et al.*, 2017)

Five isolation devices were loaded in total, one for each of the four locations and one negative control which did not contain soil, which would indicate if contamination occurred. The devices were sterilized with ethanol and labelled prior to use. Soil cell density was assumed to be 3×10^8 cells per ml based on work by Alessi *et al.* (Alessi *et al.*, 2018) and was diluted in phosphate buffered saline (PBS) to 1×10^3 cells per ml to get an average of 1 cell per 1 μ l device well. For each isolation device, 1 g soil was added to 10 ml sterile PBS (8 g NaCl, 0.2 g KCl, 1.44 g Na_2HPO_4 per L with pH adjusted to 7.4), shaken for 30 seconds then allowed to settle for three minutes. Ten microlitres of supernatant was then serially diluted in PBS and added to 5 ml 1.4% (w/v) molten agar (Formedium), giving a final concentration of 0.35% (w/v) agar. The central plate of the device was submerged in the diluted soil agar and once set, Whatman Nuclepore Track-Etched, MB PC 0.05 μ m 47 mm membranes (VWR) were placed on each side of the central plate.

The isolation devices were loaded and reassembled on site and buried at a depth of 10 cm in the locations where the soils had been sampled. The devices were intended to be left *in-situ* for two weeks, but this was reduced to 12 days due to early harvesting which destroyed both the control device and an experimental device in the high yield, high conductivity location at the southernmost sampling site (Chapter 3). The three intact devices were those from the low yield & low conductivity soil (LY LC), low yield & high conductivity soil (LY HC) and the high yield & low conductivity soil (HY LC).

4.2.3. *Culturing microbial isolates*

The isolation devices were recovered from the field and transported back to the lab in loosely tied plastic bags to retain moisture. The devices were immediately disassembled under sterile conditions with the agar plugs were carefully plated onto the soil-extract agar plates. Soil-extract agar was made using the methods used by Alessi *et al.* (Alessi *et al.*, 2018).

Briefly, 0.5 kg soil from each field location was added to 750 ml distilled water and autoclaved for 15 minutes at 121°C. The soil suspension was then centrifuged at $5,600 \times g$ for 20 minutes at

20°C. The supernatant was filtered through Whatman qualitative filter paper No. 1 (Camlab) to make soil extract. Soil extract agar was prepared with 250 ml filtered soil extract, 5 g technical agar (Formedium), 125 mg K₂HPO₄ (Fisher) and 25 mg glucose (Fisher). This was autoclaved at for 15 minutes at 121°C with 50 µg ml⁻¹ cycloheximide (SCBT) and 50 µg ml⁻¹ nystatin (Apollo scientific) added to prevent fungal growth.

Plates were incubated at room temperature for six days until colonies formed. Once colonies had formed, they were replica plated and then streak plated to check for pure culture. Single colonies were picked and grown in tryptic soy broth (TSB) (VWR) overnight. Glycerol stocks were made to a final concentration of 25% glycerol (v/v) and stored at -80°C.

To verify the assumed initial cell count, 1 g of each soil was serially diluted in PBS with 100 µl plated onto respective soil extract agar plates. Plates were incubated at room temperature for six days before colonies were counted.

4.2.4. *High-throughput nitrate and nitrite reduction assays*

All cultured isolates were scored for nitrate and nitrite reductase activity under both oxic and anoxic conditions. The colorimetric Griess assay was used to measure gain or loss of nitrite to indicate nitrate or nitrite reduction respectively.

For the nitrate reduction assay 10 µl overnight culture was added to 40 µl 0.5mM KNO₃ (Alfa Aesar) in TSB (VWR) in a 96-well plate. This was incubated for four hours at 25°C to allow microbial growth and nitrate utilisation. 50 µl 1% (w/v) sulphanilamide (Sigma) diluted in 1M HCl and 50 µl 0.1% (w/v) N-(1-naphthyl)-ethylenediamine dihydrochloride (NED) (Sigma) were added to produce to a pink chromophoric azo product if nitrite is present (Figure 26A). Reagents were prepared according to Garcia-Robledo *et al.* and stored at 4°C protected from light (García-Robledo *et al.*, 2014).

To verify if nitrate had been reduced beyond nitrite, colourless samples were further treated with 50 µl 2% (w/v) vanadium (III) chloride (Aldrich) diluted in 6M HCl to reduce any remaining

nitrate to nitrite, which could be detected. Samples were incubated at 37°C for twenty minutes for the colour change to occur. If the sample remained colourless then then nitrate had been reduced beyond nitrite and if the sample turned pink, then the isolate did not reduce the nitrate (Figure 26B). This assay was used to identify if the isolate could reduce nitrate or not, and if it could reduce nitrate beyond nitrite.

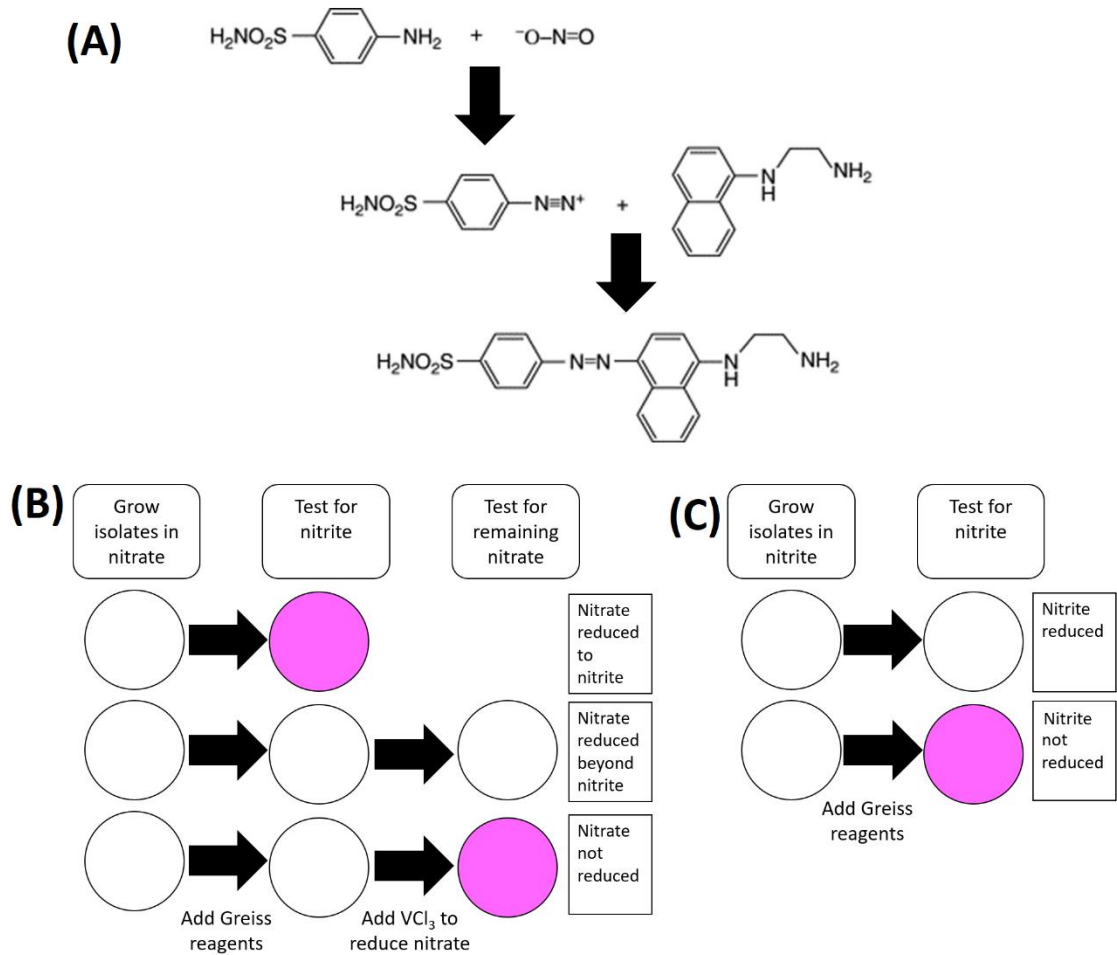


Figure 26 Schematic diagram representing the high-throughput nitrate and nitrite reduction assays. (A) Griess reaction principle. Under acidic conditions, nitrite reacts with sulphanilamide to produce a diazonium ion, which is then coupled to NED to produce a chromophoric azo product, which strongly absorbs at 540 nm. (B) nitrate reduction assay to determine whether isolated microbes can reduce nitrate to nitrite, reduce nitrate beyond nitrite or cannot reduce nitrate. (C) nitrite reduction assay to determine if isolated microbes can reduce nitrite. Figure part (A) reproduced from Giustarini et al. (Giustarini et al., 2008).

To test if nitrite could be reduced directly, a nitrite reduction assay was performed (Figure 26C). 10µl overnight culture was added to 40 µl 0.5mM KNO₂ (Alfa Aesar) in TSB in a 96-well plate. This was incubated for four hours at 25°C to allow microbial growth and nitrite utilisation. Fifty microlitres of 1% (w/v) sulphanilamide and 50 µl NED were added to produce a pink chromophoric azo product if nitrite was still present. The reaction remained colourless if all of the nitrite had been reduced by the isolate.

The assays were carried out in triplicate under both oxic and anoxic conditions to quantify the proportion of aerobic denitrifiers in the sample. For oxic assays, plates were shaken for 10 seconds every 5 minutes in a plate reader. For anoxic assays, plates were grown in an air-tight container made anoxic using AnaeroGen sachets (Thermo Scientific). The sachets contain ascorbic acid and activated carbon which reacts with air. Oxygen is rapidly absorbed, and carbon dioxide is produced. The oxygen concentration is reduced to less than 1% within 30 minutes. Anaerotest strips (Merck) were used to confirm anoxic conditions.

4.2.5. *16S rRNA sequencing of all isolates*

To identify the taxonomy of the cultured microbes, the 16S rRNA gene was sequenced. Isolates were streaked into nutrient agar plates (VWR) and grown at room temperature for 48 hours. A single colony was picked and suspended in 100 µl sterile PBS. The suspended colony was heated at 90°C for 2 minutes and centrifuged at 13,000 rpm in a microcentrifuge for 2 minutes. 20 µl of the supernatant DNA-extract was stored at -20°C prior to PCR amplification.

A nearly full length, 1465 bp, fragment of the 16S rRNA gene was amplified using primers 27F (5'-AGAGTTTGATCMTGGCTCAG) and 1492R (5'-GGWTACCTTGTTACGACTT) (Lane *et al.*, 1985) which covered variable regions 1-8. The 25 µl amplification reaction consisted of 0.4µM of each forward and reverse primer, 5 µl 5X GoTaq reaction buffer, 0.2mM dNTPs, 2mM MgCl₂, 1.25 U GoTaq DNA polymerase and 2 ul DNA extract. PCR conditions were as follows: Initial denaturation at 95°C for 90 seconds, 30 cycles consisting of denaturation at 95 °C for 30

seconds, annealing at 58 °C for 30 seconds and extension at 72 °C for 40 seconds, then final extensions at 72 °C for 10 minutes.

The size of the PCR product was confirmed by agarose gel electrophoresis and samples were purified using QIAquick PCR purification kit (Qiagen) according to the user manual with the addition of a five-minute incubation at room temperature following the additions of PE and EB and elution in 30 µl EB. The purified PCR product was quantified using a NanoDrop spectrophotometer (Thermo Fisher Scientific) and Sanger sequenced using SupremeRun (Eurofins) using the 27F primer.

Taxonomy was assigned to the 16S rRNA using the SILVA reference database version 138.1 (McLaren and Callahan, 2021). MAFFT was used for multiple sequence alignment (Madeira *et al.*, 2022) with the ape R package used to build and visualise the phylogenetic tree (Paradis and Schliep, 2019).

4.2.6. *Selection of isolates for further study*

Following 16S rRNA sequencing of all isolates, twelve were selected for further study. These isolates were chosen to represent non-model organisms, be abundant in the environment and represent each of the major phyla found in Harold Smiths field soil. These isolates were selected for whole genome sequencing to identify which nitrogen cycling genes they had and whether any inferences could be made to link gene to function.

4.2.7. *Quantifying utilised substrate*

A further 96-well plate assay was devised to test what proportion of substrate was utilised by the selected isolates. Inocula were prepared by growing each strain on nutrient agar (VWR) for 48 hours and resuspending growth in TSB (VWR) to an optical density of OD_{600 nm} = 1. Ten microlitres of cell suspension (approximately 5 x 10⁶ cells) was added to 40 µl TSB containing potassium nitrate (Alfa Aesar) or potassium nitrite (Alfa Aesar) to a final concentration of 500 µM nitrate or nitrite. Abiotic controls with an equal volume of TSB instead of inoculum were also prepared. Here, the experiments were completed as in 4.2.4. The final colorimetric results were

compared to calibration curves of between 0 – 500 μM nitrate or nitrite respectively. This experiment enabled the quantification of nitrate or nitrite loss over a four-hour period with a standardised initial cell density.

4.2.8. Nitrate loss rate experiments in pure culture

To better understand the link between gene and function, the twelve selected isolates were used in nitrate loss rate experiments with continuous measurements of oxygen and nitric oxide and regular measurements of nitrate and nitrite concentrations throughout.

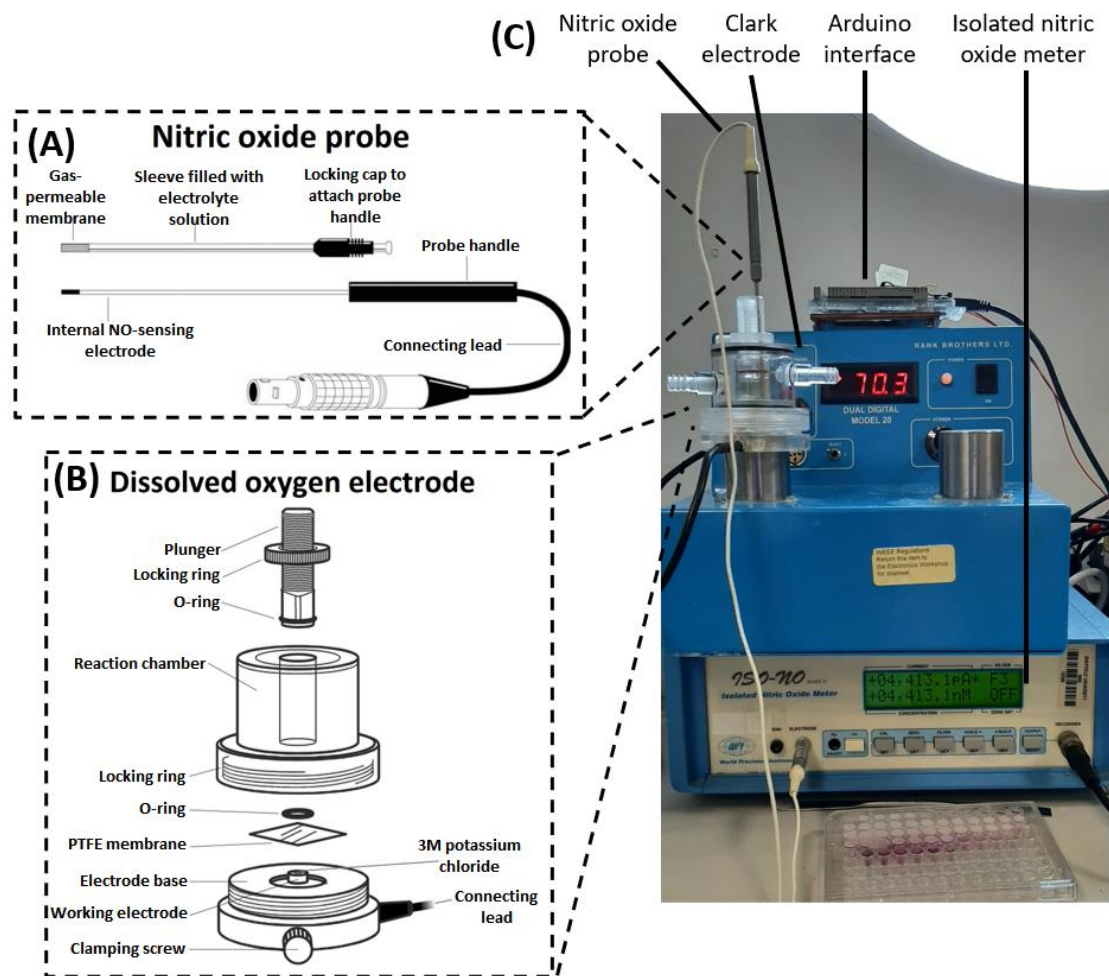
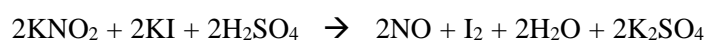


Figure 27 Nitrate loss in pure culture experimental setup. (A) Structure of the ISO-NOP nitric oxide probe. (B) Components of the dissolved oxygen (Clark) electrode. (C) Photograph of experimental setup including nitric oxide probe, Clark electrode, Arduino interface and isolated nitric oxide meter. Panels A and B adapted from WPI-Europe & Rank Brothers respectively .

Nitric oxide concentration was measured continuously throughout the experiment using an ISO-NOP nitric oxide probe (Figure 27, World Precision Instruments) coupled to an ISO-NO Mark II Isolated Nitric Oxide Meter NOMK2 (World Precision Instruments). The NO probe was suspended in the Clark electrode reaction chamber (Figure 27B-C), through a small hole drilled into the plunger, and secured with a clamp stand, so that the tip of the electrode was above the stirrer bar. The NO probe was filled with electrolyte solution (World Precision Instruments) and polarized for 12 hours in 0.1M KI/H₂SO₄ solution before use.

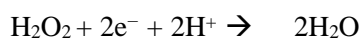
Nitric oxide calibration was performed according to the user manual. Briefly, known quantities of NO were produced by adding increasing volumes of 50 μM KNO₂ (Alfa Aesar) to 0.1 M H₂SO₄ (SLS) + 0.1 M KI (Fisher Scientific), based on the reaction below (Equation 6). The differences in current output (pA) on the isolated nitric oxide meter were recorded and used to construct a calibration curve with the known concentrations of NO. The calibration was carried out in triplicate at room temperature (20°C).



Equation 6

Oxygen concentration was measured continuously using the Clark electrode (Dissolved oxygen electrode, Figure 27B). Oxygen diffused through a 0.0127 mm PTFE membrane and is reduced at a platinum surface immediately in contact with the membrane using Equation 7.





Equation 7

To set up the Clark electrode, a droplet of 3M KCl (Sigma) was pipetted onto the silver and platinum electrodes, covered with a 1cm² piece of PTFE and sealed with a rubber 'O' ring. The incubation chamber was then secured with the locking ring. A 10mm magnetic stirrer was placed inside the reaction chamber before the sample was added and the plunger secured with the locking ring. The polarising meter was set to 0.6 V and the stirrer speed set to 9.

To calibrate the Clark electrode, 5ml Milli-Q purified water (Merck) was added to the reaction chamber, with stirrer speed set to maximum (9), and the left for approximately 1 hour for the current to stabilise. The maximum reading was assumed to represent oxygen saturated water at a concentration of 284 μM O₂ at 20°C (Benson and Krause Jr., 1980). A few crystals of sodium hydrosulphite (Sigma-Aldrich) were added two minutes after oxygen level had stabilised to react with all of the oxygen. Once the oxygen level remained level for 1 minute, the water was assumed to be fully deoxygenated. A calibration curve was then constructed with the oxygen concentration and the recorded current. The calibration was carried out in triplicate at room temperature (20°C).

Data from both the Clark electrode oxygen meter and the isolated nitric oxide meter were transferred to a computer using a custom-made Arduino interface made with a Due microcontroller board (Figure 28). The data was transferred using code written and uploaded in the Arduino IDE 1.8.19 (Appendix 2), with data points recorded every second during the three-hour experiment and the results printed to the IDE serial monitor.

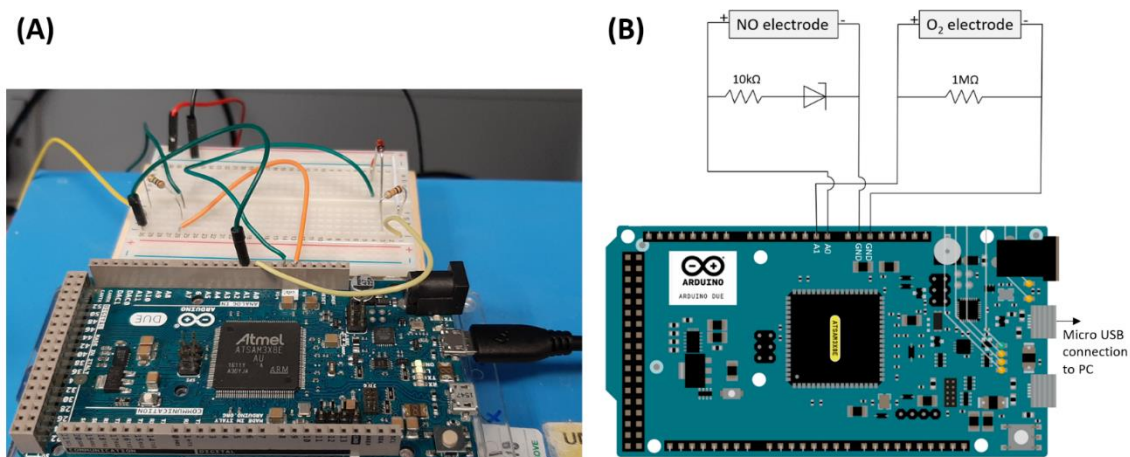


Figure 28 Arduino Due circuit to transfer data from the oxygen and nitric oxide detectors. (A) Photograph depicting breadboard mounted circuit connected to Arduino Due microcontroller board. (B) Schematic view of the circuits.

To confirm the ability of the twelve isolated strains to utilize nitrate, degradation assays were performed in TSB (VWR) with 500 μM nitrate (KNO_3 , Alfa Aesar). Inocula were prepared by growing each strain on nutrient agar for 48 hours and resuspending growth in TSB to an initial optical density of $\text{OD}_{600\text{ nm}} = 1$. Five millilitres of this inoculum (approximately 2.5×10^9 cells) were added to the reaction chamber of the Clark electrode (Figure 27B) with potassium nitrate to a final concentration of 500 μM . Abiotic controls with an equal volume of TSB instead of inoculum were also prepared.

Cultures were incubated in the reaction chamber of the Clark electrode at room temperature for three hours with a stirrer speed of 9. Fifty microlitres of sample was removed using a Hamilton syringe every fifteen minutes to measure nitrite and then nitrate concentration as described in section 4.2.4. The reaction chamber plunger was pushed into the lowest point after each sampling to avoid issues arising from increased headspace gas.

Analyses of these experiments were performed using R version 4.2.0 (R Core Team, 2022) implemented in RStudio version 2022.02.3.492 (RStudio Team, 2022). For oxygen and nitric oxide measurements, rolling averages over ten second periods were calculated using the 'rollmean' function in the zoo package (Zeileis and Grothendieck, 2005) to reduce the effects of

noise. For all chemicals rate of change was calculated as a function of time. For oxygen use, a Michaelis-Menten curve (Equation 8) was fitted to the Clark electrode data using the `drm` function of the `drc` package (Ritz *et al.*, 2015) using the `MM.3` non-linear function to specify the model. Here, v is the velocity of the reaction in $\mu\text{M s}^{-1}$, V_{\max} is the maximum rate achieved by the system in $\mu\text{M s}^{-1}$, $[S]$ represents the substrate concentration in μM and K_M is the Michaelis constant. V_{\max} and K_M values were calculated based on the model fit.

$$v = \frac{V_{\max} [S]}{K_M + [S]}$$

Equation 8

4.2.9. *Whole genome sequencing of selected isolates*

The twelve isolates selected for further study underwent whole genome sequencing to investigate the distribution of denitrification genes in bacteria that are not considered model organisms. Whole genome sequencing was done by MicrobesNG (<http://www.microbesng.com>), through Illumina short-read sequences.

The strains were grown on nutrient agar plates (VWR) overnight at 25°C. Cells were removed from the plate and resuspended in PBS. OD600 was measured and approximately 6×10^9 cells were washed in PBS and resuspended in 0.5 ml of 1 x DNA/RNA Shield buffer (Zymo Research) before being shipped to MicrobesNG (Birmingham, UK) for DNA extraction and sequencing.

DNA was then extracted from isolates using an extraction buffer containing lysozyme and RNase A, incubated for 25 minutes at 37°C. Proteinase K and RNaseA were added and incubated for 5 minutes at 65°C. Genomic DNA was purified using an equal volume of SPRI beads and resuspended in EB buffer. DNA was quantified in triplicates with the Quant-iT dsDNA HS assay (Thermo Fisher Scientific) in an Eppendorf AF2200 plate reader.

Genomic DNA libraries were prepared using Nextera XT Library Prep Kit (Illumina) following the manufacturer's protocol with the following modifications: two nanograms of DNA instead of one were used as input, and PCR elongation time was increased to one minute from 30 seconds. DNA quantification and library preparation were carried out on a Microlab STAR automated liquid handling system (Hamilton). Pooled libraries were quantified using the Kapa Biosystems Library Quantification Kit for Illumina (Roche) on a Roche light cycler 96 qPCR machine.

Libraries were sequenced on an Illumina instrument using a 250 bp paired end protocol. Reads were adapter trimmed using Trimmomatic 0.30 with a sliding window quality cutoff of Q15 (Bolger *et al.*, 2014). *De novo* assembly was performed on samples using SPAdes version 3.7 (Bankevich *et al.*, 2012), and contigs were annotated using Prokka 1.11 (Seemann, 2014).

4.3. Results

4.3.1. Isolation of culturable soil bacteria

Of the three isolation devices recovered, the soils yielded different numbers of cultivable microbes. The low yield and low conductivity soil (LY LC) yielded 53 out of 384 potential colonies (13.8%), LY HC yielded 117 colonies (30.5%), whereas HY LC had only 35 viable colonies (9.1%). The reasons for this difference may be because there are more culturable microbes in soils with high shallow conductivity which contains more moisture but would need to be confirmed through replication. Others have found only 30-40% wells were filled with colonized agar plugs (Alessi *et al.*, 2018), with an average of 43% plugs showing growth one week after plating – a return of 15% of potential colonies.

4.3.2. Diversity captured through isolation

To examine the taxonomic structure of the bacteria in our samples, a taxonomic classification was performed on the V1-V8 regions of 16S rRNA gene using the SILVA reference database (McLaren and Callahan, 2021). Of the 205 bacteria isolated, the dominant genera were *Acinetobacter* (32.7%), *Pantoea* (25.4%) and *Stenotrophomonas* (20.5%) (Figure 29). *Serratia*, *Pseudomonas*, *Chryseobacterium*, *Buttiauxella*, *Delftia*, *Paenarthrobacter*, *Bacillus* and

Citrobacter made up the remaining 21.4% of isolated bacteria. There was both considerable phylogenetic similarity and also diversity between isolates, as demonstrated by the variable branch lengths, even within genera (Figure 29).

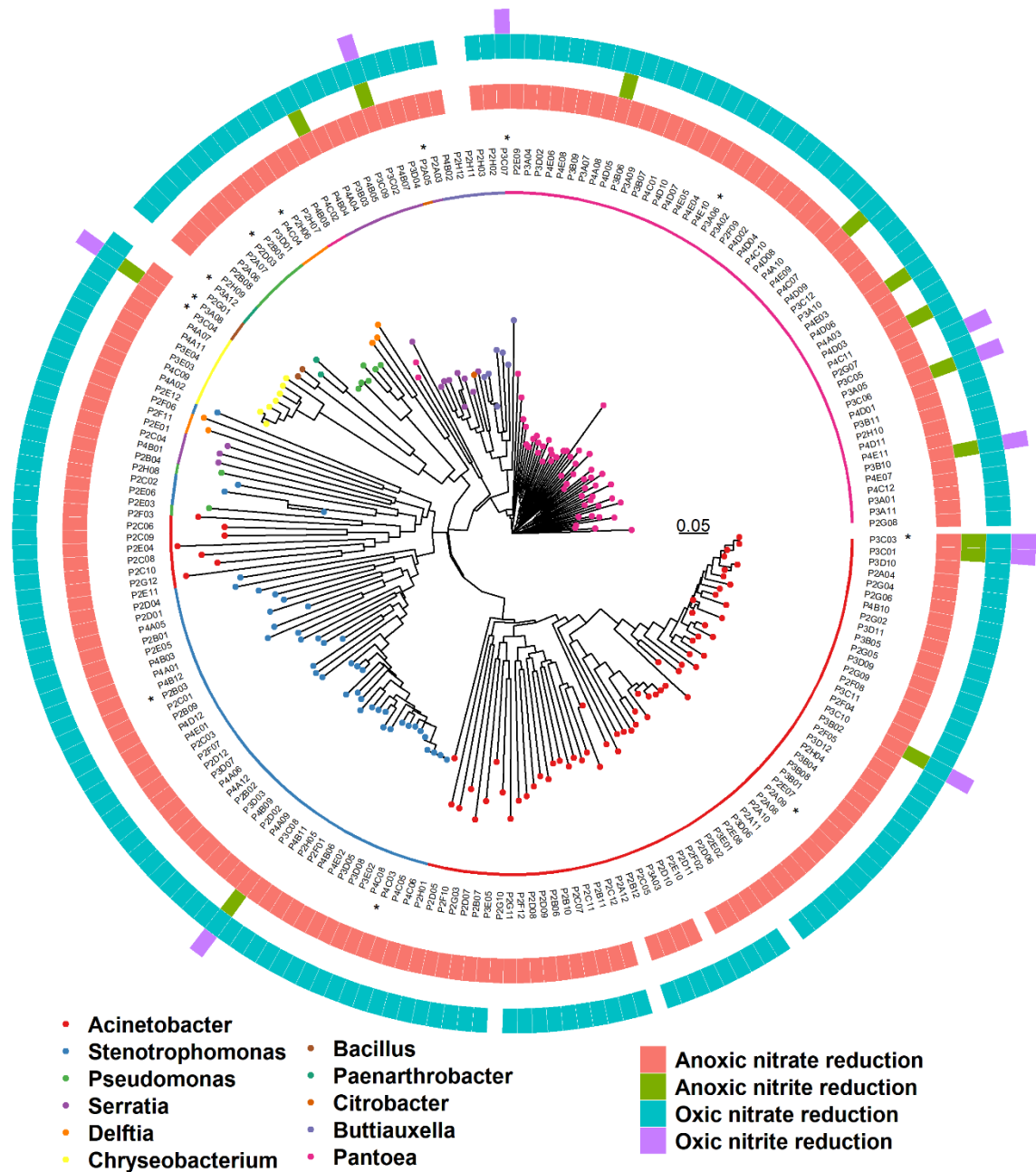


Figure 29 Phylogenetic tree of 16S rRNA for all bacteria isolated and cultured from Harold Smiths soils. Coloured tip points indicate isolate genus. Starred isolates indicate those selected for further study. Coloured bars around the outside indicate screening assay results for aerobic and anaerobic nitrate and nitrite reduction.

To understand how much diversity was captured through use of the isolation device, a species accumulation curve was made of the total bacterial population. Total bacterial population was represented by all 16S rRNA sequences from Harold Smiths field from the 2018-2020 sampling effort as described in Chapter 3. The species accumulation curve indicates that we would expect to find 155 species (± 2.59 SE) from a sampling effort of 205 samples (Figure 30). We found 159 species using the device (using a branch length of 0.05 nucleotide substitutions per site to define species). This indicates that the isolation device captured a large amount of the diversity from the soil in this relatively small sample size.

It should be noted, however, that only eleven genera were successfully cultured using the device (Figure 29), whereas environmental DNA indicates that there are at least 496 distinct genera in the soil. Whilst the isolates contained approximately the number of species that were expected from the device, they were limited to a small number of genera that were culturable under lab conditions. Increasing the sample size through more isolation devices is likely to yield a small number of different species but will likely be subject to diminishing returns, as the majority of isolates will represent “easy-to-culture” isolates that have previously been isolated.

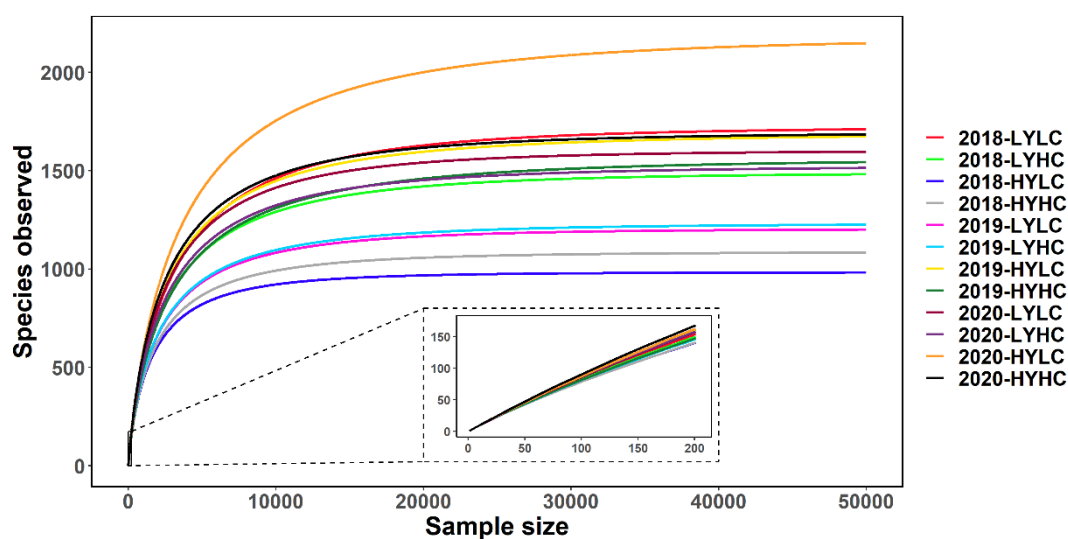


Figure 30 Species accumulation curve for Harold Smiths soil samples. Inset panel is zoomed in on 0 - 205 samples to represent the equivalent of the 205 cultured isolates.

4.3.3. High-throughput screening for nitrate & nitrite reduction

A high-throughput screening assay was developed to test whether the isolated bacteria could reduce nitrate and or nitrite under oxic and anoxic conditions. 97.1% isolates reduced the nitrate under anoxic conditions, with 96.6% still able to reduce nitrate under oxic conditions (Figure 29). Far fewer isolates reduced nitrite in this assay, with 6.34% and 4.89% of isolates reducing nitrite under anoxic and oxic conditions respectively.

Nitrate reduction was observed across all isolate genera (Figure 29). Nitrite reduction in this assay was limited to *Pantoea* (7 isolates), *Acinetobacter* (3), *Serratia* (2), *Chryseobacterium* (1), *Buttiauxella* (1), and *Stenotrophomonas* (1) isolates. Two isolates were able to reduce nitrate under anoxic conditions but were sensitive to oxygen: *Acinetobacter calcoaceticus* P2G10 and *Acinetobacter guillouiae* P3E01. Five isolates were able to reduce nitrite under anoxic conditions, but not under oxic conditions: *Pantoea agglomerans* (4 isolates) and *Serratia liquefaciens* (1 isolate).

4.3.4. Selection of isolates for further study

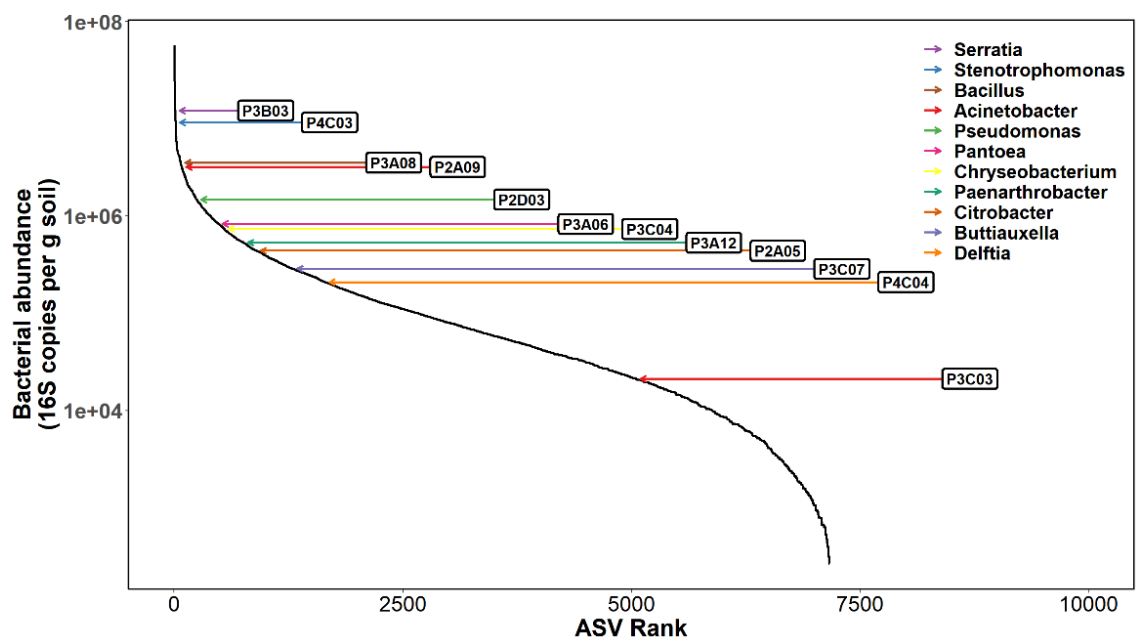


Figure 31 Rank abundance curve of 16S rRNA amplicon sequence variants from Harold Smiths field 2018-2020. Arrows indicate abundance of twelve isolates chosen for further study. Arrow colour indicates isolate genus.

Based on 16S rRNA sequencing, twelve isolates were then selected for further study. None of these represented model organisms used for the study of denitrification. One isolate was chosen from each of the genera from the isolated bacteria (Figure 29). Isolates with strongest similarities to the most abundant ASVs associated with these genera were then selected (Figure 31). 11 isolates were selected based on high abundance in Harold Smiths soils, with a second *Acinetobacter calcoaceticus* isolate (P3C03) selected based on elevated nitrite reductase activity during screening in 4.3.3. Of the twelve isolates, all could reduce nitrate apart from P3A12 (*Paenarthrobacter nitroguajacolicus*). Only three of the isolates reduced nitrite: *Acinetobacter calcoaceticus* P3C03, *Chryseobacterium lactis* P3C04 and *Buttiauxella agrestis* P3C07.

4.3.5. *Nitrate reduction profile in selected isolates*

The twelve selected isolates were then used in functional assays for nitrate and nitrite reduction. The substrate utilisation experiment showed what proportion of 500 μ M nitrate or nitrite was used over a four-hour period with a standardised starting cell density (Figure 32). Half of the isolates (P2A05, P3A06, P3A08, P3B03, P3C04 and P4C03) depleted all of the available nitrate within four hours in both anoxic and oxic conditions. Two isolates (P3C03 and P3C07) were able to reduce some of the nitrate and used more of the nitrate under anoxic conditions. Four isolates were able to reduce negligible amounts of nitrate (P2A09, P2D03, P3A12 and P4C04), with slightly more nitrate used under anoxic conditions than oxic.

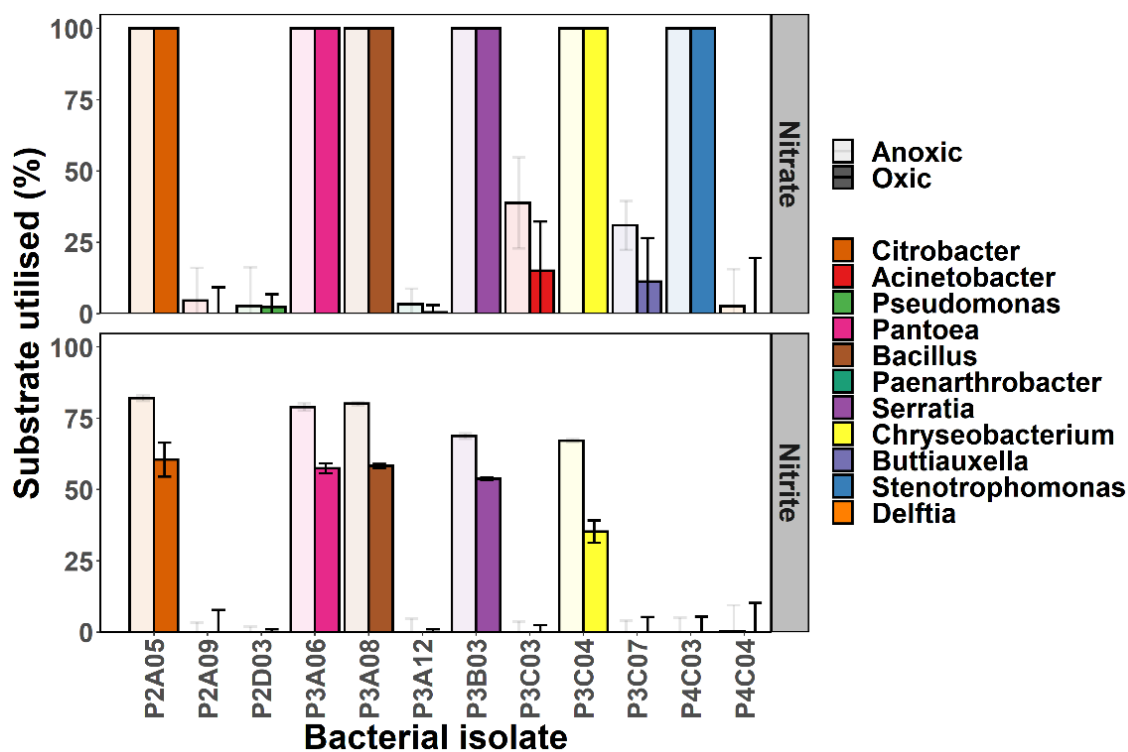


Figure 32 Percent of 500µM nitrate or nitrite used after four hours under anoxic or oxic conditions with a starting cell density of 5×10^6 cells. Bars show mean of three replicates with error bars representing standard error.

Five of the six isolates that reduced all of the nitrate were also able to reduce nitrite: P2A05, P3A06, P3A08, P3B03 and P3C04 (Figure 32). Each of these isolates reduced significantly more nitrite under anoxic conditions compared to oxic (Oxygen: $F = 232$, $Df = 1, 20$, $p = 1.79 \times 10^{-12}$). None of the other isolates showed nitrite loss above the level of the abiotic controls.

These nitrate and nitrite reduction profiles are inconsistent with those observed during the high-throughput screening assay in 4.3.3. as shown in Table 12. In this substrate utilisation experiment, three isolates that had previously demonstrated nitrate reductase activity (P2A09, P3A06 and P4C04) did not use any of the nitrate during the four hours. Additionally, one isolate that previously demonstrated considerable nitrite reductase activity, P3C03, did not reduce any nitrite. Two further isolates that had not shown nitrite reductase activity (P3A06 and P3A08) were subsequently able to utilise the nitrite. These inconsistencies may be linked to gene regulation.

Table 12 Nitrate and nitrite reduction profiles of selected bacterial isolates under oxic and anoxic conditions in three experiments: high-throughput screening, substrate utilisation and Clark electrode. + indicates loss of nitrate or nitrite. + O₂ indicates oxic conditions and - O₂ indicates anoxic.

Sample	Taxonomy	High-throughput screening				Substrate utilisation experiment				Clark electrode experiment	
		NO ₃		NO ₂		NO ₃		NO ₂		NO ₃	NO ₂
		+ O ₂	- O ₂	+ O ₂	- O ₂	+ O ₂	- O ₂	+ O ₂	- O ₂	- O ₂	- O ₂
P2A05	<i>Citrobacter werkmanii</i>	+	+			+	+	+	+	+	+
P2A09	<i>Acinetobacter guillouiae</i>	+	+								
P2D03	<i>Pseudomonas helmanticensis</i>	+	+								
P3A06	<i>Pantoea deleyi</i>	+	+			+	+	+	+	+	+
P3A08	<i>Bacillus mycoides</i>	+	+			+	+	+	+	+	+
P3A12	<i>Paenarthrobacter nitroguajacolicus</i>										
P3B03	<i>Serratia grimesii</i>	+	+			+	+	+	+	+	+
P3C03	<i>Acinetobacter calcoaceticus</i>	+	+	+	+	+	+			+	
P3C04	<i>Chryseobacterium indologenes</i>	+	+	+	+	+	+	+	+	+	
P3C07	<i>Buttiauxella agrestis</i>	+	+	+		+	+			+	+
P4C03	<i>Stenotrophomonas maltophilia</i>	+	+			+	+			+	+
P4C04	<i>Delftia lacustris</i>	+	+								

To further understand the dynamics of nitrate loss in pure culture, experiments were carried out in a Clark electrode with a nitric oxide probe (Figure 27). This allowed us to take continuous measurements of dissolved oxygen and nitric oxide whilst taking regular measurements of nitrate and nitrite concentrations every 15 minutes over three hours. This experiment used a larger culture volume and higher cell density than previous nitrate reduction experiments (4.3.3. and 4.3.5. as low cell density was found to delay the time for the media to become anoxic and begin reducing nitrate (preliminary data not shown).

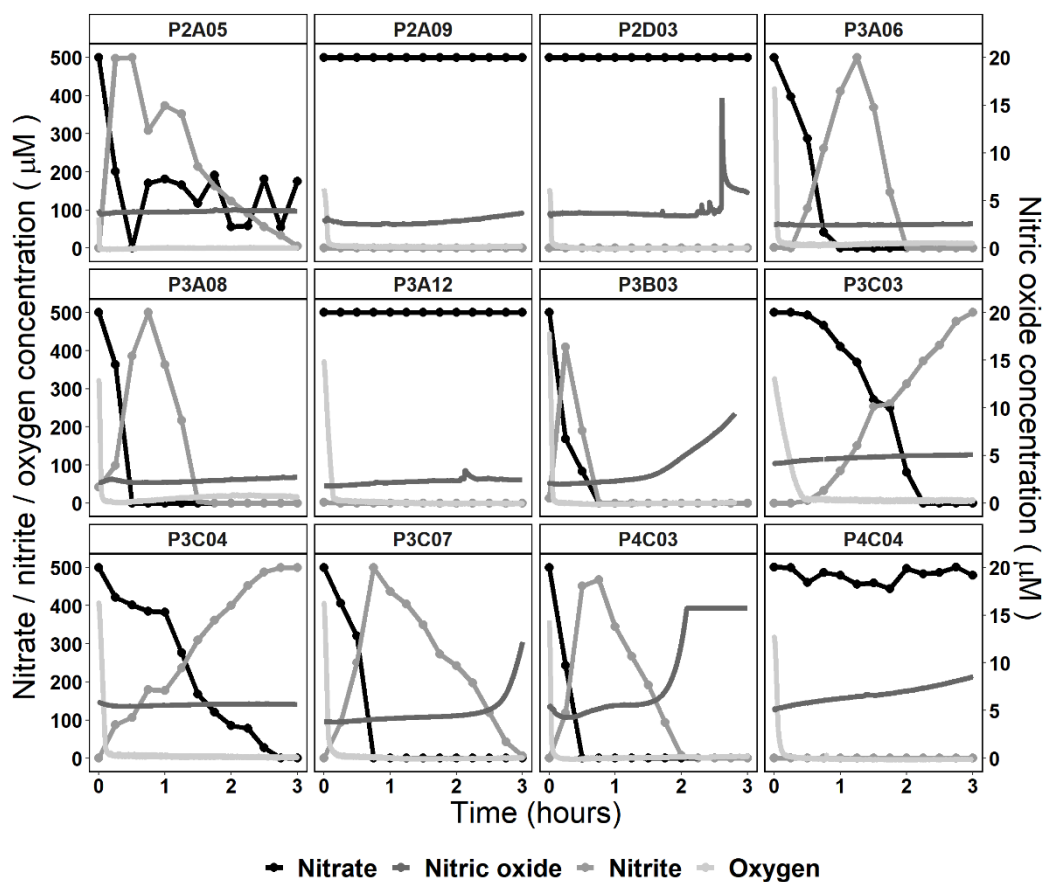


Figure 33 Nitrate loss in pure culture in 5 ml TSB supplemented with 500 μM potassium nitrate. Nitric oxide and oxygen measurements were taken continuously, with nitrate and nitrite measurements taken every 15 minutes as indicated by the points on the graph. Bacterial isolates are shown in facet name. The nitrate (black), nitrite (grey) and oxygen (light grey) scale is shown on the left axis, with nitric oxide (dark grey) on the right-hand axis.

In all samples, oxygen concentration dropped to zero with the first twenty minutes (Figure 33), and usually within the first five minutes, indicating high aerobic respiration rate and growing/proliferating cells. Rate of oxygen use was found to follow a Michaelis–Menten kinetics (Figure 34), with an average V_{max} of $2.30 \mu\text{M s}^{-1}$ (± 0.32 SE) and K_M of $45.1 \mu\text{M O}_2$ (± 6.0 SE). These isolates do not appear to use oxygen at very low concentrations, but this is likely to be an artefact of the experimental setup, with difficulties measuring oxygen accurately at low concentrations due to high background noise from electrical interference. Two of the isolates (P3C03 and P3A12) had significantly lower V_{max} rates for oxygen consumption. This may

indicate that the number of active cells in the experiments for these isolates was lower, which could affect the nitrogen use dynamics.

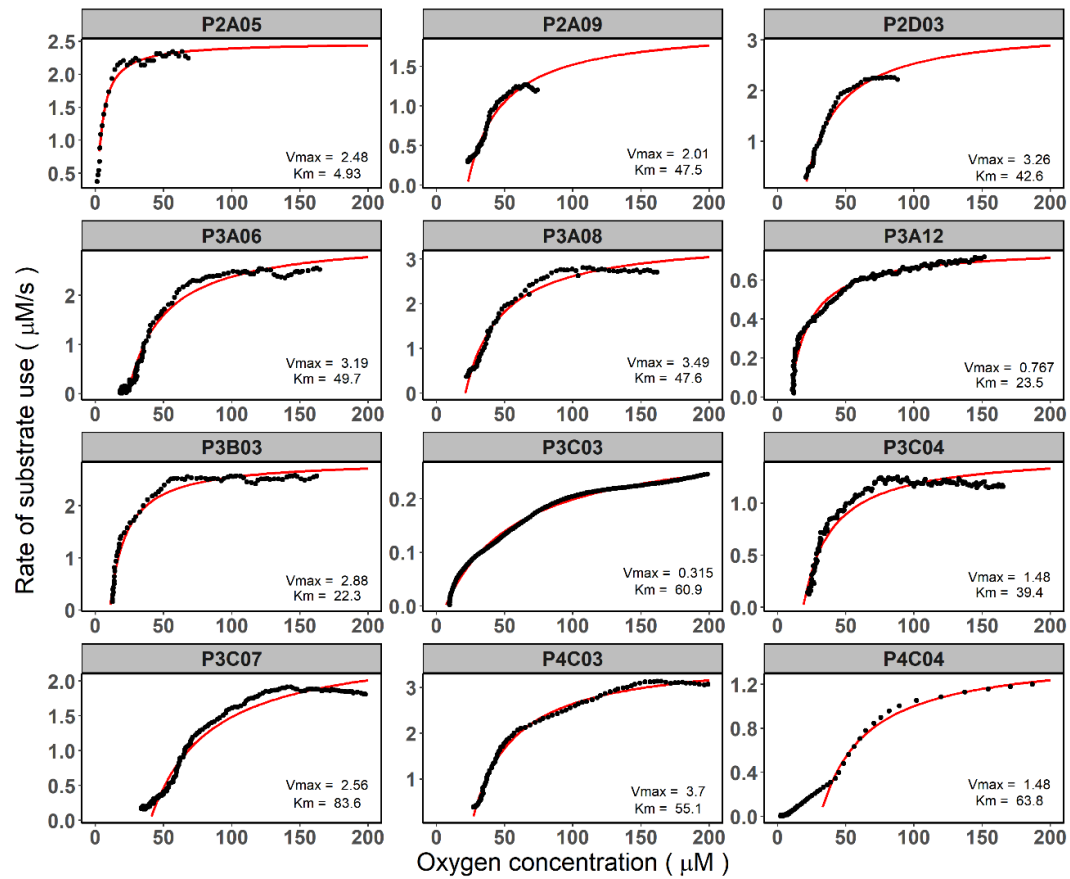


Figure 34 Rate of oxygen use in relation to dissolved oxygen concentration in Clark electrode experiments. Each panel shows a bacterial isolate. Black points show experimental data from the Clark electrode, with red line showing a Michaelis–Menten model fitted to the data. V_{max} ($\mu\text{M s}^{-1}$) and K_M (μM) values derived from the Michaelis-Menten model are shown in the bottom right of each panel.

Nitrate concentration (black points, Figure 33) began to decrease immediately in eight of the twelve isolates (P2A05, P3A06, P3A08, P3B03, P3C03, P3C04, P3C07 and P4C03). This was in accordance with nitrate utilisation experiment results (Table 12). Unlike oxygen, nitrate use does not follow Michaelis-Menten kinetics (Figure 35). Instead, the maximum rate of nitrate use ($0.291\mu\text{M s}^{-1} \pm 0.034$ SE) occurred when nitrate concentration was high (250-500 μM) but often reached peak rate later on, after an average of 46.9 minutes. Although the nitrate concentration had dropped by this point, this result may indicate the time lag between oxygen being depleted

and nitrate reducing enzymes being produced and operating at maximum capacity. This apparent lack of Michaelis-Menten kinetics is likely due to other variables impacting on the rate of nitrate reduction achievable in cells.

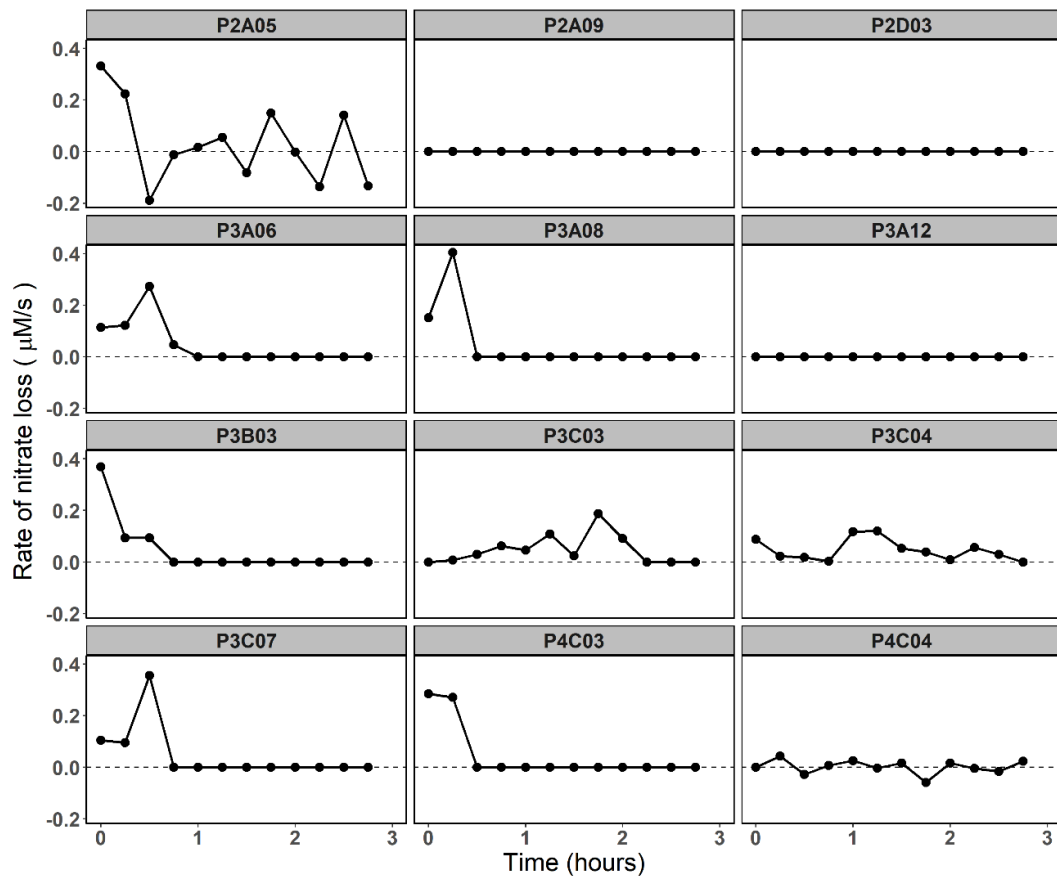


Figure 35 Rate of nitrate loss over time in Clark electrode experiments. Each panel shows a bacterial isolate. Black points show experimental data from the Clark electrode.

In terms of nitrite production and loss (grey points Figure 33), nitrite was generally produced at the same rate as nitrate was lost, with an increase in nitrite after an initial lag up to a mean maximum concentration of $486\mu\text{M} \pm 10.2 \text{ SE}$. Once nitrite concentration had reached its peak it fell more slowly back to zero or remained high for P3C03 or P3C04. The mean maximum rate of nitrite production was $0.356\mu\text{M s}^{-1} (\pm 0.0539 \text{ SE})$, whereas the mean maximum rate of nitrate loss was $0.145\mu\text{M s}^{-1} (\pm 0.0372 \text{ SE})$, indicating that nitrite production was faster than nitrite loss. Nitrite was only detected in samples showing nitrate loss (Figure 36), which could lead to a build-

up of nitrite if nitrate was unlimited. There was no relationship between the rate of nitrite production and the concentration of nitrate (data not shown). However, if measurements were taken more frequently during the initial 30 minutes of the experiment, a pattern may emerge.

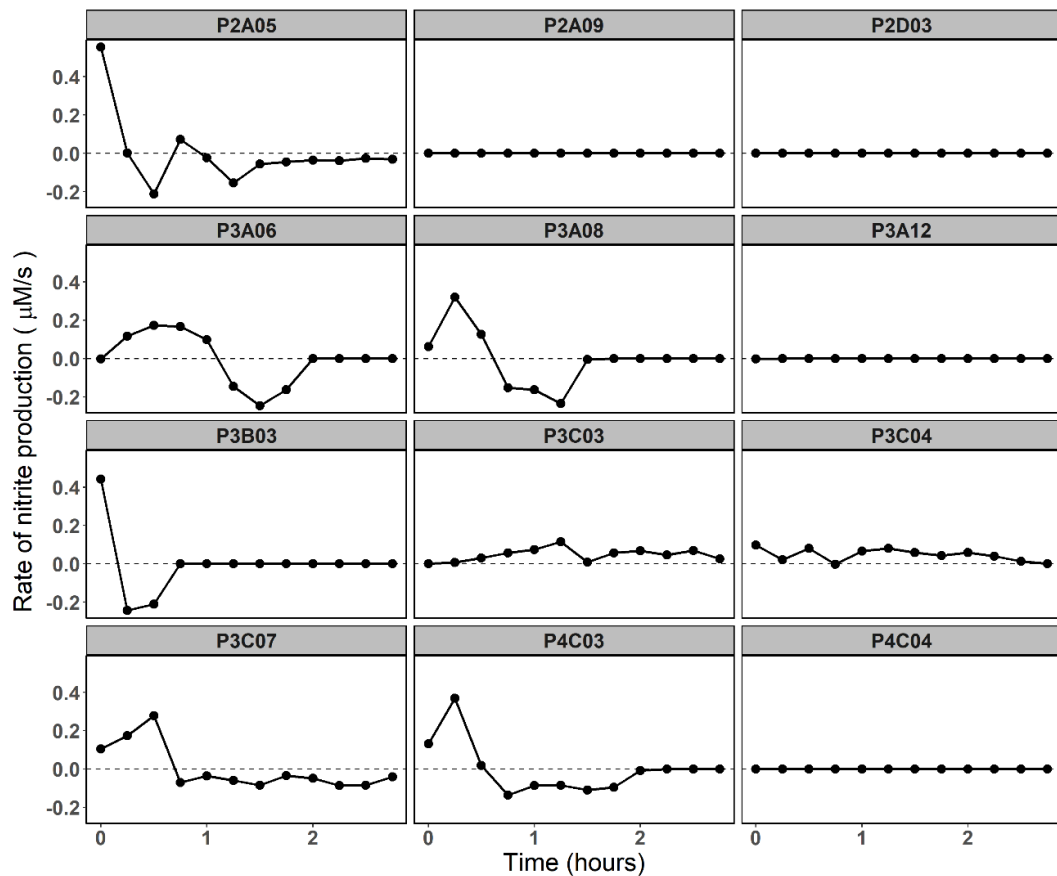


Figure 36 Rate of nitrite production and loss over time. Positive rate values indicate nitrite production with negative values showing rate of nitrite loss.

Nitric oxide (dark grey line Figure 33) concentration remained stable throughout the experiments, suggesting that nitric oxide was not produced. This suggests that nitrite reductases were not converting the nitrite into nitric oxide. The nitrite may instead have been converted into ammonium through DNRA or nitrogen assimilation pathways instead of denitrification.

To summarise, eight isolates were able to reduce nitrate under anoxic conditions in these experiments, with six of the isolates then reducing the resultant nitrite. Nitrite was produced at a higher rate than it was lost at, and nitric oxide was not detected in any of the experiments.

4.3.6. *Comparative genomic analysis of nitrogen cycling gene profiles*

The twelve isolates used in the Clark electrode experiments in 4.3.5. underwent whole genome sequencing to better understand which nitrogen cycling genes they possessed and whether these were likely to have been expressed during the aforementioned experiments. Isolates were sequenced using Illumina MiSeq 250 bp paired end sequencing, filtered to Q15, *de novo* assembled, and genes annotated using Prokka.

It was found that nine of the bacterial isolates had one or both of the denitrification/DNRA nitrate reductases *napA* or *narG* (Table 13). *NapA* is a periplasmic respiratory nitrate reductase, whereas *narG* is a membrane-bound respiratory nitrate reductase. All of the isolates containing these genes, apart from *Delftia lacustris* P4C04, were shown to reduce nitrate in the Clark electrode experiments and substrate utilisation experiments. Interestingly, P4C04 did demonstrate nitrate reductase activity in the high-throughput screening assay when the cell density was lower. All isolates apart from *Paenarthrobacter nitroguajacolicus* P3A12 had the nitrate reductase gene *nasA*. However, *nasA* is involved in assimilatory nitrate reduction and unlikely to be expressed under anoxic conditions (Figure 2). *NasA* is likely responsible for the nitrate reduction by isolates P2A09 and P2D03 during the high-throughput nitrate reduction screening experiments in 4.3.3. It is possible that all of the nitrate was reduced during the first thirty minutes before oxygen was fully removed in the anoxic experiments.

None of the isolates possessed the nitrite reductase genes *nirK* or *nirS* used for nitrite reduction in the denitrification pathway (Table 13). One of the isolates, *Citrobacter werkmanii* P2A05, had the *nrfA* gene for reducing nitrite to ammonium as part of the DNRA pathway. All of the isolates had either the *nasD* or *nirB*, an assimilatory nitrite reductase gene. This suggests that the five isolates that reduced nitrite under anoxic conditions (excluding P2A05), were doing so with *nasD/nirB* genes as part of the nitrogen assimilation pathway. This would usually take place under oxic conditions.

For nitric oxide reduction, four isolates (P2A05, P3B03, P3C04 and P4C03) have the nitric oxide reductase gene *norV*. This anaerobic nitric oxide reductase uses NADH to detoxify nitric oxide (NO), protecting several NO-sensitive enzymes. *NorW* flavorubredoxin reductase is an accessory protein for *norV*. All but two of the isolates had *norW* (Table 13). None of the isolates had *norB*, the anaerobic nitric oxide reductase gene used in the denitrification pathway. This is unsurprising given that none of the isolates had the *nirK* or *nirS* nitrite reductase genes, so none of the isolates could produce nitric oxide which would need reducing.

None of the isolates had a *nosZI* or *nosZII* nitrous-oxide reductase gene (Table 13), although this gene is often present in the absence of the other denitrification genes. The absence of *nosZ* suggests that the isolates selected were not capable of denitrification, despite the reduction of nitrate and the subsequent production and loss of nitrite.

Table 13 Nitrogen cycling gene profiles of selected bacterial isolates based on whole genome sequencing. Annotations were made using Prokka.

Isolate	Taxonomy	Nitrate reduction			Nitrite reduction			Nitric oxide reduction				Nitrous oxide reduction
		<i>napA</i>	<i>narG</i>	<i>nasA</i>	<i>nirK</i>	<i>nirS</i>	<i>nrfA</i>	<i>nasD / nirB</i>	<i>norV</i>	<i>norW</i>	<i>norB</i>	<i>nosZ</i>
		Periplasmic respiratory nitrate reductase	Membrane-bound respiratory nitrate reductase	Assimilatory nitrate reductase	Copper-containing nitrite reductase	Cytochrome cd1 containing periplasmic nitrite reductase	DNRA reduction of nitrite to ammonium	Assimilatory nitrite reduction to ammonium	NADH dependent oxidoreductase	Nitric oxide reductase FIRD-NAD(+) reductase	Anaerobic reduction of nitric oxide (denitrification)	Nitrous-oxide reductase
P2A05	<i>Citrobacter werkmanii</i>	+	+	+			+	+	+			
P2A09	<i>Acinetobacter guillouiae</i>			+				+			+	
P2D03	<i>Pseudomonas helmanticensis</i>			+				+				
P3A06	<i>Pantoea deleyi</i>		+	+				+			+	
P3A08	<i>Bacillus mycoides</i>		+	+				+			+	
P3A12	<i>Paenarthrobacter nitroguajacolicus</i>							+			+	
P3B03	<i>Serratia grimesii</i>	+	+	+				+	+		+	
P3C03	<i>Acinetobacter calcoaceticus</i>	+		+				+			+	
P3C04	<i>Chryseobacterium indologenes</i>	+	+	+				+	+		+	
P3C07	<i>Buttiauxella agrestis</i>	+		+				+			+	
P4C03	<i>Stenotrophomonas maltophilia</i>		+	+				+	+		+	
P4C04	<i>Delftia lacustris</i>	+		+				+			+	

4.4. Discussion

Previous work has shown that soil-dwelling bacteria are notoriously difficult to culture using traditional lab techniques (Staley and Konopka, 1985), with over 99% of microorganisms from the environment resisting cultivation in the laboratory (Kaeberlein *et al.*, 2002). Here we show that using in-situ cultivation facilitates the culturing of a diverse range of bacteria. This technique captures the full diversity that would be predicted by sampling effort, based on a species-accumulation curve of 16S SSU ribosomal RNA genes. In these experiments we were able to culture 205 isolates including 159 species from 11 genera. Whilst this was more than the 155 species predicted from the 16S rRNA species accumulation curve, the lack of variation in genera suggests that specific genera are selected for using this cultivation technique.

We were able to establish high-throughput screening assays for nitrate and nitrite reduction for all cultured isolates. We also performed larger-scale experiments and whole genome sequencing on abundant isolates from each genus. Together these results allow us to better understand the challenges and opportunities associated with cultivation of environmental microbes and learn more about the link between genotype and phenotype in bacteria with regard to nitrogen cycling genes. As whole-genome sequencing becomes increasingly affordable, it has the potential of becoming an important approach for identifying nitrogen cycling gene clusters, to better understand the role of microbial functional guilds in ecosystem functioning.

4.4.1. Tackling the great plate count anomaly

The ‘great plate count anomaly’, a phrase coined by Staley and Konopka, describes the gap between what is in the soil (as measured by culture-independent measures such as 16S rRNA sequencing) and what can be cultured in the lab using traditional microbiology methods (Staley and Konopka, 1985). Several alternative methods of culturing a wider range of microbes have

since been developed, including targeted phenotypic culturing (Browne *et al.*, 2016), diffusion chambers and bioreactors (Kaeberlein *et al.*, 2002; Chaudhary *et al.*, 2019), encapsulation (Zengler *et al.*, 2002) and high dilution (Rappé *et al.*, 2002) approaches. *In-situ* cultivation in diffusion chambers, such as the isolation device described here, offer advantages in terms of being high-throughput, cost effective and simultaneously combining the isolation and growth of soil dwelling bacteria.

As with previous studies (Nichols *et al.*, 2010; Alessi *et al.*, 2018), we demonstrate that the isolation device is useful for culturing a range of microbial species. However, we were unable to capture high diversity of phyla. Most of the isolated bacteria belonged to the Gammaproteobacteria phyla, but there were also Betaproteobacteria, Bacilli, Actinobacteria and Flavobacteriia. The limited number of phyla suggests that the cultivation methods skewed the results towards easily cultivable bacteria such as Gammaproteobacteria, which comprised 92% of isolated bacteria, but only 7.6% of 16S rRNA sequences. Because of this bias, it is likely that even with increased sampling effort there would be a highly diminished number of additional cultivable isolates.

Modifications to cultivation methods such as changes to the media composition, alteration of the pH and incubation temperature could increase the diversity of cultivable isolates. Previous studies have found that small alterations to media, such as autoclaving phosphate separately to agar, unlike the media preparation described here, can improve the culturability of microorganisms (Kato *et al.*, 2018). Additionally, studies using full-strength media have reported cultivation inhibition of a large proportion of soil bacteria (Olsen and Bakken, 1987), which can be overcome using media dilution. Additionally, having nitrate and/or nitrite present in the initial culturing media, as suggested by Lycus *et al.* (Lycus *et al.*, 2017), could have acted as an early enrichment step for cultivation of denitrifying bacteria, which could have contributed to culturing more diverse bacteria. On the other hand, when Heylen *et al.* compared media

containing NO_3^- and NO_2^- for isolation of denitrifiers, the results were inconclusive (Heylen *et al.*, 2006).

Broadly, the use of the custom-made isolation device allowed us to successfully isolate and culture a fairly representative range of bacteria relative to the sampling effort, but protocol modifications would be required to isolate a more diverse range of bacteria including denitrifiers.

4.4.2. *Characterisation of cultured environmental microbes*

The proposed isolation strategy allowed us to capture a range of organisms with different N reductase capabilities, shown through a range of assays. The majority of bacteria isolated from the soil were capable of nitrate reduction and that some of the bacteria also reduced nitrite. Endpoint analysis of NO_3^- and NO_2^- allowed for the quantification of substrate utilisation and time-course experiments enabled the determination of rate of substrate usage and production.

This combination of high-throughput, endpoint and time-course assays has benefits over previous work characterising N-reducing phenotypes as: (1) organisms incapable of reducing nitrate (such as P3A12) were screened for other N reductase genes and phenotypes unlike studies that only provided nitrate (Chèneby *et al.*, 2000; Hashimoto *et al.*, 2009), (2) NO was measured throughout the time-course experiments, so NO production and reduction could be studied as well and any NO-induced inhibition of nitrate or nitrite reduction (Bergaust *et al.*, 2008) and (3) combining isolation characterisation experiments with quantitative 16S rRNA amplicon sequencing enabled us to select highly abundant organisms from each genera of soil bacteria for further study.

Whilst other studies estimate that full denitrification (NO_3^- to N_2) occurs in 0.9 - 4.7% aerobic soil microbes (Chèneby *et al.*, 2000), our study did not find evidence of denitrifying bacteria. It should be noted, however, that twelve isolates that showed nitrate and nitrite reduction in the high-throughput screening assay were not selected for further study but may still be denitrifiers.

If all twelve isolates were found to be denitrifiers, this would account for 5.85% of strains isolated in this experiment. Other studies have found higher numbers of denitrifiers amongst soil organisms with 6.8% and 9.7% reported by Lycus *et al.* and Gamble *et al.* respectively (Gamble *et al.*, 1977; Lycus *et al.*, 2017). These numbers are not comparable to this study, as Lycus *et al.* included non-nitrate reducing denitrifiers and Gamble *et al.* only isolated organisms growing anaerobically, and since the number of viable anaerobes in soil is lower than the number of viable aerobes (Chèneby *et al.*, 2000), the total number of isolates would be reduced and appear to increase the proportion of denitrifiers. Taken together, these results suggest that our isolation strategy had potential but was unsuccessful for capturing denitrifying organisms, with further work required to meet the objectives given in 4.1.1.

Furthermore, if the organisms selected for further study had possessed denitrification genes beyond nitrate reductases it is unclear if they would have been expressed in the Clark electrode experimental setup given that the transition to anaerobic respiration was rapid. Previous studies note the importance of a gentle transition to anoxia, to ensure denitrifiers have the energy needed to produce denitrification enzymes. Since denitrifying bacteria are non-fermentative, they require aerobic respiration to provide energy for the initial production of the denitrification enzymes (Hassan *et al.*, 2014). Cells in the anoxic Clark electrode reaction chamber may not have had time to synthesise the required enzymes before becoming anoxic and then may have been unable to do so due to energy limitation. Additionally, the timing of gene transcription varies between organisms under anoxic conditions (Liu *et al.*, 2019), so different organisms are likely to cope differently with the swift transition to anoxia.

4.4.3. *Nitrate reduction in the absence of denitrification*

Although the approach described here was unsuccessful in isolating denitrifiers from the nitrite reduction step onwards, it was successful in isolating and characterising many nitrate-reducing bacteria and confirming the presence of *napA* or *narG* genes in nine of the twelve sequenced

isolates. Although it is thought that many organisms have both *napA* and *narG* (Frostegård *et al.*, 2022), only three of the nine *napA/narG* positive organisms had both genes. Previous metagenomic work has shown that *narG* is 2.1-6.1 times more abundant than *napA* (Frostegård *et al.*, 2022), whereas an equal number of reads annotated as *napA* and *narG* were found in our isolates, with each bacteria containing only one copy of one or both of these genes. This suggests that our isolation strategy may have preferentially selected for *napA*-type nitrate reducers, a gene that is more commonly found in Gammaproteobacteria (Smith *et al.*, 2007), a phylum that was commonly isolated in this study.

Although nitrate reduction is part of the denitrification pathway, it is also part of the nitrogen assimilation and DNRA pathways, with the presence of genes used in these pathways found in our isolates. Nitrate assimilation has long been associated with nitrogen use efficiency in agriculture, with clear correlations between the nitrate reductase enzyme activity and the yield of grain protein in several cereal crops (Eilrich and Hageman, 1973; Johnson *et al.*, 1976). It is likely that the experimental setup in this study with the isolation device has enriched for nitrate and nitrite assimilation compared to other studies which include a nitrogen source in the media (Heylen *et al.*, 2006). Here, the only nitrogen source was from the soil dilution, so was very low. By enriching for nitrate assimilating bacteria in the first stages of cultivation, this bias has been carried through, suggesting that a greater proportion of nitrate assimilators may have been cultured relative to the proportion observed in other soil samples, particularly given that nitrate assimilation generally occurs under oxic conditions (Hallin *et al.*, 2018).

Alternatively DNRA usually occurs in oxic or micro-oxic environments (Broman *et al.*, 2021). Interestingly, DNRA is found to be inhibited by increased nitrogen input (of both nitrate and nitrite, but more strongly by nitrite) (Hernández-del Amo and Bañeras, 2021). Despite the high nitrate concentration in the Clark electrode experiments, isolate P2A05 was able to reduce all of the nitrite produced through DNRA. It is clear that the interconnected nature of the nitrogen

cycle makes it a complex system to study, with the dynamics constantly in flux driven by biotic and abiotic factors.

Combining molecular techniques with physiological and biochemical studies of isolates grown in pure culture provides insight into the link between genetic potential and measured function, as well as providing context about the taxonomy of the organism itself. Due to redundant functions within the nitrogen cycle, such as nitrate reduction, being present in multiple pathways, it is clear that physiological studies alone cannot be used to predict function.

Here, by combining biochemical screens with molecular analysis it was possible to identify which processes were occurring. The variation in function during different assays can likely be attributed to regulation of the denitrification genes. The considerable variation in the regulation of nitrate and nitrite reduction found among the isolates in this study reinforced the need for more detailed knowledge about a wider range of denitrifiers than that obtained from model bacteria alone. This study supports further analysis of denitrifying bacteria as well as other functional microbial guilds by outlining a technique to isolate new representative organisms for future ecophysiological work.

Chapter 5: General Discussion

Denitrification has been extensively studied since the beginning of the 20th century (Voorhees, 1902), owing to its economic and environmental significance. Nitrogen deficiency is the major nutrient limitation for agricultural productivity (Rütting *et al.*, 2018) and denitrification is the primary route for loss of fixed nitrogen from terrestrial ecosystems (Zhang *et al.*, 2020). The resultant addition of nitrogen-rich fertilizer causes major economic costs for farmers and major environmental costs from leaching of nitrate into watercourses and emissions of environmentally harmful gases including nitrous oxide. The efficiency with which nitrogen improves crop growth varies between soils and also between environmental conditions. Understanding the basis for this variation would allow for more targeted use of nitrogen-rich fertilizers, and improved outlooks for farmers and the environment.

As a result of the sustained research into denitrification, the genes and proteins involved in the process have been systematically characterised (Zumft, 1997). Nitrogen loss is largely controlled by soil microbial processes, but the complexity of the microbial community has made it impractical to quantify the role of microbial diversity in controlling nitrogen dynamics. Despite the challenges, considerable efforts have been made to research the effects of microbial communities on denitrification (Butterbach-Bahl *et al.*, 2013). And, in addition to the problems caused by denitrification, research is increasingly focussing on investigating denitrification as a biological solution to greenhouse gas emissions (Domeignoz-Horta *et al.*, 2016).

Whilst it is clear that research has advanced our understanding of the processes and drivers involved in denitrification, consensus remains lacking concerning the contribution of different microbial communities influencing nitrogen cycling in soils. Many microbial ecology studies

focus on understanding ‘who does what?’ in a given environment, based on the concept of coupled microbial community structure and functioning. However, with a high degree of functional redundancy and clear evidence of modularity in denitrification (Graf *et al.*, 2014), it is apparent that simply knowing which taxa are present has limited value in predicting the process rates. Instead of studying the taxonomy of soil microbes in isolation, combining this with detailed analysis into the diversity and abundance of functional genes can help us to understand the broader controls over ecosystem functioning.

This thesis presents enhanced sequencing methods used to gain high resolution data on the abundance, diversity and structure of the microbial community controlling nitrogen cycling in arable soils. The cornerstone of the work presented here was an insight into the abundance and diversity of bacterial denitrifiers found in differently managed agricultural soils. This was the key to several important results: (1) microbial communities and denitrification genes are largely unaffected by long-term land management history, and cluster predominantly along spatial and environmental gradients within the field; (2) soil microbial and denitrifying communities show significant diversity over short spatial scales and also over time, with denitrifying communities exhibiting stronger distance decay effects than the total bacterial population; and (3) nitrate/nitrite degrading bacterial strains can successfully be isolated from soil and grown under lab conditions for full characterisation with *in-situ* cultivation. Additionally, there is some indication that the relative quantity of *nirK:nirS* denitrifiers may be associated with areas of unexplained low yield, but this requires further studies on a larger scale to be confirmed. These combined results demonstrate how denitrifiers can be more strongly affected by innate environmental variation relative to variation caused by agricultural management interventions; and reinforces the difficulties involved in ‘diagnosing’ a bacterial community in an environment as heterogeneous as soil.

With this in mind, and based on the key finding from Chapter 2, it is imperative to consider sampling strategy for any soil microbial experiment. The high beta diversity between samples taken just centimetres apart in Chapter 3 reinforces the need to account for within-plot variability using composite samples. Additionally, despite the experiments of Chapter 2 being carried out in a randomised block designed field trial with replication, the topography of the site (specifically a slope diagonally across the site) and resultant environmental gradients (particularly the resultant soil moisture gradient) were shown to have a much greater impact on bacterial and denitrifier diversity than the long term agricultural treatments. This indicates that block designed field experiments may not always have sufficient statistical power to identify any smaller effects of anthropogenic treatments. Therefore, it is recommended that site topography including gradients and land features are also factored into the experimental design for studies investigating variation in the soil microbiome, with prior experimental data such as that presented here used to identify possible effect sizes to then determine replicates needed in future field trials. Furthermore, it would be interesting and valuable to further understand the effect of site slopes and topographical features in shaping the microbial and denitrifying communities .

In addition to molecular techniques, this thesis highlights the continuing value of traditional culture-based experiments, with the experiments in Chapter 4 demonstrating that molecular and culture-based techniques are of most value when used in conjunction. The most informative genetic and biochemical analyses can currently only be performed on culturable organisms. Therefore, efforts should be made to effectively isolate and culture these environmentally-relevant microbes using techniques such as *in-situ* cultivation. Chapter 4 shows how bacteria can be more effectively cultivated using non-standard techniques. The major limitation of this, being that the methodology inadvertently selected for nitrogen assimilating bacteria (through lack of nitrogen addition to the initial culture media), so care should be taken to understand the

biases that experimental methodologies include. Only by isolating, culturing and characterising denitrifying bacteria from environmental samples rather than model organisms, can the results provide information relevant to predicting nitrogen cycling processes and progress the applications of this field of research.

The global nitrogen budget differs from other biogeochemical elements in that it is dominated by biological processes, with nitrogen fixation as the biggest source of fixed nitrogen and denitrification as the largest sink (Zhang *et al.*, 2020). Nitrogen is fundamental to both biosynthesis and redox cycling and as a result the nitrogen budget appears to be highly regulated by feedback cycles. Current models of nitrogen cycling, using both bottom-up (inventory, statistical extrapolation of flux measurements, process-based modelling) and top-down (atmospheric inversion) approaches struggle to incorporate soil microbial community structure (Tian *et al.*, 2020). The advancement of molecular and culture-based techniques and knowledge of denitrifying bacterial communities presented in this thesis can be used for the development of better models for nitrogen cycling which incorporate measures of microbial community diversity and function.

For example, as part of this project a simple model was developed to represent denitrification using an agent-based modelling approach (Figure 37). Here, different values were allocated to oxygen and nitrogen respiration and different costs assigned to processes such as movement and maintenance. Bacteria were then used to populate the model and outputs indicated whether each isolate would favour an oxygen or nitrogen-based respiration strategy based on different environmental parameters (with this model indicating nitrate and oxygen concentration gradients; Figure 37). Although this model was only a preliminary study within the current project, it demonstrates the potential to simulate denitrification in individuals on a community scale. With further development this model could be populated with data regarding the microbial

community structure, the internal biochemical networks within denitrifier cells and environmental parameters which affect denitrification.

Models such as these can be updated with information including gene abundance, gene regulation, resource availability, competition, and temporal & spatial variation. Furthermore, a full complement of microbial nitrogen cycling processes should be incorporated to gain a clearer picture of nitrogen cycling. Future research could build on this work by incorporating this data into a detailed functional model of how bacterial community structure affects denitrification under different environmental conditions. This model could then be used to generate testable hypotheses about the effects of human intervention on nitrogen cycling in agriculture.

The generation of data-rich denitrification models will contribute to our understanding of the within-field variability of nitrogen-use efficiency and have applications in reducing waste and increasing efficiency in agricultural processes for crop production through smarter use of nitrogen rich fertilizers.

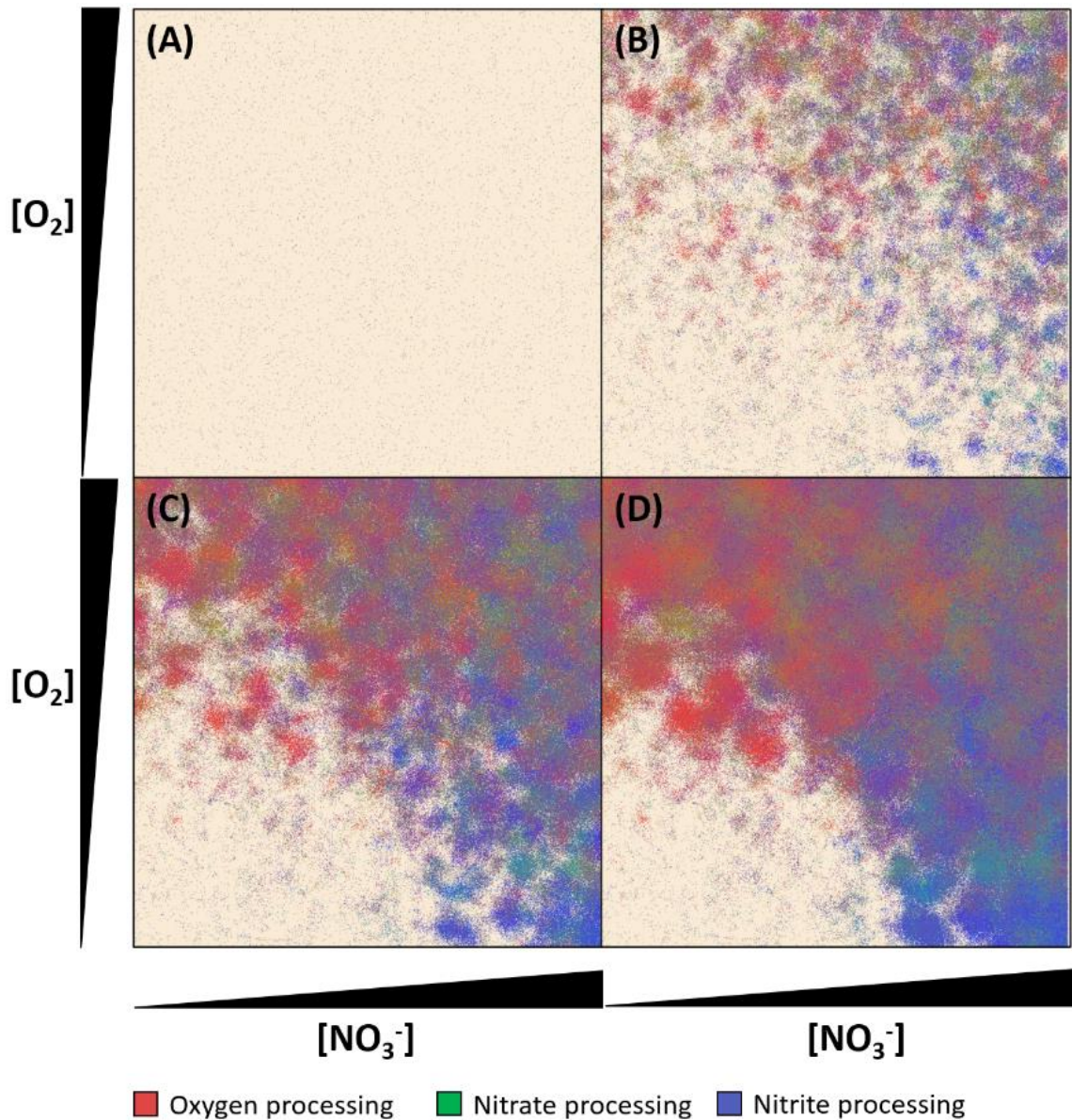




Figure 37 Outputs from agent-based denitrification model after (A) 1, (B) 50, (C) 100 and (D) 150 generations of bacterial growth. Nitrate concentration is elevated on the right-hand side of the landscape and oxygen is elevated at the top of the landscape. Red dots indicate oxygen metabolism, green shows nitrate usage and blue shows nitrite usage. In this model, oxygen respiration has a value of 8 points, nitrate respiration has a value of 5 points. Movement rate is set to 0.5 and costs 1 point and there are no maintenance costs in this scenario.

Overall, the three experimental chapters presented in this thesis demonstrate the relative importance of innate and anthropogenic environmental variation in the community assembly of

denitrifying bacteria. By focussing on functional phenotypes, combined with taxonomic distribution, we were able to better understand how the environment shapes the microbial community and vice versa. Several lines of work are still ahead, including the development of detailed predictive models incorporating the full range of nitrogen cycling processes, and also mesocosm- and field-based experiments to test the model predictions. When the impact of agricultural interventions can be accurately modelled in different contexts, nitrogen availability can be optimised to produce enough food for the growing global population.

Appendix 1: Published Manuscript:
Environmental Microbiology
(2022) 24(1), 298–308
doi:10.1111/1462-2920.15873

Long-term fertilization and tillage regimes have limited effects on structuring bacterial and denitrifier communities in a sandy loam UK soil

Claire E. Moulton-Brown ¹, Tianer Feng,² Shreiya Shivagni Kumar,² Luxi Xu,² Calvin Dytham,¹ Thorunn Helgason,¹ Julia M. Cooper² and James W. B. Moir ^{1*}

¹ Department of Biology, University of York, Heslington, York, UK.

² School of Natural and Environmental Sciences, Newcastle University, Newcastle Upon Tyne, UK.

Summary

Denitrification causes loss of available nitrogen from soil systems, thereby reducing crop productivity and increasing reliance on agrochemicals. The dynamics of denitrification and denitrifying communities are thought to be altered by land management practices, which affect the physicochemical properties of the soil. In this study, we look at the effects of long-term tillage and fertilization regimes on arable soils following 16 years of treatment in a factorial field trial. By studying the bacterial community composition based on 16S rRNA amplicons, absolute bacterial abundance and diversity of denitrification functional genes (*nirK*, *nirS* and *nosZ*), under conditions of minimum/conventional tillage and organic/synthetic mineral fertilizer, we tested how specific land management histories affect the diversity and distribution of both bacteria and denitrification genes. Bacterial and denitrifier communities were largely unaffected by land management history and clustered predominantly by spatial location, indicating that the variability in bacterial community composition in these arable soils is governed by innate environmental differences and Euclidean distance rather than agricultural management intervention.

Introduction

Below-ground biodiversity plays a major role in the functioning of soil ecosystems and is considered a

key measure of soil health and essential for the supply of ecosystem goods and services (Bardgett and van der Putten, 2014; Bender et al., 2016; Delgado-Baquerizo et al., 2016). Whilst farming practices are changing and efforts are being made to become more sustainable, in terms of meeting current food requirements whilst having minimal negative environmental effects (Rockström et al., 2017), it is important to consider what effects agricultural management practice will have on microbial communities and what the consequences of this will be for crop productivity and biogeochemical cycles.

The effect of soil microbial biodiversity on the nitrogen cycle is critical, as nitrogen is the primary limiting factor for productivity in agroecosystems (Rütting et al., 2018). To keep up with global crop demands, 110 Mt nitrogen fertilizer was applied in 2016 (FAO, 2018). Nitrogen fertilizer use remains a controversial issue, because of the need to balance high crop yield with the expense of fertilizers and the environmental impact associated with overuse, including eutrophication of waters, global warming and stratospheric ozone depletion (Ravishankara et al., 2009; IPCC, 2019; Stevens, 2019).

One option for balancing yield and environmental impact is through the use of organic fertilizers (OFs) which do not require fossil fuels for manufacture. Longterm OF amendments have been shown to increase microbial species richness relative to synthetic mineral fertilizers (SFs) (Hartmann et al., 2015; Francioli et al., 2016), which benefits ecosystem functioning. Additionally, farmers may seek to adopt different tillage practices to reduce their environmental impact. Reduced tillage, including no tillage (NT) and minimum tillage (MT), is thought to increase microbial diversity relative to conventional tillage (CT) by increasing soil organic carbon stocks (Cooper et al., 2016; Sun et al., 2016; Wang et al., 2016; Chen et al., 2020), with the added benefits of reduced soil erosion and improved water conservation (Derpsch et al., 2010). It should be noted, however, that there is often little consensus on the effects of tillage, with recent studies finding that reduced tillage does not increase soil carbon (Keel et al., 2019; Camarotto et al., 2020) or prokaryotic biodiversity (Degruene et al., 2016; Piazza et al., 2019). There is also little consensus on whether reduced tillage increases or decreases

nitrogen losses through N₂O emissions (Six et al., 2004; Rochette, 2008; Krauss et al., 2017a; Krauss et al., 2017b).

Denitrification, the microbially mediated dissimilatory reduction of nitrate to nitrogen gases, accounts for 60% of global N₂O emissions (Kroeze et al., 1999) and contributes to decreased crop productivity through loss of available nitrogen from terrestrial ecosystems (Syakila and Kroeze, 2011). Although denitrification is considered beneficial for wastewater treatment and aquatic ecosystems, in terms of removing fixed nitrogen from the ecosystem and preventing undesirable consequences such as algal bloom (Lu et al., 2014), in agriculture the loss of nitrates from fertilizers is detrimental and costly. Understanding the impact of land management practices in structuring the denitrification community may enable the mitigation of these nitrogen losses.

Whilst the effects of tillage and fertilization regimes have received considerable attention, the potential impact on denitrifying bacteria remains relatively unclear. Previous studies have looked at the effect of NT compared to CT, with results suggesting that NT leads to an increase in denitrifier abundance and activity (Wang and Zou, 2020). This effect was shown to be fertilizer dependent (with vs. without N fertilizer) (Krauss et al., 2017a; Wang and Zou, 2020). Less is known about the effects of type of nitrogen fertilizer used, or the combined effects of fertilizer type and MT on total soil and denitrifier community structure.

The highly heterogeneous soil matrix contains many micro-scale soil habitats which affect microbial activity, diversity and abundance. Whilst many studies demonstrate the impact of long-term land management of microbial and denitrifier diversity, there is a conspicuous knowledge gap in how this is linked to natural processes in shaping the denitrifying community. Despite relatively weaker biogeographic patterns being observed in microbial taxa than in plants and animals (Meyer et al., 2018), it remains plausible that microbial and denitrifier community assembly is driven by local environmental conditions, dispersal limitations and selection (Dumbrell et al., 2010; Vos et al., 2013; Domeignoz-Horta et al., 2018; Jiang et al., 2020). However, little is known about how long-term agricultural practices affect these drivers.

The initial objective of this study was therefore to gain an understanding about the impact of fertilizer regime (mineral versus organic) and tillage (minimum versus conventional) on denitrifying functional guilds in arable soils in a long-term field trial. We hypothesized that (i) MT would be associated with increased denitrifier diversity due to reduced physical disturbance, reduced aeration and increased soil organic carbon which provides optimum conditions for full

and partial denitrification; and (ii) SF would be associated with increased microbial abundance and denitrification gene diversity due to increased initial nitrate concentration relative to composted dairy manure. An additional objective of the study was to investigate the importance of inherent environmental variation within the field site, and intrinsic neutral processes, on microbial community composition. This study uses bacterial and select denitrifier gene diversity to address these specific objectives.

Results

Soil physicochemical properties

Soil physicochemical properties were measured to ascertain whether land management treatments affected soil properties, which could influence bacterial community composition. There was little chemical difference in the soil between treatments apart from extractable potassium content, which was significantly higher in soils treated with OF compared to SF (Table 1; Fertilizer: $F_{1,13} = 23.07$; $p = 0.0009$). All potassium concentrations had a K Index of 1, indicating a potential risk of potassium deficiency, whereas all soils were within range of P Index 2, the target index for arable crops (Alexander et al., 2008). Soil carbon was also slightly elevated in soils treated with OF, although this was not statistically significant ($p = 0.055$).

Treatment did not affect soil texture or pH. However, active microbial carbon biomass, measured through bacterial respiration, was greater in plots with MT compared to CT (Tillage: $F_{1,13} = 17.72$; $p = 0.002$). And, although not significant at the $p < 0.05$ level ($p = 0.054$), organic matter was also increased in sites that used MT.

The effect of tillage and fertilizer on bacterial taxa and abundance

The 16S ribosomal RNA gene sequence was used to investigate bacterial abundance and diversity. The relative abundance of each phylum remained relatively constant across plots (Fig. 1A), but clear differences were observed in the total abundance, with plots having between 1.45×10^9 and 3.41×10^{10} 16S rRNA genes per gram of soil (Fig. 1B). Although no significant difference was found between treatments due to high variance, MT appears to be associated with greater bacterial abundance. This is in accordance with the bacterial biomass result discussed above. When investigating the high sample variance further, it was clear that field-block had a significant effect on the 16S rRNA abundance in each soil sample (Block: $F_{3,12} = 5.77$; $p = 0.0111$), with Block 2 soils having significantly more 16S rRNA copies per gram of soil than any other block.

Table 1. Summary of a 16-year cropping systems management experiment at Nafferton Factorial Systems Comparison study (A) and soil physicochemical properties (B).

(A) Cropping system	MT OF	MT SF	CT OF	CT SF
Tillage	Shallow non-inversion	Shallow non-inversion	Deep inversion	Deep inversion
Fertility	Composted dairy manure	Ammonium nitrate	Composted dairy manure	Ammonium nitrate
Pest Control	None	None	None	None
Weed Control	None	None	None	None
(B) Soil chemical, physical and biological properties				
C (%)	2.24 (± 0.09)	2.16 (± 0.04)	2.21 (± 0.05)	2.06 (± 0.05)
N (%)	0.22 (± 0.009)	0.21 (± 0.003)	0.21 (± 0.009)	0.21 (± 0.005)
C:N	10.21 (± 0.11)	10.35 (± 0.08)	10.41 (± 0.25)	10.08 (± 0.21)
Extractable P (mg kg ⁻¹)	22.19 (± 2.91)	17.14 (± 3.24)	18.42 (± 4.14)	18.42 (± 3.92)
Extractable K (mg kg ⁻¹)	109.3 (± 10.1) ^a	82.6 (± 7.3) ^b	107.7 (± 12.5) ^a	68.2 (± 2.2) ^b
Moisture content (%)	23.0 (± 0.92)	22.6 (± 0.64)	22.4 (± 1.26)	22.4 (± 0.82)
pH	6.74 (± 0.10)	6.51 (± 0.13)	6.66 (± 0.08)	6.69 (± 0.16)
Clay (%)	16.50 (± 0.65)	16.50 (± 0.87)	16.50 (± 0.29)	17.25 (± 0.85)
Sand (%)	64.75 (± 0.63)	64.25 (± 1.80)	63.50 (± 1.19)	62.50 (± 1.55)
Silt (%)	18.75 (± 0.25)	19.25 (± 1.03)	20.00 (± 1.00)	20.25 (± 0.75)
Microbial biomass ($\mu\text{g C g}^{-1}$ soil)	209.6 (± 25.9) ^a	203.1 (± 33.8) ^a	143.9 (± 23.7) ^b	144.2 (± 25.7) ^b
Organic matter (%)	6.19 (± 0.19)	6.11 (± 0.10)	5.99 (± 0.13)	5.80 (± 0.16)

All values are interaction means of four replicates with standard errors given in brackets. ¹MT = minimum tillage, CT = conventional tillage, OF = organic fertilizer & SF = synthetic mineral fertilizer.

¹Means followed by the same letter in the same row are not significantly different. All soil properties measured were compared using Linear Mixed Effects model ($p < 0.05$).

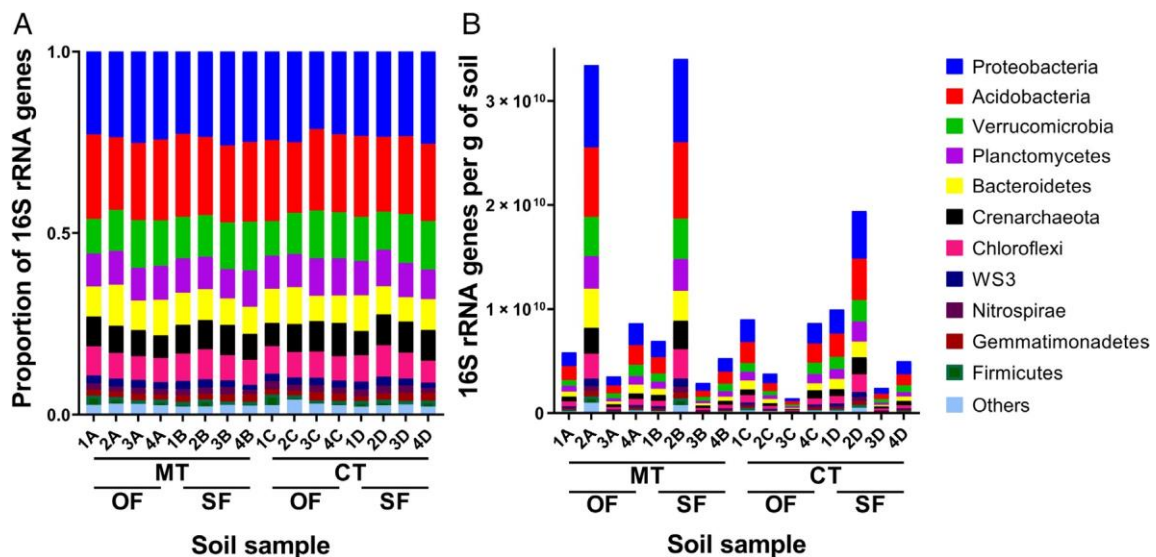


Fig. 1. Relative (A) and absolute (B) abundance of bacterial phyla in soils treated with different combinations of tillage and fertilizer. 'Others' refers to all phyla with an abundance of less than 1% across samples. Labels indicate field plot. MT and CT denote minimum and conventional tillage respectively. OF and SF denote organic and synthetic fertilizer respectively.

The dominant phyla across all samples were the Proteobacteria (with classes Alphaproteobacteria, Betaproteobacteria and Gammaproteobacteria dominating all samples) and Acidobacteria (Fig. 1). Indicator species analysis identified OTUs that were specifically associated with land management history. Although 3716 OTUs were detected in total, only 32 were associated with specific treatments, indicating that land management treatment did not affect the majority of taxa within the soil.

Five indicator species were specifically associated with plots treated with SF. These were the ammonia oxidizing *Nitrosospira multiformis*, a *Chloroflexi* in the *Kouleothrixaceae* family, a *Spartobacterium* thought to be an obligate symbiont of plant pathogenic nematodes of the *Xiphinema americanum* group (Vandekerckhove et al., 2000) and two *Phycisphaerae* [a bacterial class of mainly unknown ecophysiologicals often found in ANAMMOX communities (Costa et al., 2014)]. Two OTUs were specifically associated with MT treatments.

One is a member of the DA101 genus of the Chthoniobacteraceae family that is known to be common in grassland soils (Felske and Akkermans, 1998), the other is a Gammaproteobacteria of the Sinobacteraceae family.

The effect of tillage and fertilizer on bacterial rRNA and denitrification gene alpha diversity

To compare the effects of land management on within plot biodiversity, three measures of alpha diversity were used. The number of observed variants did not differ significantly in the 16S rRNA, nirK or nosZ amplicons, but there were approximately 32% more observed nirS variants in the MT-treated plots than the CT (Fig. 2A; Tillage: $F_{1,9} = 13.7$; $p = 0.0048$). Likewise, nirS had significantly greater Shannon diversity under MT compared to CT (Fig. 2B; Tillage: $F_{1,9} = 12.08$; $p = 0.0069$). Notably, land management treatment was not associated with any differences in variant evenness for any of the amplicons (Fig. 2C). Overall, there is very little impact of variation in tillage or fertilizer regime on below-ground biodiversity judged on the basis of 16S, nirK, nirS or nosZ alpha diversity.

All genes had significantly different levels of evenness, with 16S rRNA variants being more evenly distributed within plots compared to the other genes which had more dominant variants, particularly nirS (Fig. 2C; Evenness by gene: $F_{3,60} = 106.4$; $p = 2e^{16}$).

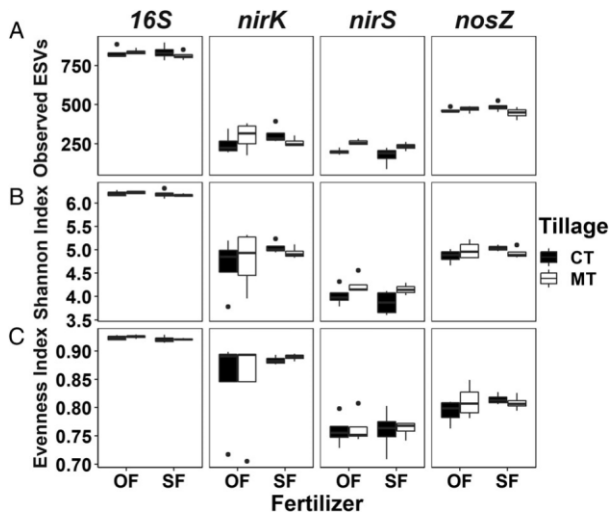


Fig. 2. Boxplots of alpha diversity measures of each sample treatment. (A) Observed ESVs by sample treatment; (B) Shannon diversity index; (C) Pielou's evenness index. Conventional tillage is shown in black, with minimum tillage shown in white. OF and SF denote organic and synthetic fertilizer respectively.

The effect of tillage, fertilizer and sample location on bacterial community composition

To explore the differences in the composition of bacterial communities between land management treatments, a nonmetric multidimensional scaling (NMDS) ordination of whole bacterial community 16S rRNA gene amplicons was constructed (Fig. 3A). To confirm if the differences between community compositions can be explained by land management factors, a PERMANOVA test was used. Neither tillage method nor fertility treatment nor a combination of the two were found to have significant effects on community composition (Tillage: $F_{1,15} = 0.73$; $p = 0.81$; Fertilizer: $F_{1,15} = 1.2$; $p = 0.18$; Tillage Fertilizer: $F_{1,15} = 0.59$; $p = 0.98$), despite block effects being included as a random factor. The variable accounting for most variance among samples was blocked, i.e. the location of the plots (Fig. 3; Block: $F_{3,15} = 5.7$; $p = 0.001$), suggesting that field location had a greater effect on soil bacterial community than either tillage or fertilizer treatments.

Amplicon analyses for the denitrification genes nirK, nirS and nosZ (clade I) were then used to ascertain whether functional diversity followed the same patterns as taxonomic diversity in the treated soils. Like bacterial taxa, the variants of the nitrite reductase gene nirK were not significantly associated with tillage or fertilizer treatment (Tillage: $F_{1,15} = 0.92$; $p = 0.53$; Fertilizer: $F_{1,15} = 1.02$; $p = 0.35$; Tillage Fertilizer: $F_{1,15} = 0.70$; $p = 0.96$), but were strongly associated with field block (Fig. 3B; Block: $F_{3,12} = 2.41$; $p = 0.001$). This was also true for nirS, which was not significantly affected by land management (Tillage: $F_{1,15} = 1.0$; $p = 0.37$; Fertilizer: $F_{1,15} = 0.65$; $p = 0.6$; Tillage Fertilizer: $F_{1,15} = 0.29$; $p = 0.99$), but was significantly affected by block (Fig. 3C; Block: $F_{3,12} = 6.18$; $p = 0.001$). The same pattern was evident in nitrous oxide reductase nosZ (Fig. 3D; Tillage: $F_{1,15} = 0.73$; $p = 0.67$; Fertilizer: $F_{1,15} = 1.0$; $p = 0.32$; Tillage Fertilizer: $F_{1,15} = 0.56$; $p = 0.92$; Block: $F_{3,12} = 3.58$; $p = 0.001$), suggesting that field-block location is the major determinant of bacterial community and denitrification functional composition.

Spatial and environmental effects on bacterial community composition

Once it became apparent that bacterial communities and denitrification genes appear largely unaffected by land management history, and cluster predominantly by field block, we began investigating the role of environmental factors and spatial location in bacterial community composition. Environmental vector fitting revealed that five soil variables: soil moisture, phosphorous, pH, silt and sand content were significantly related to total bacterial community composition (Fig. 3A; Envfit: Moisture

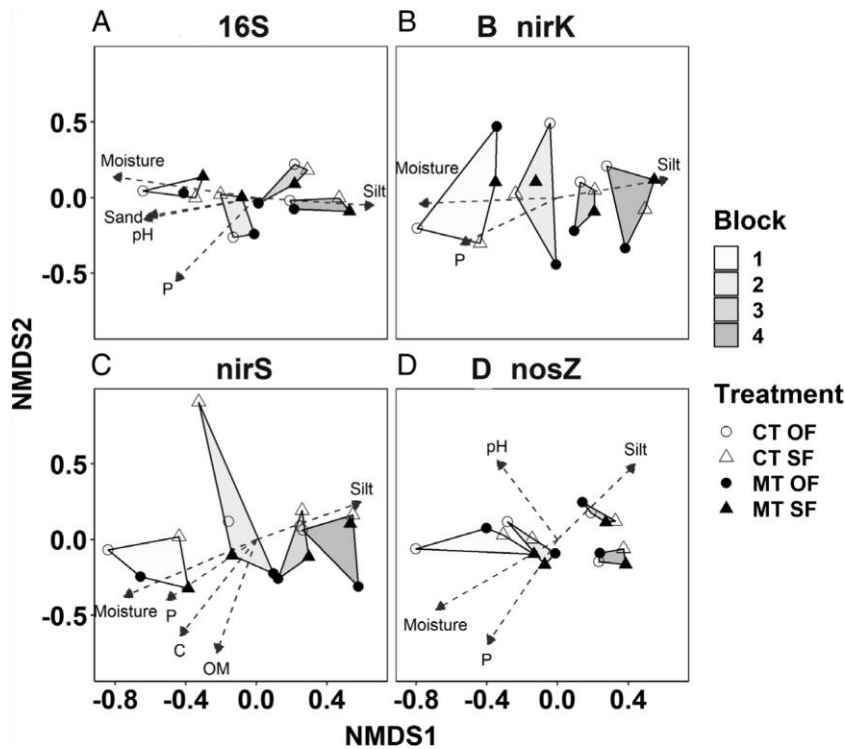


Fig. 3. Non-metric multidimensional scaling (NMFSC) of gene amplicon Bray-Curtis dissimilarity from NFSC soils. (A) Whole bacterial community 16S rRNA. (B) nirK amplicon variants. (C) nirS amplicon variants. (D) nosZ amplicon variants. Samples are indicated with points, conventional tillage (CT) plots are shown in white, with minimum tillage (MT) in black; OF is denoted by circles, SF treatments are shown by triangles. Points are grouped by polygons indicating field block, from block 1 shown in white to block 4 shown with the dark grey. Labels indicate environmental variables which significantly explain sample beta diversity.

$r^2 = 0.68$, $p = 0.001$; Phosphorus $r^2 = 0.52$, $p = 0.009$; pH $r^2 = 0.43$, $p = 0.021$; Silt $r^2 = 0.44$, $p = 0.025$; Sand $r^2 = 0.38$, $p = 0.04$). Since none of these factors was affected by land management treatment (Table 1), this suggests that innate environmental differences have more effect on bacterial community composition than long-term tillage or fertilizer treatments.

Additionally, the distribution of all the denitrification genes was significantly associated with moisture (Envfit moisture: nirK $r^2 = 0.61$, $p = 0.002$; nirS $r^2 = 0.70$, $p = 0.001$; nosZ $r^2 = 0.69$; $p = 0.001$). Phosphorus and silt were also significantly correlated with denitrification gene distribution (Fig. 3B,D). NirS variation was significantly associated with carbon content and organic matter (Envfit nirS: carbon $r^2 = 0.59$, $p = 0.005$; organic matter $r^2 = 0.61$; $p = 0.005$), suggesting that nirS organisms may be more sensitive to carbon than their nirK counterparts.

To further investigate variation in community composition, a spatial analysis was completed. A Euclidean distance matrix (with the distances between the centre of each plot) was compared against the Bray-Curtis dissimilarity matrix using a Mantel test. The test indicated that there was significant positive correlation between the physical distance between plots and their community dissimilarity for all of the amplicons tested (Fig. 4; 16S rRNA: $R^2 = 0.590$, $p = 0.001$; nirK: $R^2 = 0.429$, $p = 0.001$; nirS: $R^2 = 0.559$, $p = 0.002$; nosZ: $R^2 = 0.589$, $p = 0.001$). This result indicates a clear distance decay effect, with increased physical

distance being associated by increased dissimilarity between bacterial communities and denitrification gene distributions. Here, spatial distance is found to account for approximately 55% variation in bacterial communities and denitrification genes.

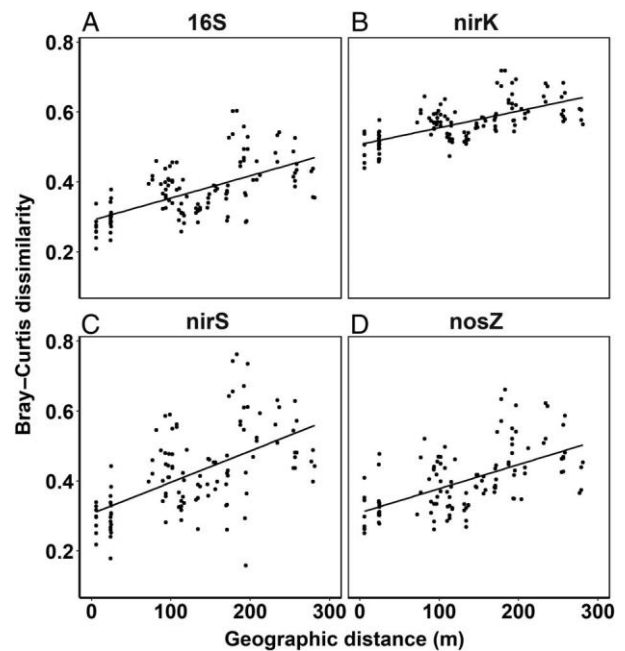


Fig. 4. Distance-decay relationship between geographic distance between samples and Bray-Curtis dissimilarity index for 16S rRNA, nirK, nirS and nosZ genes.

To separate the effects of space alone from environmental gradients on community composition, the calc. relimp function in R was used. This indicated that environmental and spatial variation together accounted for 63.6% variation in 16S rRNA diversity, with 18.9% of this attributable to space alone and 44.7% attributable to environmental variables. Spatial and environmental gradients together accounted for 28.5%, 63.0% and 50.8% of community variation in nirK, nirS and nosZ respectively. Spatial distance had a relatively stronger effect on the denitrification genes than on the overall microbial population, with space alone attributable to 13.1%, 21.1% and 22.6% of variation respectively. Together these analyses indicate that spatial distance is a major determinant of bacterial community similarity and has a much stronger effect than long-term tillage or fertilizer regimes.

Discussion

This study demonstrates that in a 16-year treatment regime there was virtually no effect of long-term tillage and fertilizer regimes on soil microbial community and denitrification gene diversity, but clear field-scale patterns across distance and environmental gradients.

MT was associated with an increase in microbial biomass, which is in accordance with several studies which demonstrate that conservation tillage systems, including NT and MT, have increase microbial biomass (Wallenstein and Hall, 2012; Zhang et al., 2012; Murugan et al., 2014). The increase is thought to be due to increased levels of microbially available, labile soil carbon and nitrogen in surface soils under conservation tillage (Chen et al., 2009). While labile C may represent a relatively small proportion of total soil organic C (Li et al., 2018), it plays a key role in driving soil microbial activity. We did not directly measure labile C in this study, but values for soil basal respiration were significantly higher in the MT treatment compared to CT, suggesting a higher proportion of labile C in the MT soils, which were not observed in this long-term field trial. A meta-analysis (Wang and Zou, 2020) indicates that no-tillage treatment leads to an increase in denitrification, N₂O and changes in nirK, nirS and nosZ abundances. Such an analysis has not been done for reduced or minimum-tillage, but the few available studies indicate that the minimum-tillage is not typically different to CT in terms of denitrification or N₂O production, but this varies between studies (Dendooven et al., 2012; Tian et al., 2012; Tellez-Rio et al., 2015; Krol et al., 2016).

The headline finding in this article is that there is no significant change in microbial community or denitrifiers gene diversity that can be linked to conventional versus MT in this arable crop setting. While substitution of organic N sources has been proposed as a strategy to reduce losses of mineral N, in this study we found no discernible difference in denitrifier populations due to N source. This may have been due to the application of equivalent levels of total N for each treatment, suggesting that the total

nitrogen supplied rather than the nitrogen source has the primary effect on denitrifier community diversity.

Environmental variation through oxygen and nitrate content; organic matter quantity, quality, and availability; redox potential; temperature; pH; and soil type are all known to affect microbial communities and denitrification (Drenovsky et al., 2004; Wallenstein et al., 2006; Enwall et al., 2010; Nadeau et al., 2019). Here, we show significant effects of moisture, potassium, pH and soil textural class on all the denitrification gene diversities. Cytochrome cd₁ type nitrite reductase nirS is further associated with increased soil carbon and soil organic matter, which may be due to the relatively greater energy demands needed for enzyme assembly for nirS type denitrifiers, which requires at least 10 genes for assembly of the mature nitrite reductase enzyme, compared to nirK type denitrifiers, which requires only a single gene (Rinaldo et al., 2016). Additionally, a combination of other physical factors, including those not measured in this experiment such as oxygen concentration, may also be important drivers of soil microbial community structure. With the majority of heterotrophic denitrifiers utilizing oxygen much of the time, denitrification genes face limited selection pressure. But, as denitrification will at times be a critical response to a bottleneck in electron acceptor availability, the capacity to rapidly pivot to denitrification can prove advantageous.

Whilst environmental gradients can be attributed to approximately 32.6% variation across all the genes studied, it remains clear that geographical distance is also a driver of microbial community and denitrifier gene diversity. Distance-decay and other spatial effects are well-known ecological phenomena (Green et al., 2004; Zhou et al., 2008; Martiny et al., 2011; O'Brien et al., 2016) that appear to be driving bacterial and denitrifier gene diversity in this study. Here, community similarity decays as a function of distance, which suggests that dispersal ability is a significant force behind the bacterial diversity observed in this study.

In this study, we used the denitrification genes nirK, nirS and nosZ as indicator genes for the denitrification process. These genes appear to show greater dispersal limitation than the background bacterial population. This may indicate that the genetic backgrounds in which these genes occur have either restricted niches or lower motility – both of which are consistent with the anoxia required for denitrification. The combination of spatial effects and environmental gradients observed here suggests that a combination of niche and neutral processes drives observed community structure and that the balance of the processes may further be related to function. Future work with greater focus of functional consequences of diversity could explore how other genes in the pathway, such as nosZII, respond to environmental change.

The United Nations promote the use of reduced tillage for improved and sustained crop production (FAO, 2015) and the use of OFs to maintain and

enhance soil productivity. This experiment demonstrates that long-term reduced tillage and OF regimes have no significant negative effects on soil physicochemical properties. Indeed, OF use led to an increase in soil potassium which may improve crop yield (Pettigrew, 2008) and MT led to increased active microbial carbon biomass, which can improve crop yield through increased nutrient cycling, suppression of soil-borne pathogenic microorganisms and the decomposition of organic matter, which is closely associated with the aboveground performance of crops (Marschner, 2007; Berg and Smalla, 2009).

This study evaluated the role of agricultural management practices on microbial and denitrification gene diversity through the use of a long-term randomized complete block field trial. Although this study focussed on the diversity of

Experimental procedures

Experiment 3 of the Nafferton Factorial Systems Comparison (NFSC) study is a long-term factorial field experiment established in 2001 in the Tyne Valley, UK

(54:59:26.3 N; 1:54:37.4 W) to compare the effects of tillage and fertilizer regimes on crops in an 8-year crop rotation (Orr et al., 2011). The soils were sampled from the site in April 2017 when all plots were planted with spelt and rye and were at the same stage in the crop rotation. The 24 m x 6 m plots were treated with synthetic mineral (SF) or organic (OF) fertilizer (100 kg total N ha⁻¹ year⁻¹ ammonium nitrate fertilizer or composted dairy manure respectively) and deep inversion CT or shallow noninversion MT, with each treatment replicated four times in blocks distributed across the field site (Fig. 5). The topsoil of the 4 ha trial site is a uniform sandy loam formed in slowly permeable glacial till deposits: Dystric Stagnosol (Soil Survey Staff, 2014).

The SF was applied in mid-April 2016, with P and K in the SF plots only added at maintenance levels based on soil analysis. Compost was added in October 2016 for the 2016/17 season, at the same total N-input level as the SF. The compost was produced onsite at Nafferton Farm from cow manure and straw and applied prior to sowing, with a fresh batch used each year. The SF used ammonium nitrate, triple superphosphate and muriate of potash as the source of NPK respectively. Treatments for fertilizer varied each year depending on the crop but have been organic or conventional for the full 16-year experiment.

The two tillage levels were also applied prior to sowing: minimum and CT. MT was shallow (<20 cm

bacterial denitrifiers possessing indicator genes nirK, nirS and nosZ, further work may focus on a broader scope of genes and organisms as well as elucidating the link between genetic diversity and functional behaviour. Here, whilst land management had a limited effect on microbial community abundance, distance and physicochemical properties were the main drivers of total bacterial and specific denitrification gene diversity. Therefore, whilst the microbial community can be identified and its genetic potential characterized, it is unlikely that long term land management strategies will significantly alter the community to improve nitrogen use efficiency. Strategies for optimizing nitrogen-use efficiency and minimizing N₂O release should be grounded on knowledge about the properties of specific, innate below-ground microbial communities, which are geographically determined and resistant to land-management interventions.

Field experiment and sampling

depth) noninversion tillage using a Dyna-Drive cultivator (Bomford Turner Ltd.) while CT treatments were mouldboard ploughed to a depth of 25–30 cm with soil inversion. All plots were sown with a 1.5 m wide Sow-Lite seed drill (Jordan Engineering Ltd.). Plots were not sprayed with pesticides during the 16-year trial to remove possible impacts on microbial and denitrifier populations. To allow for within-plot variability, 10 cores of soil (0–10 cm depth) were randomly sampled within each plot and immediately mixed to form one composite sample per plot. Soils were sieved through a 4 mm sieve then stored at 20C prior to DNA extraction.

DNA extraction and amplicon sequencing

Genomic DNA was extracted from all 16 soil samples for community 16S rRNA gene and denitrification gene amplicon sequence analysis. The denitrification genes used were nitrite reductases nirK and nirS, and nitrous oxide reductase nosZ (clade I). Details of DNA extraction and PCR amplification of 16S rRNA and denitrification genes are described in Supplementary Materials and Methods.

PCR products were purified using QIAquick PCR Purification Kit (Qiagen) and quantified using NanoDrop (Thermo Fisher Scientific). PCR products were sequenced using the Illumina MiSeq platform with 2 x 300 bp reads by the Bioscience Technology Facility, University of York.

Raw fastq files were demultiplexed, then trimmed to 100 000 reads per sample and quality-filtered using QIIME2 version 2018.2 (Bolyen et al., 2019) to a quality

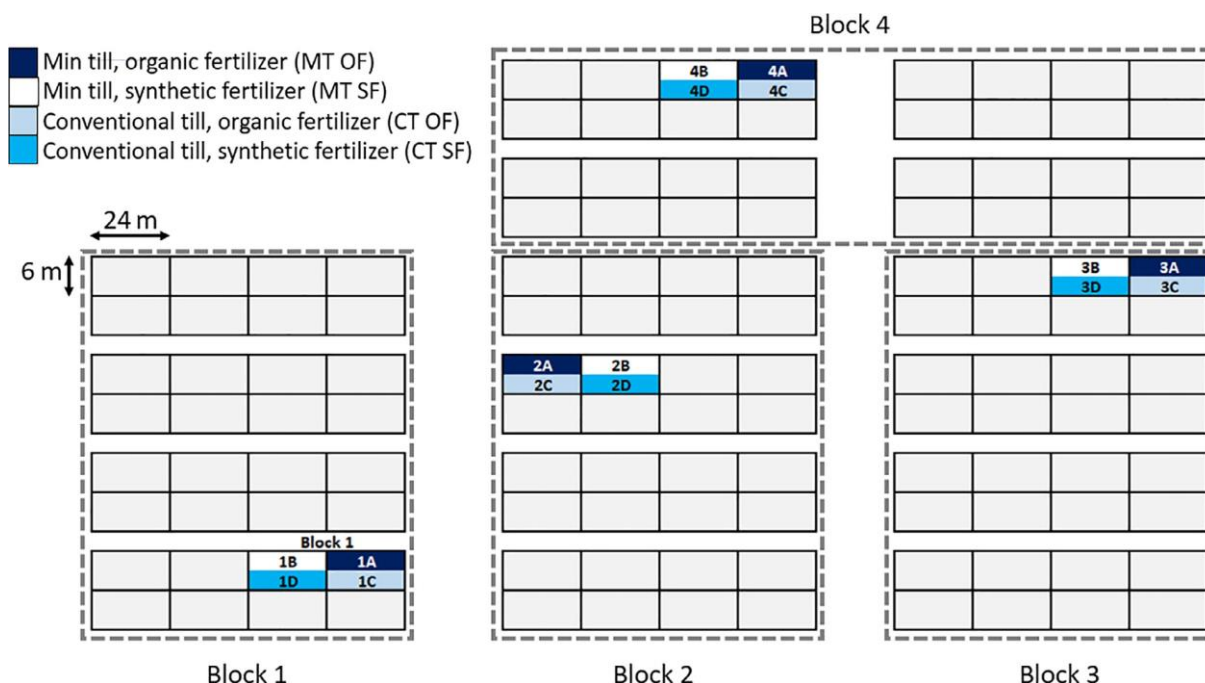


Fig. 5. Schematic of Nafferton Factorial Systems Comparison (NFSC) East Hemmel Experiment 3 Plots indicating plots used in this study. MT = minimum tillage, CT = conventional tillage, OF = organic fertilizer and SF = mineral fertilizer. Each individual plot measured 6 x 24 m (four blocks of 32 plots are separated from the other blocks by 7m).

score above 25. Sequences were denoised, dereplicated and chimaeras removed using the dada2 denoise-paired function. Feature IDs were summarized before taxonomy was assigned using the Greengenes 16S rRNA database (DeSantis et al., 2006). For denitrification genes, exact sequence variants (ESVs) were used, with reads manually verified using the FunGene database (Fish et al., 2013). Sequence data was uploaded to the European Nucleotide Archive, under accession number PRJEB49432.

Quantification of 16S rRNA

A 16S rRNA gene copy number quantification technique (Smets et al., 2016) was carried out for soils by spiking them with an internal DNA standard (*Thermus thermophilus* DSM 46338) prior to DNA extraction at an estimated 0.1% of total DNA. This strain was selected as it is unlikely to be found in UK soils as it grows optimally at 72C. Details of culture conditions and DNA extraction procedure are described in Supplementary Materials and Methods.

To determine the number of 16S rRNA genes found in each sample, the equation given by Smets et al. (2016) was used. Briefly, the number of reads assigned to each taxon is multiplied by a constant, made by multiplying the 16S copy number of the internal standard by the weight of DNA added to the sample, divided by the genome weight of the internal standard. This value is then divided by the number of reads assigned to the internal standard.

A gene copy number of two and a weight of 2.16×10^{15} g per *T. thermophilus* genome were assumed (Hallin and Ussery, 2004).

Determination of soil properties

Soil was chemically analysed for carbon and nitrogen content using the Vario MACRO Cube CN ElementalAnalyser (Elementar). Extractable phosphorus was determined using the Olsen P test (Olsen et al., 1954) and extractable potassium was determined following extraction with 1 M ammonium nitrate using a flame photometer. pH was measured in H₂O in 1:2.5 wt./vol. suspensions using a pH probe.

Gravimetric water content was calculated by dividing the mass of water lost when soil was dried at 105C for 24 h by the mass of the dry soil. Particle size distribution was determined by a Low Angle Laser Light Scattering technique using a Malvern Mastersizer 2000 optical bench with recirculating wet cell enhancement and a Hydro 2000MU sample introduction unit. Organic matter content was calculated using the Loss on Ignition method (Ball, 1964). Active soil bacterial carbon biomass was determined by substrate-induced respiration (Beare et al., 1990) through addition of glucose to the MicroResp™ system. CO₂ respiration rates were converted to ml CO₂ 100 g⁻¹ of dry soil weight h⁻¹ using the ideal gas law equation. Microbial carbon biomass was calculated using the formula described by Anderson and Domsch (1978).

Statistical and diversity analysis

Statistical and diversity analyses were performed using R version 3.5.1 (R Core Team, 2013) implemented in RStudio version 1.2.1335.1 (RStudio Team, 2018). Physicochemical soil data were analysed using two-way analysis of variance (ANOVA) using the lmer function from the lmerTest package (Kuznetsova et al., 2017), with tillage method and fertilizer type as factors and block as a random factor. Percentage data were arcsine-square root transformed prior to analysis.

The multipatt function from the indicpecies package (De Caceres and Legendre, 2009) was used to perform Dufrene–Legendre indicator species analysis to identify bacteria that were specifically associated with different treatments. Alpha diversity was compared across samples using species richness (observed OTUs/ESVs), the Shannon index and Pielou's evenness index (Shannon, 1948; Pielou, 1966). Differences in alpha diversity were tested using two-way ANOVA as described above. Beta-diversity was represented by Bray–Curtis distance matrices generated from the OTU/ESV table (Roger Bray and Curtis, 1957). Function adonis2 in the R package vegan (Oksanen et al., 2013) was used to quantify the possible effects of tillage, fertilizer and field block on beta-diversity, using the Bray–Curtis distance matrix and NMDS plots were used to visually represent community dissimilarities between samples based on the Bray–Curtis index using the metaMDS function in vegan. Distance matrices were composed using the vegdist function in vegan before Mantel tests were conducted to measure the correlation between spatial distance and Bray–Curtis dissimilarity and also between environmental data and Bray–Curtis dissimilarity using the mantel function in vegan.

Acknowledgements

This work was funded by BBSRC and Precision Decisions Ltd. training grant BB/R506400/1. Sequencing was performed by Sally James and Lesley Gilbert in the Bioscience Technology Facility (Genomics & Bioinformatics), University of York.

References

- Alexander, S., Black, A., Boland, A., Burke, J., Carton, O.T., Coulter, B.S., et al. (2008). In Major and Micro Nutrient Advice for Productive Agricultural Crops, 3rd ed, Coulter, B.S., and Lalor, S. (eds). Johnstown Castle: Wexford, Ireland, Teagasc.
- Anderson, J.P.E., and Domsch, K.H. (1978) A physiological method for the quantitative measurement of microbial biomass in soils. *Soil Biol Biochem* 10: 215–221.
- Ball, D.F. (1964) Loss-on-ignition as an estimate of organic matter and organic carbon in non-calcareous soils. *J Soil Sci* 15: 84–92.
- Bardgett, R.D., and van der Putten, W.H. (2014) Belowground biodiversity and ecosystem functioning. *Nature* 515: 505–511.
- Beare, M.H., Neely, C.L., Coleman, D.C., and Hargrove, W. L. (1990) A substrate-induced respiration (SIR) method for measurement of fungal and bacterial biomass on plant residues. *Soil Biol Biochem* 22: 585–594.
- Bender, S.F., Wagg, C., and van der Heijden, M.G.A. (2016) An underground revolution: biodiversity and soil ecological engineering for agricultural sustainability. *Trends Ecol Evol* 31: 440–452.
- Berg, G., and Smalla, K. (2009) Plant species and soil type cooperatively shape the structure and function of microbial communities in the rhizosphere. *FEMS Microbiol Ecol* 68: 1–13.
- Bolyen, E., Rideout, J.R., Dillon, M.R., Bokulich, N.A., Abnet, C.C., Al-Ghalith, G.A., et al. (2019) Reproducible, interactive, scalable and extensible microbiome data science using QIIME 2. *Nat Biotechnol* 37: 852–857.
- Camarotto, C., Piccoli, I., Dal Ferro, N., Polese, R., Chiarini, F., Furlan, L., and Morari, F. (2020) Have we reached the turning point? Looking for evidence of SOC increase under conservation agriculture and cover crop practices. *Eur J Soil Sci* 71: 1050–1063.
- Chen, H., Dai, Z., Veach, A.M., Zheng, J., Xu, J., and Schadt, C.W. (2020) Global meta-analyses show that conservation tillage practices promote soil fungal and bacterial biomass. *Agric Ecosyst Environ* 293: 106841.
- Chen, H., Hou, R., Gong, Y., Li, H., Fan, M., and Kuzyakov, Y. (2009) Effects of 11 years of conservation tillage on soil organic matter fractions in wheat monoculture in loess plateau of China. *Soil Tillage Res* 106: 85–94.
- Cooper, J.M., Baranski, M., Stewart, G., Nobel-de Lange, M., Bàrberi, P., Fließbach, A., et al. (2016) Shallow non-inversion tillage in organic farming maintains crop yields and increases soil C stocks: a meta-analysis. *Agron Sustain Dev* 36: 22.
- Costa, M.C.M.S., Carvalho, L., Leal, C.D., Dias, M.F., Martins, K.L., Garcia, G.B., et al. (2014) Impact of inocula and operating conditions on the microbial community structure of two anammox reactors. *Environ Technol* 35: 1811–1822.
- De Caceres, M., and Legendre, P. (2009) Associations between species and groups of sites: indices and statistical inference. *Ecology* 90: 3566–3574.
- Degrune, F., Theodorakopoulos, N., Dufrene, M., Colinet, G., Bodson, B., Hiel, M.P., et al. (2016) No favorable effect of reduced tillage on microbial community diversity in a silty loam soil (Belgium). *Agric Ecosyst Environ* 224: 12–21.
- Delgado-Baquerizo, M., Maestre, F.T., Reich, P.B., Jeffries, T.C., Gaitan, J.J., Encinar, D., et al. (2016) Microbial diversity drives multifunctionality in terrestrial ecosystems. *Nat Commun* 7: 1–8.
- Dendooven, L., Gutiérrez-Oliva, V.F., Patiño-Zúñiga, L., Ramírez-Villanueva, D.A., Verhulst, N., Luna-Guido, M., et al. (2012) Greenhouse gas emissions under conservation agriculture compared to traditional cultivation of maize in the central highlands of Mexico. *Sci Total Environ* 431: 237–244.
- Derpsch, R., Friedrich, T., Kassam, A., and Hongwen, L. (2010) Current status of adoption of no-till farming in the world and some of its main benefits. *Int J Agric Biol Eng* 3: 1–25.
- DeSantis, T.Z., Hugenholtz, P., Larsen, N., Rojas, M., Brodie, E.L., Keller, K., et al. (2006) Greengenes, a chimera-checked 16S rRNA gene database and

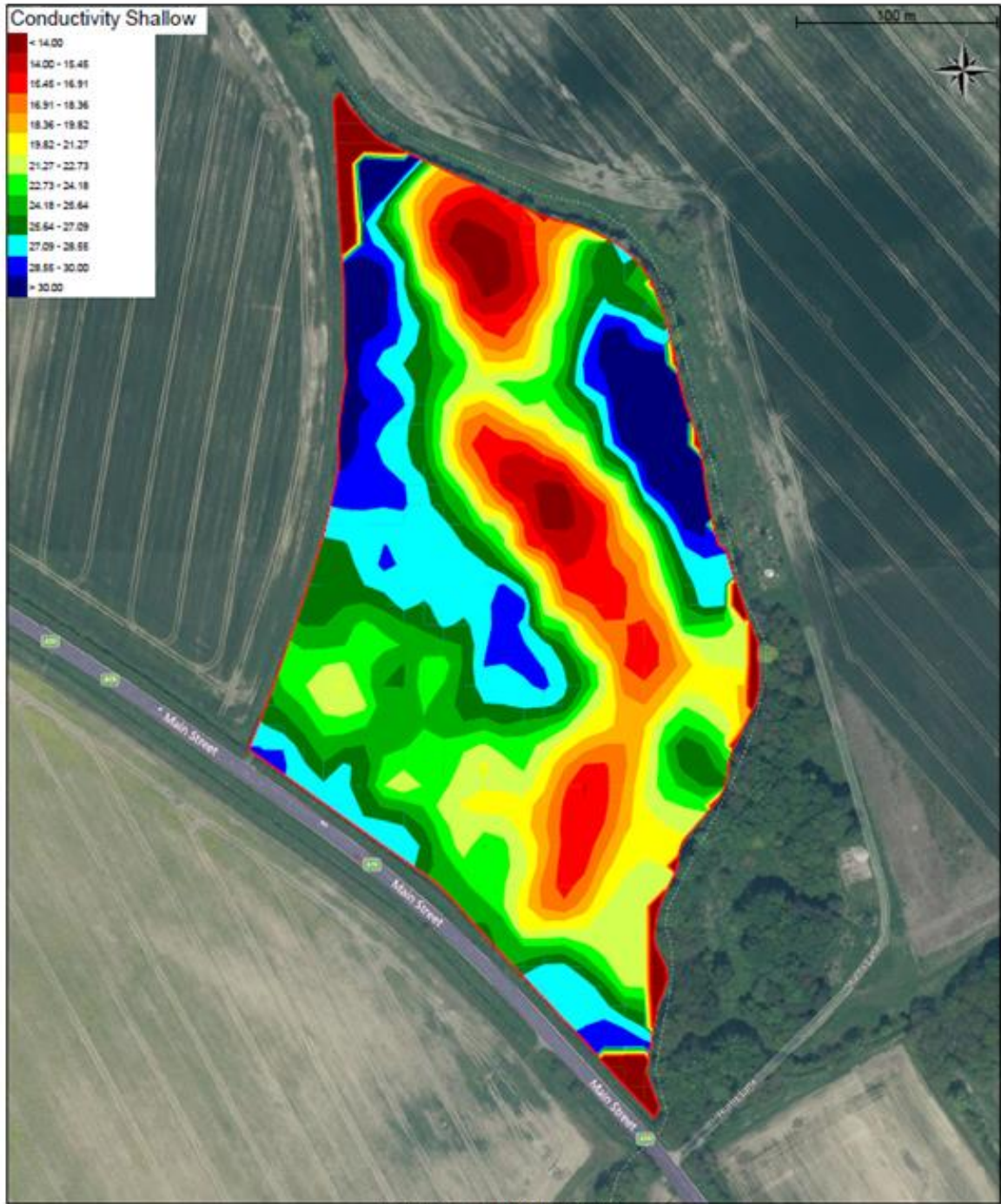
- workbench compatible with ARB. *Appl Environ Microbiol* 72: 5069–5072.
- Domeignoz-Horta, L.A., Philippot, L., Peyrard, C., Bru, D., Breuil, M.C., Bizouard, F., et al. (2018) Peaks of in situ N₂O emissions are influenced by N₂O-producing and reducing microbial communities across arable soils. *Glob Chang Biol* 24: 360–370.
- Drenovsky, R.E., Vo, D., Graham, K.J., and Scow, K.M. (2004) Soil water content and organic carbon availability are major determinants of soil microbial community composition. *Microb Ecol* 48: 424–430.
- Dumbrell, A.J., Nelson, M., Helgason, T., Dytham, C., and Fitter, A.H. (2010) Relative roles of niche and neutral processes in structuring a soil microbial community. *ISME J* 4: 337–345.
- Enwall, K., Throbäck, I.N., Stenberg, M., Söderström, M., and Hallin, S. (2010) Soil resources influence spatial patterns of denitrifying communities at scales compatible with land management. *Appl Environ Microbiol* 76: 2243–2250.
- FAO. (2015) What is Conservation Agriculture?
- FAO. (2018) World Food and Agriculture - Statistical Pocketbook 2018. Rome, Italy: FAO.
- Felske, A., and Akkermans, A.D.L. (1998) Prominent occurrence of ribosomes from an uncultured bacterium of the Verrucomicrobiales cluster in grassland soils. *Lett Appl Microbiol* 26: 219–223.
- Fish, J.A., Chai, B., Wang, Q., Sun, Y., Brown, C.T., Tiedje, J.M., and Cole, J.R. (2013) FunGene: the functional gene pipeline and repository. *Front Microbiol* 4: 1–14.
- Francioli, D., Schulz, E., Lentendu, G., Wubet, T., Buscot, F., and Reitz, T. (2016) Mineral vs. organic amendments: microbial community structure, activity and abundance of agriculturally relevant microbes are driven by long-term fertilization strategies. *Front Microbiol* 7: 1–16.
- Green, J.L., Holmes, A.J., Westoby, M., Oliver, I., Briscoe, D., Dangerfield, M., et al. (2004) Spatial scaling of microbial eukaryote diversity. *Nature* 432: 747–750.
- Hallin, P.F., and Ussery, D.W. (2004) CBS genome atlas database: a dynamic storage for bioinformatic results and sequence data. *Bioinformatics* 20: 3682–3686.
- Hartmann, M., Frey, B., Mayer, J., Mader, P., and Widmer, F. (2015) Distinct soil microbial diversity under long-term organic and conventional farming. *ISME J* 9: 1177–1194.
- IPCC. (2019) IPCC Special Report on climate change, desertification, land degradation, sustainable land management, food security, and greenhouse gas fluxes in terrestrial ecosystems summary for policymakers.
- Jiang, X., Liu, W., Yao, L., Liu, G., and Yang, Y. (2020) The roles of environmental variation and spatial distance in explaining diversity and biogeography of soil denitrifying communities in remote Tibetan wetlands. *FEMS Microbiol Ecol* 96: 1–11.
- Keel, S.G., Anken, T., Büchi, L., Chervet, A., Fliessbach, A., Flisch, R., et al. (2019) Loss of soil organic carbon in Swiss long-term agricultural experiments over a wide range of management practices. *Agric Ecosyst Environ* 286: 106654.
- Krauss, M., Krause, H.M., Spangler, S., Kandeler, E., Behrens, S., Kappler, A., et al. (2017a) Tillage system affects fertilizer-induced nitrous oxide emissions. *Biol Fertil Soils* 53: 49–59.
- Krauss, M., Ruser, R., Müller, T., Hansen, S., Mäder, P., and Gattinger, A. (2017b) Impact of reduced tillage on greenhouse gas emissions and soil carbon stocks in an organic grass-clover ley - winter wheat cropping sequence. *Agric Ecosyst Environ* 239: 324–333.
- Kroeze, C., Mosier, A.R., and Bouwman, L. (1999) Closing the global N₂O budget: a retrospective analysis 1500-1994. *Global Biogeochem Cycles* 13: 1–8.
- Krol, D.J., Jones, M.B., Williams, M., Richards, K.G., Bourdin, F., and Lanigan, G.J. (2016) The effect of renovation of long-term temperate grassland on N₂O emissions and N leaching from contrasting soils. *Sci Total Environ* 560–561: 233–240.
- Kuznetsova, A., Brockhoff, P.B., and Christensen, R.H.B. (2017) lmerTest: tests in linear mixed effects models. *J Stat Softw* 82: 1–27.
- Li, J., Wen, Y., Li, X., Li, Y., Yang, X., Lin, Z., et al. (2018) Soil labile organic carbon fractions and soil organic carbon stocks as affected by long-term organic and mineral fertilization regimes in the North China plain. *Soil Tillage Res* 175: 281–290.
- Lu, H., Chandran, K., and Stensel, D. (2014) Microbial ecology of denitrification in biological wastewater treatment. *Water Res* 64: 237–254.
- Marschner, P. (2007) Plant-microbe interactions in the rhizosphere and nutrient cycling. In *Nutrient Cycling in Terrestrial Ecosystems*, Marschner, P., and Rengel, Z. (eds). Berlin, Heidelberg: Springer.
- Martiny, J.B.H., Eisen, J.A., Penn, K., Allison, S.D., and Horner-Devine, M.C. (2011) Drivers of bacterial β -diversity depend on spatial scale. *Proc Natl Acad Sci U S A* 108: 7850–7854.
- Meyer, K.M., Memiaghe, H., Korte, L., Kenfack, D., Alonso, A., and Bohannan, B.J.M. (2018) Why do microbes exhibit weak biogeographic patterns? *ISME J* 12: 1404–1413.
- Murugan, R., Koch, H.J., and Joergensen, R.G. (2014) Long-term influence of different tillage intensities on soil microbial biomass, residues and community structure at different depths. *Biol Fertil Soils* 50: 487–498.
- Nadeau, S.A., Roco, C.A., Debenport, S.J., Anderson, T.R., Hofmeister, K.L., Walter, M.T., and Shapleigh, J.P. (2019) Metagenomic analysis reveals distinct patterns of denitrification gene abundance across soil moisture, nitrate gradients. *Environ Microbiol* 21: 1255–1266.
- O'Brien, S.L., Gibbons, S.M., Owens, S.M., HamptonMarcell, J., Johnston, E.R., Jastrow, J.D., et al. (2016) Spatial scale drives patterns in soil bacterial diversity. *Environ Microbiol* 18: 2039–2051.
- Oksanen, J., Blanchet, F.G., Friendly, M., Kindt, R., Legendre, P., McGlenn, D., et al. (2013) *Vegan: community ecology package*.
- Olsen, S.R., Cole, C.V., Watanabe, F.S., and Dean, L.A. (1954) Estimation of available phosphorus in soils by extraction with sodium bicarbonate. Washington, DC, USA: United states Department of Agriculture, p. 939.
- Orr, C.H., James, A., Leifert, C. Cooper, J.M., and Cummings, S.P., (2011) Diversity and activity of free-

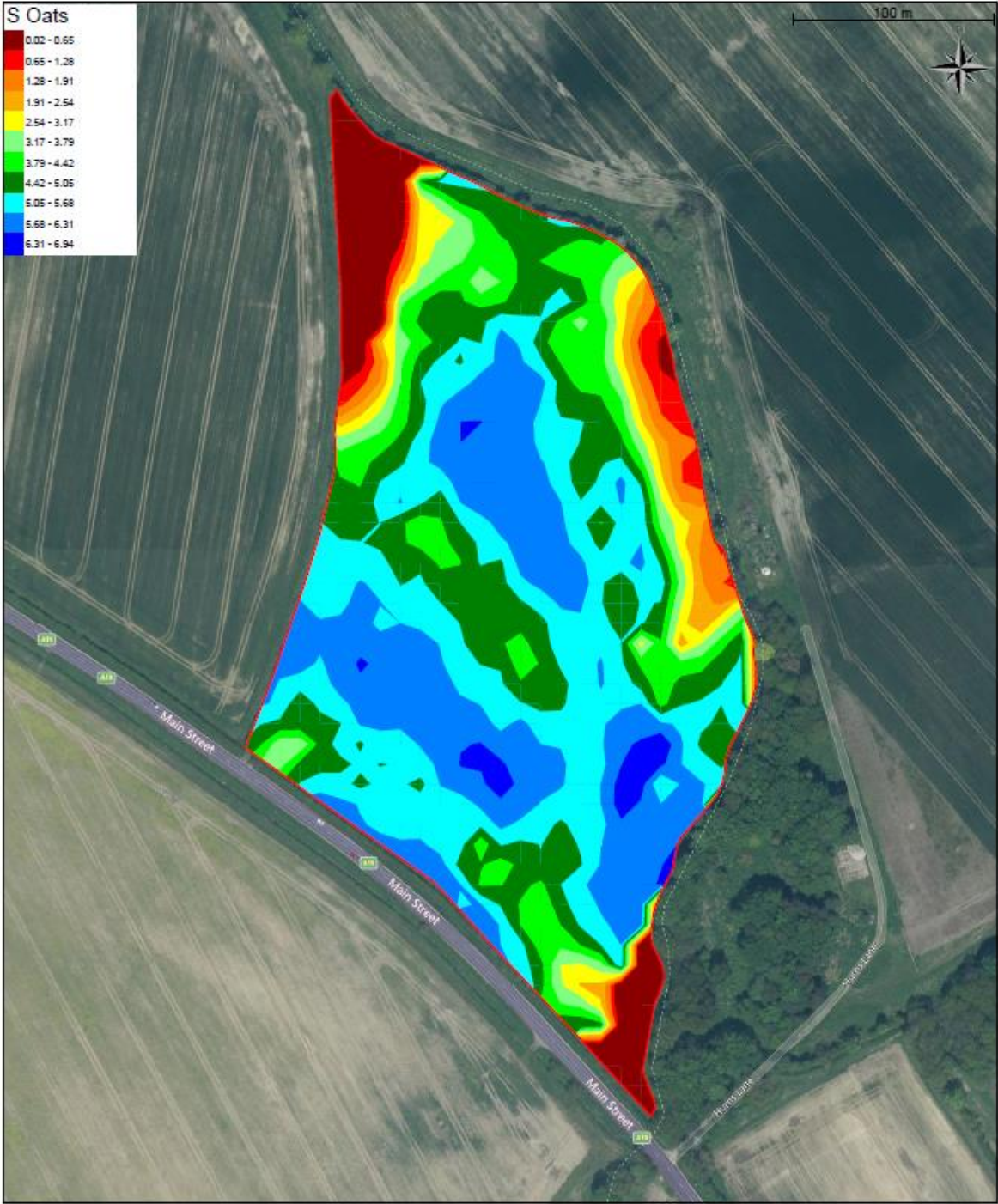
- living nitrogen-fixing bacteria and total bacteria in organic and conventionally managed soils. *Appl Environ Microbiol* 77: 911–919.
- Pettigrew, W.T. (2008) Potassium influences on yield and quality production for maize, wheat, soybean and cotton. *Physiol Plant* 133: 670–681.
- Piazza, G., Ercoli, L., Nuti, M., and Pellegrino, E. (2019) Interaction between conservation tillage and nitrogen fertilization shapes prokaryotic and fungal diversity at different soil depths: evidence from a 23-year field experiment in the Mediterranean area. *Front Microbiol* 10: 1–20.
- Pielou, E.C. (1966) The measurement of diversity in different types of biological collections. *J Theor Biol* 13: 131–144.
- R Core Team. (2013) R: A Language and Environment for Statistical Computing. Vienna: R Foundation for Statistical Computing.
- Ravishankara, A.R., Daniel, J.S., and Portmann, R.W. (2009) Nitrous oxide (N₂O): the dominant ozone-depleting substance emitted in the 21st century. *Science* 326: 123–125.
- Rinaldo, S., Giardina, G., and Cutruzzolà, F. (2016) Nitrite reductase – cytochrome cd1. In *Metalloenzymes in Denitrification: Applications and Environmental Impacts*, Moura, I., Moura, J.J.G., Pauleta, S.R., and Maia, L.B. (eds). Cambridge, UK: Royal Society of Chemistry, pp. 59–90.
- Rochette, P. (2008) No-till only increases N₂O emissions in poorly-aerated soils. *Soil Tillage Res* 101: 97–100.
- Rockström, J., Williams, J., Daily, G., Noble, A., Matthews, N., Gordon, L., et al. (2017) Sustainable intensification of agriculture for human prosperity and global sustainability. *Ambio* 46: 4–17.
- Roger Bray, J., and Curtis, J.T. (1957) An ordination of the upland forest communities of southern Wisconsin. *Ecol Monogr* 27: 326–349.
- RStudio Team. (2018) RStudio: Integrated Development for R.
- Rütting, T., Aronsson, H., and Delin, S. (2018) Efficient use of nitrogen in agriculture. *Nutr Cycl Agroecosyst* 110: 1–5.
- Shannon, C.E. (1948) A mathematical theory of communication. *Bell Syst Tech J* 27: 379–423.
- Six, J., Ogle, S.M., Breidt, F.J., Conant, R.T., Mosier, A.R., and Paustian, K. (2004) The potential to mitigate global warming with no-tillage management is only realized when practised in the long term. *Glob Chang Biol* 10: 155–160.
- Smets, W., Leff, J.W., Bradford, M.A., McCulley, R.L., Lebeer, S., and Fierer, N. (2016) A method for simultaneous measurement of soil bacterial abundances and community composition via 16S rRNA gene sequencing. *Soil Biol Biochem* 96: 145–151.
- Soil Survey Staff. (2014) *Keys to Soil Taxonomy*, 12th ed. Washington, DC: USDA-Natural Resources Conservation Service.
- Stevens, C.J. (2019) Nitrogen in the environment. *Science* 363: 578–580.
- Sun, H., Koal, P., Liu, D., Gerl, G., Schroll, R., Gattinger, A., et al. (2016) Soil microbial community and microbial residues respond positively to minimum tillage under organic farming in southern Germany. *Appl Soil Ecol* 108: 16–24.
- Syakila, A., and Kroeze, C. (2011) The global nitrous oxide budget revisited. *Greenh Gas Meas Manag* 1: 17–26.
- Tellez-Rio, A., García-Marco, S., Navas, M., Lopez-Solanilla, E., Tenorio, J.L., and Vallejo, A. (2015) N₂O and CH₄ emissions from a fallow-wheat rotation with low N input in conservation and conventional tillage under a Mediterranean agroecosystem. *Sci Total Environ* 508: 85–94.
- Tian, S., Ning, T., Zhao, H., Wang, B., Li, N., Han, H., et al. (2012) Response of CH₄ and N₂O emissions and wheat yields to tillage method changes in the North China plain. *PLoS One* 7: 1–10.
- Vandekerckhove, T.T.M., Willems, A., Gillis, M., and Coomans, A. (2000) Occurrence of novel verrucomicrobial species, endosymbiotic and associated with parthenogenesis in *Xiphinema americanum*-group species (Nematoda, Longidoridae). *Int J Syst Evol Microbiol* 50: 2197–2205.
- Vos, M., Wolf, A.B., Jennings, S.J., and Kowalchuk, G.A. (2013) Micro-scale determinants of bacterial diversity in soil. *FEMS Microbiol Rev* 37: 936–954.
- Wallenstein, M.D., and Hall, E.K. (2012) A trait-based framework for predicting when and where microbial adaptation to climate change will affect ecosystem functioning. *Biogeochemistry* 109: 35–47.
- Wallenstein, M.D., Myrold, D.D., Firestone, M.K., and Voytek, M. (2006) Environmental controls on denitrifying communities and denitrification rates: insights from molecular methods. *Ecol Appl* 16: 2143–2152.
- Wang, J., and Zou, J. (2020) No-till increases soil denitrification via its positive effects on the activity and abundance of the denitrifying community. *Soil Biol Biochem* 142: 107706.
- Wang, Z., Liu, L., Chen, Q., Wen, X., and Liao, Y. (2016) Conservation tillage increases soil bacterial diversity in the dryland of northern China. *Agron Sustain Dev* 36: 1–9.
- Zhang, B., He, H., Ding, X., Zhang, X., Zhang, X., Yang, X., and Filley, T.R. (2012) Soil microbial community dynamics over a maize (*Zea mays* L.) growing season under conventional - and no - tillage practices in a rainfed agroecosystem. *Soil Tillage Res* 124: 153–160.
- Zhou, J., Kang, S., Schadt, C.W., and Garten, C.T. (2008) Spatial scaling of functional gene diversity across various microbial taxa. *Proc Natl Acad Sci U S A* 105: 7768–7773.

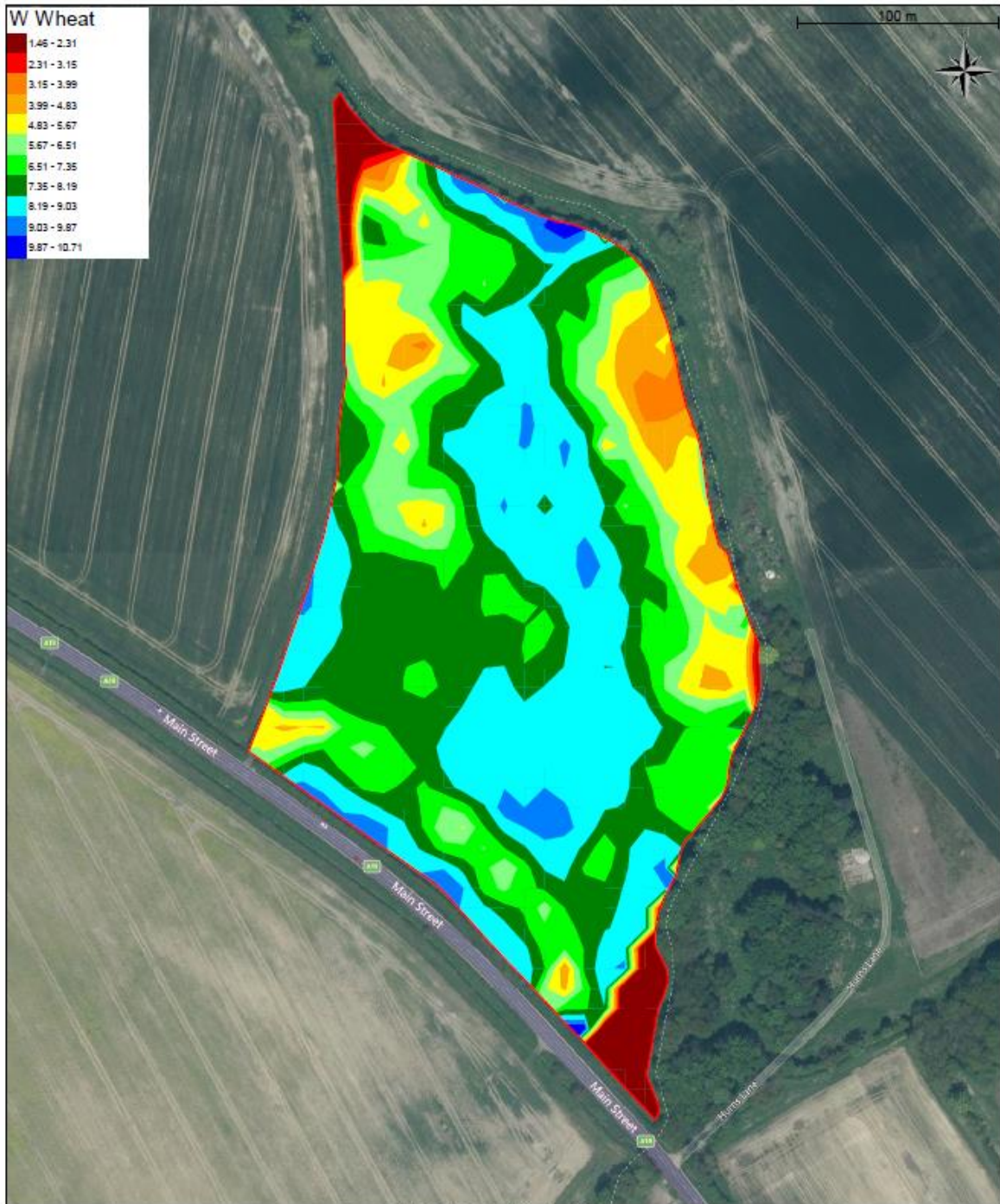
Supporting Information

Additional Supporting Information may be found in the online version of this article at the publisher's web-site: Appendix S1: Supporting Information.

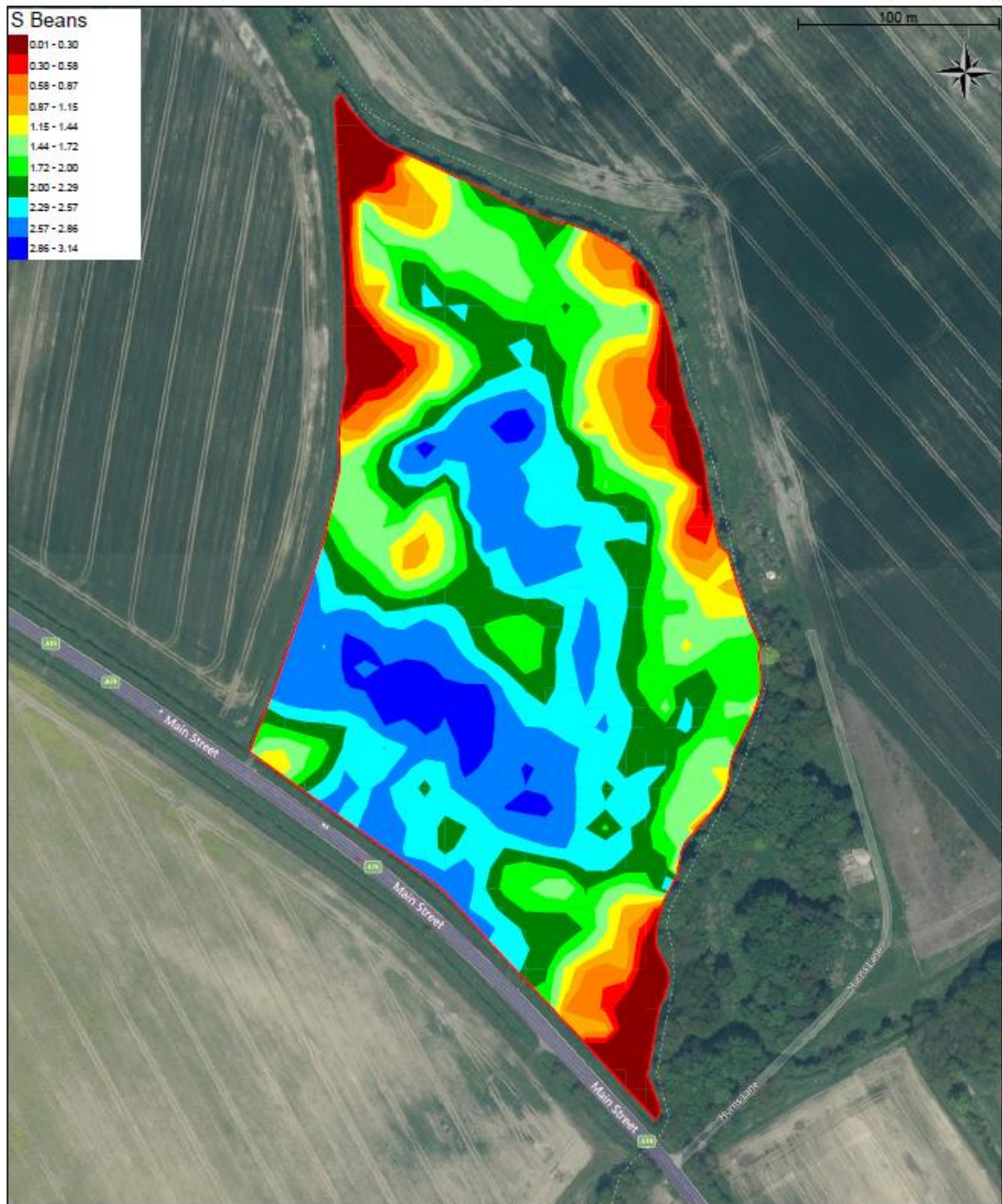
Appendix 2: Electrical conductivity and yield maps of Harold Smiths field



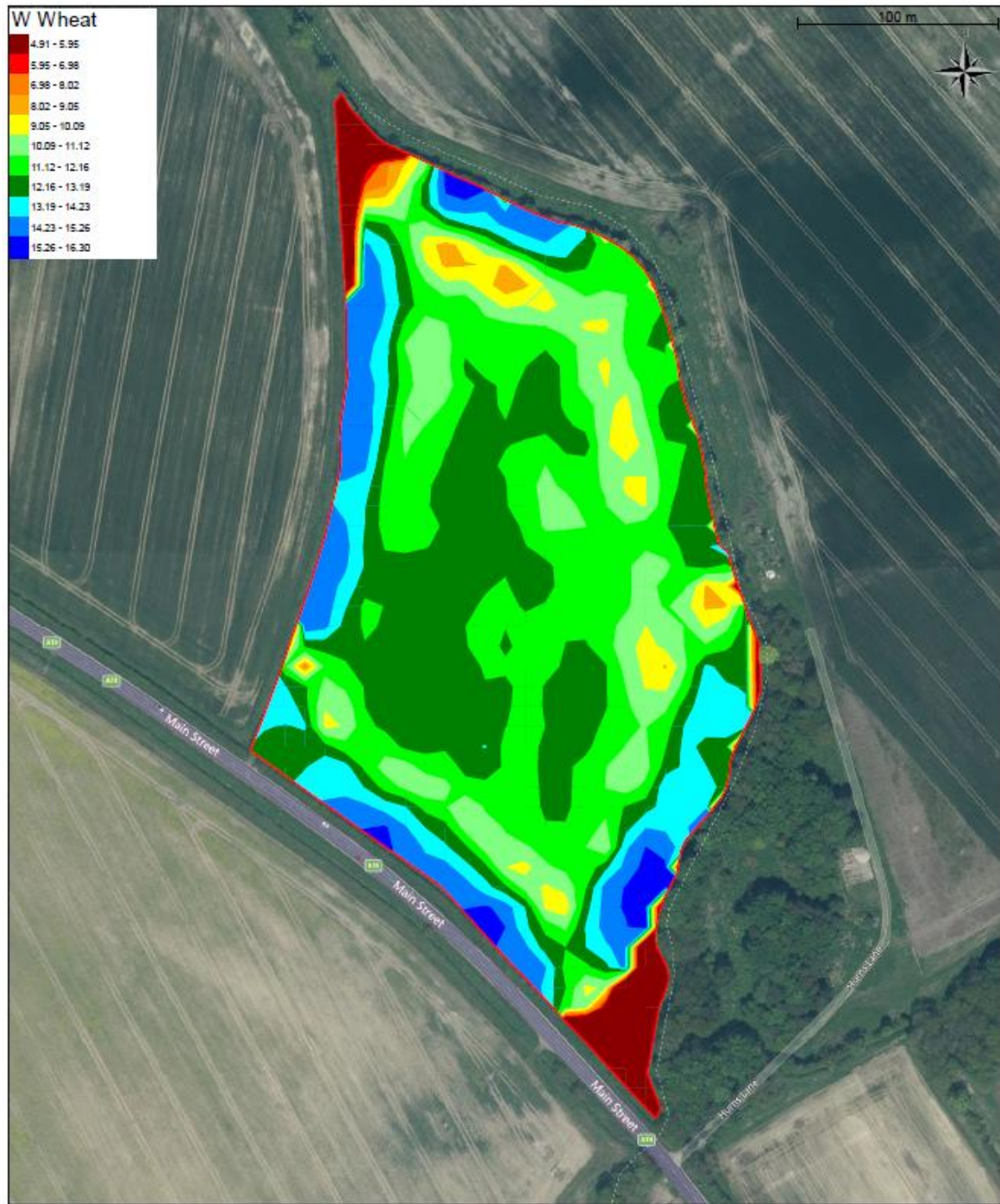




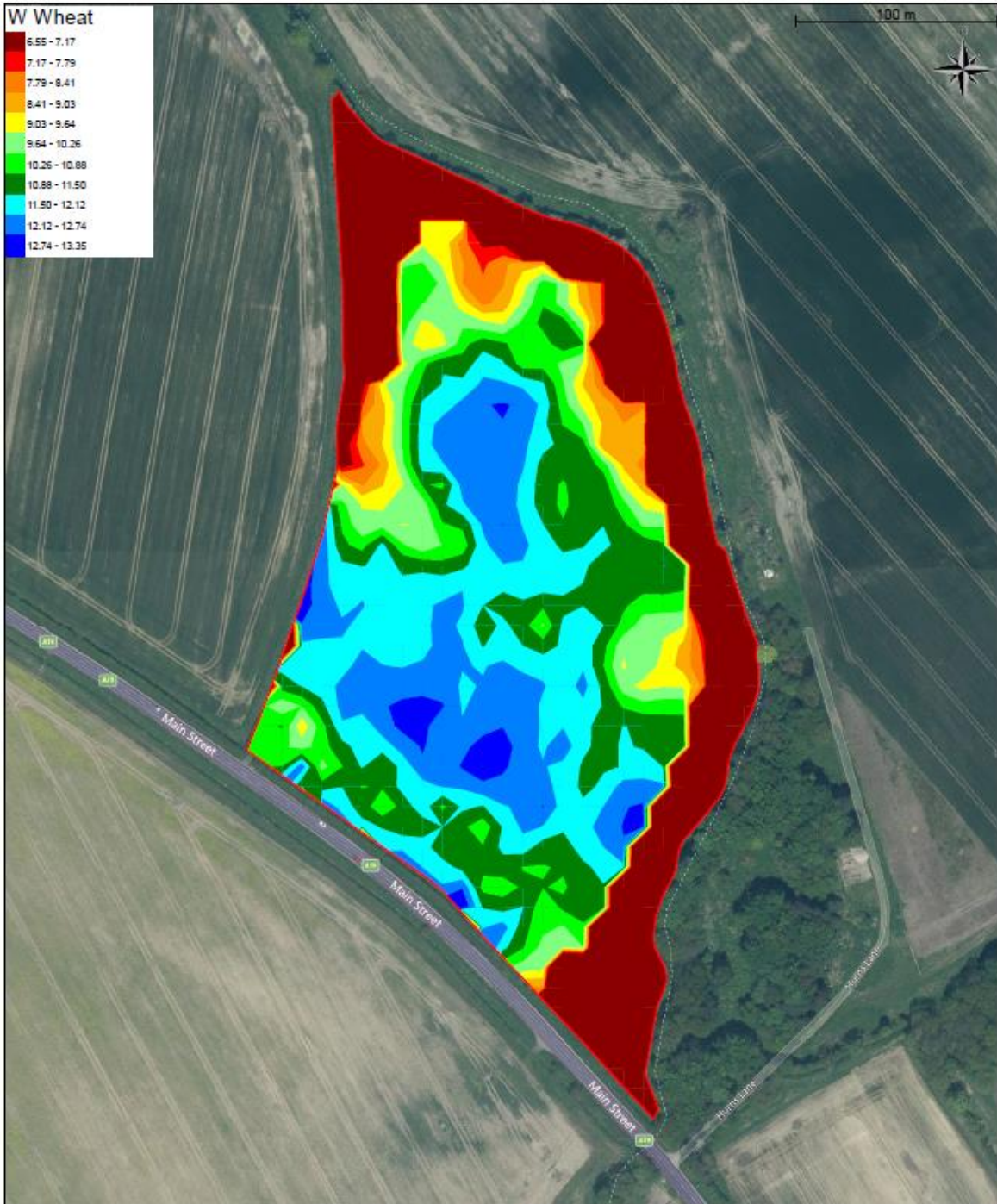
Precision Decisions is part of the Map of Ag Group



Precision Decisions is part of the Map of Ag Group



Precision Decisions is part of the Map of Ag Group



Appendix 3: Arduino code used to transfer data from nitric oxide and oxygen sensors

```
const int analogOutPinNO = A0; // Analog pin that the NO electrode circuit is attached to
const int analogOutPinOx = A1; // Analog pin the O2 electrode circuit is connected to
```

```
int t = 0; // value of assay time to output to the port
int outputValueNO = 0; // value to output to the serial port (analog out)
int outputValueOx = 0; // value to output to the serial port (analog out)
```

```
long sumValueNO = 0;
long sumValueOx = 0;
int sumN = 100;
```

```
void setup() {
  // initialize serial communications at 9600 bps:
  Serial.begin(9600);
  analogReadResolution (12); //because the Arduino Due can read 12 bits
}
```

```
void loop() {
  //adjust time value to affect assay period in seconds
  while ( t < 10800 ){
```

```

// read the analog in values:

sumValueNO = 0;

sumValueOx = 0;

for(int i = 0; i < sumN; i++){

    sumValueNO = sumValueNO + analogRead(analogOutPinNO);

    sumValueOx = sumValueOx + analogRead(analogOutPinOx);

    delay(10);

}

outputValueNO = (sumValueNO*1.0)/sumN;

outputValueOx = (sumValueOx*1.0)/sumN;

// print the results to the serial monitor:

Serial.print(millis());

Serial.print(",");

Serial.print(outputValueNO*3/4.096);    //could convert the above to the voltage by
outputValue* 3 / 4096 (3 V maximum and 12 bits equivalent to 4096 as maximum reading

Serial.print(",");

Serial.println(outputValueOx*3/4.096);

// wait 1 second before the next loop

// after the last reading:

delay(0);

t++;

}

}

```

References

- Aleklett, K., Kiers, E.T., Ohlsson, P., Shimizu, T.S., Caldas, V.E., and Hammer, E.C. (2018) Build your own soil: Exploring microfluidics to create microbial habitat structures. *ISME J* **12**: 312–319.
- Alessi, A.M., Redeker, K.R., and Chong, J.P.J. (2018) A practical introduction to microbial molecular ecology through the use of isolation chips. *Ecol Evol* **8**: 12286–12298.
- Alexander, S., Black, A., Boland, A., Burke, J., Carton, O.T., Coulter, B.S., et al. (2008) Major and micro nutrient advice for productive agricultural crops, 3rd ed. Coulter, B.S. and Lalor, S. (eds) Johnstown Castle, Co Wexford, Ireland: Teagasc.
- Amann, R.L., Ludwig, W., and Schleifer, K.H. (1995) Phylogenetic identification and in situ detection of individual microbial cells without cultivation. *Microbiol Rev* **59**: 143–169.
- Anderson, J.P.E. and Domsch, K.H. (1978) A physiological method for the quantitative measurement of microbial biomass in soils. *Soil Biol Biochem* **10**: 215–221.
- Arai, H., Igarashi, Y., and Kodama, T. (1995a) Expression of the nir and nor genes for denitrification of *Pseudomonas aeruginosa* requires a novel CRP/FNR-related transcriptional regulator, DNR, in addition to ANR. *FEBS Lett* **371**: 73–76.
- Arai, H., Igarashi, Y., and Kodama, T. (1994) Structure and ANR-dependent transcription of the nir genes for denitrification from *Pseudomonas aeruginosa*. *Biosci Biotechnol Biochem* **58**: 1286–1291.
- Arai, H., Igarashi, Y., and Kodama, T. (1995b) The structural genes for nitric oxide reductase from *Pseudomonas aeruginosa*. *Biochim Biophys Acta (BBA)-Gene Struct Expr* **1261**: 279–284.

- Arth, I., Frenzel, P., and Conrad, R. (1998) Denitrification coupled to nitrification in the rhizosphere of rice. *Soil Biol Biochem* **30**: 509–515.
- Attard, E., Recous, S., Chabbi, A., De Berranger, C., Guillaumaud, N., Labreuche, J., et al. (2011) Soil environmental conditions rather than denitrifier abundance and diversity drive potential denitrification after changes in land uses. *Glob Chang Biol* **17**: 1975–1989.
- Avery, B.W. and Bascomb, C.L. (1974) Soil survey laboratory methods. In *Soil survey of Great Britain Vol. 6*. Harpenden, U.K.
- Baas-Becking, L.G.. M. (1934) Geobiologie of inleiding tot de milieukunde.
- Babin, D., Deubel, A., Jacquiod, S., Sørensen, S.J., Geistlinger, J., Grosch, R., and Smalla, K. (2019) Impact of long-term agricultural management practices on soil prokaryotic communities. *Soil Biol Biochem* **129**: 17–28.
- Bai, E., Houlton, B.Z., and Wang, Y.P. (2012) Isotopic identification of nitrogen hotspots across natural terrestrial ecosystems. *Biogeosciences* **9**: 3287–3304.
- Bai, Z., Caspari, T., Gonzalez, M.R., Batjes, N.H., Mäder, P., Bünemann, E.K., et al. (2018) Effects of agricultural management practices on soil quality: A review of long-term experiments for Europe and China. *Agric Ecosyst Environ* **265**: 1–7.
- Bali, S., Lawrence, A.D., Lobo, S.A., Saraiva, L.M., Golding, B.T., Palmer, D.J., et al. (2011) Molecular hijacking of siroheme for the synthesis of heme and d1 heme. *Proc Natl Acad Sci* **108**: 18260–18265.
- Ball, D.F. (1964) Loss-on-ignition as an estimate of organic matter and organic carbon in non-calcareous soils. *J Soil Sci* **15**: 84–92.
- Balvočiūtė, M. and Huson, D.H. (2017) SILVA, RDP, Greengenes, NCBI and OTT — how

do these taxonomies compare? *BMC Genomics* **18**: 114.

Bankevich, A., Nurk, S., Antipov, D., Gurevich, A.A., Dvorkin, M., Kulikov, A.S., et al. (2012) SPAdes: A new genome assembly algorithm and its applications to single-cell sequencing. *J Comput Biol* **19**: 455–477.

Bardgett, R.D. and van der Putten, W.H. (2014) Belowground biodiversity and ecosystem functioning. *Nature* **515**: 505–511.

Bartnikas, T.B., Tosques, I.E., Laratta, W.P., Shi, J., and Shapleigh, J.P. (1997) Characterization of the nitric oxide reductase-encoding region in *Rhodobacter sphaeroides* 2.4. 3. *J Bacteriol* **179**: 3534–3540.

Baudoin, E., Philippot, L., Chèneby, D., Chapuis-Lardy, L., Fromin, N., Bru, D., et al. (2009) Direct seeding mulch-based cropping increases both the activity and the abundance of denitrifier communities in a tropical soil. *Soil Biol Biochem* **41**: 1703–1709.

Beare, M.H., Neely, C.L., Coleman, D.C., and Hargrove, W.L. (1990) A substrate-induced respiration (SIR) method for measurement of fungal and bacterial biomass on plant residues. *Soil Biol Biochem* **22**: 585–594.

Beeckman, F., Motte, H., and Beeckman, T. (2018) Nitrification in agricultural soils: impact, actors and mitigation. *Curr Opin Biotechnol* **50**: 166–173.

Begmatov, S., Dorofeev, A.G., Kadnikov, V. V., Beletsky, A. V., Pimenov, N. V., Ravin, N. V., and Mardanov, A. V. (2022) The structure of microbial communities of activated sludge of large-scale wastewater treatment plants in the city of Moscow. *Sci Rep* **12**: 1–14.

Behnke, G.D., Kim, N., Riggins, C.W., Zabaloy, M.C., Rodriguez-Zas, S.L., and Villamil, M.B. (2022) A Longitudinal Study of the Microbial Basis of Nitrous Oxide Emissions

Within a Long-Term Agricultural Experiment. *Front Agron* **4**:

Beijerinck, M.W. (1913) Oxydation des Mangancarbonates durch Bakterien und Schimmelpilze. *Folia Microbiol Delft* **2**:

Bender, S.F., Wagg, C., and van der Heijden, M.G.A. (2016) An Underground Revolution: Biodiversity and Soil Ecological Engineering for Agricultural Sustainability. *Trends Ecol Evol* **31**: 440–452.

Benson, B.B. and Krause Jr., D. (1980) The concentration and isotopic fractionation of gases dissolved in freshwater in equilibrium with the atmosphere. 1. Oxygen. *Limnol Oceanogr* **25**: 662–671.

Berdy, B., Spoering, A.L., Ling, L.L., and Epstein, S.S. (2017) In situ cultivation of previously uncultivable microorganisms using the ichip. *Nat Protoc* **12**: 2232–2242.

Berg, G. and Smalla, K. (2009) Plant species and soil type cooperatively shape the structure and function of microbial communities in the rhizosphere. *FEMS Microbiol Ecol* **68**: 1–13.

Bergaust, L., Shapleigh, J., Frostegård, Å., and Bakken, L.R. (2008) Transcription and activities of NO_x reductases in *Agrobacterium tumefaciens*: The influence of nitrate, nitrite and oxygen availability. *Environ Microbiol* **10**: 3070–3081.

Berks, B.C., Page, M.D., Richardson, D.J., Reilly, A., Cavill, A., Outen, F., and Ferguson, S.J. (1995) Sequence analysis of subunits of the membrane-bound nitrate reductase from a denitrifying bacterium: the integral membrane subunit provides a prototype for the dihaem electron-carrying arm of a redox loop. *Mol Microbiol* **15**: 319–331.

Berks, B.C., Richardson, D.J., Reilly, A., Willis, A.C., and Ferguson, S.J. (1995) The napEDABC gene cluster encoding the periplasmic nitrate reductase system of

Thiosphaera pantotropha. *Biochem J* **309**: 983–992.

Blagodatskaya, E. and Kuzyakov, Y. (2013) Active microorganisms in soil: critical review of estimation criteria and approaches. *Soil Biol Biochem* **67**: 192–211.

Blazewicz, S.J., Barnard, R.L., Daly, R.A., and Firestone, M.K. (2013) Evaluating rRNA as an indicator of microbial activity in environmental communities: limitations and uses. *ISME J* **7**: 2061–2068.

de Boer, A.P., Reijnders, W.N., Kuenen, J.G., Stouthamer, A.H., and van Spanning, R.J. (1994) Isolation, sequencing and mutational analysis of a gene cluster involved in nitrite reduction in *Paracoccus denitrificans*. *Antonie Van Leeuwenhoek* **66**: 111–127.

De Boer, A.P.N., Van Der Oost, J., Reijnders, W.N.M., Westerhoff, H. V, Stouthamer, A.H., and Van Spanning, R.J.M. (1996) Mutational analysis of the *nor* gene cluster which encodes nitric-oxide reductase from *Paracoccus denitrificans*. *Eur J Biochem* **242**: 592–600.

Bolger, A.M., Lohse, M., and Usadel, B. (2014) Trimmomatic: A flexible trimmer for Illumina sequence data. *Bioinformatics* **30**: 2114–2120.

Bolyen, E., Rideout, J.R., Dillon, M.R., Bokulich, N.A., Abnet, C.C., Ghalith, G.A. Al, et al. (2018) QIIME 2: Reproducible, interactive, scalable, and extensible microbiome data science. *PeerJ Prepr* **6**:e27295v2.

Braker, G., Fesefeldt, A., and Witzel, K.P. (1998) Development of PCR primer systems for amplification of nitrite reductase genes (*nirK* and *nirS*) to detect denitrifying bacteria in environmental samples. *Appl Environ Microbiol* **64**: 3769–3775.

Braker, G. and Tiedje, J.M. (2003) Nitric oxide reductase (*norB*) genes from pure cultures and environmental samples. *Appl Environ Microbiol* **69**: 3476–3483.

- Braker, G., Zhou, J., Wu, L., Devol, A.H., and Tiedje, J.M. (2000) Nitrite reductase genes (nirK and nirS) as functional markers to investigate diversity of denitrifying bacteria in pacific northwest marine sediment communities. *Appl Environ Microbiol* **66**: 2096–2104.
- Brindley, A.A., Zajicek, R., Warren, M.J., Ferguson, S.J., and Rigby, S.E.J. (2010) NirJ, a radical SAM family member of the d1 heme biogenesis cluster. *FEBS Lett* **584**: 2461–2466.
- Broman, E., Zilius, M., Samuiloviene, A., Vybernaite-Lubiene, I., Politi, T., Klawonn, I., et al. (2021) Active DNRA and denitrification in oxic hypereutrophic waters. *Water Res* **194**: 116954.
- Brown, M.D. and Schoenfish, M.H. (2019) Electrochemical nitric oxide sensors: principles of design and characterization. *Chem Rev* **119**: 11551–11575.
- Browne, H.P., Forster, S.C., Anonye, B.O., Kumar, N., Neville, B.A., Stares, M.D., et al. (2016) Culturing of “unculturable” human microbiota reveals novel taxa and extensive sporulation. *Nature* **533**: 543–546.
- Bru, D., Ramette, A., Saby, N.P.A., Dequiedt, S., Ranjard, L., Jolivet, C., et al. (2011) Determinants of the distribution of nitrogen-cycling microbial communities at the landscape scale. *ISME J* **5**: 532–542.
- Bru, D., Sarr, A., and Philippot, L. (2007) Relative abundances of proteobacterial membrane-bound and periplasmic nitrate reductases in selected environments. *Appl Environ Microbiol* **73**: 5971–5974.
- Brzezińska, M., Rafalski, P., Włodarczyk, T., Szarlip, P., and Brzeziński, K. (2011) How much oxygen is needed for acetylene to be consumed in soil? *J Soils Sediments* **11**: 1142.

- Butterbach-Bahl, K., Baggs, E.M., Dannenmann, M., Kiese, R., and Zechmeister-Boltenstern, S. (2013) Nitrous oxide emissions from soils: how well do we understand the processes and their controls? *Philos Trans R Soc B Biol Sci* **368**: 20130122–20130122.
- Butterbach-Bahl, K., Willibald, G., and Papen, H. (2002) Soil core method for direct simultaneous determination of N₂ and N₂O emissions from forest soils. *Plant Soil* **240**: 105–116.
- De Cáceres, M. and Legendre, P. (2009) Associations between species and groups of sites: Indices and statistical inference. *Ecology* **90**: 3566–74.
- Callahan, B.J., McMurdie, P.J., Rosen, M.J., Han, A.W., Johnson, A.J.A., and Holmes, S.P. (2016) DADA2: High-resolution sample inference from Illumina amplicon data. *Nat Methods* **13**: 581–583.
- Camarotto, C., Piccoli, I., Dal Ferro, N., Polese, R., Chiarini, F., Furlan, L., and Morari, F. (2020) Have we reached the turning point? Looking for evidence of SOC increase under conservation agriculture and cover crop practices. *Eur J Soil Sci* **71**: 1050–63.
- Carson, J.K., Gonzalez-Quiñones, V., Murphy, D. V, Hinz, C., Shaw, J.A., and Gleeson, D.B. (2010) Low pore connectivity increases bacterial diversity in soil. *Appl Environ Microbiol* **76**: 3936–3942.
- Casciotti, K.L. and Ward, B.B. (2001) Dissimilatory nitrite reductase genes from autotrophic ammonia-oxidizing bacteria. *Appl Environ Microbiol* **67**: 2213–2221.
- Casciotti, K.L. and Ward, B.B. (2005) Phylogenetic analysis of nitric oxide reductase gene homologues from aerobic ammonia-oxidizing bacteria. *FEMS Microbiol Ecol* **52**: 197–205.
- Chan, Y.-K., McCormic, W.A., and Watson, R.J. (1997) A new nos gene downstream from

nosDFY is essential for dissimilatory reduction of nitrous oxide by *Rhizobium* (Sinorhizobium) meliloti. *Microbiology* **143** (Pt 8): 2817–2824.

Chang, Q., Luan, Y., and Sun, F. (2011) Variance adjusted weighted UniFrac: a powerful beta diversity measure for comparing communities based on phylogeny. *BMC Bioinformatics* **12**: 118.

Changsheng Li, Frohling, S., and Frohling, T.A. (1992) A model of nitrous oxide evolution from soil driven by rainfall events: 1. Model structure and sensitivity. *J Geophys Res* **97**: 9759–9776.

Chaudhary, D.K., Khulan, A., and Kim, J. (2019) Development of a novel cultivation technique for uncultured soil bacteria. *Sci Rep* **6666**.

Chen, H., Dai, Z., Veach, A.M., Zheng, J., Xu, J., and Schadt, C.W. (2020) Global meta-analyses show that conservation tillage practices promote soil fungal and bacterial biomass. *Agric Ecosyst Environ* **293**: 106841.

Chen, H., Hou, R., Gong, Y., Li, H., Fan, M., and Kuzyakov, Y. (2009) Effects of 11 years of conservation tillage on soil organic matter fractions in wheat monoculture in Loess Plateau of China. *Soil Tillage Res* **106**: 85–94.

Chen, J.Y., Chang, W.C., Chang, T., Chang, W.C., Liu, M.Y., Payne, W.J., and LeGall, J. (1996) Cloning, characterization, and expression of the nitric oxide-generating nitrite reductase and of the blue copper protein genes of *Achromobacter cycloclastes*. *Biochem Biophys Res Commun* **219**: 423–428.

Chen, Z., Liu, J., Wu, M., Xie, X., Wu, J., and Wei, W. (2012) Differentiated response of denitrifying communities to fertilization regime in paddy soil. *Microb Ecol* **63**: 446–459.

Chen, Z., Luo, X., Hu, R., Wu, M., Wu, J., and Wei, W. (2010) Impact of long-term

fertilization on the composition of denitrifier communities based on nitrite reductase analyses in a paddy soil. *Microb Ecol* **60**: 850–861.

Chèneby, D., Hartmann, A., Hénault, C., Topp, E., and Germon, J.C. (1998) Diversity of denitrifying microflora and ability to reduce N₂O in two soils. *Biol Fertil soils* **28**: 19–26.

Chèneby, D., Philippot, L., Hartmann, A., Hénault, C., and Germon, J.C. (2000) 16S rDNA analysis for characterization of denitrifying bacteria isolated from three agricultural soils. *FEMS Microbiol Ecol* **34**: 121–128.

Chroňáková, A., Radl, V., Čuhel, J., Šimek, M., Elhottová, D., Engel, M., and Schloter, M. (2009) Overwintering management on upland pasture causes shifts in an abundance of denitrifying microbial communities, their activity and N₂O-reducing ability. *Soil Biol Biochem* **41**: 1132–1138.

Coenye, T. and Vandamme, P. (2003) Intragenomic heterogeneity between multiple 16S ribosomal RNA operons in sequenced bacterial genomes. *FEMS Microbiol Lett* **228**: 45–49.

Cole, J.R., Wang, Q., Fish, J.A., Chai, B., McGarrell, D.M., Sun, Y., et al. (2014) Ribosomal Database Project: data and tools for high throughput rRNA analysis. *Nucleic Acids Res* **42**: D633-42.

Constancias, F., Saby, N.P.A., Terrat, S., Dequiedt, S., Horrigue, W., Nowak, V., et al. (2015) Contrasting spatial patterns and ecological attributes of soil bacterial and archaeal taxa across a landscape. *Microbiologyopen*.

Conthe, M., Lycus, P., Arntzen, M., Ramos da Silva, A., Frostegård, Å., Bakken, L.R., et al. (2019) Denitrification as an N₂O sink. *Water Res* **151**: 381–387.

- Cooper, J.M., Baranski, M., Stewart, G., Nobel-de Lange, M., Bärberi, P., Fließbach, A., et al. (2016) Shallow non-inversion tillage in organic farming maintains crop yields and increases soil C stocks: a meta-analysis. *Agron Sustain Dev* **36**:
- Coskun, D., Britto, D.T., Shi, W., and Kronzucker, H.J. (2017) Nitrogen transformations in modern agriculture and the role of biological nitrification inhibition. *Nat Plants* **3**:
- Costa, M.C.M.S., Carvalho, L., Leal, C.D., Dias, M.F., Martins, K.L., Garcia, G.B., et al. (2014) Impact of inocula and operating conditions on the microbial community structure of two anammox reactors. *Environ Technol* **35**: 1811–1822.
- Cramm, R., Siddiqui, R.A., and Friedrich, B. (1994) Primary sequence and evidence for a physiological function of the flavohemoprotein of *Alcaligenes eutrophus*. *J Biol Chem* **269**: 7349–7354.
- Cramm, R., Siddiqui, R.A., and Friedrich, B. (1997) Two isofunctional nitric oxide reductases in *Alcaligenes eutrophus* H16. *J Bacteriol* **179**: 6769–6777.
- Čuhel, J., Šimek, M., Laughlin, R.J., Bru, D., Chèneby, D., Watson, C.J., and Philippot, L. (2010) Insights into the effect of soil pH on N₂O and N₂ emissions and denitrifier community size and activity. *Appl Environ Microbiol* **76**: 1870–1878.
- Cui, P., Fan, F., Yin, C., Song, A., Huang, P., Tang, Y., et al. (2016) Long-term organic and inorganic fertilization alters temperature sensitivity of potential N₂O emissions and associated microbes. *Soil Biol Biochem* **93**: 131–141.
- Dandie, C.E., Burton, D.L., Zebarth, B.J., Henderson, S.L., Trevors, J.T., and Goyer, C. (2008) Changes in bacterial denitrifier community abundance over time in an agricultural field and their relationship with denitrification activity. *Appl Environ Microbiol* **74**: 5997–6005.

- Dandie, C.E., Miller, M.N., Burton, D.L., Zebarth, B.J., Trevors, J.T., and Goyer, C. (2007) Nitric oxide reductase-targeted real-time PCR quantification of denitrifier populations in soil. *Appl Environ Microbiol* **73**: 4250–4258.
- David, M.B., McIsaac, G.F., Royer, T. V, Darmody, R.G., and Gentry, L.E. (2001) Estimated historical and current nitrogen balances for Illinois. *Sci World J* **1**: 597–604.
- Degrune, F., Theodorakopoulos, N., Dufrêne, M., Colinet, G., Bodson, B., Hiel, M.P., et al. (2016) No favorable effect of reduced tillage on microbial community diversity in a silty loam soil (Belgium). *Agric Ecosyst Environ* **224**: 12–21.
- Delgado-Baquerizo, M., Maestre, F.T., Reich, P.B., Jeffries, T.C., Gaitan, J.J., Encinar, D., et al. (2016) Microbial diversity drives multifunctionality in terrestrial ecosystems. *Nat Commun* **7**: 1–8.
- Delorme, S., Philippot, L., Edel-Hermann, V., Deulvot, C., Mougel, C., and Lemanceau, P. (2003) Comparative genetic diversity of the narG, nosZ, and 16S rRNA genes in fluorescent pseudomonads. *Appl Environ Microbiol* **69**: 1004–1012.
- Derpsch, R., Friedrich, T., Kassam, A., and Hongwen, L. (2010) Current status of adoption of no-till farming in the world and some of its main benefits. *Int J Agric Biol Eng* **3**: 1–25.
- DeSantis, T.Z., Hugenholtz, P., Larsen, N., Rojas, M., Brodie, E.L., Keller, K., et al. (2006) Greengenes, a chimera-checked 16S rRNA gene database and workbench compatible with ARB. *Appl Environ Microbiol* **72**: 5069–5072.
- van Dijk, M., Morley, T., Rau, M.L., and Saghai, Y. (2021) A meta-analysis of projected global food demand and population at risk of hunger for the period 2010–2050. *Nat Food* **2**: 494–501.
- Djigal, D., Baudoin, E., Philippot, L., Brauman, A., and Villenave, C. (2010) Shifts in size,

- genetic structure and activity of the soil denitrifier community by nematode grazing. *Eur J Soil Biol* **46**: 112–118.
- Doane, T.A. (2017) The Abiotic Nitrogen Cycle. *ACS Earth Sp Chem* **1**: 411–421.
- Domeignoz-Horta, L.A., Philippot, L., Peyrard, C., Bru, D., Breuil, M.C., Bizouard, F., et al. (2018) Peaks of in situ N₂O emissions are influenced by N₂O-producing and reducing microbial communities across arable soils. *Glob Chang Biol* **24**: 360–370.
- Domeignoz-Horta, L.A., Putz, M., Spor, A., Bru, D., Breuil, M.-C., Hallin, S., and Philippot, L. (2016) Non-denitrifying nitrous oxide-reducing bacteria - An effective N₂O sink in soil. *Soil Biol Biochem* **103**: 376–379.
- Dong, L.F., Smith, C.J., Papaspyrou, S., Stott, A., Osborn, A.M., and Nedwell, D.B. (2009) Changes in benthic denitrification, nitrate ammonification, and anammox process rates and nitrate and nitrite reductase gene abundances along an estuarine nutrient gradient (the colne estuary, United Kingdom). *Appl Environ Microbiol* **75**: 3171–3179.
- Dong, W., Sun, Y., and Luo, J. (2019) Fine mapping of key soil nutrient content using high resolution remote sensing image to support precision agriculture in Northwest China. *2019 8th Int Conf Agro-Geoinformatics, Agro-Geoinformatics 2019*.
- Doran, J.W. (1980) Soil microbial and biochemical changes associated with reduced tillage. *Soil Sci Soc Am J* **44**: 765–771.
- Drenovsky, R.E., Vo, D., Graham, K.J., and Scow, K.M. (2004) Soil water content and organic carbon availability are major determinants of soil microbial community composition. *Microb Ecol* **48**: 424–430.
- Dumbrell, A.J., Nelson, M., Helgason, T., Dytham, C., and Fitter, A.H. (2010) Relative roles of niche and neutral processes in structuring a soil microbial community. *ISME J* **4**: 337–

345.

Eilrich, G.L. and Hageman, R.H. (1973) Nitrate reductase activity and its relationship to accumulation of vegetative and grain nitrogen in wheat (*Triticum aestivum* L.). *Crop Sci* **13**: 59–66.

Eisenhauer, N., Antunes, P.M., Bennett, A.E., Birkhofer, K., Bissett, A., Bowker, M.A., et al. (2017) Priorities for research in soil ecology. *Pedobiologia (Jena)* **63**: 1–7.

Emilia Hannula, S., Kielak, A.M., Steinauer, K., Huberty, M., Jongen, R., De Long, J.R., et al. (2019) Time after time: Temporal variation in the effects of grass and forb species on soil bacterial and fungal communities. *MBio* **10**:

Enwall, K., Throbäck, I.N., Stenberg, M., Söderström, M., and Hallin, S. (2010) Soil resources influence spatial patterns of denitrifying communities at scales compatible with land management. *Appl Environ Microbiol* **76**: 2243–2250.

F. W. Preston (1980) Noncanonical distributions of commonness and rarity. *Ecology* **61**: 88–97.

FAO (2023) FAO Cereal Supply and Demand Brief February 2023.

FAO (2022) FAOSTAT statistical database.

FAO (2015) What is Conservation Agriculture?

FAO (2018) World Food and Agriculture - Statistical Pocketbook 2018, Rome, Italy: FAO.

Felske, A. and Akkermans, A.D.L. (1998) Prominent occurrence of ribosomes from an uncultured bacterium of the Verrucomicrobiales cluster in grassland soils. *Lett Appl Microbiol* **26**: 219–223.

Fenchel, T. and Finlay, B.J. (2004) The Ubiquity of Small Species: Patterns of Local and

Global Diversity. *Bioscience* **54**: 777.

Fierer, N. (2017) Embracing the unknown: Disentangling the complexities of the soil microbiome. *Nat Rev Microbiol* **15**: 579–590.

Fierer, N. and Jackson, R.B. (2006) The diversity and biogeography of soil bacterial communities. *Proc Natl Acad Sci USA* **103**: 626–631.

Fischer, H.-M. (1994) Genetic regulation of nitrogen fixation in rhizobia. *Microbiol Rev* **58**: 352–386.

Fish, J.A., Chai, B., Wang, Q., Sun, Y., Brown, C.T., Tiedje, J.M., and Cole, J.R. (2013) FunGene: The functional gene pipeline and repository. *Front Microbiol* **4**: 1–14.

Flanagan, D.A., Gregory, L.G., Carter, J.P., Karakas-Sen, A., Richardson, D.J., and Spiro, S. (1999) Detection of genes for periplasmic nitrate reductase in nitrate respiring bacteria and in community DNA. *FEMS Microbiol Lett* **183**: 275–279.

Foucher, A., Salvador-Blanes, S., Evrard, O., Simonneau, A., Chapron, E., Courp, T., et al. (2014) Increase in soil erosion after agricultural intensification: Evidence from a lowland basin in France. *Anthropocene* **7**: 30–41.

Fowler, D., Coyle, M., Skiba, U., Sutton, M.A., Cape, J.N., Reis, S., et al. (2013) The global nitrogen cycle in the twenty-first century. *Philos Trans R Soc B Biol Sci* **368**:

Fowler, D., Steadman, C.E., Stevenson, D., Coyle, M., Rees, R.M., Skiba, U.M., et al. (2015) Effects of global change during the 21st century on the nitrogen cycle. *Atmos Chem Phys* **15**: 13849–13893.

Francioli, D., Schulz, E., Lentendu, G., Wubet, T., Buscot, F., and Reitz, T. (2016) Mineral vs. organic amendments: Microbial community structure, activity and abundance of agriculturally relevant microbes are driven by long-term fertilization strategies. *Front*

Microbiol **7**: 1–16.

Franzluebbers, A.J. (1999) Microbial activity in response to water-filled pore space of variably eroded southern Piedmont soils. *Appl Soil Ecol* **11**: 91–101.

Frostegård, Å., Vick, S.H.W., Lim, N.Y.N., Bakken, L.R., and Shapleigh, J.P. (2022) Linking meta-omics to the kinetics of denitrification intermediates reveals pH-dependent causes of N₂O emissions and nitrite accumulation in soil. *ISME J* **16**: 26–37.

Galimand, M., Gamper, M., Zimmermann, A., and Haas, D. (1991) Positive FNR-like control of anaerobic arginine degradation and nitrate respiration in *Pseudomonas aeruginosa*. *J Bacteriol* **173**: 1598–1606.

Galloway, J.N., Aber, J.D., Erisman, J.W., Seitzinger, S.P., Howarth, R.W., Cowling, E.B., and Cosby, B.J. (2003) The nitrogen cascade. *Bioscience* **53**: 341–356.

Galloway, J.N., Dentener, F.J., Capone, D.G., Boyer, E.W., Howarth, R.W., Seitzinger, S.P., et al. (2004) Nitrogen cycles: Past, present, and future. *Biogeochemistry* **70**: 153–226.

Gamble, T.N., Betlach, M.R., and Tiedje, J.M. (1977) Numerically Dominant Denitrifying Bacteria from World Soils. *Appl Environ Microbiol* **33**: 926–939.

Gao, S., Xu, P., Zhou, F., Yang, H., Zheng, C., Cao, W., et al. (2016) Quantifying nitrogen leaching response to fertilizer additions in China's cropland. *Environ Pollut* **211**: 241–251.

García-Robledo, E., Corzo, A., and Pappaspyrou, S. (2014) A fast and direct spectrophotometric method for the sequential determination of nitrate and nitrite at low concentrations in small volumes. *Mar Chem* **162**: 30–36.

Gates, A.J., Luque-Almagro, V.M., Goddard, A.D., Ferguson, S.J., Roldán, M.D., and Richardson, D.J. (2011) A composite biochemical system for bacterial nitrate and nitrite

assimilation as exemplified by *Paracoccus denitrificans*. *Biochem J* **435**: 743–753.

Gerber, J.S., Carlson, K.M., Makowski, D., Mueller, N.D., Garcia de Cortazar-Atauri, I., Havlík, P., et al. (2016) Spatially explicit estimates of N₂O emissions from croplands suggest climate mitigation opportunities from improved fertilizer management. *Glob Chang Biol* **22**: 3383–3394.

Giustarini, D., Rossi, R., Milzani, A., and Dalle-Donne, I. (2008) Nitrite and Nitrate Measurement by Griess Reagent in Human Plasma: Evaluation of Interferences and Standardization. *Methods Enzymol*.

Glockner, A.B., Jüngst, A., and Zumft, W.G. (1993) Copper-containing nitrite reductase from *Pseudomonas aureofaciens* is functional in a mutationally cytochrome cd1-free background (NirS-) of *Pseudomonas stutzeri*. *Arch Microbiol* **160**: 18–26.

Glockner, A.B. and Zumft, W.G. (1996) Sequence analysis of an internal 9.72-kb segment from the 30-kb denitrification gene cluster of *Pseudomonas stutzeri*. *Biochim Biophys Acta (BBA)-Bioenergetics* **1277**: 6–12.

González, P.J., Correia, C., Moura, I., Brondino, C.D., and Moura, J.J.G. (2006) Bacterial nitrate reductases: Molecular and biological aspects of nitrate reduction. *J Inorg Biochem* **100**: 1015–1023.

Good, A.G. and Beatty, P.H. (2011) Fertilizing nature: A tragedy of excess in the commons. *PLoS Biol* **9**: e1001124.

Graf, D.R.H., Jones, C.M., and Hallin, S. (2014) Intergenomic comparisons highlight modularity of the denitrification pathway and underpin the importance of community structure for N₂O emissions. *PLoS One* **9**: e114118.

Green, J.L., Holmes, A.J., Westoby, M., Oliver, I., Briscoe, D., Dangerfield, M., et al. (2004)

- Spatial scaling of microbial eukaryote diversity. *Nature* **432**: 747–750.
- Gregory, L.G., Karakas-Sen, A., Richardson, D.J., and Spiro, S. (2000) Detection of genes for membrane-bound nitrate reductase in nitrate-respiring bacteria and in community DNA. *FEMS Microbiol Lett* **183**: 275–279.
- Griffiths, R.I., Thomson, B.C., James, P., Bell, T., Bailey, M., and Whiteley, A.S. (2011) The bacterial biogeography of British soils. *Environ Microbiol* **13**: 1642–1654.
- Groffman, P.M., Altabet, M.A., Böhlke, J.K., Butterbach-Bahl, K., David, M.B., Firestone, M.K., et al. (2006) Methods for measuring denitrification: Diverse approaches to a difficult problem. *Ecol Appl* **16**: 2091–2122.
- Gross, P.J. and Bremner, J.M. (1992) Acetone problem in use of the acetylene blockage method for assessment of denitrifying activity in soil. *Commun Soil Sci Plant Anal* **23**: 1345–1358.
- Grove, J., Tanapongpipat, S., Thomas, G., Griffiths, L., Crooke, H., and Cole, J.A. (1996) Escherichia coli K-12 genes essential for the synthesis of c-type cytochromes and a third nitrate reductase located in the periplasm. *Mol Microbiol* **19**: 467–481.
- Gruber, N. and Galloway, J.N. (2008) An Earth-system perspective of the global nitrogen cycle. *Nature* **451**: 293–296.
- Guo, X., Zhang, Xiaoning, Qin, Y., Liu, Y.X., Zhang, J., Zhang, N., et al. (2020) Host-Associated Quantitative Abundance Profiling Reveals the Microbial Load Variation of Root Microbiome. *Plant Commun* **1**: 1–17.
- Hachiya, T. and Sakakibara, H. (2016) Interactions between nitrate and ammonium in their uptake, allocation, assimilation, and signaling in plants. *J Exp Bot* **68**: 2501–2512.
- Hallin, P.F. and Ussery, D.W. (2004) CBS Genome Atlas database: A dynamic storage for

- bioinformatic results and sequence data. *Bioinformatics* **20**: 3682–3686.
- Hallin, S., Jones, C.M., Schloter, M., and Philippot, L. (2009) Relationship between N-cycling communities and ecosystem functioning in a 50-year-old fertilization experiment. *ISME J* **3**: 597–605.
- Hallin, S., Philippot, L., Löffler, F.E., Sanford, R.A., and Jones, C.M. (2018) Genomics and Ecology of Novel N₂O-Reducing Microorganisms. *Trends Microbiol* **26**: 43–55.
- Hardy, R.W., Holsten, R., Jackson, E., and Burns, R. (1968) The acetylene-ethylene assay for N₂ fixation: laboratory and field evaluation. *Plant Physiol* **43**: 1185–1207.
- Hartmann, M., Frey, B., Mayer, J., Mader, P., and Widmer, F. (2015) Distinct soil microbial diversity under long-term organic and conventional farming. *ISME J* **9**: 1177–1194.
- Hashimoto, T., Koga, M., and Masaoka, Y. (2009) Advantages of a diluted nutrient broth medium for isolating N₂-producing denitrifying bacteria of α -Proteobacteria in surface and subsurface upland soils. *Soil Sci Plant Nutr* **55**: 647–659.
- Hassan, J., Bergaust, L.L., Wheat, I.D., and Bakken, L.R. (2014) Low Probability of Initiating nirS Transcription Explains Observed Gas Kinetics and Growth of Bacteria Switching from Aerobic Respiration to Denitrification. *PLoS Comput Biol.*
- Hauck, R.D. and Melsted, S.W. (1956) Some aspects of the problem of evaluating denitrification in soils. *Soil Sci Soc Am J* **20**: 361–364.
- Hauck, R.D., Melsted, S.W., and Yankwich, P.E. (1958) Use of N-isotope distribution in nitrogen gas in the study of denitrification. *Soil Sci* **86**: 287.
- Hendriks, J., Oubrie, A., Castresana, J., Urbani, A., Gemeinhardt, S., and Saraste, M. (2000) Nitric oxide reductases in bacteria. *Biochim Biophys Acta - Bioenerg* **1459**: 266–273.

- Henry, S., Baudoin, E., López-Gutiérrez, J.C., Martin-Laurent, F., Brauman, A., and Philippot, L. (2004) Quantification of denitrifying bacteria in soils by nirK gene targeted real-time PCR. *J Microbiol Methods* **59**: 327–335.
- Henry, S., Bru, D., Stres, B., Hallet, S., and Philippot, L. (2006) Quantitative detection of the nosZ gene, encoding nitrous oxide reductase, and comparison of the abundances of 16S rRNA, narG, nirK, and nosZ genes in soils. *Appl Environ Microbiol* **72**: 5181–5189.
- Hernández-del Amo, E. and Bañeras, L. (2021) Effects of high nitrate input in the denitrification-DNRA activities in the sediment of a constructed wetland under varying C/N ratios. *Ecol Eng* **159**:
- Heylen, K., Vanparys, B., Wittebolle, L., Verstraete, W., Boon, N., Vos, P. De, and De Vos, P. (2006) Cultivation of denitrifying bacteria: Optimization of isolation conditions and diversity study. *Appl Environ Microbiol* **72**: 2637–2643.
- Hillebrand, H., Watermann, F., Karez, R., and Berninger, U.G. (2001) Differences in species richness patterns between unicellular and multicellular organisms. *Oecologia*.
- Hoeren, F.U., Berks, B.C., Ferguson, S.J., and McCarthy, J.E.G. (1993) Sequence and expression of the gene encoding the respiratory nitrous-oxide reductase from *Paracoccus denitrificans* New and conserved structural and regulatory motifs. *Eur J Biochem* **218**: 49–57.
- Hoffman, B.M., Lukoyanov, D., Yang, Z.Y., Dean, D.R., and Seefeldt, L.C. (2014) Mechanism of nitrogen fixation by nitrogenase: The next stage. *Chem Rev* **114**: 4041–4062.
- Holloway, P., McCormick, W., Watson, R.J., and Chan, Y.K. (1996) Identification and analysis of the dissimilatory nitrous oxide reduction genes, nosRZDFY, of *Rhizobium meliloti*. *J Bacteriol* **178**: 1505–1514.

- Van Holm, W., Ghesquière, J., Boon, N., Verspecht, T., Bernaerts, K., Zayed, N., et al. (2021) A Viability Quantitative PCR Dilemma: Are Longer Amplicons Better? *Appl Environ Microbiol* **87**: e0265320.
- Van Horn, D.J., Van Horn, M.L., Barrett, J.E., Gooseff, M.N., Altrichter, A.E., Geyer, K.M., et al. (2013) Factors controlling soil microbial biomass and bacterial diversity and community composition in a cold desert ecosystem: Role of geographic scale. *PLoS One* **8**: e66103.
- Horner-Devine, M.C., Lage, M., Hughes, J.B., and Bohannan, B.J.M. (2004) A taxa-area relationship for bacteria. *Nature* **432**: 750–753.
- Hou, S., Ai, C., Zhou, W., Liang, G., and He, P. (2018) Structure and assembly cues for rhizospheric nirK- and nirS-type denitrifier communities in long-term fertilized soils. *Soil Biol Biochem* **119**: 32–40.
- Houlton, B.Z. and Bai, E. (2009) Imprint of denitrifying bacteria on the global terrestrial biosphere. *Proc Natl Acad Sci U S A* **106**: 21713–21716.
- IPCC (2022) Climate Change 2022: Impacts, Adaptation, and Vulnerability. Contribution of Working Group II to the Sixth Assessment Report of the Intergovernmental Panel on Climate Change, Cambridge.
- IPCC (2019) IPCC Special Report on climate change, desertification, land degradation, sustainable land management, food security, and greenhouse gas fluxes in terrestrial ecosystems Summary for Policymakers.
- IPCC (2021) Summary for Policymakers. In: Climate Change 2021: The Physical Science Basis. Contribution of Working Group I to the Sixth Assessment Report of the Intergovernmental Panel on Climate Change, Cambridge.

- Janssen, P.H., Yates, P.S., Grinton, B.E., Taylor, P.M., and Sait, M. (2002) Improved Culturability of Soil Bacteria and Isolation in Pure Culture of Novel Members of the Divisions. *Appl Environ Microbiol* **68**: 2391–2396.
- Ji, B., Yang, K., Zhu, L., Jiang, Y., Wang, H., Zhou, J., and Zhang, H. (2015) Aerobic denitrification: A review of important advances of the last 30 years. *Biotechnol Bioprocess Eng* **20**: 643–651.
- Jiang, S.Q., Yu, Y.N., Gao, R.W., Wang, H., Zhang, J., Li, R., et al. (2019) High-throughput absolute quantification sequencing reveals the effect of different fertilizer applications on bacterial community in a tomato cultivated coastal saline soil. *Sci Total Environ* **687**: 601–609.
- Jiang, X., Liu, W., Yao, L., Liu, G., and Yang, Y. (2020) The roles of environmental variation and spatial distance in explaining diversity and biogeography of soil denitrifying communities in remote Tibetan wetlands. *FEMS Microbiol Ecol* **96**: 1–11.
- Johnson, C.B., Whittington, W.J., and Blackwood, G.C. (1976) Nitrate reductase as a possible predictive test of crop yield. *Nature* **262**: 133–134.
- Jones, C.M., Graf, D.R.H., Bru, D., Philippot, L., and Hallin, S. (2013) The unaccounted yet abundant nitrous oxide-reducing microbial community: a potential nitrous oxide sink. *ISME J* **7**: 417–426.
- Jones, C.M. and Hallin, S. (2010) Ecological and evolutionary factors underlying global and local assembly of denitrifier communities. *ISME J* **4**: 633–641.
- Jones, C.M., Spor, A., Brennan, F.P., Breuil, M.-C., Bru, D., Lemanceau, P., et al. (2014) Recently identified microbial guild mediates soil N₂O sink capacity. *Nat Clim Chang* **4**: 801–805.

- Joye, S.B. and Paerl, H.W. (1994) Nitrogen cycling in microbial mats: rates and patterns of denitrification and nitrogen fixation. *Mar Biol* **119**: 285–295.
- Jüngst, A., Wakabayashi, S., Matsubara, H., and Zumft, W.G. (1991) The nirSTBM region coding for cytochrome cd1-dependent nitrite respiration of *Pseudomonas stutzeri* consists of a cluster of mono-, di-, and tetraheme proteins. *FEBS Lett* **279**: 205–209.
- Jüngst, A. and Zumft, W.G. (1992) Interdependence of respiratory NO reduction and nitrite reduction revealed by mutagenesis of nirQ, a novel gene in the denitrification gene cluster of *Pseudomonas stutzeri*. *FEBS Lett* **314**: 308–314.
- Kaden, U.S., Fuchs, E., Hecht, C., Hein, T., Rupp, H., Scholz, M., and Schulz-Zunkel, C. (2020) Advancement of the Acetylene Inhibition Technique Using Time Series Analysis on Air-Dried Floodplain Soils to Quantify Denitrification Potential. *Geosciences* **10**:
- Kaeberlein, T., Lewis, K., and Epstein, S.S. (2002) Isolating “Uncultivable” Microorganisms in Pure Culture in a Simulated Natural Environment. *Science (80-)* **296**: 1127–1129.
- Kant, R., van Pesse, M.W.J., Palva, A., Lucas, S., Lapidus, A., del Rio, T.G., et al. (2011) Genome sequence of *Chthoniobacter flavus* Ellin428, an aerobic heterotrophic soil bacterium. *J Bacteriol* **193**: 2902–2903.
- Kato, S., Yamagishi, A., Daimon, S., Kawasaki, K., Tamaki, H., Kitagawa, W., et al. (2018) Isolation of previously uncultured slowgrowing bacteria by using a simple modification in the preparation of agar media. *Appl Environ Microbiol* **84**:
- Kawasaki, S., Arai, H., Kodama, T., and Igarashi, Y. (1997) Gene cluster for dissimilatory nitrite reductase (nir) from *Pseudomonas aeruginosa*: sequencing and identification of a locus for heme d1 biosynthesis. *J Bacteriol* **179**: 235–242.
- Keel, S.G., Anken, T., Büchi, L., Chervet, A., Fliessbach, A., Flisch, R., et al. (2019) Loss of

- soil organic carbon in Swiss long-term agricultural experiments over a wide range of management practices. *Agric Ecosyst Environ* **286**:
- van Kessel, C., Venterea, R., Six, J., Adviento-Borbe, M.A., Linnquist, B., and van Groenigen, K.J. (2013) Climate, duration, and N placement determine N₂O emissions in reduced tillage systems: A meta-analysis. *Glob Chang Biol* **19**: 33–44.
- Van Kessel, M.A.H.J., Speth, D.R., Albertsen, M., Nielsen, P.H., Op Den Camp, H.J.M., Kartal, B., et al. (2015) Complete nitrification by a single microorganism. *Nature* **528**: 555–559.
- Kim, D.G., Hernandez-Ramirez, G., and Giltrap, D.L. (2013) Linear and nonlinear dependency of direct nitrous oxide emissions on fertilizer nitrogen input: A meta-analysis. *Agric Ecosyst Environ* **168**: 53–65.
- Kim, J.M., Roh, A.S., Choi, S.C., Kim, E.J., Choi, M.T., Ahn, B.K., et al. (2016) Soil pH and electrical conductivity are key edaphic factors shaping bacterial communities of greenhouse soils in Korea. *J Microbiol*.
- King, D. and Nedwell, D.B. (1985) The influence of nitrate concentration upon the end-products of nitrate dissimilation by bacteria in anaerobic salt marsh sediment. *FEMS Microbiol Ecol* **1**: 23–28.
- Kloos, K., Hüsgen, U.M., and Bothe, H. (1998) DNA-probing for genes coding for denitrification, N₂-fixation and nitrification in bacteria isolated from different soils. *Z Naturforsch C* **53**: 69–81.
- Kloos, K., Mergel, A., Rösch, C., and Bothe, H. (2001) Denitrification within the genus *Azospirillum* and other associative bacteria. *Aust J Plant Physiol* **28**: 991–998.
- Klünemann, T., Henke, S., and Blankenfeldt, W. (2020) The crystal structure of the heme d(1)

- biosynthesis-associated small c-type cytochrome NirC reveals mixed oligomeric states in crystallo. *Acta Crystallogr Sect D, Struct Biol* **76**: 375–384.
- Knight, R., Vrbanac, A., Taylor, B.C., Aksenov, A., Callewaert, C., Debelius, J., et al. (2018) Best practices for analysing microbiomes. *Nat Rev Microbiol* **16**: 410–422.
- Kopittke, P.M., Menzies, N.W., Wang, P., McKenna, B.A., and Lombi, E. (2019) Soil and the intensification of agriculture for global food security. *Environ Int* **132**: 105078.
- Kou, Y., Liu, Y., Li, J., Li, C., Tu, B., Yao, M., and Li, X. (2021) Patterns and Drivers of nirK-Type and nirS-Type Denitrifier Community Assembly along an Elevation Gradient. *mSystems* **6**:
- Kraft, B., Strous, M., and Tegetmeyer, H.E. (2011) Microbial nitrate respiration - Genes, enzymes and environmental distribution. *J Biotechnol* **155**: 104–117.
- Krapp, A. (2015) Plant nitrogen assimilation and its regulation: A complex puzzle with missing pieces. *Curr Opin Plant Biol* **25**: 115–122.
- Krauss, M., Krause, H.M., Spangler, S., Kandeler, E., Behrens, S., Kappler, A., et al. (2017) Tillage system affects fertilizer-induced nitrous oxide emissions. *Biol Fertil Soils* **53**: 49–59.
- Krauss, M., Ruser, R., Müller, T., Hansen, S., Mäder, P., and Gattinger, A. (2017) Impact of reduced tillage on greenhouse gas emissions and soil carbon stocks in an organic grass-clover ley - winter wheat cropping sequence. *Agric Ecosyst Environ* **239**: 324–333.
- Kroeze, C., Mosier, A.R., and Bouwman, L. (1999) Closing the global N₂O budget: A retrospective analysis 1500-1994. *Global Biogeochem Cycles* **13**: 1–8.
- Kuntz, M., Berner, A., Gattinger, A., Scholberg, J.M., Mäder, P., and Pfiffner, L. (2013) Influence of reduced tillage on earthworm and microbial communities under organic

- arable farming. *Pedobiologia (Jena)* **56**: 251–260.
- Kuypers, M.M.M., Marchant, H.K., and Kartal, B. (2018) The microbial nitrogen-cycling network. *Nat Rev Microbiol* **16**: 263–276.
- Kuznetsova, A., Brockhoff, P.B., and Christensen, R.H.B. (2017) lmerTest: tests in linear mixed effects models. *J Stat Softw* **82**: 1–27.
- Kwiatkowski, A. V, Laratta, W.P., Toffanin, A., and Shapleigh, J.P. (1997) Analysis of the role of the nnrR gene product in the response of *Rhodobacter sphaeroides* 2.4. 1 to exogenous nitric oxide. *J Bacteriol* **179**: 5618–5620.
- La, H.J., Im, W.T., Ten, L.N., Kang, M.S., Shin, D.Y., and Lee, S.T. (2005) *Paracoccus koreensis* sp. nov., isolated from anaerobic granules in an upflow anaerobic sludge blanket (UASB) reactor. *Int J Syst Evol Microbiol* **55**: 1657–1660.
- Lane, D.J., Pace, B., Olsen, G.J., Stahl, D.A., Sogin, M.L., and Pace, N.R. (1985) Rapid determination of 16S ribosomal RNA sequences for phylogenetic analyses. *Proc Natl Acad Sci U S A*.
- Lawton, J.H. (1999) Are There General Laws in Ecology? *Oikos*.
- Lee, H.S., Abdelal, A.H., Clark, M.A., and Ingraham, J.L. (1991) Molecular characterization of nosA, a *Pseudomonas stutzeri* gene encoding an outer membrane protein required to make copper-containing N₂O reductase. *J Bacteriol* **173**: 5406–5413.
- Li, G., Yan, D., Xia, P., Cao, H., Lin, T., and Yi, Y. (2022) Community structure and assembly of denitrifying bacteria in epiphytic biofilms in a freshwater lake ecosystem. *J Oceanol Limnol* **40**: 1039–1050.
- Li, J., Wen, Y., Li, X., Li, Y., Yang, X., Lin, Z., et al. (2018) Soil labile organic carbon fractions and soil organic carbon stocks as affected by long-term organic and mineral

- fertilization regimes in the North China Plain. *Soil Tillage Res* **175**: 281–290.
- Liu, B., Zhang, X., Bakken, L.R., Snipen, L., and Frostegård, Å. (2019) Rapid succession of actively transcribing denitrifier populations in agricultural soil during an anoxic spell. *Front Microbiol* **9**..
- Liu, S., Lin, F., Wu, S., Ji, C., Sun, Y., Jin, Y., et al. (2017) A meta-analysis of fertilizer-induced soil NO and combined NO+N₂O emissions. *Glob Chang Biol* **23**: 2520–2532.
- Liu, W., Jiang, L., Yang, S., Wang, Z., Tian, R., Peng, Z., et al. (2020) Critical transition of soil bacterial diversity and composition triggered by nitrogen enrichment. *Ecology* **101**..
- Liu, X. and DeMoss, J.A. (1997) Characterization of NarJ, a system-specific chaperone required for nitrate reductase biogenesis in Escherichia coli. *J Biol Chem* **272**: 24266–24271.
- Liu, Y. and Sheng, Y. (2021) Iron controls the assembly processes of heterotrophic denitrifying microbial communities. *Environ Chem Lett* **19**: 1865–1872.
- Locey, K.J., Muscarella, M.E., Larsen, M.L., Bray, S.R., Jones, S.E., and Lennon, J.T. (2020) Dormancy dampens the microbial distance-decay relationship. *Philos Trans R Soc B Biol Sci* **375**..
- López-Gutiérrez, J.C., Henry, S., Hallet, S., Martin-Laurent, F., Catroux, G., and Philippot, L. (2004) Quantification of a novel group of nitrate-reducing bacteria in the environment by real-time PCR. *J Microbiol Methods* **57**: 399–407.
- Lord, E.I., Anthony, S.G., and Goodlass, G. (2002) Agricultural nitrogen balance and water quality in the UK. *Soil Use Manag* **18**: 363–369.
- Lozupone, C. and Knight, R. (2005) UniFrac: A new phylogenetic method for comparing microbial communities. *Appl Environ Microbiol* **71**: 8228–8235.

- Lu, H., Chandran, K., and Stensel, D. (2014) Microbial ecology of denitrification in biological wastewater treatment. *Water Res* **64**: 237–254.
- Luo, Z., Wang, E., and Sun, O.J. (2010) Can no-tillage stimulate carbon sequestration in agricultural soils? A meta-analysis of paired experiments. *Agric Ecosyst Environ* **139**: 224–231.
- Luque-Almagro, V.M., Gates, A.J., Moreno-Vivián, C., Ferguson, S.J., Richardson, D.J., and Roldán, M.D. (2011) Bacterial nitrate assimilation: gene distribution and regulation. *Biochem Soc Trans* **39**: 1838–1843.
- Lycus, P., Bøthun, K.L., Bergaust, L.L., Shapleigh, J.P., Bakken, L.R., and Frostegård, Å. (2017) Phenotypic and genotypic richness of denitrifiers revealed by a novel isolation strategy. *ISME J* **11**: 2219–2232.
- Ma, Y., Zilles, J.L., and Kent, A.D. (2019) An evaluation of primers for detecting denitrifiers via their functional genes. *Environ Microbiol* **21**: 1196–1210.
- Madeira, F., Pearce, M., Tivey, A.R.N., Basutkar, P., Lee, J., Edbali, O., et al. (2022) Search and sequence analysis tools services from EMBL-EBI in 2022. *Nucleic Acids Res* **50**: 276–279.
- Marschner, P. (2007) Plant-microbe interactions in the rhizosphere and nutrient cycling. In *Nutrient cycling in terrestrial ecosystems*. Marschner, P and Rengel, Z. (eds). Berlin, Heidelberg: Springer.
- Martiny, J.B.H., Eisen, J.A., Penn, K., Allison, S.D., and Horner-Devine, M.C. (2011) Drivers of bacterial β -diversity depend on spatial scale. *Proc Natl Acad Sci* **108**: 7850–7854.
- Masuda, Y., Matsumoto, T., Isobe, K., and Senoo, K. (2019) Denitrification in paddy soil as a cooperative process of different nitrogen oxide reducers, revealed by

- metatranscriptomic analysis of denitrification-induced soil microcosm. *Soil Sci Plant Nutr* **65**: 342–345.
- Mathew, R.P., Feng, Y., Githinji, L., Ankumah, R., and Balkcom, K.S. (2012) Impact of no-tillage and conventional tillage systems on soil microbial communities. *Appl Environ Soil Sci*.
- McBratney, A., Whelan, B., Ancev, T., and Bouma, J. (2005) Future directions of precision agriculture. *Precis Agric* **6**: 7–23.
- McDonald, D., Price, M.N., Goodrich, J., Nawrocki, E.P., DeSantis, T.Z., Probst, A., et al. (2012) An improved Greengenes taxonomy with explicit ranks for ecological and evolutionary analyses of bacteria and archaea. *ISME J* **6**: 610–618.
- McGill, B.J. (2003) A test of the unified neutral theory of biodiversity. *Nature*.
- McInerney, P., Adams, P., and Hadi, M.Z. (2014) Error Rate Comparison during Polymerase Chain Reaction by DNA Polymerase. *Mol Biol Int* **2014**: 287430.
- McLaren, M.R. and Callahan, B.J. (2021) Silva 138.1 prokaryotic SSU taxonomic training data formatted for DADA2.
- McMurdie, P.J. and Holmes, S. (2013) Phyloseq: An R Package for Reproducible Interactive Analysis and Graphics of Microbiome Census Data. *PLoS One* **8**..
- Melero, S., Pérez-de-Mora, A., Murillo, J.M., Buegger, F., Kleinedam, K., Kublik, S., et al. (2011) Denitrification in a vertisol under long-term tillage and no-tillage management in dryland agricultural systems: Key genes and potential rates. *Appl Soil Ecol* **47**: 221–225.
- Mergel, A., Schmitz, O., Mallmann, T., and Bothe, H. (2001) Relative abundance of denitrifying and dinitrogen-fixing bacteria in layers of a forest soil. *FEMS Microbiol Ecol* **36**: 33–42.

- Met Office (2019) MIDAS Open: UK hourly weather observation data, v201901. *Cent Environ Data Anal* 01 March 2019.
- Meyer, K.M., Memiaghe, H., Korte, L., Kenfack, D., Alonso, A., and Bohannan, B.J.M. (2018) Why do microbes exhibit weak biogeographic patterns? *ISME J* **12**: 1404–1413.
- Michotey, V.D., Méjean, V., and Bonin, P.C. (2000) Comparison of methods for quantification of cytochrome cd 1 -denitrifying bacteria in environmental marine samples. *Appl Environ Microbiol* **66**: 1564–1571.
- Milazzo, G., Caroli, S., and Braun, R.D. (1978) Tables of Standard Electrode Potentials. *J Electrochem Soc* **125**: 261C--261C.
- Miller, A.J. and Cramer, M.D. (2005) Root nitrogen acquisition and assimilation. *Plant Soil* **274**: 1–36.
- Miller, M.N., Zebarth, B.J., Dandie, C.E., Burton, D.L., Goyer, C., and Trevors, J.T. (2008) Crop residue influence on denitrification, N₂O emissions and denitrifier community abundance in soil. *Soil Biol Biochem* **40**: 2553–2562.
- Miranda, K.M., Espey, M.G., and Wink, D.A. (2001) A rapid, simple spectrophotometric method for simultaneous detection of nitrate and nitrite. *Nitric Oxide - Biol Chem* **5**: 62–71.
- Moreno-Vivián, C., Cabello, P., Martínez-Luque, M., Blasco, R., and Castillo, F. (1999) Prokaryotic Nitrate Reduction: Molecular Properties and Functional Distinction among Bacterial Nitrate Reductases. *J Bacteriol* **181**: 6573–6584.
- Mori, A.S., Isbell, F., and Seidl, R. (2018) β -Diversity, Community Assembly, and Ecosystem Functioning. *Trends Ecol Evol* **33**: 549–564.
- Mosier, A.R. (1998) Soil processes and global change. *Biol Fertil Soils* **27**: 221–229.

- Moulton-Brown, C.E., Feng, T., Kumar, S.S., Xu, L., Dytham, C., Helgason, T., et al. (2022) Long-term fertilization and tillage regimes have limited effects on structuring bacterial and denitrifier communities in a sandy loam UK soil. *Environ Microbiol* **24**: 298–308.
- Muhammed, S.E., Coleman, K., Wu, L., Bell, V.A., Davies, J.A.C., Quinton, J.N., et al. (2018) Impact of two centuries of intensive agriculture on soil carbon, nitrogen and phosphorus cycling in the UK. *Sci Total Environ* **634**: 1486–1504.
- Murugan, R., Koch, H.J., and Joergensen, R.G. (2014) Long-term influence of different tillage intensities on soil microbial biomass, residues and community structure at different depths. *Biol Fertil Soils* **50**: 487–498.
- Musafiri, C.M., Macharia, J.M., Kiboi, M.N., Ng’etich, O.K., Shisanya, C.A., Okeyo, J.M., et al. (2021) Comparison between observed and DeNitrification-DeComposition model-based nitrous oxide fluxes and maize yields under selected soil fertility management technologies in Kenya. *Plant Soil* **463**: 395–413.
- Nadeau, S.A., Roco, C.A., Debenport, S.J., Anderson, T.R., Hofmeister, K.L., Walter, M.T., and Shapleigh, J.P. (2019) Metagenomic analysis reveals distinct patterns of denitrification gene abundance across soil moisture, nitrate gradients. *Environ Microbiol* **21**: 1255–1266.
- Nekola, J.C. and White, P.S. (1999) The Distance Decay of Similarity in Biogeography and Ecology The distance decay of similarity in biogeography and ecology. *J Biogeogr* **26**: 867–878.
- Nemergut, D.R., Schmidt, S.K., Fukami, T., O’Neill, S.P., Bilinski, T.M., Stanish, L.F., et al. (2013) Patterns and processes of microbial community assembly. *Microbiol Mol Biol Rev* **77**: 342–356.
- Neubauer, H., Pantel, I., and Gotz, F. (1999) Molecular characterization of the nitrite-reducing

system of *Staphylococcus carnosus*. *J Bacteriol* **181**: 1481–1488.

Nichols, D., Cahoon, N., Trakhtenberg, E.M., Pham, L., Mehta, A., Belanger, A., et al. (2010)

Use of ichip for high-throughput in situ cultivation of “uncultivable” microbial species.

Appl Environ Microbiol **76**: 2445–2450.

Nishiyama, M., Suzuki, J., Kukimoto, M., Ohnuki, T., Horinouchi, S., and Beppu, T. (1993)

Cloning and characterization of a nitrite reductase gene from *Alcaligenes faecalis* and

its expression in *Escherichia coli*. *J Gen Microbiol* **139**: 725–733.

Nohno, T., Noji, S., Taniguchi, S., and Saito, T. (1989) The narX and narL genes encoding

the nitrate-sensing regulators of *Escherichia coli* are homologous to a family of

prokaryotic two-component regulatory genes. *Nucleic Acids Res* **17**: 2947–2957.

Noji, S., Nohno, T., Saito, T., and Taniguchi, S. (1989) The narK gene product participates in

nitrate transport induced in *Escherichia coli* nitrate-respiring cells. *FEBS Lett* **252**: 139–

143.

O’Brien, S.L., Gibbons, S.M., Owens, S.M., Hampton-Marcell, J., Johnston, E.R., Jastrow,

J.D., et al. (2016) Spatial scale drives patterns in soil bacterial diversity. *Environ*

Microbiol **18**: 2039–2051.

Oksanen, J., Blanchet, F.G., Friendly, M., Kindt, R., Legendre, P., McGlenn, D., et al. (2013)

vegan: community ecology package.

Oksanen, J., Simpson, G.L., Blanchet, F.G., Kindt, R., Legendre, P., Minchin, P.R., et al.

(2022) vegan: Community Ecology Package.

Olsen, R.A. and Bakken, L.R. (1987) Viability of soil bacteria: Optimization of plate-counting

technique and comparison between total counts and plate counts within different size

groups. *Microb Ecol* **13**: 59–74.

- Olsen, S.R., Cole, C.V., Watanabe, F.S., and Dean, L.A. (1954) Estimation of available phosphorus in soils by extraction with sodium bicarbonate. *Washington United States Department of Agriculture* **939**:
- Orr, C.H., James, A., Leifert, C., Cooper, J.M., and Cummings, S.P. (2011) Diversity and activity of free-living nitrogen-fixing bacteria and total bacteria in organic and conventionally managed soils. *Applied Environmental Microbiology* **77**: 911–919.
- Oshiki, M., Satoh, H., and Okabe, S. (2016) Ecology and physiology of anaerobic ammonium oxidizing bacteria. *Environmental Microbiology* **18**: 2784–2796.
- Palmedo, G., Seither, P., Körner, H., Matthews, J.C., Burkhalter, R.S., Timkovich, R., and Zumft, W.G. (1995) Resolution of the nirD Locus for Heme d1, Synthesis of Cytochrome cd1, (Respiratory Nitrite Reductase) from *Pseudomonas Stutzeri*. *Eur J Biochem* **232**: 737–746.
- Paradis, E. and Schliep, K. (2019) Ape 5.0: An environment for modern phylogenetics and evolutionary analyses in R. *Bioinformatics* **35**: 526–528.
- Parfitt, R.L., Baisden, W.T., Schipper, L.A., and Mackay, A.D. (2008) Nitrogen inputs and outputs for New Zealand at national and regional scales: Past, present and future scenarios. *Journal of the Royal Society of New Zealand* **38**: 71–87.
- Peakman, T., Crouzet, J., Mayaux, J.F., Busby, S., Mohan, S., Harborne, N., et al. (1990) Nucleotide sequence, organisation and structural analysis of the products of genes in the nirB–cysG region of the *Escherichia coli* K-12 chromosome. *Eur J Biochem* **191**: 315–323.
- Petersen, D.G., Blazewicz, S.J., Firestone, M.K., Herman, D.J., Turetsky, M., and Waldrop, M.P. (2012) Abundance of microbial genes associated with nitrogen cycling as indices of biogeochemical process rates across a vegetation gradient in Alaska. *Environ*

Microbiol **14**: 993–1008.

Pettigrew, W.T. (2008) Potassium influences on yield and quality production for maize, wheat, soybean and cotton. *Physiol Plant* **133**: 670–681.

Philippot, L., Clays-Josserand, A., Lensi, R., Trinsoutreau, I., Normand, P., and Potier, P. (1997) Purification of the dissimilative nitrate reductase of *Pseudomonas fluorescens* and the cloning and sequencing of its corresponding genes. *Biochim Biophys Acta (BBA)-Gene Struct Expr* **1350**: 272–276.

Philippot, L., Čuhel, J., Saby, N.P.A., Chèneby, D., Chroňáková, A., Bru, D., et al. (2009) Mapping field-scale spatial patterns of size and activity of the denitrifier community. *Environ Microbiol* **11**: 1518–1526.

Philippot, L., Piutti, S., Martin-Laurent, F., Hallet, S., and Germon, J.C. (2002) Molecular analysis of the nitrate-reducing community from unplanted and maize-planted soils. *Appl Environ Microbiol* **68**: 6121–6128.

Piazza, G., Ercoli, L., Nuti, M., and Pellegrino, E. (2019) Interaction between conservation tillage and nitrogen fertilization shapes prokaryotic and fungal diversity at different soil depths: Evidence from a 23-year field experiment in the Mediterranean area. *Front Microbiol* **10**: 1–20.

Pielou, E.C. (1966) The measurement of diversity in different types of biological collections. *J Theor Biol* **13**: 131–144.

Potapov, V. and Ong, J.L. (2017) Examining Sources of Error in PCR by Single-Molecule Sequencing. *PLoS One* **12**: e0169774.

Powlson, D.S., Stirling, C.M., Jat, M.L., Gerard, B.G., Palm, C.A., Sanchez, P.A., and Cassman, K.G. (2014) Limited potential of no-till agriculture for climate change

mitigation. *Nat Clim Chang* **4**: 678–683.

Prather, M.J., Hsu, J., DeLuca, N.M., Jackman, C.H., Oman, L.D., Douglass, A.R., et al.

(2015) Measuring and modeling the lifetime of nitrous oxide including its variability. *J Geophys Res Atmos* **120**: 5693–5705.

Privett, B.J., Shin, J.H., and Schoenfisch, M.H. (2010) Electrochemical nitric oxide sensors for physiological measurements. *Chem Soc Rev* **39**: 1925–1935.

Qian, P., Schoenau, J.J., King, T., and Japp, M. (2011) Effect of repeated manure application on potassium, calcium and magnesium in soil and cereal crops in Saskatchewan. *Can J Soil Sci* **85**: 397–403.

R Core Team (2022) R: A Language and Environment for Statistical Computing.

Ramirez, K.S., Knight, C.G., De Hollander, M., Brearley, F.Q., Constantinides, B., Cotton, A., et al. (2018) Detecting macroecological patterns in bacterial communities across independent studies of global soils. *Nat Microbiol* **3**: 189–196.

Rappé, M.S., Connon, S.A., Vergin, K.L., and Giovannoni, S.J. (2002) Cultivation of the ubiquitous SAR11 marine bacterioplankton clade. *Nature* **418**: 630–633.

Rapson, T.D. and Dacres, H. (2014) Analytical techniques for measuring nitrous oxide. *TrAC Trends Anal Chem* **54**: 65–74.

Ravishankara, A.R., Daniel, J.S., and Portmann, R.W. (2009) Nitrous oxide (N₂O): The dominant ozone-depleting substance emitted in the 21st century. *Science (80-)* **326**: 123–125.

Ray, D.K., Mueller, N.D., West, P.C., and Foley, J.A. (2013) Yield Trends Are Insufficient to Double Global Crop Production by 2050. *PLoS One* **8**.

- Ray, D.K., Ramankutty, N., Mueller, N.D., West, P.C., and Foley, J.A. (2012) Recent patterns of crop yield growth and stagnation. *Nat Commun* **3**:
- Reay, D.S., Davidson, E.A., Smith, K.A., Smith, P., Melillo, J.M., Dentener, F.J., and Crutzen, P.J. (2012) Global agriculture and nitrous oxide emissions. *Nat Clim Chang* **2**: 410–416.
- Rinaldo, S., Giardina, G., and Cutruzzolà, F. (2016) Nitrite reductase – Cytochrome cd1. In *Metalloenzymes in denitrification: Applications and environmental impacts*. Moura, I., Moura, J.J.G., Pauleta, S.R., and Maia, L.B. (eds). Royal Society of Chemistry, pp. 59–90.
- Ritz, C., Baty, F., Streibig, J.C., and Gerhard, D. (2015) Dose-response analysis using R. *PLoS One* **10**: 1–13.
- Robertson, L. a and Kuenen, J.G. (1990) Combined heterotrophic nitrification and aerobic denitrification in *Thiosphaera pantotropha* and other bacteria. *Antonie Van Leeuwenhoek* **57**: 139–152.
- Rochette, P. (2008) No-till only increases N₂O emissions in poorly-aerated soils. *Soil Tillage Res* **101**: 97–100.
- Rockström, J., Williams, J., Daily, G., Noble, A., Matthews, N., Gordon, L., et al. (2017) Sustainable intensification of agriculture for human prosperity and global sustainability. *Ambio* **46**: 4–17.
- Roco, C.A., Bergaust, L.L., Bakken, L.R., Yavitt, J.B., and Shapleigh, J.P. (2017) Modularity of nitrogen-oxide reducing soil bacteria: linking phenotype to genotype. *Environ Microbiol* **19**: 2507–2519.
- Roger, Bray, J. and Curtis, J.T. (1957) An ordination of the upland forest communities of Southern Wisconsin. *Ecol Monogr* **27**: 326–349.

- RStudio Team (2022) RStudio: Integrated Development Environment for R.
- RStudio Team (2018) RStudio: Integrated Development for R.
- Rütting, T., Aronsson, H., and Delin, S. (2018) Efficient use of nitrogen in agriculture. *Nutr Cycl Agroecosystems* **110**: 1–5.
- Ryden, J.C. (1983) Denitrification loss from a grassland soil in the field receiving different rates of nitrogen as ammonium nitrate. *J Soil Sci* **34**: 355–365.
- Sánchez, C. and Minamisawa, K. (2018) Redundant roles of Bradyrhizobium oligotrophicum Cu-type (NirK) and cd 1-type (NirS) nitrite reductase genes under denitrifying conditions. *FEMS Microbiol Lett* **365**: fny015.
- Sanford, R.A., Wagner, D.D., Wu, Q., Chee-Sanford, J.C., Thomas, S.H., Cruz-García, C., et al. (2012) Unexpected nondenitrifier nitrous oxide reductase gene diversity and abundance in soils. *Proc Natl Acad Sci* **109**: 19709–19714.
- Saunders, N.F., Houben, E.N., Koefoed, S., de Weert, S., Reijnders, W.N., Westerhoff, H. V, et al. (1999) Transcription regulation of the nir gene cluster encoding nitrite reductase of Paracoccus denitrificans involves NNR and NirI, a novel type of membrane protein. *Mol Microbiol* **34**: 24–36.
- Sawers, R.G. (1991) Identification and molecular characterization of a transcriptional regulator from Pseudomonas aeruginosa PAO1 exhibiting structural and functional similarity to the FNR protein of Escherichia coli. *Mol Microbiol* **5**: 1469–1481.
- Scala, D.J. and Kerkhof, L.J. (1998a) Nitrous oxide reductase (nosZ) gene-specific PCR primers for detection of denitrifiers and three nosZ genes from marine sediments. *FEMS Microbiol Lett* **162**: 61–68.
- Scala, D.J. and Kerkhof, L.J. (1998b) Nitrous Oxide Reductase (nosZ) gene specific Primers

for the detection of denitrifiers and the the three nosZ genes from mariene sediments. *FEMS Microbiol Lett* **162**: 61–68.

Scheer, C., Fuchs, K., Pelster, D.E., and Butterbach-Bahl, K. (2020) Estimating global terrestrial denitrification from measured N₂O:(N₂O + N₂) product ratios. *Curr Opin Environ Sustain* **47**: 72–80.

Schirmer, M., Ijaz, U.Z., D'Amore, R., Hall, N., Sloan, W.T., and Quince, C. (2015) Insight into biases and sequencing errors for amplicon sequencing with the Illumina MiSeq platform. *Nucleic Acids Res* **43**: e37.

Schlesinger, W.H. and Bernhardt, E.S. (2013) *Biogeochemistry: An Analysis of Global Change*, Elsevier Science.

Schulz, S., Kölbl, A., Ebli, M., Buegger, F., Schloter, M., and Fiedler, S. (2017) Field-Scale Pattern of Denitrifying Microorganisms and N₂O Emission Rates Indicate a High Potential for Complete Denitrification in an Agriculturally Used Organic Soil. *Microb Ecol* **74**: 765–770.

Seemann, T. (2014) Prokka: Rapid prokaryotic genome annotation. *Bioinformatics* **30**: 2068–2069.

Seitzinger, S.P., Harrison, J.A., Böhlke, J.K., Bouwman, A.F., Lowrance, R., Peterson, B., et al. (2006) Denitrification across landscapes and waterscapes: a synthesis. *Ecol Appl* **16**: 2064–2090.

Sexstone, A.J., Revsbech, N.P., Parkin, T.B., and Tiedje, J.M. (1985) Direct measurement of oxygen profiles and denitrification rates in soil aggregates. *Soil Sci Soc Am J* **49**: 645–651.

Shade, A., Gregory Caporaso, J., Handelsman, J., Knight, R., and Fierer, N. (2013) A meta-

- analysis of changes in bacterial and archaeal communities with time. *ISME J* **7**: 1493–1506.
- Shannon, C.E. (1948) A mathematical theory of communication. *Bell Syst Tech J* **27**: 379–423.
- Sheng, H., Weng, R., and He, Y. (2021) The application of (15)N isotope tracer in differentiating denitrification, anammox and DNRA during anammox start-up by adding calcium nitrate. *MethodsX* **8**: 101560.
- Shi, Y., Li, Y., Xiang, X., Sun, R., Yang, T., He, D., et al. (2018) Spatial scale affects the relative role of stochasticity versus determinism in soil bacterial communities in wheat fields across the North China Plain. *Microbiome* **6**.
- Shiro, Y. (2012) Structure and function of bacterial nitric oxide reductases: Nitric oxide reductase, anaerobic enzymes. *Biochim Biophys Acta - Bioenerg* **1817**: 1907–1913.
- Siddiqui, R.A., Warnecke-Eberz, U., Hengsberger, A., Schneider, B., Kostka, S., and Friedrich, B. (1993) Structure and function of a periplasmic nitrate reductase in *Alcaligenes eutrophus* H16. *J Bacteriol* **175**: 5867–5876.
- Six, J., Ogle, S.M., Breidt, F.J., Conant, R.T., Mosier, A.R., and Paustian, K. (2004) The potential to mitigate global warming with no-tillage management is only realized when practised in the long term. *Glob Chang Biol* **10**: 155–160.
- Smets, W., Leff, J.W., Bradford, M.A., McCulley, R.L., Lebeer, S., and Fierer, N. (2016) A method for simultaneous measurement of soil bacterial abundances and community composition via 16S rRNA gene sequencing. *Soil Biol Biochem* **96**: 145–151.
- Smith, C.J., Nedwell, D.B., Dong, L.F., and Osborn, A.M. (2007) Diversity and abundance of nitrate reductase genes (*narG* and *napA*), nitrite reductase genes (*nirS* and *nrfA*), and

- their transcripts in estuarine sediments. *Appl Environ Microbiol* **73**: 3612–3622.
- Soil Survey Staff (2014) Keys to Soil Taxonomy, 12th ed. Washington, DC: USDA-Natural Resources Conservation Service.
- Song, K., Lee, S.H., Mitsch, W.J., and Kang, H. (2010) Different responses of denitrification rates and denitrifying bacterial communities to hydrologic pulsing in created wetlands. *Soil Biol Biochem* **42**: 1721–1727.
- Sørensen, J. (1978) Denitrification rates in a marine sediment as measured by the acetylene inhibition technique. *Appl Environ Microbiol* **36**: 139–143.
- Van Spanning, R.J.M., De Boer, A.P.N., Reijnders, W.N.M., Spiro, S., Westerhoff, H. V, Stouthamer, A.H., and der Oost, J. (1995) Nitrite and nitric oxide reduction in *Paracoccus denitrificans* is under the control of NNR, a regulatory protein that belongs to the FNR family of transcriptional activators. *FEBS Lett* **360**: 151–154.
- Van Spanning, R.J.M., De Boer, A.P.N., Reijnders, W.N.M., Westerhoff, H. V, Stouthamer, A.H., and Van Der Oost, J. (1997) FnrP and NNR of *Paracoccus denitrificans* are both members of the FNR family of transcriptional activators but have distinct roles in respiratory adaptation in response to oxygen limitation. *Mol Microbiol* **23**: 893–907.
- Späti, K., Huber, R., and Finger, R. (2021) Benefits of Increasing Information Accuracy in Variable Rate Technologies. *Ecol Econ* **185**.
- Staley, J.T. and Konopka, A. (1985) Microorganisms in aquatic and terrestrial habitats. *Annu Rev Microbiol* **39**: 321–346.
- Stevens, C.J. (2019) Nitrogen in the environment. *Science (80-)* **363**: 578–580.
- Sun, H., Koal, P., Liu, D., Gerl, G., Schroll, R., Gattinger, A., et al. (2016) Soil microbial community and microbial residues respond positively to minimum tillage under organic

- farming in Southern Germany. *Appl Soil Ecol* **108**: 16–24.
- Sutton, M.A. (2011) The European Nitrogen Assessment: Sources, Effects and Policy Perspectives, Sutton, M.A., Howard, C.M., Erisman, J.W., Billen, G., Bleeker, A., Peringe, G., et al. (eds) Cambridge: Cambridge University Press.
- Syakila, A. and Kroeze, C. (2011) The global nitrous oxide budget revisited. *Greenh Gas Meas Manag* **1**: 17–26.
- Tellez-Rio, A., García-Marco, S., Navas, M., López-Solanilla, E., Rees, R.M., Tenorio, J.L., and Vallejo, A. (2014) Nitrous oxide and methane emissions from a vetch cropping season are changed by long-term tillage practices in a Mediterranean agroecosystem. *Biol Fertil Soils* **51**: 77–88.
- Tenuta, M. and Beauchamp, E.G. (2003) Nitrous oxide production from granular nitrogen fertilizers applied to a silt loam soil. *Can J Soil Sci* **83**: 521–532.
- Thomas, G., Potter, L., and Cole, J.A. (1999) The periplasmic nitrate reductase from *Escherichia coli*: a heterodimeric molybdoprotein with a double-arginine signal sequence and an unusual leader peptide cleavage site. *FEMS Microbiol Lett* **174**: 167–171.
- Throbäck, I.N., Enwall, K., Jarvis, Å., and Hallin, S. (2004) Reassessing PCR primers targeting *nirS*, *nirK* and *nosZ* genes for community surveys of denitrifying bacteria with DGGE. *FEMS Microbiol Ecol* **49**: 401–417.
- Thukral, A.K. (2017) A review on measurement of Alpha diversity in biology. *Agric Res J* **54**: 1–10.
- Ti, C., Pan, J., Xia, Y., and Yan, X. (2012) A nitrogen budget of mainland China with spatial and temporal variation. *Biogeochemistry* **108**: 381–394.

- Tian, D. and Niu, S. (2015) A global analysis of soil acidification caused by nitrogen addition. *Environ Res Lett* **10**: 24019.
- Tian, H., Xu, R., Canadell, J.G., Thompson, R.L., Winiwarter, W., Suntharalingam, P., et al. (2020) A comprehensive quantification of global nitrous oxide sources and sinks. *Nature* **586**: 248–256.
- Tiedje, J.M., Simkins, S., and Groffman, P.M. (1989) Perspectives on measurement of denitrification in the field including recommended protocols for acetylene based methods. *Plant Soil* **115**: 261–284.
- Tilman, D., Cassman, K.G., Matson, P.A., Naylor, R., and Polasky, S. (2002) Agricultural sustainability and intensive production practices. *Nature* **418**: 671–677.
- Tkacz, A., Hortala, M., and Poole, P.S. (2018) Absolute quantitation of microbiota abundance in environmental samples. *Microbiome* **6**: 1–13.
- Torsvik, V. and Øvreås, L. (2002) Microbial diversity and function in soil: From genes to ecosystems. *Curr Opin Microbiol* **5**: 240–245.
- Tosques, I.E., Shi, J., and Shapleigh, J.P. (1996) Cloning and characterization of nnrR, whose product is required for the expression of proteins involved in nitric oxide metabolism in *Rhodobacter sphaeroides* 2.4. 3. *J Bacteriol* **178**: 4958–4964.
- Tourlousse, D.M., Yoshiike, S., Ohashi, A., Matsukura, S., Noda, N., and Sekiguchi, Y. (2017) Synthetic spike-in standards for high-throughput 16S rRNA gene amplicon sequencing. *Nucleic Acids Res* **45**: e23.
- Tourna, M., Stieglmeier, M., Spang, A., Könneke, M., Schintlmeister, A., Urich, T., et al. (2011) *Nitrososphaera viennensis*, an ammonia oxidizing archaeon from soil. *Proc Natl Acad Sci U S A* **108**: 8420–8425.

- United Nations (2022a) The sustainable development goals report 2022.
- United Nations (2022b) World Population Prospects 2022, Online Edition.
- Vandekerckhove, T.T.M., Willems, A., Gillis, M., and Coomans, A. (2000) Occurrence of novel verrucomicrobial species, endosymbiotic and associated with parthenogenesis in *Xiphinema americanum*-group species (Nematoda, Longidoridae). *Int J Syst Evol Microbiol* **50**: 2197–2205.
- Vandeputte, D., Kathagen, G., D’hoë, K., Vieira-Silva, S., Valles-Colomer, M., Sabino, J., et al. (2017) Quantitative microbiome profiling links gut community variation to microbial load. *Nature* **551**: 507–511.
- Vellend, M. (2010) Conceptual synthesis in community ecology. **85**: 183–206.
- Verbaendert, I., Hoefman, S., Boeckx, P., Boon, N., and De Vos, P. (2014) Primers for overlooked *nirK*, *qnorB*, and *nosZ* genes of thermophilic Gram-positive denitrifiers. *FEMS Microbiol Ecol* **89**: 162–180.
- Viebrock, A. and Zumft, W.G. (1988) Molecular cloning, heterologous expression, and primary structure of the structural gene for the copper enzyme nitrous oxide reductase from denitrifying *Pseudomonas stutzeri*. *J Bacteriol* **170**: 4658–4668.
- Vlaeminck, S.E., Hay, A.G., Maignien, L., and Verstraete, W. (2011) In quest of the nitrogen oxidizing prokaryotes of the early Earth. *Environ Microbiol* **13**: 283–295.
- Voorhees, E.B. (1902) Studies in denitrification. *J Am Chem Soc* **24**: 785–823.
- Vos, M., Wolf, A.B., Jennings, S.J., and Kowalchuk, G.A. (2013) Micro-scale determinants of bacterial diversity in soil. *FEMS Microbiol Rev* **37**: 936–954.
- Wagg, C., Schlaeppli, K., Banerjee, S., Kuramae, E.E., and van der Heijden, M.G.A. (2019)

- Fungal-bacterial diversity and microbiome complexity predict ecosystem functioning. *Nat Commun* **10**: 1–10.
- Wallenstein, M.D., Myrold, D.D., Firestone, M.K., and Voytek, M. (2006) Environmental controls on denitrifying communities and denitrification rates: Insights from molecular methods. *Ecol Appl* **16**: 2143–2152.
- Walters, W., Hyde, E.R., Berg-lyons, D., Ackermann, G., Humphrey, G., Parada, A.E., et al. (2016) Improved Bacterial 16S rRNA Gene (V4 and V4-5) and Fungal Internal Transcribed Spacer Marker Gene Primers for Microbial Community Surveys. *mSystems* **1**: e0009-15.
- Wang, J., Chadwick, D.R., Cheng, Y., and Yan, X. (2017) Global analysis of agricultural soil denitrification in response to fertilizer nitrogen. *Sci Total Environ*.
- Wang, J. and Zou, J. (2020) No-till increases soil denitrification via its positive effects on the activity and abundance of the denitrifying community. *Soil Biol Biochem* **142**: 107706.
- Wang, J.L., Liu, K. Lou, Zhao, X.Q., Gao, G.F., Wu, Y.H., and Shen, R.F. (2022) Microbial keystone taxa drive crop productivity through shifting aboveground-belowground mineral element flows. *Sci Total Environ* **811**: 152342.
- Wang, Z., Liu, L., Chen, Q., Wen, X., and Liao, Y. (2016) Conservation tillage increases soil bacterial diversity in the dryland of northern China. *Agron Sustain Dev* **36**: 1–9.
- Watanabe, K., Kodama, Y., and Harayama, S. (2001) Design and evaluation of PCR primers to amplify bacterial 16S ribosomal DNA fragments used for community fingerprinting. *J Microbiol Methods* **44**: 253–262.
- Wei, L., Ouyang, S., Wang, Y., Shen, X., and Zhang, L. (2014) *Solirubrobacter phytolacca* sp. nov., an endophytic bacterium isolated from roots of *Phytolacca acinosa* Roxb. *Int J*

Syst Evol Microbiol **64**: 858–862.

Wei, W., Isobe, K., Nishizawa, T., Zhu, L., Shiratori, Y., Ohte, N., et al. (2015) Higher diversity and abundance of denitrifying microorganisms in environments than considered previously. *ISME J* **9**: 1954–1965.

Weisburg, W.G., Barns, S.M., Pelletier, D.A., and Lane, D.J. (1991) 16S ribosomal DNA amplification for phylogenetic study. *J Bacteriol* **173**: 697–703.

Wick, K., Heumesser, C., and Schmid, E. (2012) Groundwater nitrate contamination: Factors and indicators. *J Environ Manage* **111**: 178–186.

Yang, W.H., Traut, B.H., and Silver, W.L. (2015) Microbially mediated nitrogen retention and loss in a salt marsh soil. *Ecosphere* **6**:

Yoshinari, T. and Knowles, R. (1976) Acetylene inhibition of nitrous oxide reduction by denitrifying bacteria. *Biochem Biophys Res Commun* **69**: 705–710.

Yost, M.A., Kitchen, N.R., Sudduth, K.A., Sadler, E.J., Drummond, S.T., and Volkman, M.R. (2017) Long-term impact of a precision agriculture system on grain crop production. *Precis Agric* **18**: 823–842.

Young, J.P.W. (1992) Phylogenetic classification of nitrogen-fixing organisms. *Biol nitrogen Fixat* **1544**: 43–86.

Yuan, H., Zhang, Z., Qin, S., Zhou, S., Hu, C., Clough, T., et al. (2019) Effects of nitrate and water content on acetylene inhibition technique bias when analysing soil denitrification rates under an aerobic atmosphere. *Geoderma* **334**: 33–36.

Zeileis, A. and Grothendieck, G. (2005) Zoo: S3 infrastructure for regular and irregular time series. *J Stat Softw* **14**:

- Zengler, K., Toledo, G., Rappe, M., Elkins, J., Mathur, E.J., Short, J.M., and Keller, M. (2002) Cultivating the uncultured. *Proc Natl Acad Sci U S A* **99**: 15681–6.
- Zhang, B., He, H., Ding, X., Zhang, Xudong, Zhang, Xiaoping, Yang, X., and Filley, T.R. (2012) Soil microbial community dynamics over a maize (*Zea mays* L.) growing season under conventional - and no - tillage practices in a rainfed agroecosystem. *Soil Tillage Res* **124**: 153–160.
- Zhang, M., Zhang, L., Huang, S., Li, W., Zhou, W., Philippot, L., and Ai, C. (2022) Assessment of spike-AMP and qPCR-AMP in soil microbiota quantitative research. *Soil Biol Biochem* **166**: 108570.
- Zhang, X., Ward, B.B., and Sigman, D.M. (2020) Global Nitrogen Cycle: Critical Enzymes, Organisms, and Processes for Nitrogen Budgets and Dynamics. *Chem Rev* **120**: 5308–5351.
- Zhou, J., Kang, S., Schadt, C.W., and Garten, C.T. (2008) Spatial scaling of functional gene diversity across various microbial taxa. *Proc Natl Acad Sci* **105**: 7768–7773.
- Zhu, Y., Li, Y., Zheng, N., Chapman, S.J., and Yao, H. (2020) Similar but Not Identical Resuscitation Trajectories of the Soil Microbial Community Based on Either DNA or RNA after Flooding. *Agronomy* **10**:
- Zumft, W.G. (1997) Cell biology and molecular basis of denitrification. *Microbiol Mol Biol Rev* **61**: 533–616.
- Zumft, W.G., Viebrock-Sambale, A., and Braun, C. (1990) Nitrous oxide reductase from denitrifying *Pseudomonas stutzeri*. Genes for copper-processing and properties of the deduced products, including a new member of the family of ATP/GTP-binding proteins. *Eur J Biochem* **192**: 591–599.

